

Copyright

by

Simone Raffa Carvalho

2013

**The Dissertation Committee for Simone Raffa Carvalho Certifies that
this is the approved version of the following dissertation:**

Improved Inhalation Therapies of Brittle Powders

Committee:

Robert O. Williams III, Supervisor

Alan B. Watts

Zhengrong Cui

Jason T. McConville

James W. McGinity

Hugh D. Smyth

Improved Inhalation Therapies of Brittle Powders

by

Simone Raffa Carvalho, Farmacêutica

Dissertation

Presented to the Faculty of the Graduate School of

The University of Texas at Austin

in Partial Fulfillment

of the Requirements

for the Degree of

Doctor of Philosophy

The University of Texas at Austin

December, 2013

Dedication

To God, for blessing me with strength, wisdom and grace through all these years.

Phil 4:13: I can do everything through Him who gives me strength.

Jer 29:11: For I know the plans I have for you, declares the Lord, plans to prosper you and not to harm you, plans to give you hope and a future.

To my loving husband Thiago for all his help, endless support, patience and love.

To my dedicated parents for their love and encouragement.

Acknowledgements

First of all, I would like to thank God for giving me the opportunity to come to the United States and to earn this degree. Sincere thanks goes to my family, specially my parents Eliane and Gerson Raffa, for their unconditional love and support. I also would like to thank my grandmother Lindalva for her love and for always being present in my life.

Special thanks go to my husband Thiago. Thank you for being my friend, my love, my motivator, my inspiration and, above all, a great mentor. I would not make it without you by my side.

I would like to thank Dr. Jason McConville for giving me the opportunity to work in his research group, first as a visitor scientist and later as a doctoral student. I am grateful for his patience, advices and for trusting I was capable to endure this challenge. I cannot thank him enough for being more than an advisor but also a good friend.

I would like to express my sincere appreciation to Dr. Robert Williams III for accepting me into his research group half way through my doctorate program. I am thankful for the opportunity to work under his guidance, for the great research projects assigned to me and for always being a great mentor. I also would like to thank Dr. Alan Watts for playing a significant role as my co-advisor. Our discussions and his advices were extremely important for the success of my scientific development. A special thanks to Dr. James McGinity for his insightful professional advices and great classes. I also

would like to extend my gratitude to Dr. Hugh Smyth for all his help with my experiments and for sharing laboratory equipment. Thanks also to Dr. Zhenrong Cui for the scientific discussions and advices about my animal studies.

I would like to thank my friends Dr. H el ene Dugas, Dr. Yoen J. Son, Ashkan Yazdi, Matthew Herpin, Soraya Hengsawas and Sha Liu for their support and for sharing a great time with me down in the basement of the College of Pharmacy. Many thanks also go to Dr. Sumalee Thitinan, Dr. Javier O. Morales, Dr. Nicole Beinborn, Dr. Shih-Fan Jan, Dr. Kevin P. O'Donnell, Dr. Shayna McGill, Dr. Stephanie Bosselmann, Dr. Bo Lang and Dr. Justin R. Hughey. I also would like to thank all my fellow graduate students Dr. Yi-Bo Wang, Xinran Li, Ju Du, Ping Du, Justin Keen, Ryan Bennet, Chris Brough, and Siyuan Huang. Particularly, I would like to thank Sha Liu for helping me with my animal studies. Soraya Hengsawas made my last year in the lab so much fun. Thanks for her endless help with my experiments and for our scientific and non-scientific discussions.

I also would like to acknowledge the staff in the College of Pharmacy, Claudia McClelland, Jim Baker, Joe Adcock, Herman Schwarzer and Sharla Brewer, for their patience and support to all of us, graduate students. Mickie S. Sheppard, Yolanda Abasta and Stephanie Crouch: thank you for your help and advice with classes, scholarships and for helping us to settle in Austin. Thanks to Jay Hamman, Oliver Gomez, John Reineke for all your support with computer, videoconferencing and seminars. Thanks to Belinda G. Lehmkuhle for your patience and great job on my posters. All of you contributed to the success of my doctorate program.

Improved Inhalation Therapies of Brittle Powders

Simone Raffa Carvalho, Ph.D.

The University of Texas at Austin, 2013

Supervisor: Robert O. Williams III

Advancements in pulmonary drug delivery technologies have improved the use of dry powder inhalation therapy to treat respiratory and systemic diseases. Despite remarkable improvements in the development of dry powder inhaler devices (DPIs) and formulations in the last few years, an optimized DPI system has yet to be developed. In this work, we hypothesize that Thin Film Freezing (TFF) is a suitable technology to improve inhalation therapies to treat lung and systemic malignancies due to its ability to produce brittle powder with optimal aerodynamic properties. Also, we developed a performance verification test (PVT) for the Next Generation Cascade Impactor (NGI), which is one of the most important *in vitro* characterization methods to test inhalation.

In the first study, we used TFF technology to produce amorphous and brittle particles of rapamycin, and compared the *in vivo* behavior by the pharmacokinetic profiles, to its crystalline counterpart when delivered to the lungs of rats via inhalation. It was found that TFF rapamycin presented higher *in vivo* systemic bioavailability than the crystalline formulation. Subsequently, we investigated the use of TFF technology to produce triple fixed dose therapy using formoterol fumarate, tiotropium bromide and budesonide as therapeutic drugs. We investigated applications of this technology to

powder properties and *in vitro* aerosol performance with respect to single and combination therapy. As a result, the brittle TFF powders presented superior properties than the physical mixture of micronized crystalline powders, such as excellent particle distribution homogeneity after *in vitro* aerosolization. Lastly, we developed a PVT for the NGI that may be applicable to other cascade impactors, by investigating the use of a standardized pressurized metered dose inhaler (pMDI) with the NGI. Two standardized formulations were developed. Formulations were analyzed for repeatability and robustness, and found not to demonstrate significant differences in plate deposition using a single NGI apparatus. Variable conditions were introduced to the NGI to mimic operator and equipment failure. Introduction of the variable conditions to the NGI was found to significantly adjust the deposition patterns of the standardized formulations, suggesting that their use as a PVT could be useful and that further investigation is warranted.

Table of Contents

List of Tables	xiv
List of Figures	xvi
Chapter 1: Introduction	1
1.1 Dry Powder Inhalation for Pulmonary Delivery: Recent Advances and Continuing Challenges	2
1.2 Dry Powder Inhaler Devices	3
1.2.1. Overview	3
1.2.2. Recent Innovations in Dry Powder Inhaler Technology	6
1.3. New developments in DPI formulations and delivery	11
1.3.1. Particle surface modification	12
1.3.2. Particle Engineering Technology for Pulmonary Delivery	14
1.3.2.1. Spray drying	15
1.3.2.2. Spray-freezing methods	17
1.3.2.3. Thin film Freezing	18
1.3.2.4. Sono-crystallization	19
1.3.2.5. Fixed-Dose Drug Combination	19
1.3.3. Nanoparticles and Biodegradable Polymeric Nanocarriers	21
1.3.4. Controlled Release of Drugs for Lung Delivery	22
1.3.5. Macromolecules for Pulmonary Delivery	25
1.4. Characterization Methods of Dry Powder Inhaler Formulations	28
1.5. Conclusion	32
1.6. References	33
Chapter 2: Research Outline	55
2.1. OVERALL OBJECTIVES	55
2.2. SUPPORTING OBJECTIVES	55
2.2.1. Characterization and Pharmacokinetics Comparison Analysis of Crystalline versus Amorphous Rapamycin Dry Powder via Pulmonary Administration in Rats	55

2.2.2.	Inhaled Therapies of Fixed-dose Combinations Prepared by Thin Film Freezing	56
2.2.3.	Development of a Verification Performance Test for Cascade Impactor	57
Chapter 3: Characterization and pharmacokinetics comparison analysis of crystalline versus amorphous rapamycin dry powder via pulmonary administration in rats		59
3.1	Introduction.....	60
3.2	Materials and methods	62
3.2.1	Materials	62
3.2.2	Formulation preparation.....	62
3.2.3	Particle size analysis	64
3.2.4	Scanning Electron Microscopy (SEM)	64
3.2.5	Brunauer-Emmet-Teller (BET) specific surface area (SSA)	64
3.2.6	Thermal analysis	65
3.2.7	Powder X-ray diffraction (PXRD).....	65
3.2.8	<i>In vitro</i> aerosol performance	66
3.2.9	Chromatographic assays	67
3.2.10	<i>In vivo</i> pulmonary dosing of rats	67
3.2.11	Estimated Dose	68
3.2.12	Blood, BAL and lung analysis	69
3.2.13	Pharmacokinetics and statistical analysis	71
3.3	Results and discussion	71
3.3.1	Preformulation considerations	72
3.3.2	Physicochemical properties of formulations.....	73
3.3.2.1	Particle size and morphology of formulations	73
3.3.2.2	Crystalline state of powders and moisture content.....	74
3.3.3	<i>In vitro</i> aerosol performance	77
3.3.4	Pharmacokinetics of inhaled amorphous TFF RapaLac and crystalline RapaLac physical mixture	78
3.3.4.1	Determination of Delivered Dose	78

3.3.4.2	Pharmacokinetics Evaluation	80
3.4	Conclusion	82
3.5	Tables	83
3.6	Figures.....	86
3.7	References.....	94
Chapter 4: Inhaled Therapies of Fixed-dose Combinations Prepared by Thin Film Freezing.....		
		101
4.1	Introduction.....	102
4.2	Materials and Method	105
4.2.1	Materials	105
4.2.2	Formulation Preparation	105
4.2.3	Thermal analysis	107
4.2.4	Powder X-ray diffraction (PXRD).....	107
4.2.5	Particle size analyses.....	107
4.2.6	Scanning Electron Microscopy (SEM)	108
4.2.7	Brunauer-Emmett-Teller (BET) specific surface area (SSA) analysis	
	108	
4.2.8	Fourier Transform Infrared Spectroscopy (FTIR)	108
4.2.9	<i>In vitro</i> aerosol performance	109
4.2.10	HPLC assay.....	110
4.2.11	Statistical analysis.....	110
4.3	Results and Discussion	110
4.3.1	Particle size and morphology of formulations	110
4.3.2	Crystallinity evaluation.....	113
4.3.2.1	Budesonide	113
4.3.2.2	Tiotropium Bromide.....	114
4.3.2.3	Formoterol Fumarate.....	115
4.3.3	Triple drug combinations.....	116
4.3.4	Analysis of the samples by FTIR.....	117
4.3.5	<i>In vitro</i> aerosol performance of formulations and deposition homogeneity on the NGI.....	120

4.4	Conclusion	123
4.5	Tables	125
4.6	Figures.....	129
4.7	References.....	143
Chapter 5: Development of a Performance Verification Test for Cascade Impactors		146
5.1	Introduction.....	147
5.2	Materials and Methods.....	149
5.2.1	Materials	149
5.2.2	Formulation preparation.....	149
5.2.2.1	Rhodamine B/ethanol/propellant formulations	149
5.2.2.2	Rhodamine B/ethanol/propellant/adjuvant excipients formulations	150
5.2.3	NGI operation procedure – normal use.....	150
5.2.4	NGI operation procedure for stress testing	151
5.2.4.1	Air leakage simulation of stage 3 of the NGI.....	152
5.2.4.2	Simulation of nozzle clogging at stage 4	152
5.2.4.3	NGI analysis at low airflow rate	152
5.2.5	UV-vis spectroscopy	152
5.2.6	Statistical analysis.....	153
5.3	Results and Discussion	153
5.3.1	Formulation design	153
5.3.2	Performance of formulations	154
5.3.2.1	Rhodamine B/ethanol/propellant formulations	154
5.3.2.2	Rhodamine B/ethanol/propellant formulations/adjuvant excipients	154
5.3.2.3	Inter impactor variability.....	156
5.3.3	NGI stress testing.....	156
5.4	Conclusion	157
5.5	Tables	159
5.6	Figures.....	162

5.7 References.....	167
Bibliography	169
Vita	199

List of Tables

Table 3.1 – Particle size distribution and specific surface area of bulk lactose monohydrate and rapamycin as received from supplier, wet ball-milled lactose and rapamycin and amorphous TFF powders RapaLac_0.75% and RapaLac_0.40%.	83
Table 3.2 – Next generation cascade impactor results of RapaLac physical mixture, TFF RapaLac_0.40% and RapaLac_0.75% formulations aerosolized using the Handihaler™ device at an airflow rate of 54 L/min for 4.4 seconds.	84
Table 3.3 – Pharmacokinetic parameters for blood and pulmonary tract (lungs and BAL) rapamycin concentration in rats after single-dose inhalation of amorphous RapaLac_0.40% and crystalline RapaLac physical mixture.	85
Table 4.1 – Particle size distribution and specific surface area of bulk drugs and excipients, jet milled drugs and TFF formulations.	125
Table 4.2 – Summary of the FTIR spectrum changes showing the stretching frequency shifts for the carbonyl groups of all TFF formulations. .	126
Table 4.3 – Emitted dose and fine particle fraction for each drug from all triple combo formulations.	127
Table 4.4 – Emitted dose and percentage fine particle fraction of all single drug formulations.	128
Table 5.1 – Composition of the pMDI formulations (Rhodamine B/ethanol/propellant).	159

Table 5.2 – Composition of the pMDI formulations (Rhodamine B/ethanol/propellant/
adjuvant excipients)160

Table 5.3 – General comparison of solution based and suspension based pMDIs.161

List of Figures

- Figure 3.1 – SEM images of (a) lactose monohydrate, (b) rapamycin, (c) wet milled lactose, and (d) wet milled rapamycin.86
- Figure 3.2 – SEM images of (a) RapaLac physical mixture (b) RapaLac physical mixture at higher magnification (c) RapaLac_0.40% (w/v) and (d) RapaLac_0.75% (w/v).87
- Figure 3.3 – Powder X-ray patterns of bulk lactose monohydrate, wet ball milled lactose monohydrate, bulk rapamycin, wet ball milled rapamycin, TFF RapaLac_0.40% and TFF RapaLac_0.75%.88
- Figure 3.4 – Modulated DSC profiles of bulk lactose monohydrate, bulk rapamycin, wet ball milled lactose monohydrate, wet ball milled rapamycin, RapaLac_0.75% and RapaLac_0.40%.89
- Figure 3.5 – Thermogravimetric analyzes of rapamycin and lactose monohydrate powders as received from supplier, RapaLac_0.75% and RapaLac_0.40%.90
- Figure 3.6 – Percent deposition of RapaLac formulations on a NGI showing physical mixture RapaLac in solid dark bars, RapaLac_0.75% in striped bars and RapaLac_0.40% in dotted bars.91
- Figure 3.7 – Bronchoalveolar lavage (BAL) and lung concentration of deposited rapamycin in rats after a single-dose administration of crystalline RapaLac physical mixture and amorphous RapaLac_0.40%. Data are presented as mean \pm SD, n = 3, and normalized to ng of rapamycin per gram of lung tissue per microgram of dose.92

Figure 3.8 – Total whole blood concentration of rapamycin per microgram of dose deposited in the lungs of rats after a single-dose administration of amorphous RapaLac_0.40% and crystalline RapaLac physical mixture. Data are presented as mean \pm SD, n = 3.	93
Figure 4.1 – SEM images of (a) budesonide, (b) tiotropium bromide and (c) formoterol fumarate at magnification of 10.0k, (d) mannitol and (e) lactose monohydrate (1.0k).....	129
Figure 4.2 – SEM images of (a) jet milled budesonide (b) jet milled tiotropium (c) jet milled formoterol and the physical mixtures (d) BTF_Lac_PM (e) BTF_Man_PM (5.0k).	130
Figure 4.4 – SEM images of TFF formulations (a) For_Lac, (b) For_Man, (c) BTF_Lac, and (d) BTF_Man at magnification 1.0k.	132
Figure 4.5 – Modulated DSC heat flow thermograms of unprocessed lactose monohydrate, mannitol, budesonide, tiotropium and formoterol, physical mixture formulation of jet milled budesonide, tiotropium and formoterol with mannitol (BTF_Man) and with lactose (BTF_Lac), and jet milled tiotropium, formoterol and budesonide.....	133
Figure 4.6 – Modulated DSC heat flow thermograms of unprocessed lactose monohydrate, mannitol, budesonide, formoterol and tiotropium, TFF formulations of Bud_Man, For_Man, Tio_Man and BTF_Man.....	134
Figure 4.7 – Modulated DSC heat flow thermograms of unprocessed lactose monohydrate, mannitol, budesonide, formoterol and tiotropium, TFF formulations of BTF_Lac, Bud_Lac, For_Lac, and Tio_Lac.....	135

Figure 4.8 – Powder x-ray pattern of (a) mannitol, (b) lactose monohydrate, (c) budesonide, (d) tiotropium, (e) formoterol, (f) Bud_Man, (g) Tio_Man, (h) For_Man, (i) BTF_Man, (j) Bud_Lac, (l) Tio_Lac, (m) For_Lac and (n) BTF_Lac.....	136
Figure 4.9 – Powder x-ray pattern of (a) lactose monohydrate, (b) mannitol, (c) budesonide, (d) jet milled budesonide, (e) tiotropium, (f) jet milled tiotropium, (g) formoterol, and (h) jet milled formoterol.	137
Figure 4.10 – FTIR scans of TFF formoterol_lactose, TFF budesonide_lactose, TFF tiotropium_lactose, physical mixture of triple drug combination, TFF triple drug combination, formoterol, budesonide, tiotropium, TFF lactose and lactose.....	138
Figure 4.11 – FTIR scans of TFF formoterol_mannitol, TFF budesonide_mannitol, TFF tiotropium_mannitol, TFF triple drug combination, formoterol, budesonide, tiotropium, physical mixture of triple drug combination, TFF mannitol and mannitol.	139
Figure 4.12a – Aerodynamic particle size distribution of TFF triple combo BTF_Lac formulations deposited on a next generation cascade impactor.....	140
Figure 4.12b – Aerodynamic particle size distribution of TFF triple combo BTF_Man formulations deposited on a next generation cascade impactor.....	140
Figure 4.13a – Aerodynamic particle size distribution of TFF single drug formulations For_Lac, Tio_Lac and Bud_Lac, deposited on a next generation cascade impactor.....	141
Figure 4.13b – Aerodynamic particle size distribution of TFF single drug formulations For_Man, Tio_Man and Bud_Man, deposited on a next generation cascade impactor.....	141

Figure 4.14a – Aerodynamic particle size distribution of triple combo physical mixture BTF_Lac_PM formulations deposited on a next generation cascade impactor.....	142
Figure 4.14b – Aerodynamic particle size distribution of triple combo physical mixture BTF_Man_PM formulations deposited on a next generation cascade impactor.....	142
Figure 5.1 – Amount deposition of formulation B on a NGI. Data is presented as mean \pm SD, n = 3.	162
Figure 5.2a – Amount deposition of formulation C, D and E on a NGI. Data is presented as mean \pm SD, n = 3.....	163
Figure 5.2b – Amount deposition of formulation E.2 and E.3 on a NGI. Data is presented as mean \pm SD, n = 3	163
Figure 5.3a – Amount deposition of formulation E.4 on a NGI. Data is presented as mean \pm SD, n = 3.	164
Figure 5.3b – Combined deposition of formulations B and E.4 on a NGI. Data is presented as mean \pm SD, n = 3.....	164
Figure 5.4. Amount deposition of formulations B and E.4 on NGI I, II and III. Data is presented as mean \pm SD, n = 3. The symbol * means $\alpha < 0.05$ when compared to other groups individually and δ means $\alpha < 0.05$ when compared to each other.	165
Figure 5.5 – Amount deposition of formulations B and E.4 on NGI I at different conditions: control, damaged o-ring, partial blockage of nozzles on stage 4, and reduction of airflow rate to 25 L/min. Data is presented as mean \pm SD, n = 3. The symbol * means $\alpha < 0.05$ when compared to other groups individually and δ means $\alpha < 0.05$ when compared to each other. .	166

Chapter 1: Introduction

Abstract

The pulmonary route of administration is used to treat respiratory and systemic diseases and has gained increasing importance in the field of drug delivery due to its unique advantages including a larger surface area, avoidance of first pass metabolism, the potential for local and systemic administration. In light of some remarkable improvements in the development of dry powder inhaler (DPI) devices and formulations over the last few years, there continues to be a need for further optimized DPI systems. Recently, researchers have focused on finding ways to enhance dry powder inhalation therapy by improving the physicochemical characteristics of the powder formulation and the device performance. The aim of this manuscript is to review the most recent advances in dry powder inhaler technology. Accordingly, we provide a review of the most recent reported improvements in DPI design, mechanisms of powder dispersion, dry powder composition and delivery, and characterization methods for DPI products.

1.1 DRY POWDER INHALATION FOR PULMONARY DELIVERY: RECENT ADVANCES AND CONTINUING CHALLENGES

Advancements in pulmonary drug delivery technologies have boosted the use of dry powder inhalation therapy to treat respiratory and systemic diseases. Despite remarkable improvements in the development of dry powder inhaler devices (DPIs) and formulations in the last few years, an optimized DPI (dry powder inhaler) system has yet to be developed (1). The efficacy of inhaled therapy using a dry powder is dependent on at least four variables: the physicochemical properties of the formulation components, the design of the device, the mechanism of powder dispersion and the patient inhalation maneuver (2)(3). In order to travel through the respiratory system and reach the lungs, powder particles administered by DPIs should have an aerodynamic diameter on the range of 1-5 μm which are termed respirable particles (4). However, at such a small size the particles exhibit high adhesive and cohesive interparticulate forces and tend to agglomerate. Hence, fluidization and dispersion of the micronized particles before they enter the respiratory airways is extremely important. The principal forces involved in powder dispersion from a DPI are frictional, drag, lift, and inertial forces (5). For decades, coarse carrier particles (e.g., lactose) have been blended with the micronized drug to reduce these interparticulate forces and enhance powder flowability (6). Different DPI designs and carrier physicochemical properties will influence the aerodynamic behavior of the formulation. Aerodynamic detachment forces (i.e., the interaction of the flow stream with the drug particles attached to the carrier's surface) and mechanical detachment forces (i.e., the detachment due to collisions between the carrier-drug particles and the walls of the device) are some of the mechanisms responsible for the detachment of drugs from carrier particles (7). While bulk blended powder has shown improved flowability, interparticulate forces such as electrostatic, capillary, van der

Waals and mechanical interlocking still exist and influence powder aerosolization behavior (8)(9)(10).

Incomplete powder de-agglomeration upon inhalation results in poor generation of respirable particles and inhaled therapy performance (11). Therefore, optimization of the device-powder formulation system to generate respirable drug particles within an appropriate particle size range and consistent delivered dose is essential.

Recently, researchers have focused on finding ways to enhance dry powder inhalation therapy by improving the physicochemical characteristics of the powder formulation and device performance. The aim of this paper is to review the most recent advances in dry powder inhaler technology. Accordingly, we provide a review of the most recent reported improvements in DPI device designs and mechanisms of powder dispersion, dry powder formulations and delivery, and characterization methods for DPI products.

1.2.DRY POWDER INHALER DEVICES

1.2.1. Overview

Dry powder inhalation products are comprised of a drug formulation and a device. The generation of respirable aerosolized particles is dependent on the powder formulation properties and the characteristics of the inhaler device such as the metering dose system and the mechanism of powder dispersion during inhalation (12). DPIs are generally grouped into three categories based on the dose metering system: single-unit dose, multi-unit dose and multi-dose reservoir. The single-unit dose inhaler is the most widely utilized type of DPI which requires the patient to load the device with a hard capsule containing micronized powder formulation prior to inhalation (13). The Spinhaler[®] and

Rotahaler[®] (GlaxoSmithKline, Research Triangle Park, North Carolina, USA) are two common examples of this dose metering system. The capsule must be ruptured before the inhalation maneuver and the patient is then required to clean the remains of the broken capsule shell prior to loading the next dose into the device. These single-unit dose devices are also available as disposable systems for patient convenience which are supplied pre-loaded with one dose of the appropriate formulation and can be discarded after use. Several disposable devices are under development or in clinical trials (e.g. Cricket[™] (Mannkind Corporation, Valencia, CA, USA), however only one inhaler device, TwinCaps[®] (Hovione, New Jersey, USA) has been approved in Japan, so far. The TwinCaps[®] provides not just one but two doses of drug formulation (14). The other two categories of devices are classified as multi-dose devices. The multi-unit dose devices are available with multiple pre-metered doses stored in a sealed protective packaging (e.g. blisters, disks, cartridges or dimpled tapes), and the multi-dose reservoir has the micronized powder formulation stored in a reservoir system. In this reservoir system, individual doses are metered and dispensed by a built in mechanism under gravity (13)(15). The Turbuhaler[®], for example, is loaded with up to 200 doses each of which is metered by the patient when the grip part of the device is twisted(16). Several devices have been developed in an attempt to improve the precision of dose metering systems as well as increase formulation stability. For instance, the Clickhaler[®], another type of multi-dose device, has the formulation stored in a reservoir, which rapidly fills the dimpled metering cones when the device is actuated. Moreover, different dimple sizes on the surface of the cone allows the patient to meter different dose sizes (17)(18).

As mentioned previously, aerosolization of powder formulation within the DPI depends on the physicochemical properties of the powder, the design of the device and the mechanism of powder dispersion. According to the type of powder dispersion

mechanism, dry powder inhalers may be classified as passive or active devices. Passive devices rely solely on the energy generated by patient inspiratory flow rates to fluidize and disperse the powder. The advantage of using the breath-actuated devices is that the dose delivery no longer requires coordination with patient inhalation. However, these type of devices may present different airflow resistances requiring different levels of inspiratory effort from patients with respiratory diseases, such as asthma and chronic obstructive pulmonary disease (COPD) (19). Devices with low airflow resistance generate a low-pressure drop inside the device and may require less inspiratory effort. However, high airflow rates are usually necessary to efficiently de-agglomerate the powder. High resistance devices are more efficient for dispersion of dry powders, but also require more respiratory effort from the patient due to the high-pressure drop created inside the device and hence may not be suitable for patients with aggravated and severe pulmonary conditions (20)(21). Most of the novel DPI devices under development use the Air Classifier Technology (ACT) as a mechanism of powder dispersion(5). The high efficiency of this mechanism is based on the formation of a cyclone within the device. More specifically, a multi-channel classifier generates tangential airflow upon inhalation, which forms the cyclone within the cyclone chamber. Additionally, centrifugal energy delays the passage of large particles which increases the time for small particle detachment (22). The Novolizer[®] (Viatriis, GmbH & Co. KG, Frankfurt, Germany) was recently reported to use the aforementioned ACT as its powder dispersion mechanism (23)(24).

Active DPI devices, in most cases, possess an integrated power source dispersion unit to aerosolize the powder with compressed air. Thus, coordination between device actuation and patient breath is usually required. This system is suitable for children and patients in advanced disease states since device performance is less dependent on the

patient's inspiratory capacity (25)(26). Active devices are usually more complex and sophisticated than passive devices. A recent development is the breath-activated Aspirair™ (Vectura, Chippenham, Wiltshire, UK) active device, which utilizes compressed air as its energy source. The patient manually activates a low torque, corkscrew-type manual pump, which compresses the air immediately before the inhalation maneuver. When released inside the air chamber the air creates a vortex to disperse the powder formulation(27). Another example of an active device is the MicroDose inhaler (MicroDose Technologies, Inc., Monmouth Junction, NJ). Upon inhalation, the electronic device, which has a built-in sensor, detects the inspiratory airflow and automatically activates a piezo-electric vibrator. The piezo converts electrical energy into mechanical motion to de-aggregate the drug powder packaged in aluminum blisters. The piezo-electric vibrator creates air pressure jets, which withdraw the powder from the blister. The efficiency of the inhaler is not dependent on patient inhalation effort (28). While the active devices have been demonstrated to be very efficient to fluidize and disperse dry powder independently of the patient airflow rate, a significant challenge for the development of these devices is to produce a portable device with a built-in energy source at a low price. Therefore, passive devices are still more popular than the active devices due to low costs and simplicity of use, despite the final performance being dependent on patient airflow rate and potential inconsistent dosing (29).

1.2.2. Recent Innovations in Dry Powder Inhaler Technology

While numerous dry powder inhaler devices have been developed and marketed, there is still a lag in creating a device that meets the requirements of an ideal DPI. Computational fluid dynamics (CFD) is a well-established tool that has been used by

researchers to predict and understand more about the impact of different properties of inhaler design and airflow on inhaler dispersion performance (30). CFD has demonstrated that small changes in inhaler design can cause a significant variation on DPI performance. Coates et.al. reported that increasing the airflow rate through the AeroHaler[®] device significantly enhances the powder dispersion mechanism by increasing air turbulence and particle-device collision velocities. However, a disadvantage of increasing the airflow and particle dispersion is the subsequent increase in particle deposition on the throat and decrease of drug particles delivered to the lungs (31).

In a search for the ideal DPI technology, various devices are under development, undergoing clinical trials or have recently been marketed. There have been many innovations in the development of devices but unfortunately very limited information is provided or published. Some of these innovations are summarized below.

Elkira/Bretaris[®] Genuair[®]. A next generation multidose reservoir device and breath actuated dry powder inhaler, has been modified and optimized from the Novolizer[®] inhaler. It was approved for marketing in Europe in 2012 by the European Medicines Agency as Elkira/Bretaris[®] Genuair[®] and by the Food and Drug Administration in the United States as Tudorza Pressair[™] for the delivery of acclidinium bromide. Genuair[®] (Laboratorios Almirall, SA, Barcelona, Spain) has a multidose cartridge loaded with 200 metered doses of the medication for one month of therapy therefore does not require refilling by the patient. It is simple to use and has a visual (green and red window) and acoustic (audible click) feedback mechanism to indicate successful inhalation. Upon inhalation, airflow enters the device and generates a cyclone inside the mouthpiece and cyclone unit under medium airflow resistance. The powder is dispersed into fine particles and delivered to the patient within the first 2 liters of inhalation at a wide range of airflow rates. Data from undergoing clinical trials have

show that the delivery of acclidinium bromide by Genuair[®] has been highly accepted by patients although a potential disadvantage of the inhaler is the moderate to low lung deposition of approximately 30% of the dose (32)(33)(34).

NEXThaler[®]. The NEXT[™] or NEXThaler[®] dry powder inhaler (Chiesi Pharmaceutici, Parma, Italy) is also a medium-resistance multi-dose device, which uses a cyclone mechanism for powder dispersion localized in the mouthpiece. The powdered formulation is stored in a reservoir with a metering dose opening at the bottom. The device automatically loads the dose when the cap is opened and reloads it when the device is closed. The NEXThaler[®] device contains a tangential air inlet connected to a vortex chamber that allows high air velocity and shear force generation within the device. Under a certain airflow rate, a breath-actuated mechanism activates the dosing group allowing the dose to be taken, and the dose counter to subtract only after an effective release of the therapeutic dose (29)(35). The NEXThaler[®] was approved in Europe in 2013 and is now undergoing phase 2 clinical trials in the United States testing a combination therapy of formoterol and beclometasone dipropionate for asthmatic patients.

MedTone[®]. This is a compact and breath-powered[®] device composed of a housing with an air inlet, a valve that controls the airflow, a mixing section where the single-use cartridges are loaded with the formulation to be inserted and a mouthpiece (36). A passive de-agglomeration mechanism disperses the powder. The air stream enters the device through two inlets, passing through the cartridge, forming a cyclonic flow, which picks up, fluidizes and de-agglomerates the medicament powder in the cartridge before delivery to the patient respiratory system. A disadvantage of the device is the need to unload and reload the same cartridge immediately after the use for the second inhalation maneuver (37). MedTone[®] (MannKind Corporation, Valencia, CA, USA) was developed

for use in combination with the AFREZZA[®] Inhalation Powder, an ultra rapid-acting Technosphere[®] insulin dry powder (described later in this chapter). The inhaler is undergoing phase 3 clinical trials in the United States for the treatment of type 1 and 2 diabetes mellitus.

3M Conix[™]. The new 3M Conix[™] dry powder inhaler (3M Drug Delivery Systems, St. Paul, MN, USA) uses a reverse flow cyclone technology for efficient deagglomeration and aerosolization of the powder formulation. As the patient inhales, the airflow entering the device creates a high velocity vortex which reverses the airflow when it hits the bottom generating the energy required for deagglomeration of the micronized drug powder from the carrier through particle-particle and particle-wall collisions as well as particle shearing. The vortex de-aggregates the powder releasing the small drug particles and trapping the largest particles at the bottom of the cone avoiding oropharynx deposition. It is available as a disposable, reloadable and multidose design. 3M Conix[™] presented a higher level of fine particle fraction (FPF) albuterol sulphate when compared to the Accuhaler[™] device (GlaxoSmithKline, Brentford, UK) (1)(38).

3M[™] Taper. Two novel technologies have been combined for the development of the 3M[™] Taper DPI (3M Drug Delivery Systems, St. Paul, MN, USA). The excipient-free powdered formulation is stored inside the dimples present on the microstructured carrier tape allowing delivery of up to 120 pre-metered doses. The number and volume of dimples existing in the tape length that are presented to the dosing zone determines the dose. The dimples are only filled with micronized drug and are held in place by cohesive forces and delivered at time of inhalation. An impactor is released upon inhalation that strikes the tape and releases the inhalation powder into the airstream undergoing deagglomeration due to the high airflow shear force. The device also has an audible and visual feedback mechanism to indicate correct usage (39)(40). Adamis Pharmaceutical

Corporation has recently acquired the license to 3M™ Taper DPI technology that is currently in the development phase.

Breezhaler®. This device is a capsule based dry powder inhaler with low airflow resistance ($0.07 \text{ cm H}_2\text{O}^{1/2}/\text{L}/\text{min}$) developed to deliver glycopyrronium bromide for the treatment of patients with COPD. It is a redesign of the Novartis Aerolizer® device, with similar characteristics and peak inspiratory flow rate. However, it requires less effort from the patient to load the device and pierce the capsule. Similar to the Genuair® device, Seebri Breezhaler® (Novartis Pharma AG, Basel, Switzerland) has an acoustic feedback mechanism (whirring sound) to indicate adequate inspiratory effort. Moreover, the use of transparent capsules allows the patient to visually check that the capsule has emptied (41)(42)(43). Breezhaler® was shown to have a higher overall preference by COPD patients when compared to the Handhaler® device (44). Breezhaler® was launched in the US under the brand name Arcapta™ Neohaler™, in Japan under the brand name Onbrez® Inhalation Capsules and it has recently been approved in Europe under the name Seebri® Breezhaler®. In 2013, the European and Japanese regulatory authorities approved the use of Ultibro® Breezhaler®, a fixed-dose combination of indacaterol and glycopyrronium to treat COPD patients.

Cricket™ and Dreamboat™. MannKind Corporation has also developed two other high resistance dry powder inhaler devices to dispense powdered insulin that work in a similar way. When the patient inhales, Cricket™ (single use) and Dreamboat™ (re-usable) inhalers form two airflow inlet streams that converge into one. The first stream fluidizes and carries the Technosphere® inhalation powder from the reservoir into the second by-pass inlet stream. At the intersection where the two streams meet each other, the turbulence and shear force is high enough to break up and disperse the particles for inhalation. Due to the high resistance design, both inhalers efficiently disperse the dry

powder formulations at low airflow rates. As mentioned previously, high resistance devices require enormous effort from the patient to inhale the powder (45)(46)(47)(48). Cricket™ is a single-use device, which is meant to be discarded after use by the patient. The devices are currently in phase 1 clinical trials.

Swinghaler®. The Swinghaler® (PT. Otsuka Indonesia, Jakarta, Indonesia), another type of multiuse reservoir device, has recently been developed to facilitate a patient's use during inhalation. The dose is metered by a "swing back system" that prevents double dosing. Further research is required to confirm the robustness of this type of mechanism as a means of drug delivery (49)(50).

A novel active and multi-dose dry powder inhaler (DPI) was recently developed to deliver small doses of pure drug formulation. The device holds a multi-dose disk loaded with 12-64 metered doses that has been filled with the drug powder by a rotating fluidized bed powder dispensing device (51)(52). The disk is placed between the air tubule and compress chamber. The powder fluidizing mechanism is generated by two airflow designs generated from an exterior source of gas, which disperse the agglomerates of powder into fine particle fractions. The primary airflow creates a positive pressure inside the sealed chamber and passes through the drug pocket, carrying the powder along the air tubule. The second airflow creates additional shear flow above the drug pocket (53). *In vivo* studies have shown a high lung deposition of about 57% of the aerosolized dose.

1.3. NEW DEVELOPMENTS IN DPI FORMULATIONS AND DELIVERY

The efficacy of dry powder inhalation therapy is dependent not only on the design of the device, but also on a more efficient powder formulation with enhanced

aerosolization properties. Traditionally, most DPI formulations are either comprised of only micronized drug particles or a blend of drug and carrier particles prepared in dry powder form. As previously discussed, cohesion and adhesion interparticulate interaction forces play a significant role in the generation of the fine particle fraction, which is the fraction of the dose that is most likely delivered to the lungs with particle sizes between 1 and 5 μm (4). Interparticulate interaction forces are directly influenced by particle size distribution, particle density, morphology, surface roughness, surface energy, carrier material, carrier flow, and the presence of fine particle excipients amongst other properties (54)(55). Therefore, any modification of the physicochemical and/or surface properties of powders can significantly affect drug dispersion and DPI performance, and consequently enhance or worsen therapeutic outcome.

1.3.1. Particle surface modification

New technologies to improve carrier particle flowability and detachment from the drug have been developed through the modification of particle size, shape and/or surface properties to increase particle respirable fraction. Pollen-shaped hydroxyapatite (HA) carrier particles were synthesized with geometric diameters ranging from 21.1 to 48.6 μm and effective densities ranging from 0.21 to 0.41 g/cm^3 . Carr's compressibility index and angle of slide confirmed the better flowability of HA particles when compared to the conventional lactose carrier. The pollen-shaped surface of HA particles reduced the particle-particle, particle-surface interactions and aggregation that is usually seen with conventional lactose and increased the final FPF when compared to lactose (56)(57). Similarly, Shen et al. reported a new approach to fabricate inhalable spore-like particles. First, a high gravity controlled precipitation (HGCP) method was used to prepare hollow

spore-like nanoparticles. Then, a nanosuspension was prepared with these particles using insulin as a model drug, which was spray dried to generate particles with uniform size and controlled morphology. After aerosolization, the formulation presented higher FPF (80%) and smaller MMAD values at different dosages than Exubera[®] (33%)(58). The improved performance of this formulation may be directly related to the reduction of adhesive and cohesive forces and consequently, powder agglomeration. Mechano-fusion or mechanical dry coating has been widely investigated for the surface modification of dry powders (59)(60). It has been reported that powders mechano-fused with magnesium stearate yield modified physicochemical properties that significantly improved powder aerosolization. Such improvement in aerosolization was related to the surface modification of the particles and reduction of powder intrinsic cohesion (61). Improving the formulation by means of using another coating technology has been reported. A carrier-free l-leucine coated micronized salbutamol sulphate powder formulation was prepared by physical vapour deposition (PVD) (62). The study reports that the FPF of coated particles resulted in 47% of the aerosolized dose, which is 3-4 times higher than other micronized particles using the same DPI device (Easyhaler[®]). Furthermore, the emitted dose and fine particle fraction decreased with increasing surface roughness (63). The use of magnesium stearate and l-leucine as coating materials has also improved the aerosolization performance of salbutamol sulfate from mixtures with polycaprolactone microspheres. When the microspheres were coated with salbutamol sulfate, the *in vitro* powder performance was very low with FPF 0%. On the other hand, when the microspheres were precoated with magnesium stearate and l-leucine, the FPF values increased to about 11%. The presence of both materials reduced the strong adhesion between drug and carrier(64).

1.3.2. Particle Engineering Technology for Pulmonary Delivery

Advances in the field of particle engineering technology have enabled the development of dry powder inhaler systems with high drug aerosolization efficiency and more accurate pulmonary dosing. Particle engineering has enabled the development of carrier-free powder formulations, the delivery of nanoparticles encapsulated into biodegradable carriers, fixed-dose combination dosing among others. The aerodynamic diameter (d_a) dictates how the aerosol particles will deposit in the respiratory system. The aerodynamic diameter is defined as the diameter of a sphere of unit density with equivalent terminal settling velocity, while still travelling in the air, as the particle in study, as shown in Equation 1 (65)(9):

$$d_{aer} = d_g \sqrt{\frac{\rho}{x \cdot \rho_0}} \quad \text{Equation 1}$$

Where d_{aer} is the aerodynamic diameter, d_g the geometric diameter, ρ_p the particle density, ρ_0 the unit density (usually from water), X is the shape factor. Particles with aerodynamic diameter sizes between 1 and 5 μm are most likely able to deposit deep in the lungs (4). Researchers have used particle-engineering technologies to alter physicochemical properties of particles, such as reduction of particle size and/or density, modification of particle shape and surface characteristics, and creation of new polymorphism or amorphous forms in order to enhance particle aerodynamic properties increasing lung deposition and solubility.

Milling is one of the oldest and most common particle processing techniques used in the pharmaceutical industry. Different processes may be used such as dried or wet pearl-ball milling, jet milling or high-pressure homogenization. Only the most recent

advancements are reviewed in this chapter. The different milling processes will not be reviewed and the reader is referred to several articles (66)(67)(68).

1.3.2.1. Spray drying

Spray drying has been established as a standard technique to produce engineered dry powders. This technique has enabled the development of many types of particles and remains a well reported topic nowadays. In the spray drying process, a drug and excipient solution is sprayed through nozzles into a drying chamber where a hot air cyclone evaporates the solvent. The particles are carried out by the hot air and are collected in a cyclone vessel. Particle size and shape are determined by the formulation and process parameters such as the concentration of the feed solution and the size of the droplets, which is controlled by the atomization. Several atomizers are available for use with spray drying and the final choice depends on the desired particle properties. The most popular atomizers used by the industry are rotary atomizers, pressure nozzles, two-fluid nozzles and ultrasonic atomizers (69)(70). Folded shells and porous low-density particles are characteristics of powders produced by spray drying. The low-density characteristic allows the delivery of drug aerosol particles with large volumes, improved aerodynamic properties and enhanced lower respiratory tract deposition. The PulmoSpheres™ process produces particles that are formed through the atomization of a submicron oil-in-water emulsion stabilized by phospholipid, producing light porous particles with improved aerodynamic properties (71). In 2013, the US Food and Drug Administration (FDA) approved TOBI® Podhaler™ (Tobramycin Inhalation Powder or TIP) for the management of cystic fibrosis. Novartis TIP is prepared using the hollow PulmoSphere™ technology.

Recently, spray drying has been widely used for the pulmonary delivery of proteins such as insulin (72), peptides (73) and virus dry powder formulations. Bacteriophages, viruses that infect and kill bacteria, have successfully been produced by spray drying when used at low-temperature. Bacteriophages are spray dried with an inactive excipient such as lactose, trehalose or leucine that work as a bulk agent and protectant agent during the process (74). The spray dried phages exhibit enhanced aerosolization performance with minimal reduction in activity (75).

Spray dried polymeric microcarrier systems prepared with biodegradable and biocompatible polymers such as poly (DL-lactide-coglycolide acid) (PLGA) have enabled the development of several engineered particles loaded with drug micro and nanoparticles for lung delivery (76)(77). Spray drying has been shown to be a suitable process for processing nanosuspension of polymer-encapsulated nanoparticles such as small interfering RNA (siRNA), into a more stable dry powder formulation. The nanosuspension is spray dried with sugar excipients to enhance stability and aerodynamic properties (78)(79)(80).

Spray drying is suitable to produce polymorphic powders with different surface structures. Aerosolization properties of a novel excipient-free dry powder formulation of rifampicin were drastically improved by the polymorphic transformation of its crystalline form I structure into a flake-like crystal hydrate. Rifampicin dihydrate was prepared by the recrystallization of rifampicin in an anhydrous ethanol solution followed by the spray drying technique. It was reported that after DPI aerosolization, the formulation exhibited a low MMAD value of 2.2 μm and an high FPF (68%) which was due to the decreased tendency of powder agglomeration of the thin flaky structures (81). New polymorphic and amorphous forms were also produced for glycine(82), mannitol (83)(84) and trehalose (85).

Spray drying technology has been explored to produce cocrystals. Cocrystal formation of two or more molecules might be an alternative to overcome poor physicochemical properties of molecules such as solubility and stability (86). Recently, cocrystals of theophylline and urea were prepared by spray drying techniques for inhalation delivery. The use of different process parameters produced highly crystalline cocrystals with different particle properties, such as size and surface energy (87)(88).

1.3.2.2. *Spray-freezing methods*

The pharmaceutical industry and academia have been investigating the use of spray freeze-drying technology (SFD) for over a decade now. In SFD an aqueous drug solution is sprayed into a cold vapor over a cryogenic liquid to form droplets. The droplets are then lyophilized generating nano- and micronized powder with good flowability. (89)(89). The time required for the droplets to freeze and the air-liquid interface formed on the surface of the droplets may result in broad particle size distribution and protein aggregation (90). To overcome this problem a new technology was developed named spray freezing in liquid (SFL). In this process, the solution is sprayed directly into liquid nitrogen by an insufflated nozzle at a faster speed compared to SFD. This process produces amorphous powder with a high surface area and low-density exhibiting good flowability(91)(92).

Recently, the thermal ink-jet spray freeze-drying technique has also been studied for the preparation of engineered inhalable drug particles. This technique consists of the atomization of an aqueous drug solution by a modified printer (Hewlett-Packard) into liquid nitrogen followed by freeze-drying. Mueannoom et al. reported that porous particles could be attained when prepared from solutions of salbutamol sulphate with

concentrations up to 15% w/v after spray-freeze drying. However, particles prepared from 5% w/v salbutamol solutions presented the best strength and aerodynamic properties. When compared with the commercial micronized formulation, which contains the drug blended with lactose, the spray-freeze dried formulation produced lower percentage FPF values and MMAD above 5 μm .(93) Spherical, highly porous excipient-free particles were also a result of this technology(94). While this process seems to be suitable to prepare inhalable particles, further optimization studies are necessary to enhance powder dispersion and aerodynamic properties.

1.3.2.3. *Thin film Freezing*

The thin film freezing (TFF) technique has been used to enhance drug powder properties and make it suitable for pulmonary delivery. In this process, a drug solution containing a stabilizer excipient with high glass transition temperature is rapidly frozen onto a rotating cryogenic substrate in a drop wise manner. The frozen disks are collected and freeze dried for solvent removal (95). The engineered particles generated from this process form a low density brittle matrix of powder that are easily dispersed when aerosolized from a DPI device presenting great aerodynamic properties (96). The quench cooling process avoids nucleation and crystallization and usually generates amorphous particles. This technology may be an alternative to preparing formulations using thermally labile and poorly water-soluble actives. Recently, Beinborn and coworkers reported that particles prepared from a voriconazole solution without the stabilizing excipients using this technique were microstructures and presented crystalline low-density properties. On the other hand, powder prepared from a drug solution with stabilizing excipients resulted in nanostructured and amorphous low-density aggregate

particles (97). Additional *in vivo* studies in mice showed that the microstructure crystalline formulation presented a better aerodynamic performance than the nanostructured amorphous formulation, which had the highest lung deposition and slowest dissolution rate.(98)

1.3.2.4. Sono-crystallization

In this procedure, ultrasound waves are applied during the anti-solvent crystallization process of the drug solution to control the precipitation. The ultrasound induces nucleation and crystallization increasing reproducibility and particle size uniformity(99). Process variables such as high sonication amplitude, time, concentration and temperature influenced particle size distribution. Fine elongated crystal-shaped salbutamol sulphate particles were successfully prepared by sonocrystallization(100). The powder formulation prepared with these fine elongated crystal particles showed favored aerosolization performance when compared to the spray dried formulation and micronized formulation (101).

1.3.2.5. Fixed-Dose Drug Combination

Combination therapy has been used for many years for the management of COPD patients. The Global Initiative for chronic obstructive lung disease recommends the use of a combination of bronchodilators with different mechanisms and duration of action therapy to increase the degree of bronchodilation while decreasing side effects. The main objective is to improve quality of life by preventing disease progression, exacerbation and providing symptomatic relieve (102). The first dual combination therapy comprising an inhaled corticosteroid (ICS) and a long-acting beta agonist (LABA) together in one

inhaler was marketed a decade ago by GlaxosmithKline as Seretide/Advair Diskus[®] (103). Advair containing fluticasone propionate (ICS) with salmeterol xinafoate (LABA) proved more effective in reducing the effects of asthma and COPD when used in combination than when used individually(104). Additionally, it has been hypothesized that the success of Advair can be attributed to the synergistic action of fluticasone and sameterol, when both drugs co-deposit at the target cells (105). When dual therapy is not enough to control exacerbation and breathlessness, the use of a third component such as a long acting muscarinic antagonist is advised (103)(106).

Formulations of fixed-dose drug combinations must ensure powder homogeneity and delivery of a uniform dose to the patients particularly when the ratio of each drug present in the formulation significantly differs. In an attempt to reach these requirements and achieve co-deposition of drugs in the lungs, particle engineering has been used in place of a simple blending of micronized drugs with coarse carrier particles. Pearl Therapeutics (California, US) has used spray-drying process to prepare a triple fixed-dose combination formulation. First, an emulsion of DSPC (1,2-distearoyl-sn-glycero-3-phosphocholine) and anhydrous calcium chloride are spray dried to form porous microparticles. Subsequently, the porous particles and micronized glycopyrrolate, formoterol fumarate and mometasone furoate were co-suspended in 1,1,1,2-tetrafluoroethane (HFA 134a) propellant. The drug microparticles irreversibly adhere to the porous particle surfaces forming a stable suspension with equivalency in dose delivered for each drug (107). Another attempt to prepare a homogeneous formulation of a triple fixed-dose combination was reported by Price et al. The solution atomization and crystallization method (SAX[™]) is a sonocrystallization method that involves the formation of drug concentrated droplets followed by treatment with ultrasound waves to create cavitation bubbles for fast nucleation and crystallization. This process produced a

powder formulation with good dose delivery homogeneity and reasonable aerodynamic properties (108).

1.3.3. Nanoparticles and Biodegradable Polymeric Nanocarriers

Nanoparticles for pulmonary delivery have been extensively investigated. The use of nanoparticles may enhance lung deposition of drugs, increase drug dissolution velocity due to the decrease of particle size, as described by Noyes-Whitney equation. Moreover, pulmonary epithelial cell internalization of nanoparticles of less than 0.5 μm is at least 10-times more than particles in the micron size range between 1 and 3 μm (109). Additionally, nanoparticle systems may prolong drug release, enable cell specific targeted drug delivery or modified biological distribution of drugs(110). An efficient nanoparticulate drug delivery system should ensure high drug loading capacity in order to reduce the quantity of polymer load required for administration. However, lung delivery of nanoparticles is unviable due to the high particle-particle interactions and low lung deposition, a consequence of the low-inertia of the particles. Thus, to improve pulmonary deposition, nanoparticles are, in most cases, encapsulated in different excipients. Several technologies have been used to produce nanoparticles for pulmonary delivery, e.g. wet milling(111), spray drying(77), double emulsion followed by spray drying(112), nanoparticle flocculation(113), supercritical fluid extraction(114) and ionotropic generation followed by spray drying(115).

In order to increase therapeutic potency of salbutamol sulphate, a nanoparticle formulation was prepared using a liquid anti-solvent method followed by spray drying and blending with a lactose carrier. *In vitro* tests have shown a 13.9% increase in generation of respirable fraction of the nano-formulation when compared to the

micronized salbutamol blend formulation. *In vivo* studies in healthy human volunteers also reported enhanced total lung deposition by about 2-3 fold and lower oropharyngeal depositions ($25.3 \pm 4.5\%$) with nano-salbutamol formulation compared to the micronized formulation ($58.4 \pm 6.1\%$). confirming its suitability for inhalation delivery.(116)

Biodegradable polymeric nanocarriers prolong the retention time of drugs in the lungs and may reduce alveolar macrophage uptake.(117) Several polymers have been utilized for the development of pulmonary formulations. The polymers must be biodegradable and biocompatible to ensure patient safety and minimal toxicity(118). Poly(lactic-co-glycolic acid) (PLGA) has been extensively investigated as a nanocarrier for drug delivery systems intended for oral and intravenous administration(119)(120). Studies suggest that PLGA is safe for inhalation therapy(121). For example, Dailey et al. suggest that, at the same particle size, biodegradable PLGA nanocarriers may produce less inflammatory response *in vivo* than non-biodegradable polystyrene particles. However, the use of PLGA may not be recommended for therapies that require frequent dosing due to the slow rate of biodegradation (weeks to months) and the high potential for lung accumulation(117).

1.3.4. Controlled Release of Drugs for Lung Delivery

Dry powder formulations with controlled release profiles would allow for once daily delivery of drugs and greatly improve patient compliance. The development of a drug formulation with controlled release is difficult due to the efficient pulmonary clearance pathways, such as mucociliary and macrophage clearance, rapid absorption into the systemic circulation and safety of slow release excipients when delivered to the lungs(2). Therefore, an effective controlled release pulmonary drug delivery system has

yet to be developed. This field has been explored mainly for the delivery of antibiotics and insulin formulations. Nanoparticles have also been investigated for the sustained delivery of antibiotics to the lungs. The local treatment of pulmonary infections using inhaled antibiotics is highly promising once the infection is located in the endobronchial space(122). The efficacy of the treatment is dependent on drug targeting to the site of infection and on the concentration of drug deposited in the lungs. The high dose of antibiotics necessary to treat lung infections and kill the bacteria makes lung delivery of antibiotics more suitable than oral or intravenous delivery resulting in reduced side effects(122).

In order to prolong treatment activity, the use of polymeric materials such as (D,L)-poly(lactic glycolic acid) (PLGA), chitosan, poly(ethylene glycol) (PEGs) and different type of particles such as liposomes and small crystalline particles have been investigated(123). Dry powder rifampicin porous nanoparticle-aggregate particles (PNAP) were prepared by encapsulating rifampicin in PLGA nanoparticles using a solvent evaporation technique followed by spray drying. *In vitro* and *in vivo* data showed an initial burst in release of rifampicin in the first minutes followed by the release of the remaining drug in the next six to eight hours(124). Using an adaptation of spray drying, biodegradable poly(D,L-lactide-co-glycolide (PLGA) nano-spray dried particles were prepared and successfully achieved drug release of 8 hours(77). The incoming liquid feed is atomized by a vibrating-mesh actuated by a piezoelectric element into a drying chamber. The generated nano-sized particles are collected by an electrostatic particle collector due to the highly charged characteristics(125). This new spray-drying technology generates homogeneous solid nanoparticles with high formulation yields. Recently, a dry powder formulation using PLGA nanoparticles for tobramycin inhalation was investigated. Tobramycin was embedded in PLGA nanoparticles by a modified

emulsion/solvent diffusion technique. The tobramycin PLGA nanoparticles were then embedded in lactose microcarrier by spray drying improving powder flow. Afterwards, hydrophilic polymers, e.g. alginate and chitosan were added to the nanoparticles enhancing drug entrapment within nanoparticles with release up to a month and improving size and surface properties of final particles, respectively(76). Voriconazole-containing PLGA porous nanoparticles (VNPs) were prepared using a multiple-emulsification technique. The porous particles contained 30% (w/w) drug loading, enhanced aerodynamic properties compared to the non-porous particles. When administered to rodents, 20% of porous VNPs are released in the initial 2 hours by controlled release for 15 days(126). As a side note, the use of inhaled mannitol has been investigated as an excipient in co-spray-dried formulations with antibiotics. Mannitol may increase the osmotic pressure of the lung fluids, reducing mucous viscosity and increasing mucus clearance of patients with pulmonary infection.(127) Moreover, combination of co-spray dried antibiotics formulations have shown increased therapeutic effects and stability compared to single spray dried formulations.(128)

Swellable microparticles used as drug carriers for controlled pulmonary delivery have also been reported recently(129). Smyth et al. developed a novel biodegradable carrier for pulmonary sustained drug delivery. Poly(ethylene glycol) grafted onto N-phthaloyl chitosan (PEG-g-NPHCs) was synthesized and self-assembled into nanoparticles and encapsulated in swellable sodium alginate hydrogel microspheres via spray drying and ionotropic crosslinking in an aqueous solution. *In vitro* studies showed that the prepared microspheres had aerodynamic diameters between 1.02 and 2.63 μm and an enhanced FPF of 31.52%. Additionally, an *in vitro* sustained release profile was confirmed by the microparticle swelling that started after less than 2 minutes and enzymatic degradation that occurred within the first 2 hours(115). To enhance

aerodynamic properties and control drug release, highly porous large PLGA microparticles was developed. PLGA microparticles were produced by a double-emulsion method and ammonium bicarbonate, an effervescent pore forming agent, and added to the internal aqueous phase. Ammonium bicarbonate decomposes into ammonia and carbon dioxide creating the porous structures in the microparticles. The large porous microparticles (10 – 20 μm in diameter) presented high encapsulation efficiency of doxorubicin (~100%), good aerodynamic properties with FPF of ~ 32% and ability to avoid phagocytosis by macrophages(130).

Even though the development of a sustained drug release profile has been successfully reported, further studies are necessary to demonstrate the drug release profile *in vivo* and to evaluate the biologic compatibility of the new delivery system.

1.3.5. Macromolecules for Pulmonary Delivery

Pulmonary delivery of dry powder formulations to treat local and systemic diseases of patients is convenient since invasive procedures and supervision by a health provider are not required. Pulmonary delivery may be a good alternative as a non-invasive route of administration of peptides and proteins, due to their vulnerability to intestinal enzymes, first pass metabolism and poor membrane permeability(131). The biologic activity of a protein is highly dependent on its secondary, tertiary and quaternary structures, which are held together by weak physical interactions such as electrostatic and Van der Waals forces. Proteins may easily undergo conformational changes and lose biological activity. Therefore, the formulation of proteins for therapeutic use with good physical and chemical stability may be challenging. Exubera[®] (Pfizer, New York, NY/Nektar Therapeutics, San Carlos, CA) was the first dry powder inhaled insulin

product approved by the Food and Drug Administration (FDA) in 2006. However, one year later (2007), the product was phased out due to low acceptance by patients and health care providers, and a reported increase incidence of lung cancer in ex-smoker patients(26). AFREZZA[®] (MannKind Corporation, Valencia, CA, USA), currently under FDA review for approval, is a drug-device product consisting of pre-metered ultra rapid human insulin that will be used as an inhalation treatment for diabetes mellitus type 1 and type 2. (132) AFREZZA[®] uses Technosphere[®] technology to deliver insulin as an inhalation powder. Technosphere[®] is a drug carrier product formed by fumaryl diketopiperazine (FDKP), which can self-assemble into microparticles with size diameters of 2 to 5 μm and dried by lyophilization. The porous microparticles formed have large surface areas in which peptides and proteins can be later adsorbed to. The formulation was prepared to be delivered using the MedTone[®] DPI (MannKind Corporation).(45)

Al Qadi et al. developed a microencapsulated insulin-loaded chitosan nanoparticles by ionotropic gelation for lung delivery. The nanoparticles were co-spray dried afterwards with mannitol to enhance aerodynamic properties. *In vivo* studies in rats and the monitoring of plasmatic glucose levels after dosing have shown that microencapsulated insulin-loaded chitosan nanoparticles induced a more pronounced and prolonged hypoglycemic effect compared to the controls(72). Spray drying and spray freeze-drying are suitable processes to prepare dried protein formulations. However, in both processes, the protein formulations are subject to cold or hot shear stresses, which may degrade the product. Recently, enhanced stability of protein formulations when glass forming agents, such as sugars, are included has been reported.(133)

Insulin dry powder formulation has also been developed as large porous PLGA particles, loaded with insulin, and prepared by a double emulsion technique using

hydroxypropyl- β -cyclodextrin (HP β CD). HP β CD was used as an osmotic agent to create an osmotic pressure between the internal and the external aqueous phases of the emulsion, which does not modify protein integrity(134). The large porous particles successfully presented good aerodynamic properties and prolonged hypoglycemic effect(135).

Dry powder pulmonary vaccine delivery has also gained attention lately. However, more studies are required showing formulation improvements, clinical efficacy and safety before the first formulation gets approved and becomes commercially available on the market(136). Recent studies have shown some promising results in this field. ISCOMATRIXTM, a saponin-based adjuvant, has been successfully used for pulmonary delivery.(137)(138) The deep lung administration of the vaccine formulation was able to induce both a mucosal and systemic immune response.(139) Antigens, such as, polysaccharides, proteins and peptides are usually unstable in liquid formulations and achieve low absorption and uptake across epithelial barriers. Therefore, antigens and proteins should be formulated with excipients that protect them from degradation and enhance absorption rate. A protein formulation of spray-dried IgG1 using mannitol as the stabilizer agent achieved high levels of stability. Additionally, a 20% concentration of mannitol allowed for the best stabilizing capability. The study also reported that it was necessary to reduce the solids content of the formulation to 2.5% to improve aerodynamic properties.(140) Chitosan (a cationic polysaccharide) has also been shown to exhibit absorption enhancement and immunoadjuvant properties when formulated with antigens, peptides and proteins(141). Calcitonin has been formulated for pulmonary delivery by an ionic gelation technique with a derivative of glycol chitosan named glycol chitosan thioglycolic acid (GCS-TGA). The calcitonin-loaded GCS-TGA demonstrated high permeation characteristics and a prolonged and pronounced hypocalcemic effect(142).

Small interfering RNAs (siRNAs) are an efficient therapy against viral infections and respiratory disorders, such as cystic fibrosis and respiratory syncytial virus. Because siRNAs are quickly degraded by nucleases, local administration via pulmonary delivery may be suitable. Therefore, formulations for lung delivery should protect siRNAs from degradation by nucleases, enhance intracellular uptake, prolong local deposition by avoidance of macrophage clearance and present non-toxicity (143). siRNA has been successfully formulated with nanocarriers using chitosan(144), oligofectamine (145), and PEGylated polyethylenimine (PEG-PEI)(146) for pulmonary and intranasal delivery. In order to reach the lungs, siRNA was loaded into PLGA nanoparticles using a spray drying process. To enhance aerosolization properties, the nanoparticles were further dispersed in different sugar excipients like trehalose, lactose and mannitol. The optimization of the spray drying process generated microparticles with up to 50% (w/w) nanoparticle inclusion with suitable aerodynamic properties and minimal degradation of the siRNA(78).

1.4.CHARACTERIZATION METHODS OF DRY POWDER INHALER FORMULATIONS

The United State Pharmacopeia (USP) General Chapter <601> Aerosols, Nasal Sprays, Metered-Dose Inhalers, and Dry Powder Inhalers and the United States Food and Drug Administration draft guidance – Metered Dose Inhaler (MDI) and Dry Powder Inhaler (DPI) Drug Products require dry powder inhalers to meet specific standard test methods:

- Delivered-Dose Uniformity
- Aerodynamic Size Distribution

Delivered-Dose Uniformity: The USP describes standard test methods and apparatus specifications, which should be used to determine the values for both methods (147)(148). The first test determines the uniformity of the drug delivered per dose. At least 9 out of the 10 actuated doses should fall between 75% to 125% of the specific targeted dose. The USP apparatus is used for testing at an airflow rate, which will generate a pressure drop inside the device of 4 kPa. The test flow duration, in seconds, is determined by:

$$T = 240/Q_{out}$$

where Q_{out} is the volume of air passing through the air flowmeter. The test should be performed for sufficient time so that 4 liters of air are withdrawn through the device at the test flow rate Q_{out} . Dose consistency with low variability rates should be achieved besides variation of patient's inspiratory flow rate (149).

Aerodynamic Particle Size Distribution: Particle size distribution is one of the most important pharmaceutical characteristics of DPIs. More specifically, the aerodynamic particle size distribution (APSD) of the aerosol leaving the inhaler is used to determine its performance. The USP recommends the use of a cascade impactor (CI) to assess the APSD of the emitted dose of inhalation formulations. The CI fractionates and collects drug particles by aerodynamic diameter through a series of collection plates (stages) enabling the formulator to measure the aerodynamic particle size distribution of the drug and to quantify the mass of drug deposited in each stage (147). The USP describes several types of apparatus used to measure APSD for inhalation aerosols, including multi-stage liquid impinge (MSLI), Anderson cascade impactor and the most recently introduced, next generation cascade impactor (NGI). Each has its own design specifications and different nominal stage cut-off diameters and therefore, APSD data

from different impactors should not be compared (150). Aerodynamic particle size distribution and the mass balance (drug deposited throughout the apparatus, inhaler and accessories) should be reported. Moreover, when a log-normal distribution is obtained, the mass median aerodynamic diameter (MMAD) and the geometric standard deviation (GSD) should be determined (147). Many factors may affect accuracy and robustness of the cascade impaction measurement including particle bounce, re-entrainment and wall losses (151). The use of a greasy material to coat the collection plates has been suggested to reduce variability of cascade impactor measurements (152).

The laser diffraction technique has been widely used for the measuring, at real time, of particle size distribution aerosolized from DPI. The test is relatively easy to perform and can quickly generate and process the data results (153). However, the technique measures the geometric instead of aerodynamic size of the particles and the effect of particle non-sphericity is not taken into consideration (154). Many studies have compared the laser diffraction measurements of inhalation formulations with the data obtained from cascade impactors (155). Overall, the studies report that laser diffraction is a reliable method to use for studying particle size distribution of dry powder aerosol formulations (156).

Since efficient dry powder inhalation therapy depends on both device and formulation aerosolization ability, complete knowledge and understanding of the physicochemical properties of the particles and aerodynamic behavior are essential for the development of an ideal DPI formulation (157).

Scanning Electron Microscopy: Microscopic evaluation of powders is commonly used to characterize particle morphology, size and shape of DPI formulations. In addition, it can also be used to detect the presence of large particles and agglomerates of drug and carriers due to its enhanced resolution (158). Many studies have reported the

use of Scanning Electron Microscopy (SEM) technique to investigate the properties of engineered particles produced by a variety of techniques such as spray-drying (159) and spray-freeze drying (160). Characterization of lactose surface roughness, morphology and size have also been extensively studied (161)(162)(163).

Atomic Force Microscopy (AFM): AFM is a useful tool for the investigation of the adhesive properties of dry powder formulations using pico-newton resolution, which measures interactions between particles in a variety of controlled environmental conditions (164). It provides information on surface reactivity, surface energy and on interaction forces involved in binary drug systems such as carriers and drugs used in the process of DPI development (165)(166).

Inverse Gas Chromatography (IGC): This technique is useful for the investigation of particle surface energy and the adhesive properties between dry powder particles. In this method, inert polar and nonpolar gases are eluted in a constant flow through a column packed with the solid analyte. Interactions between the gaseous probe molecules and the stationary phase determines the retention volume, which is used to determine the free energy of adsorption and other thermodynamic surface parameters (8). IGC analysis can be performed under different environmental conditions and do not require pre-treatment of the particles, which make it a suitable method for powder surface characterization (167)(168)(169). Accordingly, specific surface areas of carrier and drug particles may be determined via nitrogen adsorption using the Brunauer, Emmett, and Teller (BET) gas adsorption method (60)(7).

Dissolution Method: There is no standardized test method to characterize the dissolution properties of the emitted dose of inhalation formulations. Although a few dissolution methods have been developed in the last decade, none have yet been approved. Dry powder formulation has been added directly to an apparatus II dissolution

tester (paddle method) as reported by Asada et al (170). In another study, the powdered formulation was wrapped up by glass fiber filters and placed in a basket dissolution apparatus to prevent powder from escaping to the medium (171). Recently, Yoen-Ju et al. developed a membrane-containing cassette that is connected to the collection plates of the NGI. After aerosolization of the formulation in the cascade impactor, a polycarbonate membrane is placed on the top of the cassettes which is then placed in the dissolution vessels of a commercially available dissolution apparatus containing 100 mL of simulated lung fluid (SLF) and modified simulated lung fluid (mSLF) (172).

1.5.CONCLUSION

Recent advancements in DPI systems have significantly contributed to the improvement of DPI therapy efficacy by enhancing formulation aerosolization and drug bioavailability. Additionally, DPIs have been shown to be an excellent system to deliver drugs such as antibiotics. Particle engineering technologies have played an important role in the development of optimized powder formulations by enhancing stability properties. Different techniques have also shown to enhance particle physicochemical properties and thus, formulation dispersion. Moreover, engineered particle formulations usually require reduced amounts of excipient/carriers that may induce adverse events. Most of the new DPI technologies that are commercially approved or are under investigation are passive devices even though extensive research still continues for active device development. Although several novel DPI-formulation systems have been recently approved or are under clinical trial investigations, more improvements are still required in order to increase patient compliance and therapy efficiency as well as reduce adverse therapy events and production costs.

1.6. REFERENCES

1. Islam N, Cleary MJ. Developing an efficient and reliable dry powder inhaler for pulmonary drug delivery – A review for multidisciplinary researchers. *Medical Engineering & Physics*. 2012 May;34(4):409–27.
2. Smyth HDC, Hickey AJ. Carriers in Drug Powder Delivery: Implications for Inhalation System Design. *American Journal of Drug Delivery*. 2005;3(2):117–32.
3. Lavorini F, Magnan A, Dubus JC, Voshaar T, Corbetta L, Broeders M, et al. Effect of incorrect use of dry powder inhalers on management of patients with asthma and COPD. *Respir Med*. 2008 Apr;102(4):593–604.
4. Carvalho TC, Peters JI, Williams III RO. Influence of particle size on regional lung deposition – What evidence is there? *International Journal of Pharmaceutics*. 2011 Mar 15;406(1–2):1–10.
5. De Boer AH, Hagedoorn P, Gjaltema D, Goede J, Frijlink HW. Air classifier technology (ACT) in dry powder inhalation: Part 1. Introduction of a novel force distribution concept (FDC) explaining the performance of a basic air classifier on adhesive mixtures. *International Journal of Pharmaceutics*. 2003 Jul 24;260(2):187–200.
6. De Boer AH, Chan HK, Price R. A critical view on lactose-based drug formulation and device studies for dry powder inhalation: Which are relevant and what interactions to expect? *Advanced Drug Delivery Reviews*. 2012 Mar 15;64(3):257–74.
7. Donovan MJ, Kim SH, Raman V, Smyth HD. Dry powder inhaler device influence on carrier particle performance. *J Pharm Sci*. 2012 Mar;101(3):1097–107.
8. Hickey AJ, Mansour HM, Telko MJ, Xu Z, Smyth HD., Mulder T, et al. Physical characterization of component particles included in dry powder inhalers. I.

Strategy review and static characteristics. *Journal of pharmaceutical sciences*. 2007;96(5):1282–301.

9. Chow AHL, Tong HHY, Chattopadhyay P, Shekunov BY. Particle engineering for pulmonary drug delivery. *Pharm Res*. 2007 Mar;24(3):411–37.

10. Thalberg K, Berg E, Fransson M. Modeling dispersion of dry powders for inhalation. The concepts of total fines, cohesive energy and interaction parameters. *Int J Pharm*. 2012 May 10;427(2):224–33.

11. NEWMAN SP, BUSSE WW. Evolution of dry powder inhaler design, formulation, and performance. *Respiratory Medicine*. 2002 May;96(5):293–304.

12. De Koning J., van der Mark T., Coenegracht PM., Tromp TF., Frijlink H. Effect of an external resistance to airflow on the inspiratory flow curve. *International Journal of Pharmaceutics*. 2002 Mar 2;234(1–2):257–66.

13. Daniher DI, Zhu J. Dry powder platform for pulmonary drug delivery. *Particuology*. 2008 Aug;6(4):225–38.

14. Friebel C, Steckel H. Single-use disposable dry powder inhalers for pulmonary drug delivery. *Expert Opin Drug Deliv*. 2010 Dec;7(12):1359–72.

15. Son Y-J, McConville JT. Advancements in Dry Powder Delivery to the Lung. *Drug Development and Industrial Pharmacy*. 2008 Jan;34(9):948–59.

16. Wetterlin K. Turbuhaler - a New Powder Inhaler for Administration of Drugs to the Airways. *Pharm Res*. 1988 Aug;5(8):506–8.

17. Thibert R, Parry-Billings M, Shott M. Clickhaler® dry powder inhaler: focussed in vitro proof of principle evaluation of a new chemical entity for asthma. *International Journal of Pharmaceutics*. 2002 Jun 4;239(1–2):149–56.

18. Parry-Billings M, Birrell C, Oldham L, O'Callaghan C. Inspiratory flow rate through a dry powder inhaler (Clickhaler (R)) in children with asthma. *Pediatr Pulmonol.* 2003 Mar;35(3):220–6.
19. Tarsin WY, Pearson SB, Assi KH, Chrystyn H. Emitted dose estimates from Seretide® Diskus® and Symbicort® Turbuhaler® following inhalation by severe asthmatics. *International Journal of Pharmaceutics.* 2006 Jun 19;316(1–2):131–7.
20. Al-Showair RAM, Tarsin WY, Assi KH, Pearson SB, Chrystyn H. Can all patients with COPD use the correct inhalation flow with all inhalers and does training help? *Respiratory Medicine.* 2007 Nov;101(11):2395–401.
21. Cegla UH. Pressure and inspiratory flow characteristics of dry powder inhalers. *Respiratory Medicine.* 2004 Apr;98, Supplement 1:S22–S28.
22. De Boer AH, Hagedoorn P, Gjaltema D, Goede J, Kussendrager KD, Frijlink HW. Air classifier technology (ACT) in dry powder inhalation Part 2. The effect of lactose carrier surface properties on the drug-to-carrier interaction in adhesive mixtures for inhalation. *International Journal of Pharmaceutics.* 2003 Jul 24;260(2):201–16.
23. De Boer AH, Hagedoorn P, Gjaltema D, Goede J, Frijlink HW. Air classifier technology (ACT) in dry powder inhalation - Part 3. Design and development of an air classifier family for the Novolizer (R) multi-dose dry powder inhaler. *Int J Pharm.* 2006 Mar 9;310(1-2):72–80.
24. Kohler D. The Novolizer®: overcoming inherent problems of dry powder inhalers. *Respiratory Medicine.* 2004 Apr;98, Supplement 1:S17–S21.
25. Crowder T, Hickey A. Powder specific active dispersion for generation of pharmaceutical aerosols. *International Journal of Pharmaceutics.* 2006 Dec 11;327(1–2):65–72.

26. Harper NJ, Gray S, De Groot J, Parker JM, Sadrzadeh N, Schuler C, et al. The design and performance of the Exubera((R)) pulmonary insulin delivery system. *Diabetes Technol Ther.* 2007 Jun;9:S16–S27.
27. Morton DAV, Staniforth JN. Systemic pulmonary delivery: Success through integrated formulation and device development. 2006; Available from: <http://www.ondrugdelivery.com/publications/pulmonary.pdf>
28. Brown BA-S, Rasmussen JA, Becker DP, Friend DR. A piezo-electronic inhaler for local & systemic applications. *Drug Delivery Technol.* 2004;4(8):90–3.
29. Islam N, Gladki E. Dry powder inhalers (DPIs)—A review of device reliability and innovation. *International Journal of Pharmaceutics.* 2008 Aug 6;360(1–2):1–11.
30. Coates MS, Chan HK, Fletcher DF, Chiou H. Influence of mouthpiece geometry on the aerosol delivery performance of a dry powder inhaler. *Pharmaceutical research.* 2007;24(8):1450–6.
31. Coates MS, Chan H-K, Fletcher DF, Raper JA. Influence of Air Flow on the Performance of a Dry Powder Inhaler Using Computational and Experimental Analyses. *Pharmaceutical Research.* 2005 Aug 24;22(9):1445–53.
32. Chrystyn H, Niederlaender C. The Genuair (R) inhaler: a novel, multidose dry powder inhaler. *Int J Clin Pract.* 2012 Mar;66(3):309–17.
33. Newman SP, Sutton DJ, Segarra R, Lamarca R, de Miquel G. Lung Deposition of Aclidinium Bromide from Genuair (R), a Multidose Dry Powder Inhaler. *Respiration.* 2009;78(3):322–8.
34. Magnussen H, Watz H, Zimmermann I, Macht S, Greguletz R, Falques M, et al. Peak inspiratory flow through the Genuair® inhaler in patients with moderate or severe COPD. *Respiratory Medicine.* 2009 Dec;103(12):1832–7.

35. Brambilla G, Cocconi D, Armani A, Smith S, Lye EL, Burge S. Designing a Novel Powder Inhaler: The NEXT DPI. *Respiratory Drug Delivery*; 2006. p. 553–5.
36. Rave K, Potocka E, Boss AH, Marino M, Costello D, Chen R. Pharmacokinetics and linear exposure of AFRESA™ compared with the subcutaneous injection of regular human insulin. *Diabetes, Obesity and Metabolism*. 2009;11(7):715–20.
37. Steiner SS, Poole TA, Fog PB, Pohl R, Crick M, Feldstein R. United States Patent: 7464706 - Unit dose cartridge and dry powder inhaler [Internet]. 7464706, 2008 [cited 2012 Jul 5]. Available from: http://patft.uspto.gov/netacgi/nph-Parser?Sect1=PTO1&Sect2=HITOFF&d=PALL&p=1&u=%2Fnetahhtml%2FPTO%2Fsrc_hnum.htm&r=1&f=G&l=50&s1=7,464,706.PN.&OS=PN/7,464,706&RS=PN/7,464,706
38. Needham M, Fradley G, Cocks A. Investigating the Efficiency of the 3M Conix™ of Reverse Cyclone Technology for DPI Drug Delivery. 2010. p. 369–72.
39. Kelley J, Stein S, Robison T, Wang Z, Bohlke A, Simons J, et al. Comparative Performance of the High Efficiency 3M™ Taper Dry Powder Inhaler Device. 2011. p. 247–52.
40. Stein S, Robison T, Wang Z, Hodson D, Alband T. The 3M Taper Dry Powder Inhaler Device. *Respiratory Drug Delivery*; 2010. p. 377–80.
41. Pavkov R, Mueller S, Fiebich K, Singh D, Stowasser F, Pignatelli G, et al. Characteristics of a capsule based dry powder inhaler for the delivery of indacaterol. *Current Medical Research and Opinion*. 2010 Nov;26(11):2527–33.
42. Pavkov R, Singh D, Reitveld I. Concept1 (a New Single Dose Dry Powder Inhaler) Peak Inspiratory Flow Rate Study with COPD Patients. 2008. p. 683–6.

43. Chapman KR, Rennard SI, Dogra A, Owen R, Lassen C, Kramer B. Long-term Safety and Efficacy of Indacaterol, a Long-Acting β 2-Agonist, in Subjects With COPD A Randomized, Placebo-Controlled Study. *Chest*. 2011 Jul 1;140(1):68–75.
44. Chapman KR, Fogarty CM, Peckitt C, Lassen C, Jadayel D, Dederichs J, et al. Delivery characteristics and patients' handling of two single-dose dry-powder inhalers used in COPD. *Int J Chron Obstruct Pulmon Dis*. 2011;6:353–63.
45. Richardson PC, Boss AH. Technosphere((R)) Insulin technology. *Diabetes Technol Ther*. 2007 Jun;9:S65–S72.
46. Kling J. Dreamboat sinks prospects for fast approval of inhaled insulin. *Nature Biotechnology*. 2011 Mar;29(3):175–6.
47. Shah S, Smutney C, Saviano V, Kinsey S, Ridley D. A Dry Powder Delivery Technology Embodied in a Single Use Re-useable and Single Use Disposable Format. 2012. p. 577–80.
48. Kinsey PS, Adamo B, Smutney CC, Polidoro JM, others. Dry powder inhaler. D597,657, 2009.
49. Chang YS, Park MJ, Bai C, Cai B, Kartasasmita C, Margono BP, et al. Comparative study of patients in correct usage of and preference for the Swinghaler and Turbuhaler multidose inhalers. *J Asthma*. 2012;49(7):750–6.
50. Lertchanaruengrith P, Rattanasukol P, Suratannon N, Voraphani N, Chatchatee P, Ngamphaiboon J. The Ability and Predictive Factors of Preschool Children to Use Swinghaler Device. *Journal of Allergy and Clinical Immunology*. 2012 Feb;129(2, Supplement):AB74.
51. Zhang X, Ma Y, Zhang L, Zhu J, Jin F. The development of a novel dry powder inhaler. *Int J Pharm*. 2012 Jul 15;431(1-2):45–52.

52. Chan H-K, Young PM, Traini D, Coates M. Dry powder inhalers: challenges and goals for next generation therapies. *Pharm Technol Eur.* 2007;19(4):19–24.
53. Zhu J, Wen J, Ma Y, Zhang H. Dry powder inhaler [Internet]. 8037880, 2011 [cited 2012 Jul 6]. Available from: <http://www.google.com/patents?id=GSn5AQAAEBAJ>
54. Le VNP, Thi THH, Robins E, Flament MP. Dry Powder Inhalers: Study of the Parameters Influencing Adhesion and Dispersion of Fluticasone Propionate. *AAPS PharmSciTech.* 2012 Jun;13(2):477–84.
55. Adi S, Adi H, Tang P, Traini D, Chan H, Young PM. Micro-particle corrugation, adhesion and inhalation aerosol efficiency. *European journal of pharmaceutical sciences.* 2008;35(1-2):12–8.
56. Hassan MS, Lau R. Inhalation performance of pollen-shape carrier in dry powder formulation with different drug mixing ratios: Comparison with lactose carrier. *Int J Pharm.* 2010 Feb 15;386(1-2):6–14.
57. Hassan MS, Lau R. Feasibility Study of Pollen-Shape Drug Carriers in Dry Powder Inhalation. *J Pharm Sci.* 2010 Mar;99(3):1309–21.
58. Shen Z-G, Chen W-H, Jugade N, Gao L-Y, Glover W, Shen J-Y, et al. Fabrication of inhalable spore like pharmaceutical particles for deep lung deposition. *Int J Pharm.* 2012 Jul 1;430(1-2):98–103.
59. Bose S, Bogner RH. Solventless pharmaceutical coating processes: a review. *Pharm Dev Technol.* 2007;12(2):115–31.
60. Zhou Q (Tony), Denman JA, Gengenbach T, Das S, Qu L, Zhang H, et al. Characterization of the Surface Properties of a Model Pharmaceutical Fine Powder

Modified with a Pharmaceutical Lubricant to Improve Flow via a Mechanical Dry Coating Approach. *J Pharm Sci.* 2011 Aug;100(8):3421–30.

61. Zhou QT, Qu L, Larson I, Stewart PJ, Morton DAV. Improving aerosolization of drug powders by reducing powder intrinsic cohesion via a mechanical dry coating approach. *Int J Pharm.* 2010 Jul 15;394(1-2):50–9.

62. Raula J, Thielmann F, Naderi M, Lehto V-P, Kauppinen EI. Investigations on particle surface characteristics vs. dispersion behaviour of l-leucine coated carrier-free inhalable powders. *International Journal of Pharmaceutics.* 2010 Jan 29;385(1–2):79–85.

63. Raula J, Lahde A, Kauppinen EI. Aerosolization behavior of carrier-free L-leucine coated salbutamol sulphate powders. *Int J Pharm.* 2009 Jan 5;365(1-2):18–25.

64. Tuli RA, Dargaville TR, George GA, Islam N. Polycaprolactone microspheres as carriers for dry powder inhalers: Effect of surface coating on aerosolization of salbutamol sulfate. *J Pharm Sci.* 2012 Feb;101(2):733–45.

65. De Boer AH, Gjaltema D, Hagedoorn P, Frijlink HW. Characterization of inhalation aerosols: a critical evaluation of cascade impactor analysis and laser diffraction technique. *Int J Pharm.* 2002 Dec 5;249(1-2):219–31.

66. Rasenack N, Muller BW. Micron-size drug particles: Common and novel micronization techniques. *Pharmaceutical Development and Technology.* 2004;9(1):1–13.

67. Nakach M, Authelin J-R, Chamayou A, Dodds J. Comparison of various milling technologies for grinding pharmaceutical powders. *International Journal of Mineral Processing.* 2004 Dec 10;74, Supplement:S173–S181.

68. Bentham A., Kwan C., Boerefijn R, Ghadiri M. Fluidised-bed jet milling of pharmaceutical powders. *Powder Technology.* 2004 Mar 30;141(3):233–8.

69. Vehring R. Pharmaceutical Particle Engineering via Spray Drying. *Pharm Res.* 2008 May;25(5):999–1022.
70. Bittner B, Kissel T. Ultrasonic atomization for spray drying: a versatile technique for the preparation of protein loaded biodegradable microspheres. *J Microencapsul.* 1999 Jun;16(3):325–41.
71. Geller DE, Weers J, Heuerding S. Development of an Inhaled Dry-Powder Formulation of Tobramycin Using PulmoSphere™ Technology. *J Aerosol Med Pulm Drug Deliv.* 2011 Aug;24(4):175–82.
72. Al-Qadi S, Grenha A, Carrión-Recio D, Seijo B, Remuñán-López C. Microencapsulated chitosan nanoparticles for pulmonary protein delivery: In vivo evaluation of insulin-loaded formulations. *Journal of Controlled Release.* 2012 Feb 10;157(3):383–90.
73. Li H-Y, Seville PC, Williamson IJ, Birchall JC. The use of amino acids to enhance the aerosolisation of spray-dried powders for pulmonary gene therapy. *The Journal of Gene Medicine.* 2005;7(3):343–53.
74. Vandenheuvel D, Singh A, Vandersteegen K, Klumpp J, Lavigne R, Van den Mooter G. Feasibility of spray drying bacteriophages into respirable powders to combat pulmonary bacterial infections. *Eur J Pharm Biopharm.* 2013 Aug;84(3):578–82.
75. Matinkhoo S, Lynch KH, Dennis JJ, Finlay WH, Vehring R. Spray-dried respirable powders containing bacteriophages for the treatment of pulmonary infections. *J Pharm Sci.* 2011 Dec;100(12):5197–205.
76. Ungaro F, d' Angelo I, Coletta C, d' Emmanuele di Villa Bianca R, Sorrentino R, Perfetto B, et al. Dry powders based on PLGA nanoparticles for pulmonary delivery of antibiotics: Modulation of encapsulation efficiency, release rate and lung

deposition pattern by hydrophilic polymers. *Journal of Controlled Release*. 2012 Jan 10;157(1):149–59.

77. Beck-Broichsitter M, Schweiger C, Schmehl T, Gessler T, Seeger W, Kissel T. Characterization of novel spray-dried polymeric particles for controlled pulmonary drug delivery. *J Control Release*. 2012 Mar 10;158(2):329–35.

78. Jensen DMK, Cun D, Maltesen MJ, Frokjaer S, Nielsen HM, Foged C. Spray drying of siRNA-containing PLGA nanoparticles intended for inhalation. *Journal of Controlled Release*. 2010 Feb 25;142(1):138–45.

79. Jensen DK, Jensen LB, Koocheki S, Bengtson L, Cun D, Nielsen HM, et al. Design of an inhalable dry powder formulation of DOTAP-modified PLGA nanoparticles loaded with siRNA. *Journal of Controlled Release*. 2012 Jan 10;157(1):141–8.

80. Cun D, Jensen DK, Maltesen MJ, Bunker M, Whiteside P, Scurr D, et al. High loading efficiency and sustained release of siRNA encapsulated in PLGA nanoparticles: Quality by design optimization and characterization. *European Journal of Pharmaceutics and Biopharmaceutics*. 2011 Jan;77(1):26–35.

81. Son Y-J, McConville JT. A new respirable form of rifampicin. *Eur J Pharm Biopharm*. 2011 Aug;78(3):366–76.

82. Yu L, Ng K. Glycine crystallization during spray drying: the pH effect on salt and polymorphic forms. *J Pharm Sci*. 2002 Nov;91(11):2367–75.

83. Grohganz H, Lee Y-Y, Rantanen J, Yang M. The influence of lysozyme on mannitol polymorphism in freeze-dried and spray-dried formulations depends on the selection of the drying process. *International Journal of Pharmaceutics*. 2013 Apr 15;447(1–2):224–30.

84. Duret C, Wauthoz N, Sebti T, Vanderbist F, Amighi K. New Respirable and Fast Dissolving Itraconazole Dry Powder Composition for the Treatment of Invasive Pulmonary Aspergillosis. *Pharm Res.* 2012 Oct 1;29(10):2845–59.
85. Sou T, Kaminskas LM, Nguyen T-H, Carlberg R, McIntosh MP, Morton DAV. The effect of amino acid excipients on morphology and solid-state properties of multi-component spray-dried formulations for pulmonary delivery of biomacromolecules. *European Journal of Pharmaceutics and Biopharmaceutics.* 2013 Feb;83(2):234–43.
86. Vishweshwar P, McMahon JA, Bis JA, Zaworotko MJ. Pharmaceutical co-crystals. *J Pharm Sci.* 2006 Mar;95(3):499–516.
87. Alhalaweh A, Kaialy W, Buckton G, Gill H, Nokhodchi A, Velaga SP. Theophylline Cocrystals Prepared by Spray Drying: Physicochemical Properties and Aerosolization Performance. *AAPS PharmSciTech.* 2013 Jan 8;14(1):265–76.
88. Alhalaweh A, Velaga SP. Formation of Cocrystals from Stoichiometric Solutions of Incongruently Saturating Systems by Spray Drying. *Cryst Growth Des.* 2010 Aug;10(8):3302–5.
89. Cheow WS, Ng MLL, Kho K, Hadinoto K. Spray-freeze-drying production of thermally sensitive polymeric nanoparticle aggregates for inhaled drug delivery: Effect of freeze-drying adjuvants. *International Journal of Pharmaceutics.* 2011 Feb 14;404(1–2):289–300.
90. Yu Z, Johnston KP, Williams III RO. Spray freezing into liquid versus spray-freeze drying: Influence of atomization on protein aggregation and biological activity. *European Journal of Pharmaceutical Sciences.* 2006 Jan;27(1):9–18.
91. Rogers TL, Nelsen AC, Hu J, Brown JN, Sarkari M, Young TJ, et al. A novel particle engineering technology to enhance dissolution of poorly water soluble

drugs: spray-freezing into liquid. *European Journal of Pharmaceutics and Biopharmaceutics*. 2002 Nov;54(3):271–80.

92. Hu J, Johnston KP, Williams III RO. Spray freezing into liquid (SFL) particle engineering technology to enhance dissolution of poorly water soluble drugs: organic solvent versus organic/aqueous co-solvent systems. *European Journal of Pharmaceutical Sciences*. 2003 Nov;20(3):295–303.

93. Mueannoom W, Srisongphan A, Taylor KMG, Hauschild S, Gaisford S. Thermal ink-jet spray freeze-drying for preparation of excipient-free salbutamol sulphate for inhalation. *Eur J Pharm Biopharm*. 2012 Jan;80(1):149–55.

94. Sharma G, Mueannoom W, Buanz ABM, Taylor KMG, Gaisford S. In vitro characterisation of terbutaline sulphate particles prepared by thermal ink-jet spray freeze drying. *International Journal of Pharmaceutics*. 2013 Apr 15;447(1–2):165–70.

95. Overhoff KA, Engstrom JD, Chen B, Scherzer BD, Milner TE, Johnston KP, et al. Novel ultra-rapid freezing particle engineering process for enhancement of dissolution rates of poorly water-soluble drugs. *European Journal of Pharmaceutics and Biopharmaceutics*. 2007 Jan;65(1):57–67.

96. Watts AB, Wang Y-B, Johnston KP, Williams RO. Respirable Low-Density Microparticles Formed In Situ from Aerosolized Brittle Matrices. *Pharmaceutical Research*. 2013 Mar;30(3):813–25.

97. Beinborn NA, Lirola HL, Williams RO. Effect of process variables on morphology and aerodynamic properties of voriconazole formulations produced by thin film freezing. *Int J Pharm*. 2012 Jun 15;429(1-2):46–57.

98. Beinborn NA, Du J, Wiederhold NP, Smyth HDC, Williams III RO. Dry powder insufflation of crystalline and amorphous voriconazole formulations produced by thin film freezing to mice. *European Journal of Pharmaceutics and Biopharmaceutics*

[Internet]. [cited 2012 Jul 2];(0). Available from: <http://www.sciencedirect.com/science/article/pii/S0939641112001348>

99. Luque de Castro MD, Priego-Capote F. Ultrasound-assisted crystallization (sonocrystallization). *Ultrasonics Sonochemistry*. 2007 Sep;14(6):717–24.

100. Ruecroft G, Parikh D. Sonocrystallisation Particle Engineering for Inhalable Medicines. *J Pharm Pharmacol*. 2010 Oct;62(10):1470–1.

101. Dhumal RS, Biradar SV, Paradkar AR, York P. Particle engineering using sonocrystallization: Salbutamol sulphate for pulmonary delivery. *International Journal of Pharmaceutics*. 2009 Feb 23;368(1–2):129–37.

102. Bjerg A, Lundbäck B, Lötvall J. The future of combining inhaled drugs for COPD. *Current Opinion in Pharmacology*. 2012 Jun;12(3):252–5.

103. Salama RO, Young PM, Rogueda P, Lallement A, Iliev I, Traini D. Advances in drug delivery: is triple therapy the future for the treatment of chronic obstructive pulmonary disease? *Expert Opin Pharmacother*. 2011 Aug;12(12):1913–32.

104. Barnes PJ. Scientific rationale for inhaled combination therapy with long-acting β 2-agonists and corticosteroids. *Eur Respir J*. 2002 Jan 1;19(1):182–91.

105. Nelson HS, Chapman KR, Pyke SD, Johnson M, Pritchard JN. Enhanced synergy between fluticasone propionate and salmeterol inhaled from a single inhaler versus separate inhalers. *J Allergy Clin Immunol*. 2003 Jul;112(1):29–36.

106. Barnes PJ. Triple inhalers for obstructive airways disease: will they be useful? *Expert Rev Respir Med*. 2011 Jun;5(3):297–300.

107. Vehring R, Lechuga-Ballesteros D, Joshi V, Noga B, Dwivedi SK. Cosuspensions of Microcrystals and Engineered Microparticles for Uniform and Efficient Delivery of Respiratory Therapeutics from Pressurized Metered Dose Inhalers. *Langmuir*. 2012 Oct 23;28(42):15015–23.

108. Parikh D, Burns J, Hipkiss D, Usmani O, Price R. Improved localized lung delivery using smart combination respiratory medicines. *Eur Respiratory Disease*. 2012;8(1):40–5.
109. Bailey MM, Berkland CJ. Nanoparticle formulations in pulmonary drug delivery. *Med Res Rev*. 2009 Jan 1;29(1):196–212.
110. Pison, U, Welte, T, Giersig, M, Groneberg, DA. Nanomedicine for respiratory diseases. *European Journal of Pharmacology*. 2006 Mar 8;533(1-3):341–50.
111. Yang W, Johnston KP, Williams III RO. Comparison of bioavailability of amorphous versus crystalline itraconazole nanoparticles via pulmonary administration in rats. *European Journal of Pharmaceutics and Biopharmaceutics*. 2010 May;75(1):33–41.
112. Bhambere D, Shirivastava B, Sharma P, Bukane N, Gide P. Preparation and Optimization of Dry PLGA Nanoparticles by Spray Drying Technique. *Part Sci Technol*. 2013 Sep 3;31(5):533–40.
113. Murthy VS, Cha JN, Stucky GD, Wong MS. Charge-driven flocculation of poly(L-lysine)-gold nanoparticle assemblies leading to hollow microspheres. *J Am Chem Soc*. 2004 Apr 28;126(16):5292–9.
114. Mayo AS, Ambati BK, Kompella UB. Gene delivery nanoparticles fabricated by supercritical fluid extraction of emulsions. *Int J Pharm*. 2010 Mar 15;387(1-2):278–85.
115. El-Sherbiny IM, Smyth HDC. Biodegradable nano-micro carrier systems for sustained pulmonary drug delivery: (I) Self-assembled nanoparticles encapsulated in respirable/swellable semi-IPN microspheres. *International Journal of Pharmaceutics*. 2010 Aug 16;395(1–2):132–41.

116. Bhavna, Ahmad FJ, Mittal G, Jain GK, Malhotra G, Khar RK, et al. Nano-salbutamol dry powder inhalation: A new approach for treating broncho-constrictive conditions. *Eur J Pharm Biopharm.* 2009 Feb;71(2):282–91.
117. Dailey LA, Jekel N, Fink L, Gessler T, Schmehl T, Wittmar M, et al. Investigation of the proinflammatory potential of biodegradable nanoparticle drug delivery systems in the lung. *Toxicology and Applied Pharmacology.* 2006 Aug 15;215(1):100–8.
118. Pilcer G, Amighi K. Formulation strategy and use of excipients in pulmonary drug delivery. *INTERNATIONAL JOURNAL OF PHARMACEUTICS.* 2010 Jun 15;392(1-2):1–19.
119. Fonseca C, Simoes S, Gaspar R. Paclitaxel-loaded PLGA nanoparticles: preparation, physicochemical characterization and in vitro anti-tumoral activity. *Journal of Controlled Release.* 2002;83(2):273–86.
120. Mittal G, Sahana DK, Bhardwaj V, Ravi Kumar MNV. Estradiol loaded PLGA nanoparticles for oral administration: Effect of polymer molecular weight and copolymer composition on release behavior *in vitro* and *in vivo*. *Journal of Controlled Release.* 2007;119(1):77–85.
121. Hara K, Tsujimoto H, Tsukada Y, Huang CC, Kawashima Y, Tsutsumi M. Histological examination of PLGA nanospheres for intratracheal drug administration. *International Journal of Pharmaceutics.* 2008 May 22;356(1–2):267–73.
122. Geller D. Aerosol antibiotics in cystic fibrosis... including discussion with Volsko TA, Flume PA, Ratjen FA, Geller DE, Davies JC. *Respiratory Care.* 2009 May;54(5):658–70.
123. Shoyele SA. Controlling the release of proteins/peptides via the pulmonary route. In: Jain KK, editor. *Methods in Molecular Biology.* 2008. p. 141–8.

124. Sung J, Padilla D, Garcia-Contreras L, VerBerkmoes J, Durbin D, Peloquin C, et al. Formulation and Pharmacokinetics of Self-Assembled Rifampicin Nanoparticle Systems for Pulmonary Delivery. *Pharmaceutical Research*. 2009;26(8):1847–55.
125. Li X, Anton N, Arpagaus C, Belleteix F, Vandamme TF. Nanoparticles by spray drying using innovative new technology: The Büchi Nano Spray Dryer B-90. *Journal of Controlled Release*. 2010 Oct 15;147(2):304–10.
126. Sinha B, Mukherjee B, Pattnaik G. Poly-lactide-co-glycolide nanoparticles containing voriconazole for pulmonary delivery: in vitro and in vivo study. *Nanomedicine : nanotechnology, biology, and medicine*. 2013 Jan 1;9(1):94–104.
127. Adi H, Young PM, Chan H-K, Agus H, Traini D. Co-spray-dried mannitol–ciprofloxacin dry powder inhaler formulation for cystic fibrosis and chronic obstructive pulmonary disease. *European Journal of Pharmaceutical Sciences*. 2010 Jun 14;40(3):239–47.
128. Adi H, Young PM, Chan H-K, Stewart P, Agus H, Traini D. Cospray dried antibiotics for dry powder lung delivery. *J Pharm Sci*. 2008 Aug;97(8):3356–66.
129. El-Sherbiny IM, McGill S, Smyth HDC. Swellable Microparticles as Carriers for Sustained Pulmonary Drug Delivery. *J Pharm Sci*. 2010 May;99(5):2343–56.
130. Yang Y, Bajaj N, Xu P, Ohn K, Tsifansky MD, Yeo Y. Development of highly porous large PLGA microparticles for pulmonary drug delivery. *Biomaterials*. 2009 Apr;30(10):1947–53.
131. Brain JD. Inhalation, Deposition, and Fate of Insulin and Other Therapeutic Proteins. *Diabetes Technology & Therapeutics*. 2007 Jun;9(s1):S–4–S–15.

132. Neumiller JJ, Campbell RK, Wood LD. A Review of Inhaled Technosphere Insulin. *Ann Pharmacother.* 2010 Jul 1;44(7/8):1231–9.

133. Saluja V, Amorij J-P, Kapteyn JC, de Boer AH, Frijlink HW, Hinrichs WLJ. A comparison between spray drying and spray freeze drying to produce an influenza subunit vaccine powder for inhalation. *Journal of Controlled Release.* 2010 Jun 1;144(2):127–33.

134. Ungaro F, De Rosa G, Miro A, Quaglia F, La Rotonda MI. Cyclodextrins in the production of large porous particles: Development of dry powders for the sustained release of insulin to the lungs. *Eur J Pharm Sci.* 2006 Aug;28(5):423–32.

135. Ungaro F, Bianca R d'Emmanuele di V, Giovino C, Miro A, Sorrentino R, Quaglia F, et al. Insulin-loaded PLGA/cyclodextrin large porous particles with improved aerosolization properties: In vivo deposition and hypoglycaemic activity after delivery to rat lungs. *J Control Release.* 2009 Apr 2;135(1):25–34.

136. Sou T, Meeusen EN, de Veer M, Morton DAV, Kaminskas LM, McIntosh MP. New developments in dry powder pulmonary vaccine delivery. *Trends Biotechnol.* 2011 Apr;29(4):191–8.

137. Maraskovsky E, Schnurr M, Wilson NS, Robson NC, Boyle J, Drane D. Development of prophylactic and therapeutic vaccines using the ISCOMATRIX adjuvant. *Immunol Cell Biol.* 2009 Jul;87(5):371–6.

138. Vujanic A, Wee JLK, Snibson KJ, Edwards S, Pearse M, Quinn C, et al. Combined mucosal and systemic immunity following pulmonary delivery of ISCOMATRIXTM adjuvanted recombinant antigens. *Vaccine.* 2010 Mar 19;28(14):2593–7.

139. Wee JLK, Scheerlinck J-PY, Snibson KJ, Edwards S, Pearse M, Quinn C, et al. Pulmonary delivery of ISCOMATRIX influenza vaccine induces both systemic

and mucosal immunity with antigen dose sparing. *Mucosal Immunol.* 2008 Nov;1(6):489–96.

140. Schüle S, Schulz-Fademrecht T, Garidel P, Bechtold-Peters K, Frieß W. Stabilization of IgG1 in spray-dried powders for inhalation. *European Journal of Pharmaceutics and Biopharmaceutics.* 2008 Aug;69(3):793–807.

141. Amidi M, Mastrobattista E, Jiskoot W, Hennink WE. Chitosan-based delivery systems for protein therapeutics and antigens. *Advanced Drug Delivery Reviews.* 2010 Jan 31;62(1):59–82.

142. Makhlof A, Werle M, Tozuka Y, Takeuchi H. Nanoparticles of glycol chitosan and its thiolated derivative significantly improved the pulmonary delivery of calcitonin. *International Journal of Pharmaceutics.* 2010 Sep 15;397(1–2):92–5.

143. Merkel OM, Kissel T. Nonviral Pulmonary Delivery of siRNA. *Acc Chem Res.* 2012 Jul 17;45(7):961–70.

144. Kong X, Zhang W, Lockey RF, Auais A, Piedimonte G, Mohapatra SS. Respiratory syncytial virus infection in Fischer 344 rats is attenuated by short interfering RNA against the RSV-NS1 gene. *Genet Vaccines Ther.* 2007;5:4.

145. Tompkins SM, Lo C-Y, Tumpey TM, Epstein SL. Protection against lethal influenza virus challenge by RNA interference in vivo. *PNAS.* 2004 Jun 8;101(23):8682–6.

146. Merkel OM, Beyerle A, Librizzi D, Pfestroff A, Behr TM, Sproat B, et al. Nonviral siRNA delivery to the lung: investigation of PEG-PEI polyplexes and their in vivo performance. *Mol Pharm.* 2009 Aug;6(4):1246–60.

147. General Chapters <601> Aerosols, Nasal Sprays, Metered-dose Inhalers, and Dry Powder Inhaler. *United States Pharmacopeia.* 35th-NF ed.

148. Guidance for Industry - Metered Dose Inhaler (MDI) and Dry Powder Inhaler (DPI) Drug Products - Chemistry, Manufacturing, and Controls Documentation. Food and Drug Administration. 1998. p. 1 – 61.
149. Hindle M, Byron P. Dose Emissions from Marketed Dry Powder Inhalers. *Int J Pharm.* 1995 Mar 28;116(2):169–77.
150. Taki M, Marriott C, Zeng X-M, Martin GP. Aerodynamic deposition of combination dry powder inhaler formulations in vitro: A comparison of three impactors. *International Journal of Pharmaceutics.* 2010 Mar 30;388(1–2):40–51.
151. Dunbar C, Kataya A, Tiangbe T. Reducing bounce effects in the Andersen cascade impactor. *International Journal of Pharmaceutics.* 2005 Sep 14;301(1–2):25–32.
152. Bonam M, Christopher D, Cipolla D, Donovan B, Goodwin D, Holmes S, et al. Minimizing variability of cascade impaction measurements in inhalers and nebulizers. *AAPS PharmSciTech.* 2008;9(2):404–13.
153. Stevens N, Shrimpton J, Palmer M, Prime D, Johal B. Accuracy assessments for laser diffraction measurements of pharmaceutical lactose. *Meas Sci Technol.* 2007 Dec;18(12):3697–706.
154. Pilcer G, Vanderbist F, Amighi K. Correlations between cascade impactor analysis and laser diffraction techniques for the determination of the particle size of aerosolised powder formulations. *International Journal of Pharmaceutics.* 2008 Jun 24;358(1–2):75–81.
155. Zeng X-M, MacRitchie H, Marriott C, Martin G. Correlation between Inertial Impaction and Laser Diffraction Sizing Data for Aerosolized Carrier-based Dry Powder Formulations. *Pharmaceutical Research.* 2006;23(9):2200–9.

156. Martin G, MacRitchie H, Marriott C, Zeng X-M. Characterisation of a Carrier-Free Dry Powder Aerosol Formulation Using Inertial Impaction and Laser Diffraction. *Pharmaceutical Research*. 2006;23(9):2210–9.
157. Kaialy W, Alhalaweh A, Velaga SP, Nokhodchi A. Effect of carrier particle shape on dry powder inhaler performance. *International Journal of Pharmaceutics*. 2011 Dec 12;421(1):12–23.
158. Shur J, Price R. Advanced microscopy techniques to assess solid-state properties of inhalation medicines. *Advanced Drug Delivery Reviews*. 2012 Mar 30;64(4):369–82.
159. Adi H, Traini D, Chan H-K, Young PM. The influence of drug morphology on the aerosolisation efficiency of dry powder inhaler formulations. *J Pharm Sci*. 2008 Jul;97(7):2780–8.
160. Mohri K, Okuda T, Mori A, Danjo K, Okamoto H. Optimized pulmonary gene transfection in mice by spray–freeze dried powder inhalation. *Journal of Controlled Release*. 2010 Jun 1;144(2):221–6.
161. Kaialy W, Martin GP, Larhrib H, Ticehurst MD, Kolosionek E, Nokhodchi A. The influence of physical properties and morphology of crystallised lactose on delivery of salbutamol sulphate from dry powder inhalers. *Colloid Surf B-Biointerfaces*. 2012 Jan 1;89:29–39.
162. Guchardi R, Frei M, John E, Kaerger JS. Influence of fine lactose and magnesium stearate on low dose dry powder inhaler formulations. *International Journal of Pharmaceutics*. 2008 Feb 4;348(1–2):10–7.
163. Ferrari F, Cocconi D, Bettini R, Giordano F, Santi P, Tobbyn M, et al. The surface roughness of lactose particles can be modulated by wet-smoothing using a high-shear mixer. *AAPS PharmSciTech*. 2004;5(4).

164. Harder C, Lesniewska E, Laroche C. Study of ageing of dry powder inhaler and metered dose inhaler by atomic force microscopy. *Powder Technology*. 2011 Mar 25;208(2):252–9.
165. Berard V, Lesniewska E, Andres C, Pertuy D, Laroche C, Pourcelot Y. Affinity scale between a carrier and a drug in DPI studied by atomic force microscopy. *Int J Pharm*. 2002 Oct 24;247(1-2):127–37.
166. Bérard V, Lesniewska E, Andrès C, Pertuy D, Laroche C, Pourcelot Y. Dry powder inhaler: influence of humidity on topology and adhesion studied by AFM. *International Journal of Pharmaceutics*. 2002 Jan 31;232(1–2):213–24.
167. Jones MD, Young P, Traini D. The use of inverse gas chromatography for the study of lactose and pharmaceutical materials used in dry powder inhalers. *Adv Drug Deliv Rev*. 2012 Mar 15;64(3):285–93.
168. Pilcer G, Wauthoz N, Amighi K. Lactose characteristics and the generation of the aerosol. *Advanced Drug Delivery Reviews*. 2012 Mar 15;64(3):233–56.
169. Das S, Larson I, Young P, Stewart P. Understanding lactose behaviour during storage by monitoring surface energy change using inverse gas chromatography. *Dairy Sci Technol*. 2010 Jun;90(2-3):271–85.
170. Asada M, Takahashi H, Okamoto H, Tanino H, Danjo K. Theophylline particle design using chitosan by the spray drying. *International Journal of Pharmaceutics*. 2004 Feb 11;270(1–2):167–74.
171. Jaspert S, Bertholet P, Piel G, Dogné J-M, Delattre L, Evrard B. Solid lipid microparticles as a sustained release system for pulmonary drug delivery. *European Journal of Pharmaceutics and Biopharmaceutics*. 2007 Jan;65(1):47–56.

172. Son Y-J, McConville JT. Development of a standardized dissolution test method for inhaled pharmaceutical formulations. *International Journal of Pharmaceutics*. 2009 Dec 1;382(1-2):15-22.

Chapter 2: Research Outline

2.1.OVERALL OBJECTIVES

The primary objective of the work presented in this dissertation was to investigate the use of a novel technology named Thin Film Freezing (TFF) to produce dry powder formulation with enhanced characteristics for inhalation therapy. The characteristics of the brittle dry powder produced by TFF were investigated and its suitability to be delivered to the lungs. Moreover, it was developed a performance verification test (PVT) for the Next Generation Cascade Impactor (NGI), which is one of the most important *in vitro* characterization methods to test inhalation products.

2.2.SUPPORTING OBJECTIVES

2.2.1. Characterization and Pharmacokinetics Comparison Analysis of Crystalline versus Amorphous Rapamycin Dry Powder via Pulmonary Administration in Rats

Rapamycin (Sirolimus, RAPA) is a carboxylic lactone-lactam macrolide antibiotic with antifungal activity and great immunosuppressive and antitumor properties. Numerous noted side effects, such as nephrotoxicity, eyelid edema and hyperlipidemia, have impeded its use in treatment for a prolonged time. Recently, RAPA has been investigated for treating women diagnosed with lymphangiomyomatosis (LAM), a progressive, cystic lung disease associated with inappropriate activation of mammalian target of rapamycin (mTOR) signaling, which regulates cellular growth and lymphangiogenesis. TFF technology was used to produce amorphous and brittle particles

of rapamycin for inhalation therapy. The powder formulation was prepared using lactose as a stabilizing agent for the unstable amorphous form of rapamycin. It is known that polymorphic and amorphous forms of poorly water-soluble drugs have been developed to enhance local and/or systemic bioavailability when delivered via pulmonary route. Also, a crystalline counterpart formulation of rapamycin was prepared by wet ball milling using coarse lactose as a carrier and bulk agent. The goal of this investigation, presented in Chapter 3, was to assess and compare the *in vivo* behavior and pharmacokinetic profiles of crystalline and amorphous rapamycin when delivered to the lungs of rats via inhalation. An estimated dose at which mice were to be exposed to was calculated for each formulation to be delivered.

2.2.2. Inhaled Therapies of Fixed-dose Combinations Prepared by Thin Film Freezing

The use of a combination of bronchodilators with different mechanisms and durations of action may increase the degree of bronchodilation in a patient with chronic obstructive pulmonary disease (COPD) whilst decreasing side effects experienced. Furthermore, concentrating the use of multiple medicines in one inhaler may improve patient compliance. When exacerbation or breathlessness persists in patients taking long-acting β 2-agonists (LABA) and inhaled corticosteroids (ICS) dual combination, the use of a triple inhalation therapy of LABA, ICS and long-acting muscarinic antagonist (LAMA) would be advised. It has also been hypothesized that the success of fixed combo formulations can be attributed to the synergistic action of the drugs when co-deposited at the target cells.

The aim of this study was to investigate the use of TFF technology to produce triple fixed dose therapy using formoterol fumarate (LABA), tiotropium bromide

(LAMA) and budesonide (ICS) as therapeutic drugs. Thin Film Freezing (TFF) has shown to be a suitable particle engineering method to produce brittle powder matrices for pulmonary delivery. The rapid freezing of drug solution onto a cryogenic surface prevents segregation and heterogeneity of the solutes. We investigated applications of this technology to powder properties and *in vitro* aerosol performance with respect to single and combination therapy. The aerosol performance of TFF powder combination was compared to the physical mixture of micronized crystalline powders prepared using jet milling process. It is known that one of most challenges in formulating a fixed dose combination lies in the ability to achieve dose uniformity and co-deposition in a powder blend of two or more actives with coarse carrier particles. Therefore particle engineering may be a good alternative to produce a fixed dose therapy in powder form where all drugs are present within a single particle, resulting in improved content uniformity, co-deposition and co-location of drugs at the target of action.

2.2.3. Development of a Verification Performance Test for Cascade Impactor

Cascade impactors (CIs) are used as the standard test method for assessing the performance of therapeutic aerosols. It is widely known that variation in the cascade impactor data can occur over time, due to improper cleaning resulting in erosion, corrosion and/or occlusion of the nozzles or even a poorly implemented standard operational procedure (SOP). As such the impactor manufacturers and the United States Pharmacopeia (USP) recommend that routine mensuration of the test apparatus should be implemented. In most cases, the apparatus is sent back to the manufacture for cleaning and mensuration. The goal of this investigation was to develop a standard performance verification test (PVT) could be used in house to provide routine validation of impactor

apparatus. We investigated the use of a standardized pressurized metered dose inhaler (pMDI) with the NGI. Two standardized formulations were developed. Formulations were analyzed for repeatability and robustness. Variable conditions were introduced to the NGI to mimic operator and equipment failure.

Chapter 3: Characterization and pharmacokinetics comparison analysis of crystalline versus amorphous rapamycin dry powder via pulmonary administration in rats

Abstract

The pharmacokinetics of inhaled rapamycin (RAPA) is compared for amorphous versus crystalline dry powder formulations. The amorphous formulation of RAPA and lactose (RapaLac) was prepared by thin film freezing (TFF) using lactose as the stabilizing agent in the weight ratio 1:1. The crystalline formulation was prepared by wet ball milling RAPA and lactose and posteriorly blending the mixture with coarse lactose (micronized RAPA/micronized lactose/coarse lactose = 0.5:0.5:19). While both powders presented good aerosolization performance for lung delivery, TFF formulation exhibited better *in vitro* aerodynamic properties than the crystalline physical mixture. Single-dose 24 hours pharmacokinetic studies were conducted in Sprague-Dawley rats following inhalation of the aerosol mist in a nose-only inhalation exposure system. Lung deposition was higher for the crystalline group than for the TFF group. Despite higher pulmonary levels of drug that were found for the crystalline group, the systemic circulation (AUC₀₋₂₄) was higher for the amorphous group (23 ng·h/mL) than for crystalline group (16.0 ng·h/mL) based on a two-compartmental analysis. Lung level profiles suggest that TFF powder stays in the lung for the same period of time as the crystalline powder but it presented higher *in vivo* systemic bioavailability due to its greater surface area and increased FPF at a more distal part of the lung.

3.1 INTRODUCTION

Rapamycin (Sirolimus, RAPA) is a carboxylic lactone-lactam macrolide antibiotic with antifungal activity and great immunosuppressive and antitumor properties (1). RAPA has been used both with and without cyclosporine in order to prevent organ rejection in patients after kidney transplant and as an alternative immunosuppressant for lung transplantation (2). Numerous noted side effects, such as hypertension, hyperlipidemia and nephrotoxicity, have impeded its use in treatment for a prolonged time (3). Recently, systemic RAPA has been investigated for treating women diagnosed with pulmonary involvement with lymphangiomyomatosis (LAM). LAM is a progressive, cystic lung disease associated with inappropriate activation of mammalian target of rapamycin (mTOR) signaling, which regulates cellular growth and lymphangiogenesis. In 2011, the Multicenter International LAM Efficacy of Sirolimus (MILES) Trial was performed. This double-blind, placebo-controlled trial showed promising results in phases 1 and 2, where oral doses of RAPA successfully inhibited mTOR and stabilized lung function in patients with moderate to severe LAM (4)(5). Unfortunately, the disease progressed when rapamycin was discontinued and the systemic toxicities were felt to be too significant for long term use in young females.

RAPA is currently approved for prophylaxis of rejection for kidney allograft patients and it is only commercially available for oral administration (e.g. Rapamune[®]) due to its poor water solubility (2.6 µg/mL) (6). The oral bioavailability of RAPA from Rapamune[®] oral solution is approximately 14% (7)(8). The oral bioavailability was reportedly improved to about 27% reducing the particle size (9)(10). Therefore, because of the relatively low oral bioavailability, a higher dose of RAPA is given to the patient in order to reach the desired drug therapeutic window (7)(11). Such high dosages may be the cause of various adverse effects. To further improve RAPA solubility, numerous oral

formulations have been developed e.g. solid dispersion nanoparticles using a supercritical antisolvent process (12), liposomes (13) and solid dispersion and complexation with hydrophilic excipients (14).

To our knowledge, rapamycin has never been used to treat systemic or local diseases via pulmonary inhalation. Pulmonary drug delivery is a non-invasive route of administration which presents several advantages such as avoidance of first pass metabolism and large mucosal surface area for drug absorption; a characteristic which allows this method to be an ideal candidate in applications involving local and systemic administration (15).

Polymorphic and amorphous forms of poorly water-soluble drugs have been developed to enhance local and/or systemic bioavailability when delivered via the pulmonary route. Wei et al. compared the bioavailability of amorphous versus crystalline itraconazole nanoparticles via pulmonary administration in rats. After inhalation of the same dose of nebulized itraconazole dispersions, the C_{\max} of the nanocrystalline dispersion was 50 ng/ml at 2.7 hours with an AUC_{0-24} of 662 ng h/mL. The C_{\max} of amorphous dispersion was 180 ng/mL at 4 hours and AUC_{0-24} of 2543 ng h/mL, in systemic circulation. The authors relate the significantly higher systemic bioavailability value of the amorphous system to the increased supersaturated environment, which would result in an increased drug permeation (16). Despite these findings, in another study, the administration of amorphous voriconazole nanoparticles to the lungs of mice did not present enhanced systemic bioavailability when compared to the crystalline counterpart. Beinborn et al. associate these results to the prolonged residence time of crystalline voriconazole in the lungs when compared to the amorphous system (17).

The aim of this study is to assess and compare the *in vivo* behavior and pharmacokinetic profiles of crystalline and amorphous rapamycin when delivered to the

lungs of rats via inhalation. We hypothesize that the solubility enhancement of amorphous rapamycin in the lung fluids will increase *in vivo* systemic bioavailability. Techniques used in this study include thin film freezing technology (TFF) in order to produce amorphous rapamycin respirable powder and wet ball milling to prepare the crystalline rapamycin powder.

3.2 MATERIALS AND METHODS

3.2.1 Materials

Rapamycin (Sirolimus) was purchased from Tecoland Corporation (Irvine, California) and lactose monohydrate (lactose, Lactohale[®] LH 200) was kindly donated by Friesland Foods Domo (Zwolle, Netherlands). High performance liquid chromatography (HPLC) grade acetonitrile and methanol were purchased from Fisher Scientific (Fair Lawn, NJ). Water was purified by reverse osmosis (MilliQ, Millipore, France).

3.2.2 Formulation preparation

Thin Film Freezing technology was used for the preparation of amorphous and low density dry powder (18). In brief, a cosolvent mixture of acetonitrile and water (3:2) was used to dissolve rapamycin and lactose in the ratio of 1 to 1. To investigate the influence of solid loading on TFF powder aerosolization, two formulations were prepared with different final solid loading concentrations: 0.40% and 0.75% (w/v). The solution was rapidly frozen on a cryogenically cooled (-80°C) stainless steel surface by thin film freezing. The frozen films were collected in a container filled with liquid nitrogen to avoid melting. The frozen formulation was transferred to a -70°C freezer until the liquid

nitrogen was completely evaporated, and then transferred to a VirTis Advantage Lyophilizer (VirTis Company Inc., Gardiner, NY) for solvent removal. Formulation was lyophilized over 24 h at -40°C at a pressure of 400 mTorr. The temperature was gradually increased to 25°C over 24 h with a pressure less than 200 mTorr, and kept at 25°C for 24 h.

For comparison purposes, the equivalent crystalline physical mixture of rapamycin and lactose in the same weight ratio as described previously was prepared. First, micronized rapamycin and lactose were prepared using wet ball milling in a ceramic jar with zirconia grinding media (1/2" radius end cylinder) (US Stoneware, East Palestine, OH). Five grams of rapamycin powder was added to 25 mL of purified water and milled at 100 rpm at 20°C for 48 hours. Likewise, lactose was dispersed in acetonitrile and ball milled at 100 rpm at 20°C for 48 hours. The obtained slurry collected from the ceramic jar and from triple rinsing of milling media was frozen at -80 °C and then lyophilized using a VirTis Advantage Lyophilizer (VirTis Company Inc., Gardiner, NY) for solvent removal. The dry powder products were stored in a desiccator under vacuum at room temperature until further use. After particle size reduction, lactose monohydrate and rapamycin were sieved through a 100 µm and 45µm mesh. Equivalent amounts of micronized lactose and rapamycin were accurately weighed and mixed using the geometric dilution technique. The mixed powder was then mixed with coarse lactose LH200 in the ratio 1 to 19, again using geometric dilution technique. The final mixture was then transferred to a stainless steel mixing vessel. The vessel was placed in a Turbula Blender T2F (Bachofen, Switzerland) and mixing was carried out for 20 min at 48 revolutions per minute (rpm).

3.2.3 Particle size analysis

Measurements of particle size distributions of rapamycin and lactose, before and after wet ball milling, were performed by laser diffraction (HELOS, Sympatec GmbH, Clausthal-Zellerfeld, Germany). A small amount of bulk lactose was dispersed in 10 mL 0.01% tween 80 mineral oil and a small amount of rapamycin was dispersed in 10 mL 0.01% tween 80 in deionized water. The samples were sonicated for 5 minutes and diluted with enough solvent to produce light obscuration in the range of 10–20%. Results are presented as $D_{(x)}$ and span, where X is the cumulative percentile of particles under the referred size (e.g. $D_{(50)}$ corresponds to the median diameter of the particles). Span is a measurement of particle size distribution calculated as $[(D_{(90)} - D_{(10)})/D_{(50)}]$. The sizes reported are average values taken from at least 3 measurements.

3.2.4 Scanning Electron Microscopy (SEM)

Analysis of powder morphologies and estimation of particle size of all samples were performed using SEM. Samples were placed on carbon tape and coated with gold/palladium (60/40) for 20 seconds under argon atmosphere using a Cressington Sputter Coater 208 HR (Cressington Scientific Instruments, Watford, England). The SEM images were captured using a SmartSEM[®] graphical user interface software in a Carl Zeiss Supra[®] 40VP (Carl Zeiss, Oberkochen, Germany) operated under vacuum, at a working distance of 19 mm and at 5 kV of Electron High Tension (EHT).

3.2.5 Brunauer-Emmet-Teller (BET) specific surface area (SSA)

Powder porosity was determined through the measurement of the specific surface area (SSA) using a Monosorb MS-22 rapid surface area analyzer (Quantachrome Instruments, Boynton Beach, Florida). The instrument uses a modified BET equation for

SSA determination. Samples were degassed in a Thermoflow™ Degasser for at least 2 hours at 25°C using 30% nitrogen in helium as the desorbate gas.

3.2.6 Thermal analysis

Thermal properties and the degree of crystallinity of the powders were analyzed using a 2920 modulated differential scanning calorimetry (mDSC) (TA Instruments, New Castle, DE) equipped with a refrigerated cooling system. Dry nitrogen was used as the purge gas through the mDSC cell at a flow rate of 40 mL/min. Sample weights varying between 3 and 8 mg were placed into open aluminum pans and hermetically sealed (kit 0219-0041, Perkin-Elmer Instruments, Norwalk, CT). Experiments were performed at a heating rate of 10°C/min and modulation temperature amplitude of 1°C/min, in the range of 20 to 300°C. The data was analyzed using TA Universal Analysis 2000 software (TA Instruments, New Castle, DE).

Powders were analyzed for residual moisture content using Mettler Toledo TGA/DSC 1 - Thermogravimetric Analyser (Mettler-Todedo, Columbus, OH) operated at a ramp rate of 10°C/min from a temperature of 40 to 350°C. Samples were prepared by weighing powders in a crucible. The sample weights varied between 5 and 8 mg. Crucibles were covered with a lid to avoid evaporation of any solvent residue by air/nitrogen gas present in the equipment chamber.

3.2.7 Powder X-ray diffraction (PXRD)

Crystallinity properties of bulk rapamycin and lactose, wet ball milled powders and TFF formulations were investigated using a Philips Model 1710 X-ray diffractometer (Philips Electronic Instruments Inc. Mahwah, NJ) with primary monochromated radiation

(CuK. α_1 , $\lambda = 1.54056 \text{ \AA}$) emitting at an accelerating voltage of 40 kV and 30 mA. The samples were placed into a stage and scanned for diffraction patterns from 5° to 35° on the 2-theta scale at a step size of $0.03^\circ/\text{second}$ and a dwell time of 2 seconds.

3.2.8 *In vitro* aerosol performance

The Next Generation Pharmaceutical Impactor (NGI) (MSP Corporation, Shoreview, MN) was used to determine the aerodynamic properties of the TFF-amorphous and crystalline physical mixture formulations of rapamycin. Cascade impactor was assembled and operated in accordance to the USP General Chapter <601> Aerosol, Nasal Spray, Metered-dose Inhalers and Dry Powder Inhalers (19). The samples were filled into size 3 HPMC capsules and aerosolized using a Handihaler[®] device. Measurements were performed for 4.4 seconds at a pressure drop of 4kPa across the device corresponding to a flow rate of 54 L/min through the device which was calibrated using a TSI mass flowmeter (Model 4000, TSI Inc., St. Paul, MN). The NGI collection plates were coated with 1% (v/v) silicone oil in hexane to prevent particle bounce, fracture and reentrainment. After aerosolization, samples were collected using known volumes of diluent and analyzed by high performance liquid chromatography (HPLC).

Total emitted dose (TED) was calculated as the percentage of drug emitted from the DPI. Fine particle fraction (FPF) was calculated as the percentage of loaded drug aerosol smaller than $5 \mu\text{m}$. Mass median aerodynamic diameter (MMAD) and geometric standard deviation (GSD) were calculated based on the dose deposited on stages 1 through MOC.

3.2.9 Chromatographic assays

High performance liquid chromatography method was modified from a previous report (20). *In vitro* samples of rapamycin were quantified using a Dionex 3000 HPLC system equipped with UV detector set at 278 nm wavelength. A 90 μ L injection volume was injected into a Waters Symmetry C₁₈, 5 μ m guard column connected to a Waters Symmetry C₈ 3.5 μ m 75 x 4.6 mm reversed-phase column (Waters Corp., Milford, MA). The column temperature was maintained at 50°C. The mobile phase consisted of 1360 mL deionized water, 1200 mL methanol, and 1440 mL acetonitrile (34:40:36) running at flow rate of 1 mL/min. Rapamycin exists in two isomeric forms in solution, a lactone and lactam form and both forms show equivalent therapeutic activity. The retention time is approximately 21 minutes for lactone (major isomer peak) and 27 minutes for lactam (minor isomer) (21). The quantification of rapamycin present in the samples is the result of the summation of both peak areas. All samples were kept at 4°C and protected from light until time of analysis due to the instability of rapamycin in solution (20).

3.2.10 *In vivo* pulmonary dosing of rats

The protocol for the animal study was approved by the Institutional Animal Care and Use Committee (IACUC) at the University of Texas at Austin, Austin, TX. Jugular vein pre-catheterized and non-catheterized Sprague-Dawley rats weighting between 225–275 grams were purchased from Charles River Laboratories (Wilmington, MA). Animals were housed two per cage, subjected to 12 h /12 h light and darkness cycles with access to food and water *ad libitum*. A nose-only inhalation exposure system (NOIES) equipped with a compressor and brush generator capable of dosing 24 rats at a time was used (CH Technologies (USA) Inc., Westwood, NJ, USA). Prior to dosing, animals were individually acclimated for 30 minutes per day for four days in restraint tubes. Catheters

were flushed two times before the study with heparinized normal saline. Animals were divided in 2 groups for dosing of TFF and physical mixture (i.e., crystalline) formulations, and each group was comprised of 4 jugular vein pre-catheterized rats for blood sample collection and 12 non-catheterized rats for collection of bronchoalveolar lavage (BAL) fluid and lung harvesting. Rapamycin formulations were loaded into a feed cylinder connected to a rotating brush generator. At an airflow rate of 33 L/min, animals in the TFF group were dosed for 5 minutes and animals in the physical mixture group were dosed for 10 minutes. Times of exposures were determined according to equation 1 below. Following dosing, animals were placed back into their respective cages. A series of 0.3 mL blood samples were collected following exposure to the powder aerosol through the jugular vein catheters at 0.25, 1, 2, 4, 8, 12 and 24 hours post dosing and transferred into pre-heparinized micro-centrifuge tubes. The volume of blood withdrawn from rats was replaced with same volume of warmed sterile saline solution. To investigate the amount of drug deposited in the lower respiratory tract, the lining of the respiratory tract was washed for collection of fluids (i.e., bronchoalveolar lavage). The trachea was cannulized and 3 mL of saline solution was inserted and removed twice from the lungs for proper washing. The lungs were subsequently harvested. Three non-catheterized rats in each dosing group were sacrificed at 0.25, 1, 4, 12 and 24 hour. Rats used for blood sample collection were sacrificed after the 24 hours time point and BAL was performed and lung tissues were harvested. All samples were transferred to centrifuge tubes and immediately transferred to -80°C freezer.

3.2.11 Estimated Dose

To estimate the dose inhaled by the rats during this study, the following equation was used:

$$\text{Delivered Dose (mg)} = C \times \text{RMV} \times D \quad \text{Equation 1}$$

Where C is the measured drug concentration in air (mg L^{-1}), RMV is the species-specific respiratory minute volume or the volume of air inhaled in one minute (Lmin^{-1}), and D is the duration of exposure (min). To determine the portion of the delivered dose that was deposited in the lungs, the percent deposition in relationship to the particle size distribution was estimated based on rodent dosimetry findings reported by Kuehl et al. (22).

3.2.12 Blood, BAL and lung analysis

Quantification of rapamycin in blood, lung tissue and bronchoalveolar lavage (BAL) solution samples were performed according to previous published procedures with modifications (23)(24)(25). Samples were analyzed using a HPLC system consisted of a Shimadzu SCL-10A Controller, LC-10AD pump with a FCV-10AL mixing chamber, SIL-10AD autosampler, and an AB Sciex API 3200 tandem mass spectrometer with turbo ion spray. The analytical column was a Grace Alltima C18 (4.6 x 150 mm, 5 μ) purchased from Alltech (Deerfield, IL) and was maintained at 60°C during the chromatographic runs using a Shimadzu CTO-10A column oven. Mobile phase A contained 10 mM ammonium formate and 0.1% formic acid dissolved in HPLC grade methanol. Mobile phase B contained 10 mM ammonium formate and 0.1% formic acid dissolved in 90% HPLC grade methanol. The flow rate of the mobile phase was 0.5 ml/min. RAPA was eluted with a step gradient. The column was equilibrated with 100% mobile phase B. At 6.10 minutes after time of injection, the system was switched to 100% mobile phase A. Finally, at 15.1 minutes the system was switched back to 100% mobile phase B in preparation for the next injection. The RAPA transition was detected

at 931.6 Da (precursor ion) and the daughter ion was detected at 864.5 Da. Ascomycin (ASCO) was detected at 809.574 Da and the daughter ion was 756.34 Da.

Quantification of rapamycin in rat whole blood: RAPA was quantified in uncoagulated rat blood (EDTA). Briefly, 100 μ L of calibrator and unknown whole blood samples were mixed with 10 μ L of 0.5 μ g/mL ASCO (internal standard), and 300 μ L of a solution containing 0.1% formic acid and 10 mM ammonium formate dissolved in 95% HPLC grade methanol. The samples were vortexed vigorously for 2 min, and then centrifuged at 15,000 g for 5 min at 23°C. Subsequent centrifugations were performed under the same conditions. Supernatants were transferred to 1.5 ml microfilterfuge tubes and spun at 15,000 g for 1 minute and then 40 μ L of the final extracts were injected into the LC/MS/MS. The ratio of the peak area of RAPA to that of the internal standard ASCO (response ratio) for each unknown sample was compared against a linear regression of calibrator response ratios at 0, 1.25, 3.13, 6.25, 12.5, 50, and 100 ng/mL to quantify RAPA. The concentration of RAPA was expressed as ng/mL whole blood.

Quantification of rapamycin in rat lung tissue: RAPA was quantified in rat lung tissue according to the following protocol. The lungs weighed an average of 1.8 grams. Briefly, 100 mg of calibrator, control, and unknown tissue samples were mixed by sonication (three 5 sec bursts) with 10 μ L of 0.5 μ g/mL ASCO (internal standard) and 300 μ L of a solution containing 0.1% formic acid and 10 mM ammonium formate dissolved in 95% HPLC grade methanol. After sonication, the samples were vortexed vigorously for 2 min, and then centrifuged at 15,000 g for 5 min at 23°C (subsequent centrifugations were performed under the same conditions). Supernatants were transferred to 1.5 mL microfilterfuge tubes and spun at 15,000 g for 1 minute and then 40 μ L of the final extracts were injected into the LC/MS/MS. The ratio of the peak area of RAPA to that of the internal standard ASCO (response ratio) for each unknown sample was compared

against a linear regression of calibrator response ratios at 0, 1.56, 3.13, 6.25, 12.5, 50, and 100 µg/g to quantify RAPA. The concentration of RAPA was expressed as µg/g of tissue.

Quantification of rapamycin in BAL solutions: RAPA was quantified in BAL solutions according to the following protocol. Briefly, 100 µL of calibrator, control, and unknown samples were mixed by vortexing with 10 µL of 0.5 µg/mL ASCO (internal standard) and 200 µL of a solution containing 0.1% formic acid and 10 mM ammonium formate dissolved in 95% HPLC grade methanol for 2 min. After vortexing, the samples were transferred to 1.5 ml microfilterfuge tubes and then centrifuged at 15,000 g for 1 min at 23°C. Filtrates were transferred to autosampler tubes and 40 µL of the final extracts were injected into the LC/MS/MS. The ratio of the peak area of RAPA to that of the internal standard ASCO (response ratio) for each unknown sample was compared against a linear regression of calibrator response ratios at 0, 2.5, 10, 40, 160, 640, and 2560 ng/mL to quantify RAPA. The concentration of RAPA was expressed as ng RAPA/mL BAL solution.

3.2.13 Pharmacokinetics and statistical analysis

The data is expressed as mean ± standard deviation (SD). Pharmacokinetic parameters were determined using a two compartmental analysis with assistance from Phoenix[®] WinNonlin[®] 5.3 (Pharsight, St. Louis, MO). The average data at each time point for lung, BAL and blood data were modeled simultaneously in a single model.

3.3 RESULTS AND DISCUSSION

3.3.1 Preformulation considerations

Rapamycin, a hydrophobic drug, is soluble in most organic solvents but is practically insoluble in water (2.6 µg/mL) and in approved parenteral excipients, e.g. ethanol and tween 80 (6). Thus, rapamycin has only been commercialized in solution containing polysorbate 80, phosphatidylcholine, propylene glycol, mono- and di-glycerides, ethanol, soy fatty acids and ascorbyl palmitate and tablet oral dosage forms, which have a very low bioavailability of approximately 14 to 20%, respectively (7). In this study, thin film freezing technology (TFF) was used to increase bioavailability of rapamycin and produce powder capable of aerosolization. TFF was first developed to increase water solubility of lipophilic drug molecules and subsequently enhance bioavailability of BSC class II drugs such as itraconazole and danazol (26)(16). In addition to improving drug solubility, TFF has also been shown to produce low-density brittle matrix powders capable of aerosolization and delivery to the airway (27). The use of excipients with high glass transition temperature (T_g) enables the formation of the amorphous form of the compounds by TFF and prevents recrystallization. Lactose monohydrate, one of the US Food and Drug Administration (FDA)-approved sugar carriers and excipient for delivery to the lungs, has a T_g of about 102°C (28). Lactose plays an important role as excipient to improve stability of lyophilized formulations and as carrier in most DPI formulations to enhance powder aerosolization behavior (29)(30). In this TFF formulation, however, lactose does not act as a carrier, but as a matrix excipient to enable aerosolization by brittle fracture. Water and acetonitrile were used during manufacture as a co-solvent system to allow dissolution of the poorly water-soluble rapamycin as well as hydrophilic lactose monohydrate. Overhoff et al. found that acetonitrile is a suitable organic solvent to be used with TFF technology due to its good heat transfer properties, which results in fast cooling rates and high supersaturation and

nucleation rates. Furthermore, acetonitrile is miscible in water, has a freezing point of -45°C, density of 1.42 g/mL, and viscosity of 0.36 cP at 20°C (31). Due to the low viscosity and low freezing point properties of acetonitrile, the time of droplet spreading on the cryogenic surface is faster than its freezing time with subsequent fast freezing. These characteristics allow the formation of thin and homogeneous frozen disks with uniform particle sizes. The final powder presents high surface area and potentially fast dissolution rates (18).

3.3.2 Physicochemical properties of formulations

3.3.2.1 Particle size and morphology of formulations

In order to effectively compare the TFF formulation of rapamycin and lactose (1:1) to a traditional micronized formulation, both rapamycin and lactose needed to be milled into respirable particles and blended with carrier lactose. Particle size analyses by laser diffraction and scanning electron microscopic images of lactose and rapamycin showed that the particles are unsuitable for pulmonary delivery as presented in bulk material. SEM image of lactose displays an irregular shape and broad particle size distribution, varying from 5 to 160 μm as shown in Figure 3.1. Accordingly, laser diffraction analyzes demonstrate a D_{50} of 39.78 μm and span values of 2.43, which confirms the broad particle size distribution. Specific surface area measurement (SSA) of lactose shows a small surface area value of 0.34 m^2/g (Table 3.1), typical for larger particle sizes. Bulk rapamycin also presented irregular shape surface morphologies (Figure 3.1) and broad particle size distribution with D_{50} value of 28 μm and span value of 2.21. The SSA value of 0.57 m^2/g was slightly greater than lactose.

The use of wet ball milling technique for 48 hours was efficient and considerably reduced the particle size of bulk rapamycin and lactose and consequently increased specific surface area. Micronized rapamycin presented a D_{50} value of 5.22 μm and SSA value of 14.29 m^2/g while lactose presented a D_{50} value of 6.41 μm and SSA value of 10.76 m^2/g (Table 3.1). Even though laser diffraction results of wet ball milled powders showed D_{50} values greater than the values suitable for lung delivery, SEM images of both powders revealed particles in the sub-micron range exhibiting irregular to round-shaped morphologies (Figures. 3.1c and 3.1d). While the particle size measured of both milled powders was slightly larger than desirable for pulmonary delivery, it was adequate to insure delivery in the animal exposure study designed. SEM images of the physical mixture of micronized rapamycin and lactose with coarse lactose are shown in Fig. 3.2a and 3.2b. The images show micronized powders adhered to the coarse lactose surfaces, which may improve powder dispersion and aerosolization at the time of inhalation.

SSA measurements of TFF powder formulations show a significant increase in surface area due to the low density powder matrix formed after lyophilization of the frozen discs (Table 3.1). The increase in surface area was greater for the RapaLac_0.40% than for the RapaLac_0.75% formulation, which was prepared from the most diluted drug solution. The difference in powder density is confirmed in the SEM images (Fig. 3.2c and 3.2d). With approximately half the solids compared to the 0.75% formulation and the same bulk volume, the 0.40% formulation would be expected to have a higher surface area.

3.3.2.2 Crystalline state of powders and moisture content

The PXRD patterns of all samples are shown in Figure 3.3. Bulk lactose exhibits high intensity peaks (2θ) at 16.04, 19.10 and 19.25, indicating its crystalline structure,

which is similar to the data reported elsewhere (32). Crystallinity state of lactose is also evident by the two characteristic endothermic peaks at 151.7°C and 218.5°C shown in Figure 3.4. The first endothermic peak is due to dehydration and the second peak represents the melting point of monohydrate α -lactose form (33). Bulk rapamycin exhibits high intensity peaks at 5.15, 9.80, 14.87, 15.65, 19.61, 20.03 and 22.22 degrees of 2θ . The endothermic peak of rapamycin was found to be 192.16°C close to the temperature range of 187 to 193°C reported previously (12). Wet ball milled rapamycin and lactose also exhibit the characteristic PXRD patterns of bulk powders but with smaller intensities. The reduction of peak intensity and broadening seen on the PXRD patterns are indications of crystallinity loss due to the use of high-energy input process to reduce particle size. The milling process disrupts the crystal structure on the particle surface and creates amorphous domains (34). The DSC profile of wet milled lactose confirms its crystallinity state with endothermic peaks at 136.4 and 220.9°C. The peaks present less intensity and a small shift, which may be related to the loss of crystallinity of the powder. Moreover, the first endothermic peak characteristic of dehydration is almost nonexistent, most likely due to dehydration caused by the lyophilization cycle. Even though the milling process generated some amorphous domains on the rapamycin and lactose particles, the powders were predominantly crystalline. Wet ball milled rapamycin also presented a smaller endothermic peak at 178.1°C possibly due to the presence of amorphous domains in the crystalline powder, as shown in Figure 3.4.

The PXRD patterns of both TFF formulations show a broad and diffused halo pattern with an absence of crystalline peaks. Such findings suggest that the formulations are in the amorphous state. Unfortunately, the PXRD technique has a 10% limit of detection for amorphous materials and a more sensitive technique would be necessary to investigate for the presence of any crystal lattice in the formulations (35). However,

further investigation with mDSC of RapaLac_0.40% and RapaLac_0.75% indicate that both formulations exist in the amorphous form as shown in Figure 3.4. Both TFF formulations presented a recrystallization peak at the temperature range of 188 to 192°C and a single endothermic melting peak at the temperature range of 215 to 216°C. The first peak indicates the recrystallization of the formulations in the glassy state and the second peak indicates further melting of crystals.

Thermogravimetric analyses of the bulk powders and TFF formulations were used to determine the residual moisture content present in the samples. The thermogram profile of rapamycin (Figure 3.5) exhibits initial decomposition at temperature of approximately 195°C. Alternatively, lactose monohydrate exhibits an initial 5% weight loss at temperature ranging from 100 to 155°C, which indicates dehydration of the molecules. The decomposition temperature was found to be about 220°C. Thermogram profiles of RapaLac_0.40% and RapaLac_0.75% were similar and indicate that both formulations exhibit minimal solvent evaporation of only 3.2% through temperatures ranging from 45 to 110°C. Indeed, the actual moisture content of TFF formulations might be smaller than the values found in this study as the powders were exposed to the environment during sample preparation and may have absorbed some ambient moisture. Furthermore, thermal decomposition of the formulations started at temperatures of about 180°C. The results indicate that the lyophilization cycles were suitable to prepare formulations in accordance with the standard limits of less than 5% moisture content (36). It is important to maintain a low moisture content in order to reduce chemical degradation of the active compound and to reduce physical instability of the formulation (30).

3.3.3 *In vitro* aerosol performance

The next generation cascade impactor (NGI) is a standardized apparatus recommended by the pharmacopeia for assessing the aerosol aerodynamic particle size distribution from a dry powder inhaler.(37) The cascade impactor attempts to predict how an aerosol will deposit in the airways during inhalation. Only aerosol particles with aerodynamic size smaller than 5 μm may deposit in the lower airways.(38) The aerodynamic properties of the crystalline physical mixture and the TFF formulations were investigated using the NGI. The aerosol properties of the coarse blend and TFF formulations are shown in Table 3.2. RapaLac physical mixture had the smallest TED, 78.92%, and the smallest FPF, 36.79%, when compared to the TED and FPF values of RapaLac_0.40% and RapaLac_0.75% (97.14 and 72.11%, and 94.71 and 61.29%, respectively). The superior performance of the TFF powder formulation is likely due to the ease in fracturing of the brittle powder matrix resulting in low density aerosolized particles. Additionally, low interparticulate adhesion due reduction of electrostatic and van der Waals forces may contribute to improved performance. Surprisingly, the MMAD of the physical mixture was smaller (1.81 μm) than the MMAD values of the RapaLac_0.40% and RapaLac_0.75% (2.1 and 2.43 μm , respectively). However, the GSD value, which indicates the magnitude of dispersity from the particle size distribution, is greater for the physical mixture (4.26) than for the RapaLac_0.40% and RapaLac_0.75% (2.25 and 2.76 μm , respectively). GSD results suggest that the TFF formulations have a narrower aerodynamic particle size distribution than the physical mixture formulation.

The influence of solid loading concentration on aerosolization performance of TFF RAPA formulation was investigated in this study. As described before, TFF powder generated from more diluted solutions (RapaLac_0.40%) yielded a less dense powder

matrix with greater specific surface area. Apparently, these characteristics also have influence on the aerosolization performance of the formulations (Figure 3.6). Even though both TFF powders presented better aerosolization performance compared to the milled formulation, TFF powder prepared from the 0.40% (w/v) solid loading solution exhibited better results using the dry powder inhaler device by generating greater FPF values with smaller MMAD and GSD values than the least porous powder (Table 3.2). Therefore, amorphous RapaLac_0.40% powder and crystalline RapaLac physical mixture were chosen for *in vivo* studies.

3.3.4 Pharmacokinetics of inhaled amorphous TFF RapaLac and crystalline RapaLac physical mixture

3.3.4.1 Determination of Delivered Dose

Therapeutic dose necessary to prevent lung allograft rejection in rats when administered orally is approximately 2.5 mg/kg/day (39)(40)(41). When given orally, the bioavailability of rapamycin in rats is less than 4% and only approximately 2.05% of this dose is distributed to the lungs which is the equivalent of around 410 ng of rapamycin (42). In this study, a dose of approximately 19.3 µg of amorphous TFF powder and 32.7 µg of crystalline powder was estimated to be delivered to the rats. The dose was calculated by drawing a set flow (1.5 liter/min) through a filter for a set duration during the exposure. Of the delivered dose, the amount of lung deposition was predicted based on findings from a SPECT/CT imaging deposition study(22). Particle size distribution was determined during animal exposures using a Mercer cascade impactor. Data from Mercer impaction was applied to the particle size/deposition correlation demonstrated by Kuehl et al. to determine rapamycin lung deposition of 1.0 µg and 1.5 µg for TFF and crystalline formulations respectively.

The first time point (15 minutes) was considered for the determination of the actual amount of rapamycin delivered to rats as follows (Eq. 2):

$$m_{0T} = m_{0BAL} + m_{0lung} + m_{0blood} \quad \text{Equation 2}$$

Where m_{0T} is the total amount delivered and m_{0BAL} , m_{0lung} and m_{0blood} are the amounts of rapamycin found in the BAL, lung and blood samples at the first time point, respectively. From equation 2, the following equation can be derived:

$$m_{0T} = C_{0BAL} \cdot V_{BAL} + C_{0lung} \cdot W_{lung} + C_{0blood} \cdot V_{blood} \quad \text{Equation 3}$$

Where C_{0BAL} is the concentration of rapamycin in BAL sample at the first time point; V_{BAL} is the volume of saline collected from the BAL procedure (5 mL); C_{0lung} is the concentration of rapamycin in the lung sample at the first time point; W_{lung} is the lung weight; C_{0blood} is the concentration of rapamycin in the blood sample at the first time point; and V_{blood} is the blood volume of rats based on rat weight according to equation 4 from Lee et al (43):

$$V_{blood} = 0.06 \cdot W_{rat} + 0.77 \quad \text{Equation 4}$$

Where W_{rat} is the body weight of the rats. According to this estimation, the total amounts of lung deposition were 332.7 ng and 2749.1 ng for TFF and physical mixture, respectively. These estimated amounts were used as the dose for each treatment group for the discussion of the pharmacokinetics parameters.

3.3.4.2 Pharmacokinetics Evaluation

During dosing, the aerosol particles inhaled by the animals that are smaller than 5 μm are more likely to be deposited in the deep lungs. The rate of absorption of drug into the systemic circulation depends on the particle physical state and its physicochemical properties. When deposited in the solid state, drug particles have to dissolve into the epithelial lining fluid prior to absorption into the lung tissue (44). Rapamycin is a highly lipophilic drug, with logP value greater than 5 and a molecular weight (MW) of 914.2 g/mol (45). Based on the findings from Patton and co-workers, absorption of a molecule with such physicochemical properties (logP and MW) through the respiratory tract and into systemic circulation can be expected within a few minutes (46).

The amount of drug per gram of lung tissue found in the BAL samples was less than that found in the lung tissue (Figure 3.7). For the two-compartmental analysis, these amounts were combined. Table 3.3 shows the PK parameters derived from this model. To facilitate data comparison, pharmacokinetic parameters of the pulmonary tract and blood were reported as per microgram of drug deposited.

The initial concentration found in the pulmonary tract (C_0) was much higher for the crystalline group (1529.1 ng/g) than for the TFF group (165.9 ng/g) as shown in Table 3.3. The higher initial concentration found for the crystalline group is due to the higher initial dose deposition in the lungs and the faster systemic absorption of the TFF powder. Accordingly, the total amount of drug present in pulmonary tract (AUC_{0-24}) was 7560.6 ng·h/g and 731.1 ng·h/g for the crystalline and TFF groups, respectively. Once in the interstitial tissue, drug molecules are absorbed into the systemic circulation. Despite higher pulmonary tract levels of drug that were found for the crystalline group, the extension to absorption in the blood or the area under the curve over 24 hours (AUC_{0-24}) was higher for the amorphous group (23 ng·h/mL) than for crystalline group (16.0

ng·h/mL), as shown in Table 3.3. Figure 3.8 shows that, for a normalized dose (per μg) delivered, the initial concentration of rapamycin in the blood from the TFF arm is about five times greater than that of the crystalline group, suggesting a faster absorption rate of the TFF formulation. This finding is confirmed by the k_{12}/k_{21} ratios: 2:1 and 1:1 for the TFF and the crystalline formulations, respectively. Dissolution is the rate-limiting step for the crystalline group and results in high BAL levels, reduced absorption from the lung fluid and systemic bioavailability. Moreover, lung level profiles at 12-24 hours suggest that TFF powder stays in the lung for the same period of time as the crystalline powder but with more surface area and based on increased FPF at a more distal part of the lung. The fast rate of absorption of rapamycin from the lungs into the blood is confirmed by the fact that C_{max} values of both groups were found at the first time point as seen in Figure 3.8 (46).

Many mechanisms are responsible for the elimination of drug from the pulmonary tract (47). Once deposited in the lungs, drugs may be eliminated by mucociliary or cough clearance, alveolar macrophages and by drug metabolism in the mucus or lung tissue (cytochrome P450 enzymes). Slowly dissolving drug, in the size ranging from 1.5 to 3 μm , deposited in the alveolar region are more susceptible to being phagocytized by alveolar macrophages(48)(49). Crystalline rapamycin is kinetically more stable and has less surface area when compared to the amorphous TFF formulation. This likely results in a slower dissolution rate in lung fluids and renders the particles more vulnerable to macrophage clearance. TFF rapamycin, on the other hand, is a more thermodynamically unstable amorphous material, which may present increased solubility and hence a faster dissolution rate than its crystalline counterpart (50). The enhanced solubility will create a supersaturated environment directly influencing bioavailability (51). As explained above, as a lipophilic molecule, rapamycin is absorbed rapidly once dissolved in biological fluid.

Due to the increase in solubility, amorphous rapamycin is similar to giving rapamycin in a nebulized solution. Therefore, the slow decline of crystalline rapamycin levels in the pulmonary tract points to a slower dissolution/absorption from lung fluid.

3.4 CONCLUSION

An amorphous formulation of rapamycin was successfully prepared by Thin Film Freezing technology and compared to its crystalline physical mixture counterpart. The low-density brittle dry powder rapamycin formulation exhibit enhanced *in vitro* aerodynamic properties than the physical mixture formulation. Following single dose administration in rats, amorphous TFF rapamycin formulation presented higher *in vivo* systemic bioavailability than its crystalline counterpart. The slow dissolution rate of the crystalline formulation reduced absorption from the lung fluid and reduced systemic bioavailability. Moreover, lung level profiles at 12-24 hours suggest that TFF powder stays in the lung for the same period of time as the crystalline powder but with more surface area and based on increased FPF at a more distal part of the lung.

3.5 TABLES

Samples	Particle size (μm)				SSA \pm SD (m^2/g)
	D ₁₀	D ₅₀	D ₉₀	Span	
Lactose LH200	4.13 \pm 0.11	39.78 \pm 1.32	100.9 \pm 0.27	2.43	0.34 \pm 0.02
Rapamycin	2.8 \pm 0.54	28.83 \pm 3.05	66.46 \pm 10.39	2.21	0.57 \pm 0.08
Wet ball milled lactose	1.34 \pm 0.08	6.41 \pm 0.82	26.05 \pm 3.41	3.85	10.76 \pm 0.01
Wet ball milled rapamycin	1.15 \pm 0.005	5.22 \pm 0.07	13.57 \pm 0.60	2.38	14.29 \pm 0.25
RapaLac_0.75%	-	-	-	-	69.57 \pm 6.25
RapaLac_0.40%	-	-	-	-	85.72 \pm 19.86

Table 3.1 – Particle size distribution and specific surface area of bulk lactose monohydrate and rapamycin as received from supplier, wet ball-milled lactose and rapamycin and amorphous TFF powders RapaLac_0.75% and RapaLac_0.40%.

Formulation	TED (%)	FPF (%)	MMAD (μm)	GSD
RapaLac physical mixture	78.92	36.79	1.81	4.26
RapaLac_0.40%	97.14	72.11	2.1	2.25
RapaLac_0.75%	94.71	61.29	2.43	2.76

Table 3.2 – Next generation cascade impactor results of RapaLac physical mixture, TFF RapaLac_0.40% and RapaLac_0.75% formulations aerosolized using the Handihaler™ device at an airflow rate of 54 L/min for 4.4 seconds.

Pharmacokinetics Parameters	TFF		Crystalline	
	BAL + Lung	Blood	BAL + Lung	Blood
C_0	165.9 ng/g	0 ng/mL	1529.1 ng/g	0 ng/mL
C_{max}	-	3.375 ng/mL	-	4.920 ng/mL
t_{max}	-	0.25h	-	0.25h
AUC_{0-24}	731.1 ng·h/g	23.0 ng·h/mL	7560.6 ng·h/g	16.0 ng·h/mL
AUC_{blood} to $AUC_{BAL+Lung}$ ratio		0.031		0.002
k_{10} (h^{-1})		0.24		0.24
k_{12} (h^{-1})		0.78		0.75
k_{21} (h^{-1})		0.39		0.74
K_{el} (h^{-1})		0.02		0.02

Table 3.3 – Pharmacokinetic parameters for blood and pulmonary tract (lungs and BAL) rapamycin concentration in rats after single-dose inhalation of amorphous RapaLac_0.40% and crystalline RapaLac physical mixture.

3.6 FIGURES

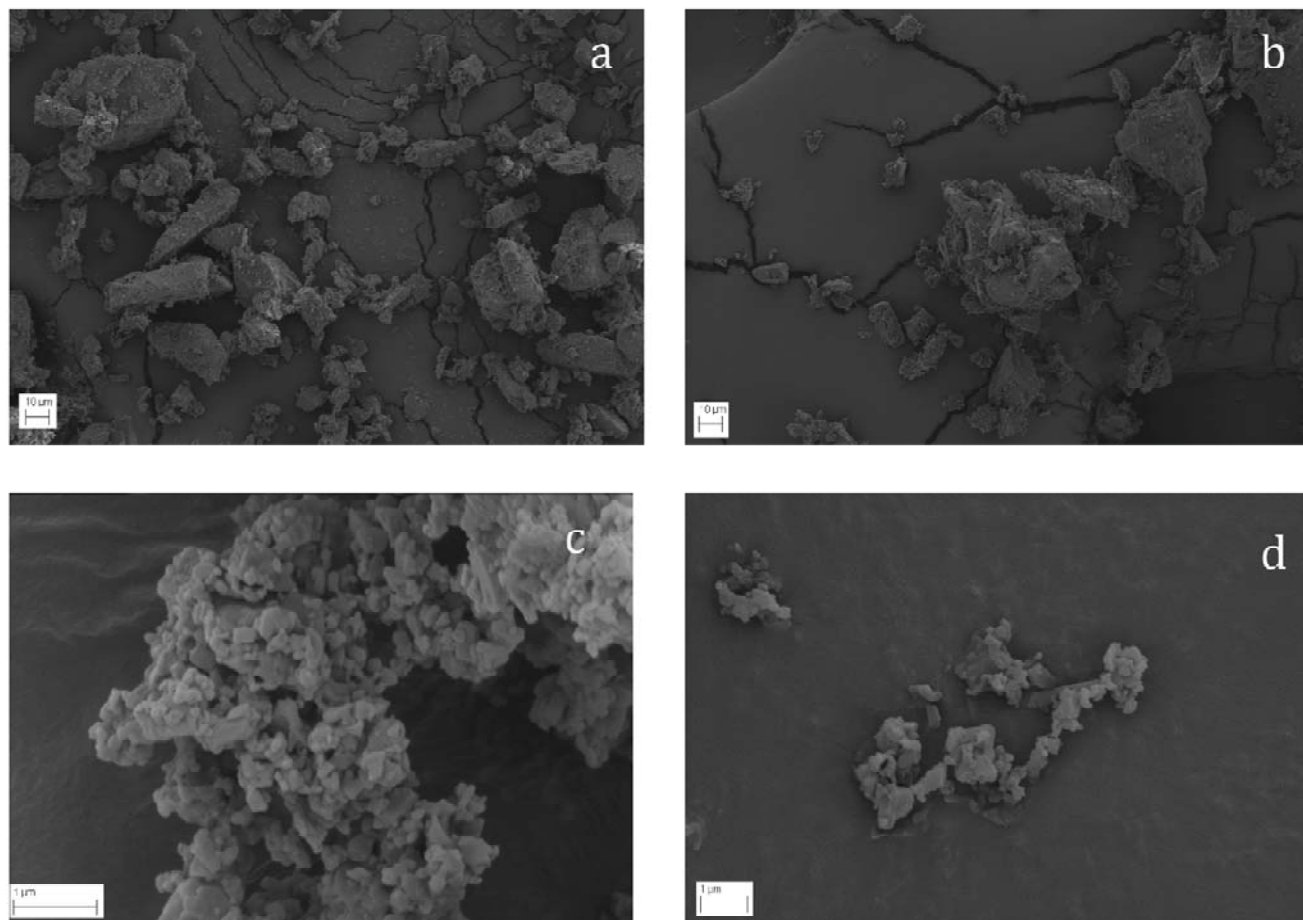


Figure 3.1 – SEM images of (a) lactose monohydrate, (b) rapamycin, (c) wet milled lactose, and (d) wet milled rapamycin.

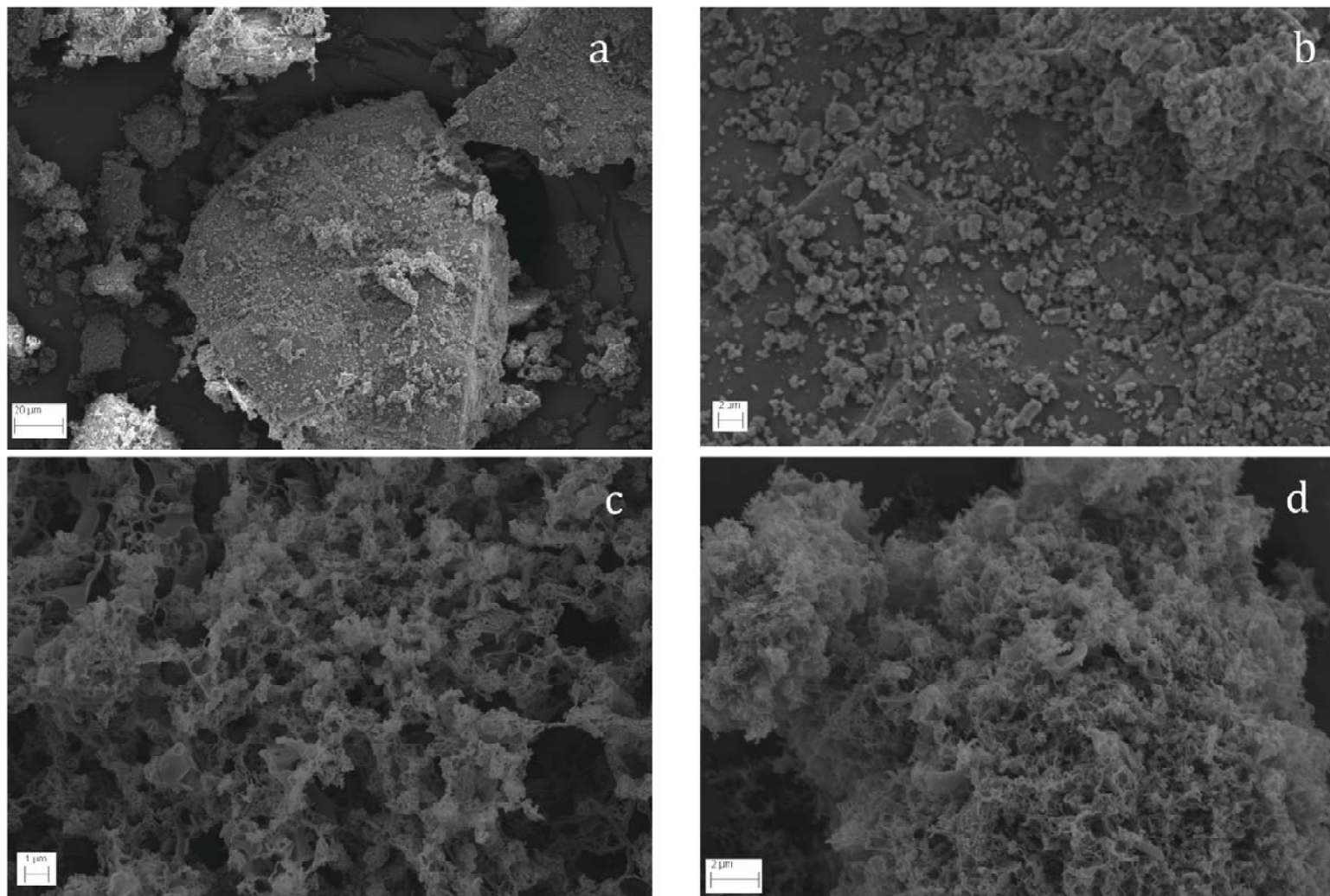


Figure 3.2 – SEM images of (a) RapaLac physical mixture (b) RapaLac physical mixture at higher magnification (c) RapaLac_0.40% (w/v) and (d) RapaLac_0.75% (w/v).

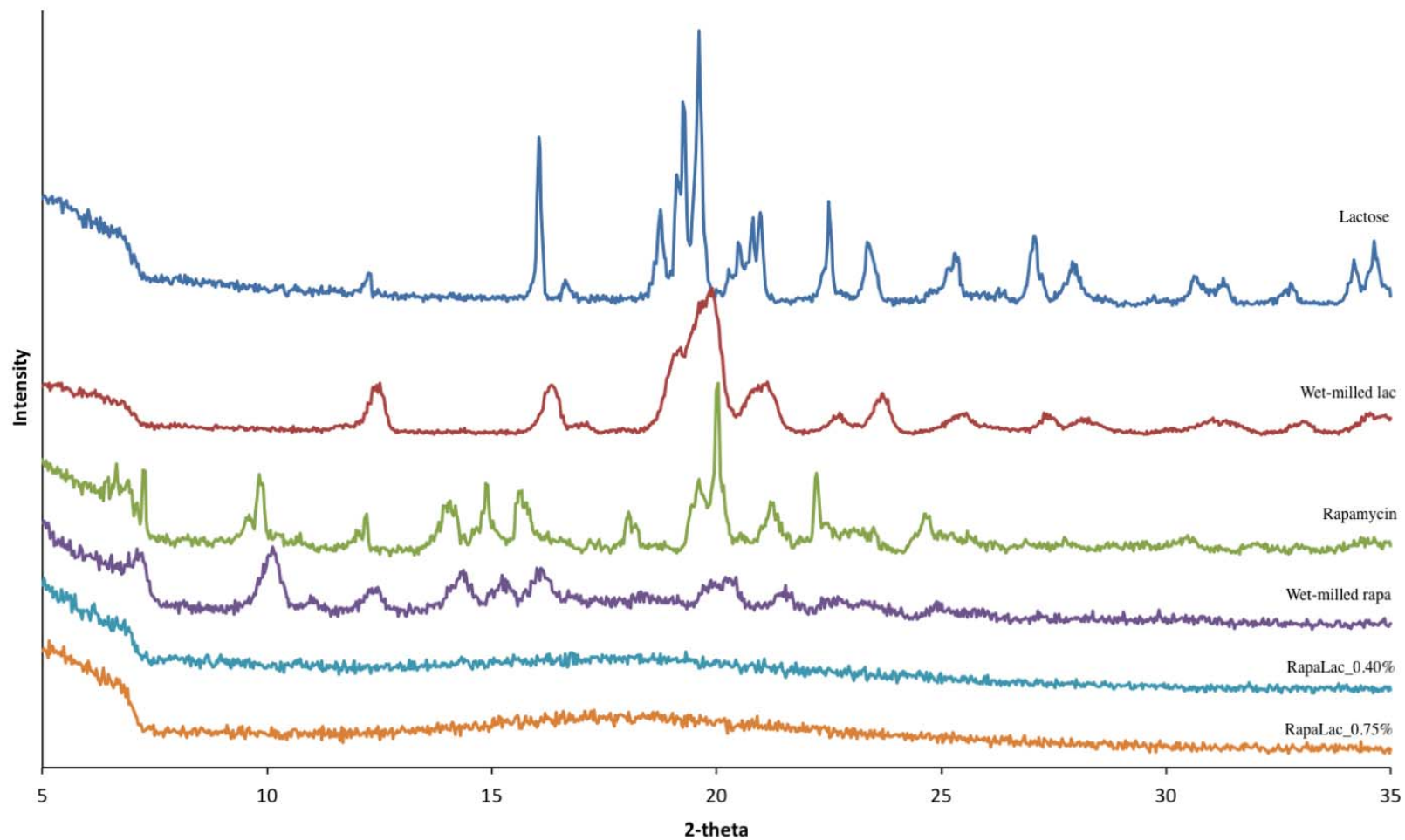


Figure 3.3 – Powder X-ray patterns of bulk lactose monohydrate, wet ball milled lactose monohydrate, bulk rapamycin, wet ball milled rapamycin, TFF RapaLac_0.40% (w/v) and TFF RapaLac_0.75% (w/v).

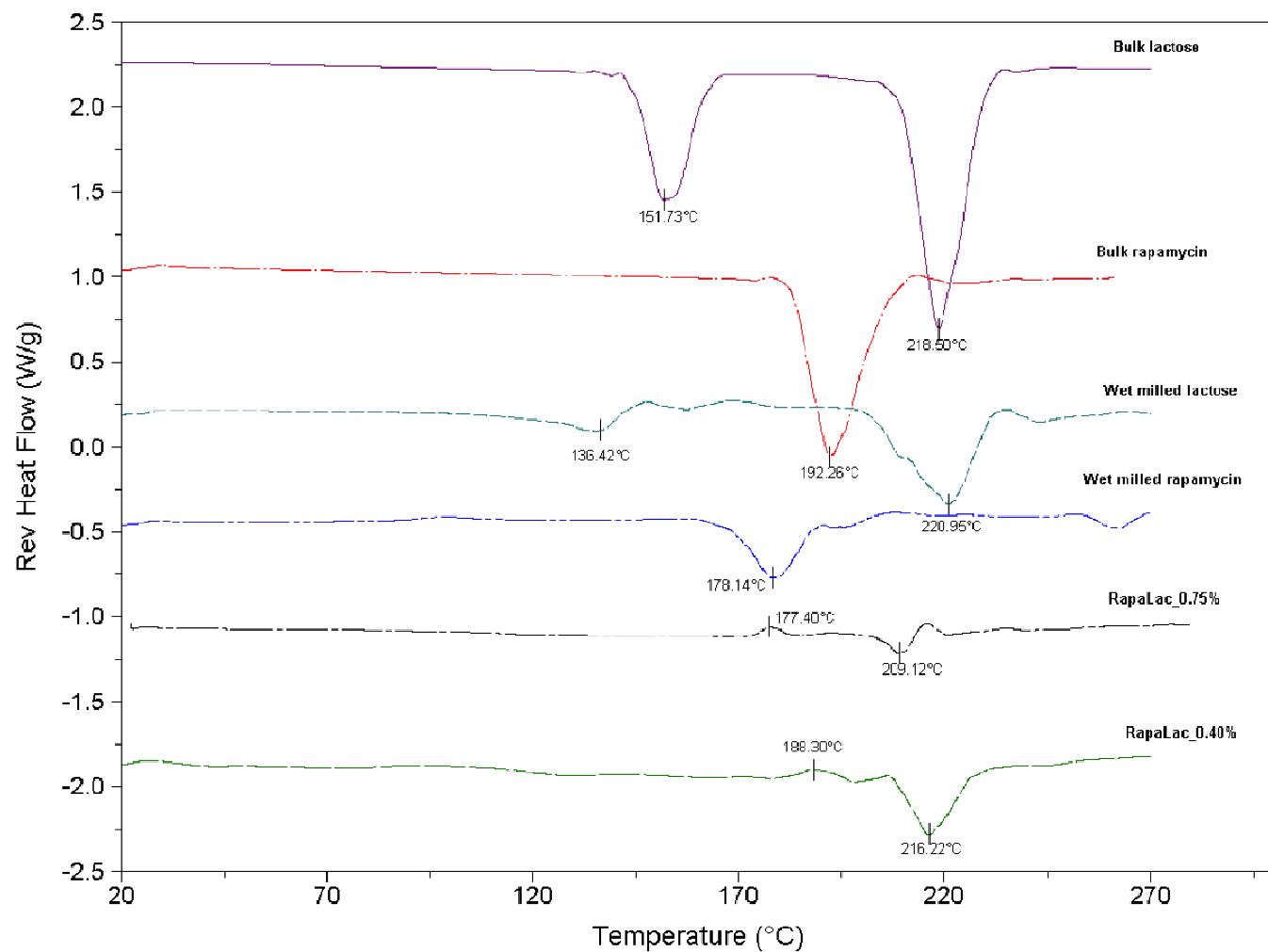


Figure 3.4 – Modulated DSC profiles of bulk lactose monohydrate, bulk rapamycin, wet ball milled lactose monohydrate, wet ball milled rapamycin, RapaLac_0.75% and RapaLac_0.40%.

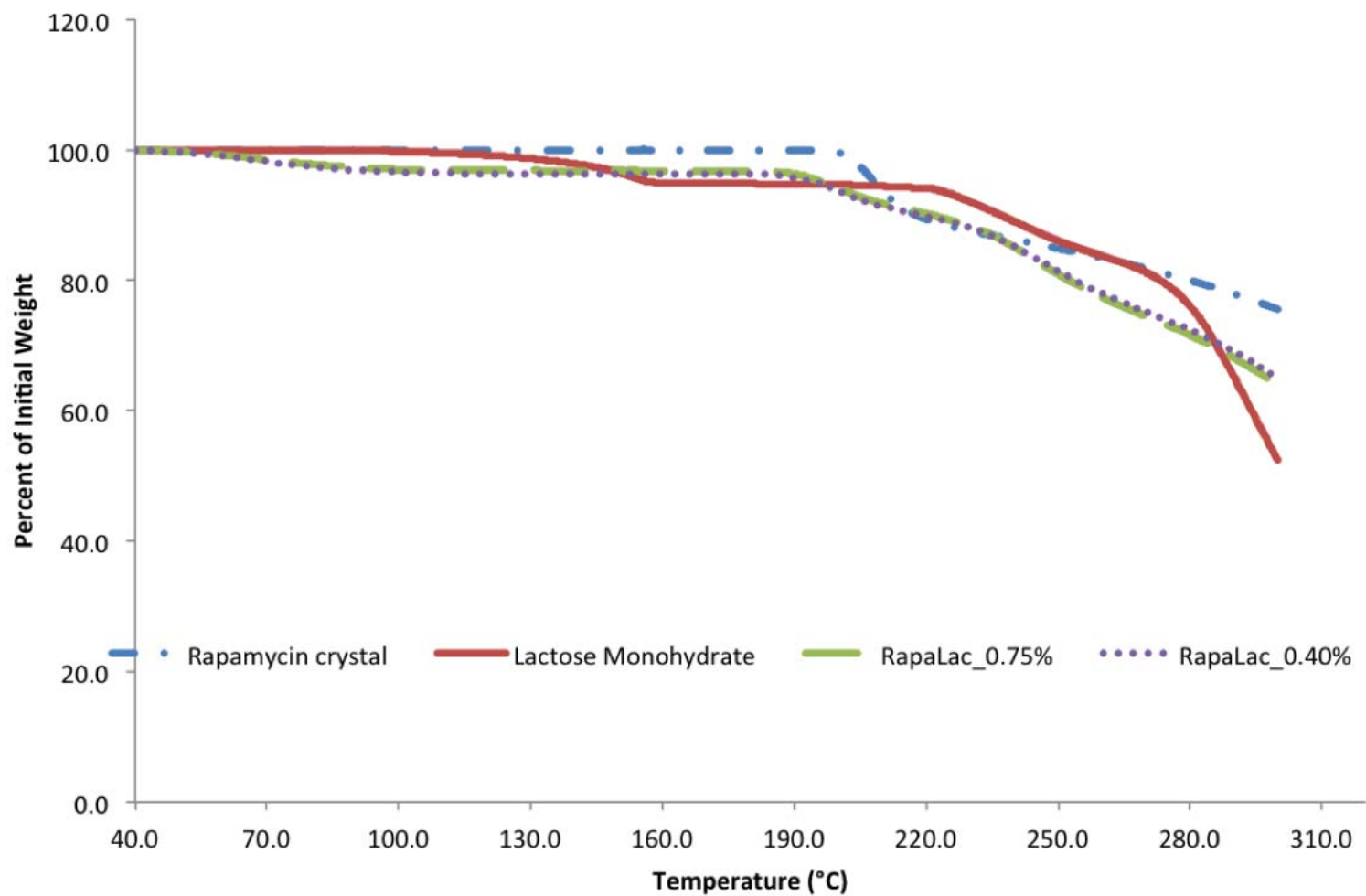


Figure 3.5 – Thermogravimetric analyzes of rapamycin and lactose monohydrate powders as received from supplier, RapaLac_0.75% and RapaLac_0.40%.

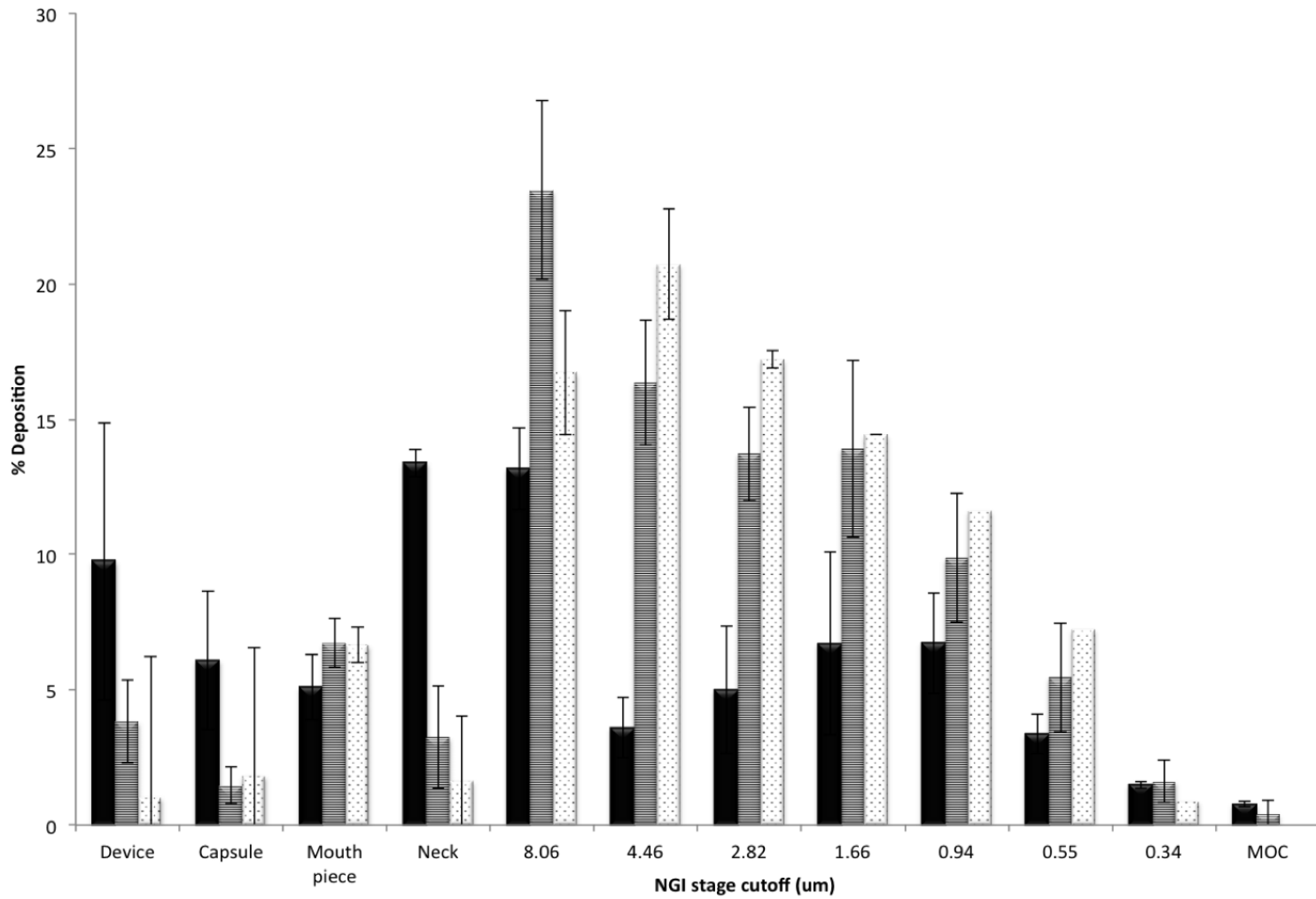


Figure 3.6 – Percent deposition of RapaLac formulations on a NGI showing physical mixture RapaLac in solid dark bars, RapaLac_0.75% in striped bars and RapaLac_0.40% in dotted bars.

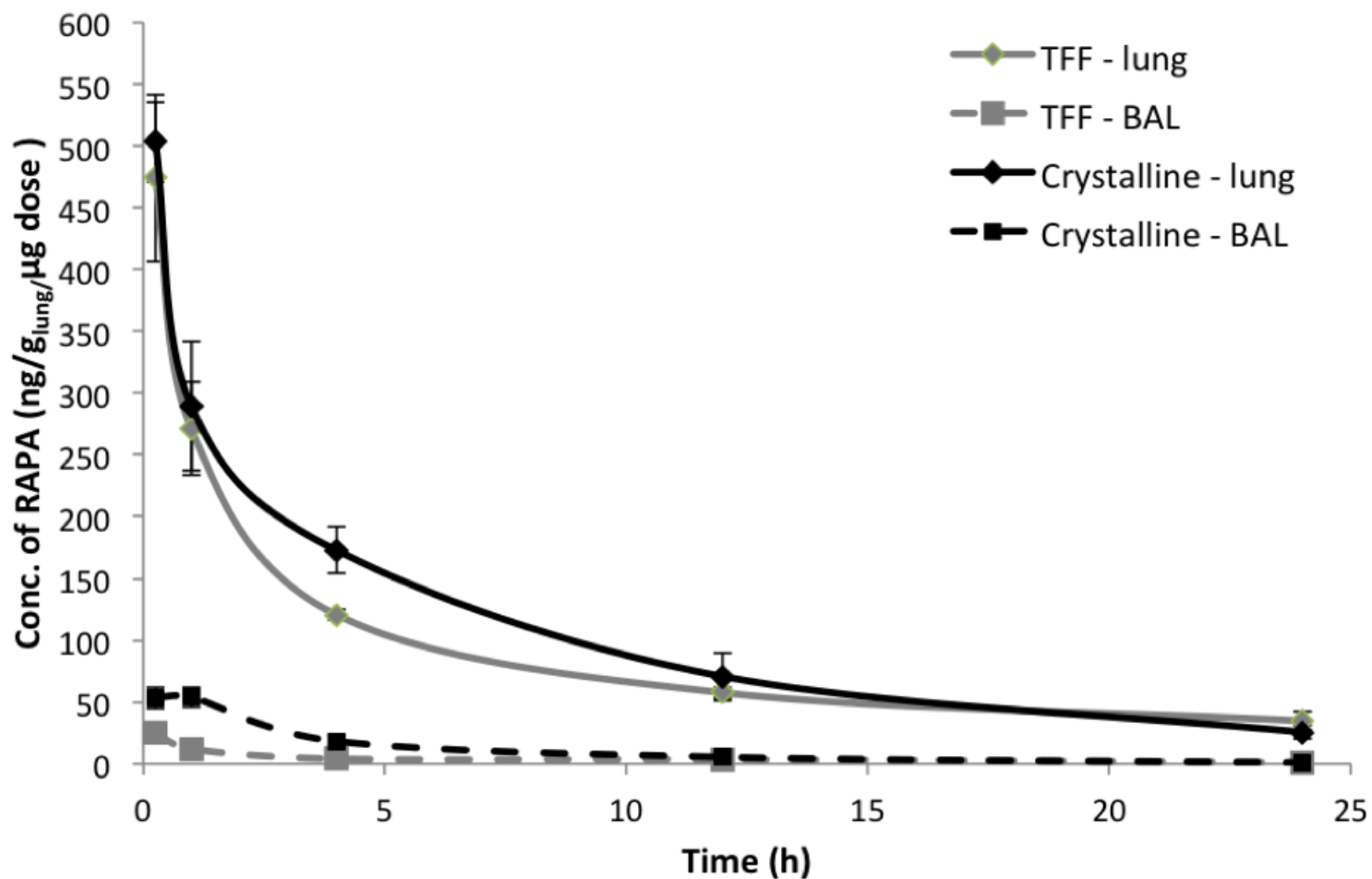


Figure 3.7 – Bronchoalveolar lavage (BAL) and lung concentration of deposited rapamycin in rats after a single-dose administration of crystalline RapaLac physical mixture and amorphous RapaLac_0.40%. Data are presented as mean ± SD, n = 3, and normalized to ng of rapamycin per gram of lung tissue per microgram of dose.

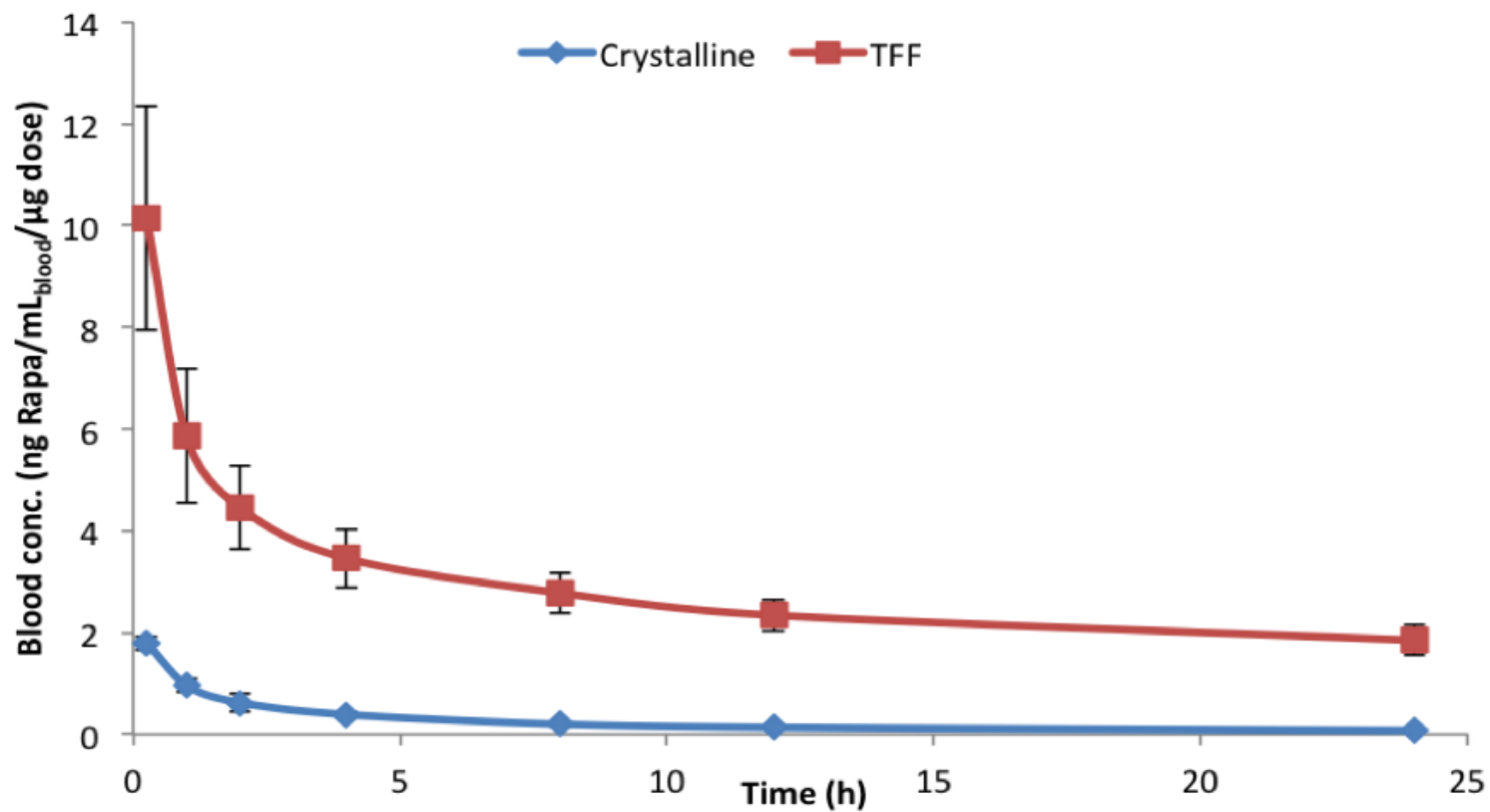


Figure 3.8 – Total whole blood concentration of rapamycin per microgram of dose deposited in the lungs of rats after a single-dose administration of amorphous RapaLac_0.40% and crystalline RapaLac physical mixture. Data are presented as mean \pm SD, n = 3.

3.7 REFERENCES

1. Sehgal S. Sirolimus: its discovery, biological properties, and mechanism of action. *Transplant Proc.* 2003 May;35(3, Supplement):S7–S14.
2. Chhajed PN, Dickenmann M, Bubendorf L, Mayr M, Steiger J, Tamm M. Patterns of pulmonary complications associated with sirolimus. *Respiration.* 2006;73(3):367–74.
3. Stuckey LJ, Bartos CE, McCullough HA, Florn RD, Lama VN, Lin J, et al. Use of Sirolimus in Lung Transplantation: A Single Center Experience. *J Heart Lung Transplant.* 2013 Apr;32(4, Supplement):S89.
4. McCormack FX, Inoue Y, Moss J, Singer LG, Strange C, Nakata K, et al. Efficacy and Safety of Sirolimus in Lymphangiomyomatosis. *N Engl J Med.* 2011;364(17):1595–606.
5. Taveira-DaSilva AM, Hathaway O, Stylianou M, Moss J. Changes in lung function and chyloous effusions in patients with lymphangiomyomatosis treated with sirolimus. *Ann Intern Med.* 2011 Jun 21;154(12):797–805, W–292–293.
6. Simamora P, Alvarez JM, Yalkowsky SH. Solubilization of rapamycin. *Int J Pharm.* 2001 Feb 1;213(1–2):25–9.
7. MacDonald A, Scarola J, Burke JT, Zimmerman JJ. Clinical pharmacokinetics and therapeutic drug monitoring of sirolimus. *Clin Ther.* 2000;22, Supplement 2(0):B101–B121.
8. Hauss DJ. *Oral Lipid-Based Formulations: Enhancing the Bioavailability of Poorly Water-Soluble Drugs.* CRC Press; 2007.
9. Shen L-J, Wu F-LL. Nanomedicines in renal transplant rejection - focus on sirolimus. *Int J Nanomedicine.* 2007;2(1):25–32.

10. Müller R, Junghanns. Nanocrystal technology, drug delivery and clinical applications. *Int J Nanomedicine*. 2008 Oct;295.
11. Kahan BD, Chang JY, Sehgal SN. Preclinical evaluation of a new potent immunosuppressive agent, rapamycin. *Transplantation*. 1991 Aug;52(2):185–91.
12. Hwang S-J, Min-Soo Kim, Jeong-Soo Kim, Hee Jun Park, Won Kyung Cho, Kwang-Ho Cha. Enhanced bioavailability of sirolimus via preparation of solid dispersion nanoparticles using a supercritical antisolvent process. *Int J Nanomedicine*. 2011 Nov;2997.
13. Alemdar AY, Sadi D, McAalister VC, Mendez I. Liposomal formulations of tacrolimus and rapamycin increase graft survival and fiber outgrowth of dopaminergic grafts. *Cell Transplant*. 2004;13(3):263–71.
14. Preetham AC, Satish CS. Formulation of a Poorly Water-Soluble Drug Sirolimus in Solid Dispersions to Improve Dissolution. *J Dispers Sci Technol*. 2011;32(6):778–83.
15. Patton JS, Byron PR. Inhaling medicines: delivering drugs to the body through the lungs. *Nat Rev Drug Discov*. 2007 Jan 1;6(1):67–74.
16. Yang W, Johnston KP, Williams III RO. Comparison of bioavailability of amorphous versus crystalline itraconazole nanoparticles via pulmonary administration in rats. *Eur J Pharm Biopharm*. 2010 May;75(1):33–41.
17. Beinborn NA, Du J, Wiederhold NP, Smyth HDC, Williams III RO. Dry powder insufflation of crystalline and amorphous voriconazole formulations produced by thin film freezing to mice. *Eur J Pharm Biopharm* [Internet]. [cited 2012 Jul 2];(0). Available from: <http://www.sciencedirect.com/science/article/pii/S0939641112001348>
18. Overhoff KA, Engstrom JD, Chen B, Scherzer BD, Milner TE, Johnston KP, et al. Novel ultra-rapid freezing particle engineering process for enhancement of

dissolution rates of poorly water-soluble drugs. *Eur J Pharm Biopharm.* 2007 Jan;65(1):57–67.

19. General Chapters <601> Aerosols, Nasal Sprays, Metered-dose Inhalers, and Dry Powder Inhaler. United States Pharmacop. 35th-NF ed.

20. Cattaneo D, Perico N, Gaspari F. Assessment of sirolimus concentrations in whole blood by high-performance liquid chromatography with ultraviolet detection. *J Chromatogr B.* 2002 Jul 15;774(2):187–94.

21. Ricciutelli M, Di Martino P, Barboni L, Martelli S. Evaluation of rapamycin chemical stability in volatile-organic solvents by HPLC. *J Pharm Biomed Anal.* 2006 Jun 7;41(3):1070–4.

22. Kuehl PJ, Anderson TL, Candelaria G, Gershman B, Harlin K, Hesterman JY, et al. Regional particle size dependent deposition of inhaled aerosols in rats and mice. *Inhal Toxicol.* 2012 Jan;24(1):27–35.

23. Harrison DE, Strong R, Sharp ZD, Nelson JF, Astle CM, Flurkey K, et al. Rapamycin fed late in life extends lifespan in genetically heterogeneous mice. *Nature.* 2009 Jul 16;460(7253):392–U108.

24. Miller RA, Harrison DE, Astle CM, Baur JA, Boyd AR, Cabo R de, et al. Rapamycin, But Not Resveratrol or Simvastatin, Extends Life Span of Genetically Heterogeneous Mice. *J Gerontol A Biol Sci Med Sci.* 2011 Feb 1;66A(2):191–201.

25. Majumder S, Caccamo A, Medina DX, Benavides AD, Javors MA, Kraig E, et al. Lifelong rapamycin administration ameliorates age-dependent cognitive deficits by reducing IL-1 ss and enhancing NMDA signaling. *Aging Cell.* 2012 Apr;11(2):326–35.

26. Rogers TL, Nelsen AC, Hu J, Brown JN, Sarkari M, Young TJ, et al. A novel particle engineering technology to enhance dissolution of poorly water soluble drugs: spray-freezing into liquid. *Eur J Pharm Biopharm.* 2002 Nov;54(3):271–80.
27. Watts AB, Wang Y-B, Johnston KP, Williams RO. Respirable Low-Density Microparticles Formed In Situ from Aerosolized Brittle Matrices. *Pharm Res.* 2013 Mar;30(3):813–25.
28. Haque MK, Kawai K, Suzuki T. Glass transition and enthalpy relaxation of amorphous lactose glass. *Carbohydr Res.* 2006 Aug 14;341(11):1884–9.
29. Steckel H, Bolzen N. Alternative sugars as potential carriers for dry powder inhalations. *Int J Pharm.* 2004 Feb 11;270(1-2):297–306.
30. Baheti A, Kumar L, Bansal AK. Excipients used in lyophilization of small molecules. *J Excipients Food Chem.* 2010;1(1):41–54.
31. FisherScientific, Material Safety Data Sheet: Acetonitrile [HPLC]. 2009.
32. Garnier S, Petit S, Coquerel G. Dehydration mechanism and crystallisation behaviour of lactose. *J Therm Anal Calorim.* 2002;68(2):489–502.
33. Monajjemzadeh F, Hassanzadeh D, Valizadeh H, Siahi-Shadbad MR, Mojarrad JS, Robertson TA, et al. Compatibility studies of acyclovir and lactose in physical mixtures and commercial tablets. *Eur J Pharm Biopharm.* 2009 Nov;73(3):404–13.
34. Rasenack N, Muller BW. Micron-size drug particles: Common and novel micronization techniques. *Pharm Dev Technol.* 2004;9(1):1–13.
35. Saleki-Gerhardt A, Ahlneck C, Zografi G. Assessment of disorder in crystalline solids. *Int J Pharm.* 1994 Jan 25;101(3):237–47.

36. Commissioner O of the. Inspection Guides - Lyophilization of Parenterals (7/93) [Internet]. [cited 2013 Sep 17]. Available from: <http://www.fda.gov/ICECI/Inspections/InspectionGuides/ucm074909.htm>
37. Mohammed H, Roberts DL, Copley M, Hammond M, Nichols SC, Mitchell JP. Effect of Sampling Volume on Dry Powder Inhaler (DPI)-Emitted Aerosol Aerodynamic Particle Size Distributions (APSDs) Measured by the Next-Generation Pharmaceutical Impactor (NGI) and the Andersen Eight-Stage Cascade Impactor (ACI). *AAPS PharmSciTech*. 2012 Jun 8;13(3):875–82.
38. Carvalho TC, Peters JI, Williams III RO. Influence of particle size on regional lung deposition – What evidence is there? *Int J Pharm*. 2011 Mar 15;406(1–2):1–10.
39. Dijoseph J, Sharma R, Chang J. The Effect of Rapamycin on Kidney-Function in the Sprague-Dawley Rat. *Transplantation*. 1992 Mar;53(3):507–13.
40. Meiser BM, Wang J, Morris RE. Rapamycin: A New and Highly Active Immunosuppressive Macrolide with an Efficacy Superior to Cyclosporine. In: Melchers F, Albert ED, Boehmer H, Dierich MP, Pasquier L, Eichmann K, et al., editors. *Prog Immunol* [Internet]. Berlin, Heidelberg: Springer Berlin Heidelberg; 1989 [cited 2013 Jun 21]. p. 1195–8. Available from: http://link.springer.com/content/pdf/10.1007/978-3-642-83755-5_159.pdf#page-1
41. Hausen B, Boeke K, Berry GJ, Segarra IT, Christians U, Morris RE. Suppression of acute rejection in allogeneic rat lung transplantation: a study of the efficacy and pharmacokinetics of rapamycin derivative (SDZ RAD) used alone and in combination with a microemulsion formulation of cyclosporine. *J Heart Lung Transplant Off Publ Int Soc Heart Transplant*. 1999 Feb;18(2):150–9.

42. Napoli KL, Wang M-E, Stepkowski SM, Kahan BD. Distribution of sirolimus in rat tissue. *Clin Biochem.* 1997 Mar;30(2):135–42.
43. Lee H, Blaufox M. Blood-Volume in the Rat. *J Nucl Med.* 1985;26(1):72–6.
44. Tolman JA, Williams RO. Advances in the pulmonary delivery of poorly water-soluble drugs: influence of solubilization on pharmacokinetic properties. *Drug Dev Ind Pharm.* 2010;36(1):1–30.
45. Yanez JA, Forrest ML, Ohgami Y, Kwon GS, Davies NM. Pharmacometrics and delivery of novel nanoformulated PEG-b-poly(epsilon-caprolactone) micelles of rapamycin. *Cancer Chemother Pharmacol.* 2008 Jan;61(1):133–44.
46. Patton, John S., Fishburn, C. Simone, Weers, Jeffrey G. The Lungs as a Portal of Entry for Systemic Drug Delivery (thoracic). *Am Thorac Soc.* 2004;1(4):338–44.
47. Ferin J. Pulmonary retention and clearance of particles. *Toxicol Lett.* 1994 Jun;72(1–3):121–5.
48. Lombry C, Edwards DA, Preat V, Vanbever R. Alveolar macrophages are a primary barrier to pulmonary absorption of macromolecules. *Am J Physiol-Lung Cell Mol Physiol.* 2004 May 1;286(5):L1002–L1008.
49. Labiris NR, Dolovich MB. Pulmonary drug delivery. Part I: Physiological factors affecting therapeutic effectiveness of aerosolized medications. *Br J Clin Pharmacol.* 2003 Dec;56(6):588–99.
50. Alonzo DE, Zhang GG., Zhou D, Gao Y, Taylor LS. Understanding the behavior of amorphous pharmaceutical systems during dissolution. *Pharm Res.* 2010;27(4):608–18.

51. Vaughn JM, McConville JT, Crisp MT, Johnston KP, Williams III RO. Supersaturation Produces High Bioavailability of Amorphous Danazol Particles Formed by Evaporative Precipitation into Aqueous Solution and Spray Freezing into Liquid Technologies. *Drug Dev Ind Pharm*. 2006 Jun;32(5):559–67.

Chapter 4: Inhaled Therapies of Fixed-dose Combinations Prepared by Thin Film Freezing

Abstract

The use of Thin Film Freezing technology (TFF) to produce a triple fixed dose therapy with enhanced aerosol properties was investigated. Formoterol fumarate (LABA), tiotropium bromide (LAMA) and budesonide (ICS) were used as therapeutic drugs and lactose monohydrate and mannitol were used as sugar excipients. We investigated applications of this technology to powder properties and *in vitro* aerosol performance with respect to single and combination therapy. The aerosol performance of TFF powder combination was compared to the physical mixture of micronized crystalline powders prepared using jet milling process. TFF powder prepared with lactose produced amorphous, low-density matrix with greater specific surface area than mannitol powder forming few hydrogen bonding interactions. TFF powder prepared with mannitol produced crystalline, low-density matrix with strong hydrogen bonding interactions. As a result, the brittle TFF powders presented superior properties than the physical mixture of micronized crystalline powders, such as excellent particle distribution homogeneity after *in vitro* aerosolization.

4.1 INTRODUCTION

Chronic obstructive pulmonary disease (COPD) is a chronic inflammatory disease characterized by a slow progressive development of airflow limitation that is not fully reversible (1). Currently, the therapies available to treat COPD are efficient in managing the progress of the disease and reducing the severity and frequency of exacerbations (2). However, to date, none of the existing medications for COPD are capable of eradicating the disease. Asthma, another example of airways inflammatory disease, is characterized by excessive sensitivity of the lungs or airways to various environmental triggers (3). Unlike COPD, asthma reactions are reversible and in most cases, controlled by the use of medication (4).

According to the Global initiative for chronic obstructive lung disease, the use of a combination of bronchodilators with different mechanisms and durations of action may increase the degree of bronchodilation in a patient whilst decreasing side effects experienced. Furthermore, concentrating the use of multiple medicines in one inhaler may improve patient compliance (5). The most common forms of combination therapies involve the use of two active bronchodilators such as short-acting β 2-agonists (SABA) and anticholinergic/long-acting muscarinic antagonist (LAMA) or long-acting β 2-agonists (LABA) and inhaled corticosteroids (ICS) in one inhaler. When exacerbation or breathlessness persists in patients taking LABA/ICS dual combination, the use of a triple inhalation therapy of LABA, LAMA and ICS would be advised (6)(7)(8). A significant example was seen in 2001, when GlaxoSmithKline (United Kingdom) launched Seretide/Advair Diskus[®], a product which combines ICS and LABA. The result of fluticasone propionate (ICS) with salmeterol xinafoate (LABA) proved more effecting in reducing the effects of asthma and COPD when used in combination than when used individually. Additionally, it has been hypothesized that the success of Advair can be

attributed to the synergistic action of fluticasone and sameterol, when both drugs co-deposit at the target cells (9). Another example of fixed combination therapy is Symbicort[®] launched by Astrazeneca in 2007. This product involves the amalgamation of budesonide (ICS) and formoterol fumarate dehydrate (LABA) which offers 12 hours symptom relief for asthmatic patients, a significant improvement on previous therapies (10)

Tiotropium bromide (LAMA) has only been approved for the treatment of COPD. However in 2013, a phase III clinical trial named PrimoTinA-asthma conducted by Boehringer Ingelheem, reported the safety and efficacy of the use of tiotropium bromide to treat patients with asthma. Moreover, the use of tiotropium bromide (LAMA) has yielded positive results in asthmatic patients already using ICS and LABA therapy.

One of most challenges in formulating a fixed dose combination lies in the ability to achieve dose uniformity and co-deposition in a powder blend of two or more actives with coarse carrier particles. Additional difficulties are encountered when blending drugs that are prepared from mechanically milled micronized particles due to the interparticulate forces and formation of amorphous domains. Adi et al. reported the successful formulation and co-deposition of a triple therapy drug formulation. No significant difference was found between the drugs in the cascade impactor stage depositions (11). However, the triple therapy was formulated as a solution based pressurized metered dose inhaler (pMDI), where all three drugs were dissolved in the propellant. Solution pMDIs are not a suitable technique for the preparation of a wide variety of drugs that are insoluble in the solvent (usually ethanol) and/or the propellant. Likewise, the presence of multiple drugs in solution, most probably, will present stability issues. Therefore, particle engineering may be a good alternative to produce a fixed dose therapy in powder form where all drugs are present within a single particle, resulting in

improved content uniformity, co-deposition and co-location of drugs at the target of action. This increases the potential of synergistic action. Price et al. reported the use of a sonocrystallization particle engineering method (SAX™) to produce crystalline spheroidal particles of two drugs. This technology has shown to efficiently deliver each component with co-deposition of the particles within the cascade impactor. Even though this technology is considered an efficient means to produce fixed dose formulations, the process of production process may be over engineered due to the number of steps and complex equipment required (10). Formulation of triple fixed-dose combination has also been developed by Pearl Therapeutics (California, US). An emulsion of DSPC (1,2-distearoyl-sn-glycero-3-phosphocholine) and anhydrous calcium chloride are prepared and spray dried to form porous microparticles. Sequentially, the porous microparticles are mixed with micronized drugs, which are then cosuspended in 1,1,1,2-tetrafluoroethane (HFA 134a) propellant. The drug microparticles irreversibly adheres to the porous particle surfaces forming a stable suspension with equivalency in dose delivered for each drug (12). The creation of cocrystals comprising 2 or 3 drugs in the same crystal lattice having the same properties seems to be a good alternative produce fixed-dose combination formulation. However, the production of cocrystals is difficult and requires micronization and blending with a coarse carrier (13)(14).

Thin Film Freezing (TFF) has shown to be a suitable particle engineering method to produce brittle powder matrices for pulmonary delivery (15). The rapid freezing of drug solution onto a cryogenic surface prevents segregation and heterogeneity of the solutes. When freezing is complete, the formulation is lyophilized and generates a low-density matrix powder, which is easily aerosolized and dispersible at the time of inhalation(15). The aim of this study is to investigate the use of TFF technology to produce triple fixed dose therapy using formoterol fumarate (LABA), tiotropium bromide

(LAMA) and budesonide (ICS) as therapeutic drugs. We investigated powder properties and *in-vitro* aerosol performance with respect to single and combination therapies.

4.2 MATERIALS AND METHOD

4.2.1 Materials

Budesonide, formoterol fumarate and tiotropium bromide were purchased from Chemieliva Pharmaceutical Co. (Chongqing, China). D-(+)-Mannitol was purchased from Acrōs Organics (Geel, Belgium) and lactose monohydrate (Lactohale® LH 200) was kindly donated by Friesland Foods Domo (Zwolle, Netherlands). High performance liquid chromatography (HPLC) grade acetonitrile was purchased from Fisher Scientific (Fair Lawn, NJ) and perchloric acid 8% w/v aqueous was purchased from Ricca Chemicals (Arlington, TX). Water was purified by reverse osmosis (MilliQ, Millipore, France).

4.2.2 Formulation Preparation

Thin Film Freezing technology was used for the preparation of low-density dry powder as described elsewhere (16). Triple combo formulations were prepared using the weight ratio of 1:2:35.5 for formoterol, tiotropium and budesonide, respectively. The ratio chosen was based on the typical doses used to treat COPD patients, according to the Global initiative for chronic Obstructive Lung Disease (GOLD), Inc. The following mixtures were prepared by dissolving the components in a co-solvent mixture of three parts of acetonitrile and two parts of water: budesonide/tiotropium/formoterol and mannitol (BTF_Man), budesonide and mannitol (Bud_Man), tiotropium and mannitol (Tio_Man), formoterol and mannitol (For_Man), budesonide/tiotropium/formoterol and

lactose (BTF_Lac), budesonide and lactose (Bud_Lac), tiotropium and lactose (Tio_Lac), formoterol and lactose (For_Lac). The ratio of drug(s) to sugar excipient was 1 to 1 and the final solid loading concentration was 0.50% (w/v).

Solutions were rapidly frozen on a cryogenically cooled (-80°C) stainless steel surface using the thin film freezing apparatus. The frozen disks were collected in a container filled with liquid nitrogen to avoid melting. The frozen formulations were transferred to a -70°C freezer until complete evaporation of the liquid nitrogen and then transferred to a VirTis Advantage Lyophilizer (VirTis Company Inc., Gardiner, NY) for solvent removal. Formulations were lyophilized over 24 h at -40°C at pressure of 400 mTorr, temperature was gradually ramped to 25°C over 24 h with pressure less than 200 mTorr, and kept at 25°C for 24 h.

For comparison purposes, the equivalent physical mixtures of budesonide/tiotropium bromide/formoterol fumarate and mannitol (BTF_Man_PM) and budesonide/tiotropium bromide/formoterol fumarate and lactose (BTF_Lac_PM) were prepared using the same weight ratio as described previously. The actives were micronized using a fluid energy laboratory jet-o-miser (Fluid Energy, Telford, PA) with pusher pressure set at 80 psi and the gridding pressures set at 100 psi. Precise amounts of micronized powders were weighed and mixed using the geometric dilution technique and then transferred to a stainless steel vessel. The vessel was placed in a Turbula mixer (Glen greston Ltd., Middx, UK) and mixing was carried out for 20 min at 45 revolutions per minute (rpm). Formulations were sieved through 100 and 45 µm mesh size before and after mixing.

4.2.3 Thermal analysis

The TA Instruments modulated Differential Scanning Calorimeter (mDSC 2920) (New Castle, DE), equipped with a refrigerated cooling system, was used to analyse the thermal properties and the degree of crystallinity of the powders. Dry nitrogen was used as the purge gas for the mDSC cell at a flow rate of 40 mL/min. Sample weights of 4 to 10 mg were placed into open aluminum pans and hermetically sealed (kit 0219-0041, Perkin-Elmer Instruments, Norwalk, CT). Experiments were carried out in the range of 10 to 350°C at a heating rate of 10°C/min and modulation temperature amplitude of 1°C/min. Data was analyzed using TA Universal Analysis 2000 software (TA Instruments, New Castle, DE).

4.2.4 Powder X-ray diffraction (PXRD)

Crystallinity properties of the dried powders of raw actives as purchased as well as the jet milled and TFF powder formulations were investigated using a Philips 1710 X-ray diffractometer (Philips Electronic Instruments Inc. Mahwah, NJ). Measurements were taken from 5° to 35° on the 2-theta scale at a step size of 0.03°/s and a dwell time of 5s.

4.2.5 Particle size analyses

Measurement of particle size distributions of budesonide, tiotropium bromide and formoterol fumarate before and after jet milling were measured by laser diffraction (HELOS, Sympatec GmbH, Clausthal-Zellerfeld, Germany). A small amount of formoterol fumarate and Tiotropium bromide were separately dispersed in 10 mL 0.01% tween 80 mineral oil and a small amount of budesonide was dispersed in 10 mL 0.01% tween 80 in deionized water. The samples were sonicated for 5 minutes and diluted with enough solvent to produce light obscuration in the range of 15–20%. The sizes reported

are average values of at least 3 measurements. The results are presented as $D_{(x)}$ and span, where X is the cumulative percentile of particles under the referred size (e.g. $D_{(50)}$ corresponds to the median diameter of the particles). Span is a measurement of particle size distribution calculated as $[(D_{(90)} - D_{(10)})/D_{(50)}]$.

4.2.6 Scanning Electron Microscopy (SEM)

Powder morphologies and estimation of particle sizes were determined using a SEM. Samples were placed on carbon tape and coated with gold/palladium (60/40) for 20 seconds under high vacuum using a Cressington 208 Benchtop Sputter Coater (Watford, England). The SEM images were captured using a SmartSEM[®] graphical user interface software in a Carl Zeiss Supra[®] 40VP (Carl Zeiss, Oberkochen, Germany) operated under vacuum, at a working distance of 19 mm and at 5 kV of Electron High Tension (EHT).

4.2.7 Brunauer-Emmett-Teller (BET) specific surface area (SSA) analysis

Powder porosity was determined through the measurement of the specific surface area (SSA) using a Monosorb MS-22 rapid surface area analyzer (Quantachrome Instruments, Boynton Beach, Florida). The instrument uses a modified BET equation for SSA determination. Samples were degassed in a Thermoflow[™] Degasser for at least 2 hours at 25°C using 30% nitrogen in helium as the desorbate gas.

4.2.8 Fourier Transform Infrared Spectroscopy (FTIR)

FTIR spectroscopy was used to characterize chemical interactions and/or amorphous and crystalline polymorphs of each sample. FTIR scans of dry samples were collected on a Nicolet IR100 spectrometer (Thermo Fisher Scientific, Pittsburgh, PA)

equipped with a Deuteriated tri-glyceride sulfate (dTGS) detector. KBr disc method was used with approximately 1% (w/w) sample loading. A total of 32 scans were accumulated at a resolution of 4 cm^{-1} in the region of 4000 to 600 cm^{-1} .

4.2.9 *In vitro* aerosol performance

Aerodynamic particle size distribution and deposition homogeneity were evaluated by the Next Generation Cascade Impactor (NGI) (MSP Corporation, Shoreview, MN) using a Handihaler[®] device attached to the induction port by a mouthpiece adaptor made of silicon. The cascade impactor was assembled and operated in accordance to the USP General Chapter <601> Aerosol, Nasal Spray, Metered-dose Inhalers and Dry Powder Inhalers. The device was run for 4.4 seconds at a pressure drop of 4kPa across the device corresponding to a flow rate of 54 L/min, which was calibrated using a TSI mass flowmeter (Model 4000, TSI Inc., St. Paul, MN). The NGI collection plates were coated with 1% (v/v) silicone oil in hexane to prevent particle bounce, fracture and reentrainment. Three capsules were fired in sequence into the NGI and the experiments were performed in triplicate for each formulation under investigation. After aerosolization, samples were collected using known volumes of diluent and analyzed by high performance liquid chromatography (HPLC).

Emitted dose (ED) was calculated as the percentage of drug emitted from the DPI. Fine particle fraction (FPF) was calculated as the sum of assayed dose deposited on stages 2 through micro-orifice collector (MOC) corresponding to particles with and aerodynamic diameter $\leq 4.46\ \mu\text{m}$. Mass median aerodynamic diameter (MMAD) was calculated via regression of a log-probability plot of cumulative percent versus cut-off diameter and geometric standard deviation (GSD) was calculated as the square root of the 84th/16th percentile.

4.2.10 HPLC assay

Chemical analyses of all drugs were performed using a Dionex 3000 HPLC system equipped with UV detector set at 230 nm wavelength. A 20 μL injection volume was injected into a Inertisil C₈ 5 μm 150 x 4.6 mm reversed-phase column (Thermo Fisher Scientific, Waltham, MA) maintained at 26°C. Gradient elution was used and the mobile phase consisted of a 0.2 % v/v perchloric acid solution as solvent-A and acetonitrile as solvent-B, running at a flow rate of 1.2 mL/min and run time of 10 minutes, as described elsewhere(17). The method was tested with regard to variability, recovery, linearity, detection limit and range, and shown to be suitable for this study.

4.2.11 Statistical analysis

The data is expressed as a mean \pm standard deviation (SD). Statistical analyses were performed using NCSS/PASS software Dawson edition. Significant differences between formulations and between the percentage distributions of all three drugs on the NGI stages were analyzed using One-way ANOVA ($p < 0.05$).

4.3 RESULTS AND DISCUSSION

4.3.1 Particle size and morphology of formulations

Particle size analyzes by laser diffraction and scanning electron microscopy images of the bulk drug and excipient powders showed that the sizes of the particles are not suitable for lung delivery. SEM images of budesonide and tiotropium display irregular shape with D₅₀ values of 22.11 ± 16.92 and 5.14 ± 0.03 μm respectively and

broad particle size distributions confirmed by the large span values of 2.31 and 2.14 (Table 4.1 and Figures 4.1a and 4.1b). Formoterol, on the other hand, displays a plate-like shape with D_{50} values of $6.27 \pm 0.97 \mu\text{m}$ and greater span value of 7.75 (Table 4.1 and Figure 4.1c). In addition, specific surface area measurements (SSA) gave small surface area values of $3.05 \pm 0.21 \text{ m}^2/\text{g}$ for budesonide, $2.08 \pm 0.13 \text{ m}^2/\text{g}$ for tiotropium and $2.97 \pm 0.05 \text{ m}^2/\text{g}$ for formoterol indicating that the bulk powders contain large particles.

Coarse lactose and mannitol were used as carriers to enhance powder dispersion at time of aerosolization. SEM images of both powders show irregular shape with D_{50} values of $39.78 \pm 1.32 \mu\text{m}$ for lactose and $52.70 \pm 0.59 \mu\text{m}$ for mannitol. Although the particle sizes of lactose and mannitol were bigger than those of the raw drugs, nevertheless, the particle size distributions were similar with span values of 2.43 and 1.80, respectively (Table 4.1 and Figures 4.1d and 4.1e).

In order to prepare the triple combo physical mixture formulations for comparison purposes with the TFF formulations, particle size reduction of the three drug powders was necessary. Laser diffraction results indicate that the size reduction process was only significant for bulk budesonide powder with D_{50} values of $3.40 \pm 0.09 \mu\text{m}$ and broad particle size distribution with span value of 2.58. Interestingly, the SSA of bulk budesonide decreased to $2.75 \pm 0.13 \text{ m}^2/\text{g}$ regardless of the reduction in particle size (Table 4.1). This could be due to aggregation of the micron size particles, which can be caused by cohesive forces generated during the uncontrolled milling process resulting in electrostatically charged particles with heterogeneous shapes as shown Figure 4.2a. Laser diffraction results of tiotropium and formoterol show a slight reduction in particle size after milling process with D_{50} values of 4.65 ± 0.04 and $4.51 \pm 0.02 \mu\text{m}$, respectively. Moreover, particle size distribution of tiotropium shows a small reduction with span value of 2.0 where as formoterol showed a significant reduction in particle size range

with span value of 1.96 (Table 4.1). SEM images of tiotropium and formoterol show agglomerated micronized powders with irregular shapes and the SSA results confirm the reduction in particle sizes with increased values to 2.86 ± 0.11 and 5.08 ± 0.26 m²/g, respectively (Figures 4.2b and 4.2c). SEM images of the physical mixture of micronized drugs with coarse lactose and coarse mannitol are shown in Figures 4.2d and 4.2e. The images show micronized drug powders adhered to the coarse lactose and mannitol surfaces, which may improve powder dispersion and aerosolization at the time of inhalation. Due to the mixture with coarse lactose and mannitol, the physical mixture formulations produced small SSA values of 0.43 ± 0.05 and 0.32 ± 0.03 m²/g (Table 4.1).

SSA measurements of TFF powder formulations show a significant increase in surface area due to the highly porous cake powder formed after lyophilization of the frozen discs (Table 4.1). Tiotropium formulations produced the least porous cakes with SSA values of 38.79 ± 0.81 m²/g for Tio_Man and 48.90 ± 2.42 m²/g for Tio_Lac. The SSA values for budesonide were much higher than those of the tiotropium formulations with values of 46.97 ± 2.22 m²/g for Bud_Man and 90.39 ± 6.15 m²/g for Bud_Lac. Formoterol formulations, however, presented the greatest SSA values of 64.14 ± 0.68 m²/g for For_Man and 193.86 ± 10.63 m²/g for For_Lac. The triple combo formulations also produced large SSA values of 54.55 ± 1.10 m²/g for BTF_Man and 81.31 ± 1.71 m²/g for BTF_Lac. These are very similar to the SSA values of budesonide formulations, as the triple combo has a high percentage of formulations (Table 4.1). The difference in powder density and porosity can be seen in the SEM images. Powder formulations with greater SSA values also show a more porous cake structure as shown in Figures 4.3 and 4.4.

4.3.2 Crystallinity evaluation

4.3.2.1 Budesonide

Budesonide was supplied as a micronized powder. PXRD pattern of budesonide exhibit high intensity peaks at 11.81° , 15.2° , 15.77° , 18.14° and 22.46° of 2Θ , indicating its crystalline structure, which is in accordance with data reported by Tajber et al, as shown in Figure 4.9c (18). The mDSC profile of bulk budesonide powder shows a single endothermic melting peak at 251.4°C (Figure 4.5) similar to the data reported by Velaga et al. confirming its crystalline properties(19). After jet milling process, micronized budesonide powder remained crystalline as shown by mDSC peak profile (Figure 4.5) and PXRD pattern (Figure 4.9c). The mDSC profile shows a slight shift of the endothermic melting peak with peak maxima at 252.6°C . Accordingly, PXRD pattern shows a reduction in the peak intensities but the sample remains mostly crystalline. The observed shift of endotherm peak and the reduction of the PXRD peak intensities may be a result of a change in the crystalline structure of the powder at the time of comminution. The milling process disrupts the crystal structure on the particle surface and creates amorphous domains (20).

Thin film freezing (TFF) of budesonide formulation prepared with mannitol yielded partially crystalline powders, as confirmed by the mDSC (Figure 4.6) and PXRD (Figure 4.8f) results. The PXRD pattern of Bud_Man shows peaks with small intensities characterizing a partially crystalline formulation. From the mDSC profile, Bud_Man exhibit one exothermic recrystallization peak at 126.2°C and two endothermic melting peaks, one at 167.4°C , corresponding to the melting point of mannitol and the second at 242.3°C corresponding to the melting of budesonide. These results confirm the partially amorphous nature of the Bud_Man formulation. Kim et al. investigated the

physicochemical characteristics of mannitol after lyophilization and reported that lyophilized mannitol yields a partially crystalline powder as a consequence of the low glass transition temperature of the pure amorphous powder, which is observed at 13°C. The study also reports that the relative concentration of crystalline mannitol in the formulation should be above 30% (w/w) in order to be detected by PXRD (15).

Regarding the PXRD pattern of TFF Bud_Lac formulation, shown in Figure 4.8j, broad and diffuse halos were present with an absence of the characteristic crystalline peaks, indicating an amorphous structure. Figure 4.7 shows the modulated DSC thermogram which indicates two recrystallization events, in which the first peak may represent the recrystallization of lactose at 131.4°C, and the second peak may represent the recrystallization of budesonide at 180.2°C. The recrystallization events confirm that an amorphous structure is formed by the ultra rapid freezing process. Two endothermic melting peaks are also observed, which may correspond to the melting of lactose at 212.8°C and budesonide at 245.7°C. The two exothermic and endothermic peaks may indicate the formation of a solid dispersion system and a posterior phase separation of budesonide and lactose at the time of analysis (16).

4.3.2.2 Tiotropium Bromide

The PXRD pattern of tiotropium bromide exhibits crystalline high intensity peaks at 5.81°, 16.13°, 19.79°, and 26.6° of 2 Θ (Figure 4.9e). The crystallinity of this sample is confirmed by the mDSC profile of the bulk tiotropium powder, which exhibits a single endothermic melting peak at 219.0°C (Figure 4.5). Micronized tiotropium powder obtained by jet milling remained crystalline, indicated by the absence of an exothermic recrystallization peak and the presence of an endothermic melting peak at 219.3°C in the mDSC profile (Figure 4.5). However, the PXRD pattern shows a significant decrease in

the intensity of crystalline peak diffractions, probably as a result of the loss of powder crystallinity and the formation of amorphous domains (14).

The TFF Tio_Man formulation, which was prepared with mannitol as a stabilizing sugar, has also shown to be partially crystalline, as observed on the PXRD by less intense crystalline peak diffractions which are similar to those of tiotropium and mannitol (Figure 4.8g). The partial crystallinity of Tio_Man is confirmed by an exothermic recrystallization peak at 134.3°C followed by an endothermic melting peak at 158.8°C (Figure 4.6). Remarkably, only a single recrystallization and melting peak were present. The PXRD pattern of the TFF Tio_Lac formulation is shown in Figure 4.8l. Similar to Bud_Lac, the Tio_Lac powder exhibits broad and diffuse halos with an absence of the characteristic crystalline peaks indicating an amorphous structure. The amorphous form of the powder is confirmed by the mDSC thermogram (Figure 4.7). The thermogram profile shows an exothermic recrystallization event at 67.9°C, and two endothermic melting peaks at 119.7°C most likely due to lactose and at 189.2°C most likely a result of tiotropium.

4.3.2.3 Formoterol Fumarate

The PXRD pattern of formoterol fumarate is shown in Figure 4.9g where crystalline high intensity peaks can be seen at 5.75°, 15.29°, 16.10°, 18.38°, 19.76° and 26.60° of 2 θ . The PXRD pattern indicates that the material analyzed is a dihydrate polymorph of formoterol fumarate, as reported by Tajber et al. and Jarring et al. (12)(17). A modulated DSC heat flow thermogram of formoterol shows two endothermic melting peaks occurring at 118.2°C and at 143.54°C, as shown in Figure 4.5. When analyzed by mDSC reverse heat flow, the thermogram of formoterol fumarate displays three endotherm peaks at 111.4, 123.1 and 139.1°C (data not shown). Tajber et al. have also

investigated the thermodynamic properties of formoterol fumarate and reported the findings of three melting peaks. The first and largest peak occurred at approximately 122°C which was anticipated as a dehydration event. The last two peaks appeared at approximately 130°C and 150°C. The PXRD pattern of jet milled formoterol shows that the material has remained mostly in the crystalline form with peak diffractions presenting only a slight reduction in intensity as seen in Figure 4.9h. The mDSC profile confirms the crystalline state of the micronized material showing the first peak at 118.3°C and the second peak at 142.3°C (Figure 4.5).

The TFF For_Man powder, when subjected to PXRD analysis, displayed small peak diffractions indicating the presence of crystalline structures (Figure 4.8h). The crystallinity of the material is also confirmed by the presence of a single endothermic melting peak at 161.2°C, which may be related to the melting of mannitol. The melting peak of formoterol was not observed which suggests that the material was in the amorphous state (Figure 4.6). The mDSC reverse heat thermogram analysis of TFF For_Lac powder exhibits a recrystallization peak at 152.9°C and a following melting peak at 163.8°C (data not shown). The mDSC heat flow thermogram shows a melting peak at 158.4°C as well as a peak at 67.19°C that could represent the glass transition temperature of the formulation (Figure 4.7). PXRD confirms the amorphous characteristics of the powder exhibiting a halo pattern with absence of crystalline peaks (Figure 4.8m).

4.3.3 Triple drug combinations

Much like the TFF single drug formulations, the PXRD pattern of TFF BTF_Man has shown to be crystalline exhibiting small intensity diffraction peaks (Figure 4.8i). The mDSC thermogram of BTF_Man powder exhibits an exothermic recrystallization peak at

141.2°C followed by two endothermic peaks. The first and largest peak occurred at 165.4°C, most likely corresponding to the melting of mannitol and the second peak occurred at 236.5°C possibly representing the melting of budesonide (Figure 4.6). Furthermore, the TFF BTF_Lac powder displayed broad and diffuse haloes with an absence of the characteristic crystalline peaks, indicating an amorphous structure. The mDSC thermogram profile is characteristic of an amorphous formulation showing two exothermic recrystallization peaks at 130.9 and 170.0°C. This was followed by two endothermic melting peaks at 207.2°C, which may be related to the melting of lactose, and at 245.7°C, which corresponds to the melting of budesonide. It was hypothesized that the lactose and budesonide peaks would be more evident in the characterization of the triple combo formulations due to the largest amount of these materials in the formulation.

4.3.4 Analysis of the samples by FTIR

The IR frequencies of OH stretching vibrations are affected by hydrogen bonding of these groups. However, in this study, the OH stretching region of the binary- and tertiary mixtures of drugs is dominated by the broad envelopes due to the effects of thermal excitation on these vibrational modes for lactose and mannitol. As such, it is impossible to determine if there are shifts due to hydrogen bonding interactions in this region of the spectra. In contrast, the carbonyl-stretching region of the IR spectra provides some insight in to possible hydrogen bonding interactions of these functional groups of the drugs. In the case of tiotropium bromide, there is a significant 20 cm^{-1} shift in the frequency of the ester carbonyl stretch in the binary Tio_Lac formulation from 1749 to 1729 cm^{-1} . A smaller shift of carbonyl of about 15cm^{-1} is observed in the binary Tio_Man formulation from 1749 to 1734. These shifts are commensurate with hydrogen bonding interactions, which result in decreases in carbonyl stretching frequency, as

shown in Figure 4.10. In addition to the apparently stronger hydrogen-bonding interaction between tiotropium and lactose as evidenced by this carbonyl stretching frequency shift, further evidence for interaction comes from analysis of the lower frequency region of the IR spectra. The most pronounced feature in this region is the apparent absence of the lactose $\sim 900\text{-}870\text{ cm}^{-1}$ bands in the Tio_Lac formulation. These bands are resolved in raw lactose, but appear as a single broad band in TFF-processes lactose. In the binary mixture, these bands may possibly be shifted to $\sim 860\text{ cm}^{-1}$; although a 860 cm^{-1} band also appears in the spectrum for tiotropium alone, it is much less intense than the band from the binary formulation. Because this region of the IR spectrum consists of transitions with substantial coupling, it is impossible to make a definitive assignment for the origin of this band, and thus to the nature of the interaction that gives rise to its spectral change. However, in light of the evidence for tiotropium carbonyl hydrogen bonding, it is likely that this change is due to hydrogen bonding interactions with lactose (Figure 4.10).

The IR spectra of the binary For_Lac and Bud_Lac formulations show more modest shifts in the carbonyl region. In the case of formoterol, the carbonyl-stretching band at 1687 cm^{-1} shifts slightly to 1660 cm^{-1} , accompanied by a marked decrease in intensity. The saturated ketone carbonyl-stretching band of budesonide moves slightly from 1722 cm^{-1} to 1712 cm^{-1} in the binary formulation. Similarly, the dienone carbonyl also shifts slightly, from 1666 cm^{-1} to 1650 cm^{-1} , in the binary formulation. These shifts indicate that there is minimal hydrogen bonding to these carbonyl groups in the binary formulation.

The IR spectrum of the BTF_Lac formulation is dominated by the major component budesonide and shows little change in carbonyl stretch peak positions relative to the corresponding binary drug-lactose formulation.

In the case of the formulations with mannitol, a slightly different picture emerges from analysis of the IR spectra. In binary drug-mannitol mixtures, there are only slight changes in the carbonyl stretching bands when compared to spectra of the drugs alone, as seen in Figure 4.11. For example, the tiotropium carbonyl band shifts from 1749 to 1734 cm^{-1} , the formoterol formamide carbonyl band shifts from 1687 to 1664 cm^{-1} , but the budesonide saturated ketone carbonyl band remains unchanged at 1723 cm^{-1} . In contrast, in the ternary formulation, the saturated ketone carbonyl band for budesonide is even further shifted to lower frequency than in the case of the binary mixture, from 1717 to 1710 cm^{-1} . In contrast, the dienone carbonyl band for budesonide remains unchanged from the binary mixture. Together, these IR band shifts indicate that there is a significant hydrogen bond interaction involving budesonide in the ternary mixture in mannitol, in contrast to the case of the lactose ternary mixture, for which there is little evidence of interactions.

The IR spectrum for the physical mixture formulation prepared with lactose (BTF_Lac_PM) is dominated by the bands for formoterol, despite the fact that this is the least component by weight in the formulation. It is hypothesized that this result may be due to the low content uniformity of the powder formulation, which may have produced a KBr disk also not uniform. As a result, the portion of the KBr disk that was in the beam of the FTIR had mostly formoterol generating a spectrum similar to the spectrum of formoterol. In contrast, the physical mixture with mannitol has the carbonyl bands unchanged from the raw drugs as it was expected. A summary of the FTIR spectrum changes showing the stretching frequency shifts for the carbonyl groups of all TFF formulations is presented in Table 4.2.

4.3.5 *In vitro* aerosol performance of formulations and deposition homogeneity on the NGI

Aerodynamic particle size distribution of TFF formulations and physical mixtures were assessed using the NGI at 54 L/min and a Handihaler® dry powder inhaler device. Particle size distribution of the triple combo powder formulation prepared with lactose (BTF_Lac) is shown in Figure 4.12a. Importantly, analyses of the percentage stage-by-stage distribution of all three drugs present in the formulation were not statistically different. Thin film freezing powders are prepared from a diluted drug solution, which are rapidly frozen and freeze dried straight after (10). The resultant cake powder is homogenous and porous, which is easily dispersible under an inhalation air stream. Therefore, the results were in accordance with the hypothesis that each component of the formulation would be homogeneously distributed throughout the lyophilized cake and consequently homogeneously dispersed at time of aerosolization. A small difference in values was noticed in the percentage FPF for all three components, which were 31.65 ± 10.25 , 26.18 ± 0.67 and $33.08 \pm 9.19\%$ for formoterol, tiotropium and budesonide, respectively, as seen in Table 4.3.

Aerodynamic particle size distribution of the triple combo formulation prepared with mannitol (BTF_Man) is shown in Figure 4.12b. As expected, the percentage stage-by-stage powder depositions of the three drugs present in the formulation were not statistically different. The distribution similarity is also seen in the percentage FPF values of 52.95 ± 3.91 , 52.96 ± 3.48 and $53.60 \pm 2.89\%$ for formoterol, tiotropium and budesonide, respectively (Table 4.3). Interestingly, BTF_Man formulation presented the greatest percentage FPF, regardless the higher specific surface area (SSA) and porosity of BTF_Lac formulation. The inferior performance of BTF_Lac may be related to water sorption to the particle surfaces, which function as plasticizer on amorphous powder. The plasticizing effect may reduce powder fracture at time of aerosolization and increase

particle density due to collapse of the cake structure. This phenomenon may also be the reason why the stage-by-stage percentage depositions of all three drugs for the BTF_Lac powder were not as homogeneously distributed as the percentage depositions of the BTF_Man. Therefore, it is recommended that when preparing TFF formulations with lactose, the powder should be manipulated under a controlled low humidity environment. As expected, the emitted doses of the two TFF triple combo formulations were above 90% due to the fact that the brittle cake powders are easily dispersible and emitted from the dry powder inhaler and capsule(15).

When aerosolized individually, the stage distribution and aerosol performance of each TFF formulation prepared with a single drug was statistically different. The difference is particularly significant for stage 1 where the amount of tiotropium deposited was almost double the amount of formoterol and budesonide for lactose and mannitol formulations, as seen in Figure 4.13a and 4.13b. The difference in aerosol performance among the single drug TFF formulations is also confirmed by the FPF values as shown in Table 4.4. The percentage FPF for formoterol, tiotropium and budesonide formulations (For_Lac, Tio_Lac and Bud_Lac) prepared with lactose were 55.51 ± 5.79 , 22.56 ± 5.75 and $58.67 \pm 4.28\%$, respectively. Also, percentage FPF deposition of formoterol, tiotropium and budesonide prepared with mannitol (For_Man, Tio_Man and Bud_Man) were 58.32 ± 5.99 , 37.45 ± 0.71 and $64.62 \pm 1.28\%$, respectively, showing a very significant difference. Single drugs prepared with mannitol presented greater percentage FPF than formulations prepared with lactose. This phenomenon is in accordance with the hypothesis that hygroscopic lactose formulations are susceptible to water sorption to the powder surfaces and posterior collapse of the lyophilized cake structure. It is important to notice that TFF formulations prepared with tiotropium presented the smallest FPF and SSA values, which may be related to the powder physicochemical characteristics. Thus,

tiotropium may be responsible for the low aerosolization performance and FPF values generated by the triple combo formulations. These results imply that when patients are treated with multiple administrations of single drug formulations they may not benefit from co-deposition of drugs in the lungs and from a potential synergistic action(21)(22). Similarly to the triple combo TFF formulations, high percentage values of emitted doses from the inhalers were seen for all single drug formulations, which is a characteristic of the TFF powders (Table 4.4)

The difference in stage distribution and aerosol performance of the triple combo formulations prepared by physically blending the jet milled drug powders with coarse lactose or mannitol (BTF_Lac_PM and BTF_Man_PM) particles also were investigated. The stage-by-stage powder depositions of the BTF_Man_PM formulation were significantly different as shown in Figure. 4.14b. The three drugs presented a very different percentage deposition from each other with a high percentage of powder being deposited in the induction port. Although the percentage deposition of all three drugs on the cascade impactor stages were significantly different, the percentage FPF for all three drugs of the BTF_Man_PM formulation were similar presenting values of 26.36 ± 03.84 , 28.65 ± 0.30 and $25.80 \pm 1.96\%$ for formoterol, tiotropium and budesonide, respectively (Table 4.3). Additionally, the percentage emitted dose values reduced from above 90% to approximately 70 to 80% for BTF_Man_PM and BTF_Lac_PM due to the high amount of powder remaining in the capsules after aerosolization of both formulations, as shown in Table 4.3. The lower emitted dose and higher neck deposition of the physical mixture formulations may contribute to variable dosing with potential for under or overdosing specially if the powder mixture is comprised of potent drugs(5)(23).

Surprisingly, the stage-by-stage powder depositions of the BTF_Lac_PM formulation were not statistically different as shown in Figure 4.14a. The BTF_Lac_PM

also showed low aerosolization performance presenting percentage FPF values of 28.64 ± 3.89 , 25.22 ± 3.56 and $25.05 \pm 5.82\%$ for formoterol, tiotropium and budesonide, respectively. However, deposition through stages 3 to 5, where particle sizes between 1-3 μm deposit and have the highest probability to reach the deep lungs, is more homogeneous for the TFF formulations than for the BTF_Lac_PM. Also, the difference of powder aerosolization performance between the physical mixtures prepared with lactose and mannitol suggests the lack of robustness of the preparation process. The low aerosol performance of the physical mixture formulations may be related to the size and surface properties of the particles. As discussed previously, mechanical comminution produces electrostatically charged particles, which, in most cases, become agglomerated due to their cohesive and adhesive behavior. These strong interparticulate forces require a much higher shearing force inside the inhaler to deagglomerate and disperse the particles at the time of aerosolization. Consequently, aerosolization of physical mixture formulations usually generates incomplete powder dispersion and variations in aerosol performance which may influence pulmonary drug delivery (24)(25).

4.4 CONCLUSION

Thin film freezing technology demonstrated to be suitable to prepare a triple drug combination formulation. The triple combo drug formulations produced with TFF technology presented superior properties than the physical mixture of micronized powders exhibiting good particle distribution homogeneity after *in vitro* aerosolization. TFF formulations prepared with lactose were amorphous while mannitol formulation powders were crystalline. The crystallinity of the powders seems to not influence the aerodynamic properties of the formulations. The hygroscopic characteristic of lactose

formulations may be the responsible for the inferior aerodynamic properties of lactose formulation due to possible water sorption onto lactose particles.

Future research should investigate the effect of formulation and process variables on the particle structure, aerodynamic properties and chemical and physical stability of the systems.

4.5 TABLES

Samples	Particle size (μm)				SSA \pm SD (m^2/g)
	D ₁₀	D ₅₀	D ₉₀	Span	
Budesonide	1.63 \pm 1.25	22.11 \pm 16.92	52.7 \pm 2.42	2.31	3.05 \pm 0.21
Tiotropium bromide	1.10 \pm 0.01	5.14 \pm 0.03	12.11 \pm 0.07	2.14	2.08 \pm 0.13
Formoterol fumarate	1.16 \pm 0.05	6.27 \pm 0.97	49.78 \pm 7.84	7.75	2.97 \pm 0.05
Lactose monohydrate	4.13 \pm 0.11	39.78 \pm 1.32	100.9 \pm 0.27	2.43	0.34 \pm 0.03
Mannitol	6.88 \pm 0.07	52.70 \pm 0.59	101.91 \pm 0.41	1.8	0.22 \pm 0.001
Jet milled budesonide	0.91 \pm 0.01	3.40 \pm 0.09	9.7 \pm 0.30	2.58	2.75 \pm 0.13
Jet milled tiotropium bromide	1.09 \pm 0.79	4.65 \pm 0.04	10.39 \pm 0.04	2.0	2.86 \pm 0.11
jet milled formoterol fumarate	1.45 \pm 1.01	4.51 \pm 0.02	10.29 \pm 0.07	1.96	5.08 \pm 0.26
BTF_Lac_PM	-	-	-		0.43 \pm 0.05
BTF_Man_PM	-	-	-		0.32 \pm 0.03
Bud_Man	-	-	-		46.97 \pm 2.22
Tio_Man	-	-	-		38.79 \pm 0.81
For_Man	-	-	-		64.14 \pm 0.68
BTF_Man	-	-	-		54.55 \pm 1.10
Bud_Lac	-	-	-		90.39 \pm 6.15
Tio_Lac	-	-	-		48.90 \pm 2.42
For_Lac	-	-	-		193.86 \pm 10.63
BTF_Lac	-	-	-		81.31 \pm 1.71

Table 4.1 – Particle size distribution and specific surface area of bulk drugs and excipients, jet milled drugs and TFF formulations.

Formulation	Chemical group	Stretching frequency shift (cm ⁻¹)	H-bonding		Comments
			yes	no	
Tio_Lac	Ester carbonyl	1749 to 1729			Strong H-bonding.
	-	~ 900 to 860	x		Undefined band. Likely formation of H-bonding.
For_Lac	Formamide carbonyl	1687 to 1660	x		Market decrease in intensity. Slight frequency shift. Minimal H-bonding formation.
Bud_Lac	Ketone carbonyl	1722 to 1712	x		Slight frequency shift. Minimal H-bonding formation.
	Dienone carbonyl	1666 to 1650			
BTF_Lac	Ketone carbonyl	1722 to 1712	x		Slight frequency shift. Minimal H-bonding formation.
Tio_Man	Ester carbonyl	1749 to 1734		x	Slight frequency shift. Minimal H-bonding formation.
For_Man	Formamide carbonyl	1687 to 1664		x	Slight frequency shift.
Bud_Man	Ketone carbonyl	1723		x	Remains unchanged.
	Dienone carbonyl	1666			
BTF_Man	Ketone carbonyl	1717 to 1710	x		Further shift to lower frequency than Bud_Man. Strong H-bonding.
	Dienone carbonyl	1666			Remains unchanged.

Table 4.2 – Summary of the FTIR spectrum changes showing the stretching frequency shifts for the carbonyl groups of all TFF formulations.

Formulation	Formoterol Fumarate	Tiotropium Bromide	Budesonide
BTF_Lac			
ED	94.68 ± 1.33	97.20 ± 0.70	92.73 ± 0.72
FPF	31.65 ± 10.25	26.18 ± 0.67	33.08 ± 9.19
BTF_Man			
ED	98.74 ± 1.69	98.81 ± 2.05	96.08 ± 1.57
FPF	52.95 ± 3.91	52.96 ± 3.48	53.60 ± 2.89
BTF_Lac_PM			
ED	69.04 ± 7.22	73.46 ± 6.78	83.68 ± 10.88
FPF	28.64 ± 3.98	25.22 ± 3.56	25.05 ± 5.82
BTF_Man_PM			
ED	85.06 ± 3.56	83.95 ± 3.46	80.00 ± 2.37
FPF	26.36 ± 3.84	28.65 ± 0.30	25.80 ± 1.96

Table 4.3 – Emitted dose and fine particle fraction for each drug from all triple combo formulations.

Formulation	ED	FPF
For_Lac	96.84 ± 6.04	55.51 ± 5.79
For_Man	97.08 ± 0.28	58.32 ± 5.99
Tio_Lac	95.81 ± 0.84	22.56 ± 5.75
Tio_Man	93.93 ± 0.44	37.45 ± 0.71
Bud_Lac	93.59 ± 2.08	58.67 ± 4.28
Bud_Man	95.2 ± 0.68	64.06 ± 1.28

Table 4.4 – Emitted dose and percentage fine particle fraction of all single drug formulations.

4.6 FIGURES

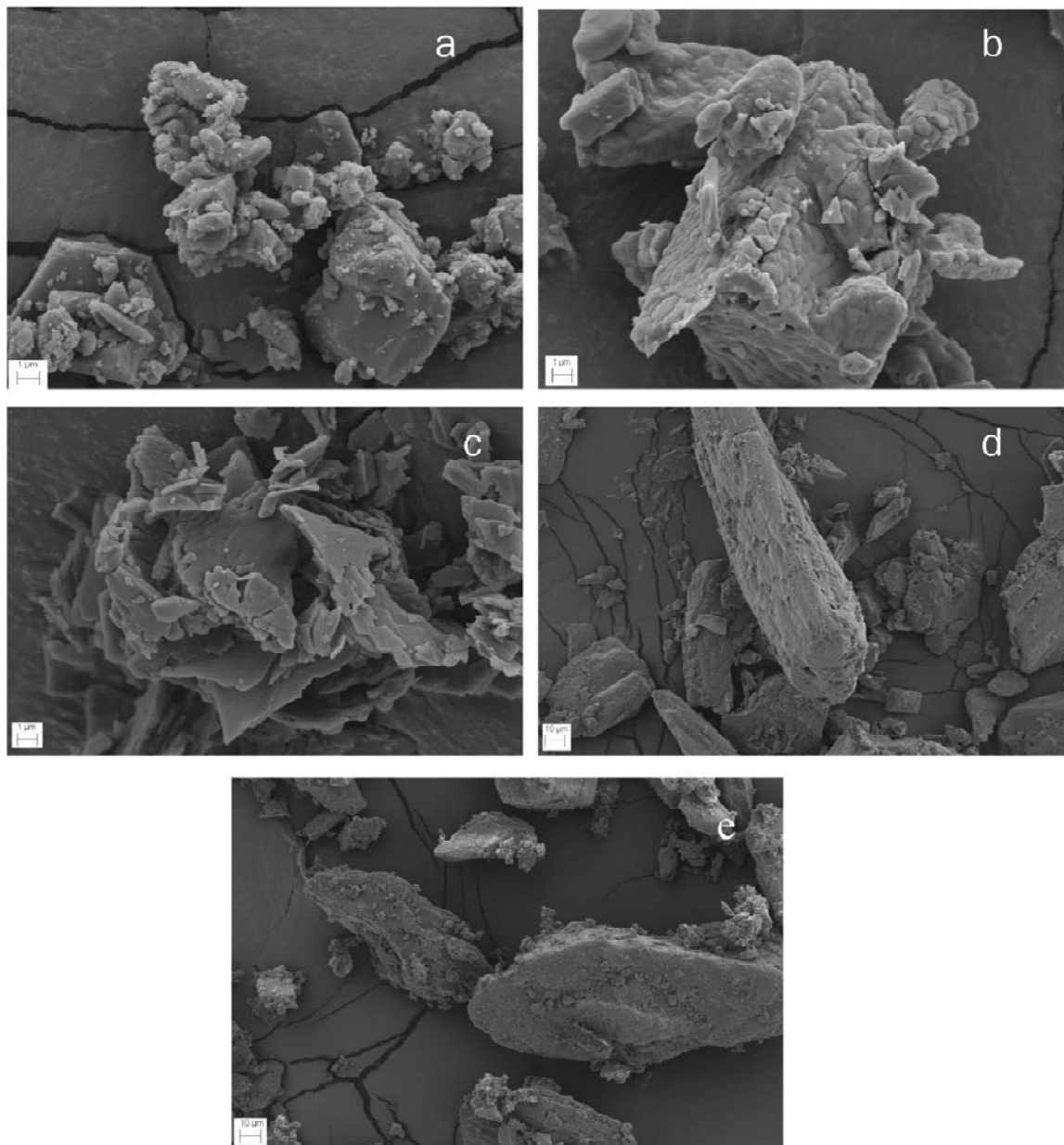


Figure 4.1 – SEM images of (a) budesonide, (b) tiotropium bromide and (c) formoterol fumarate at magnification of 10.0k, (d) mannitol and (e) lactose monohydrate (1.0k).

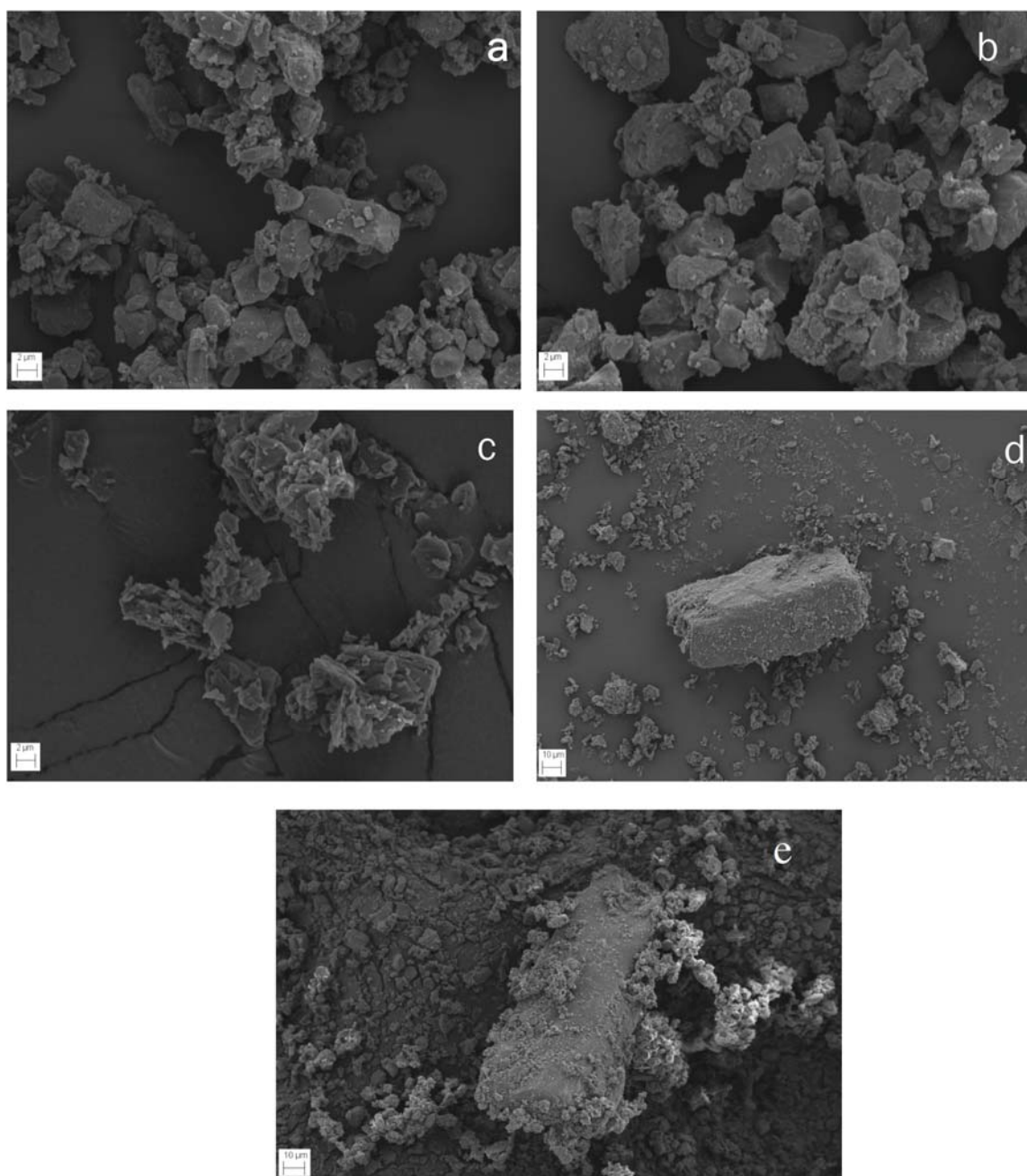


Figure 4.2 – SEM images of (a) jet milled budesonide (b) jet milled tiotropium (c) jet milled formoterol and the physical mixtures (d) BTF_Lac_PM (e) BTF_Man_PM (5.0k).

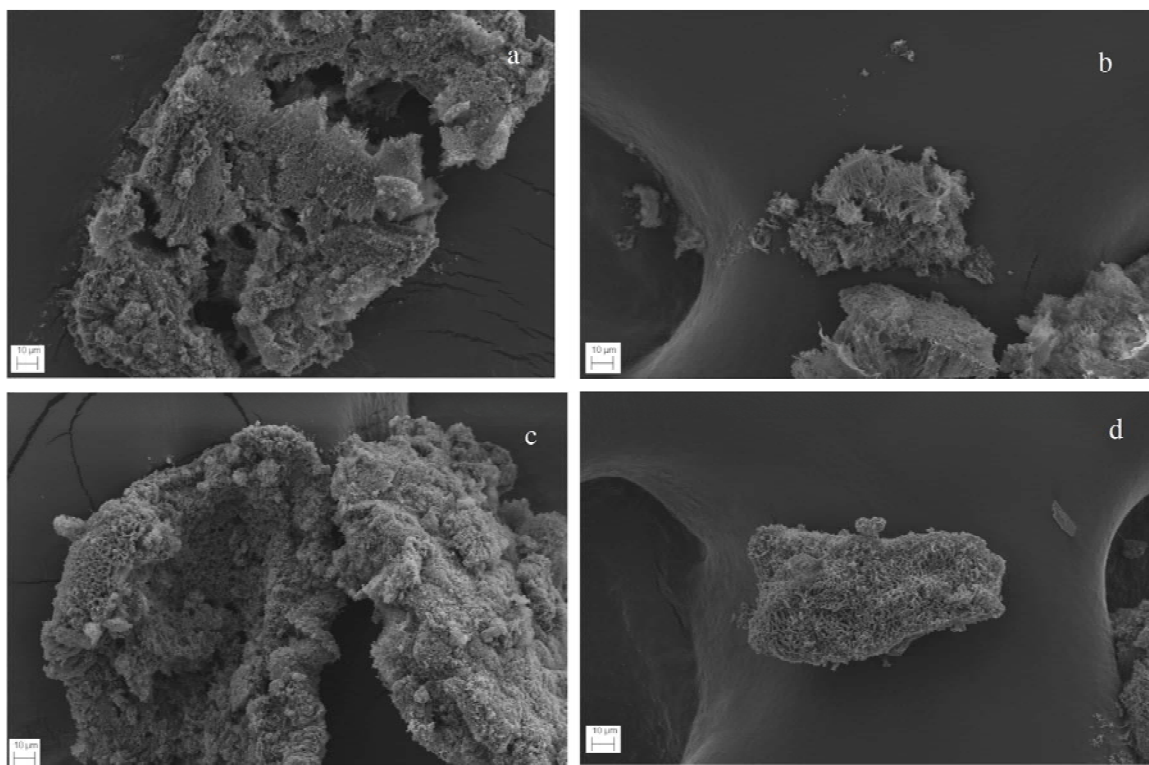


Figure 4.3 – SEM images of TFF formulations (a) Bud_Lac, (b) Bud_Man, (c) Tio_Lac, and (d) Tio_Man at magnification 1.0k.

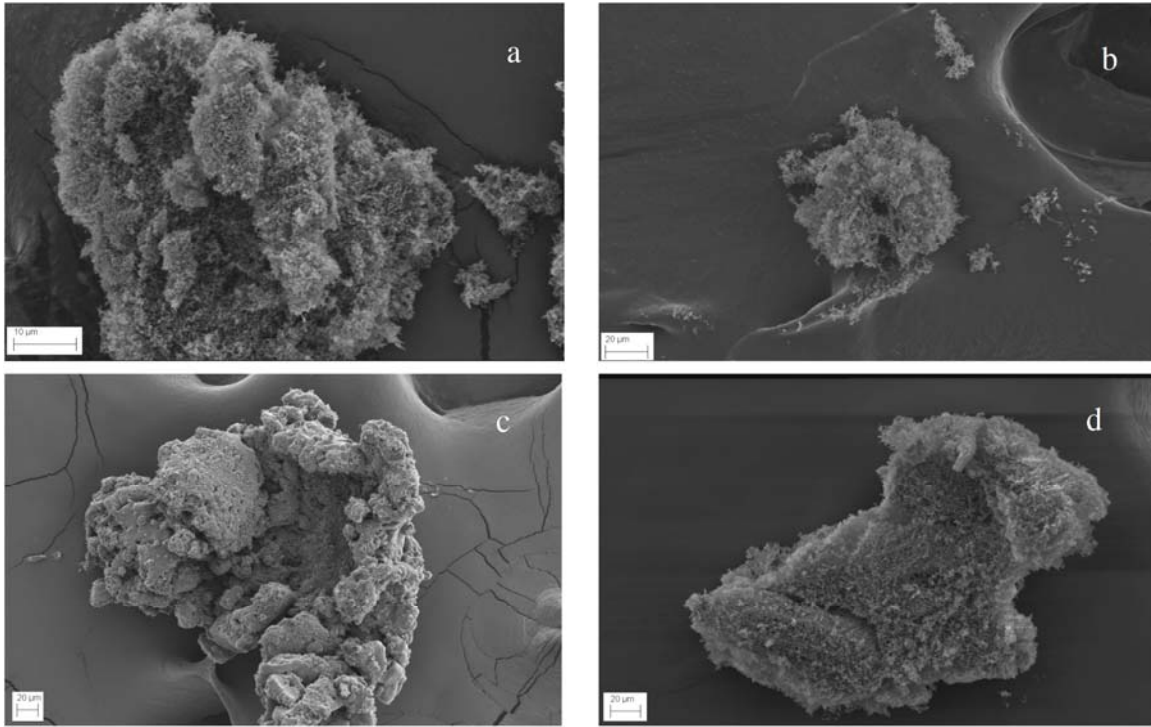


Figure 4.4 – SEM images of TFF formulations (a) For_Lac, (b) For_Man, (c) BTF_Lac, and (d) BTF_Man at magnification 1.0k.

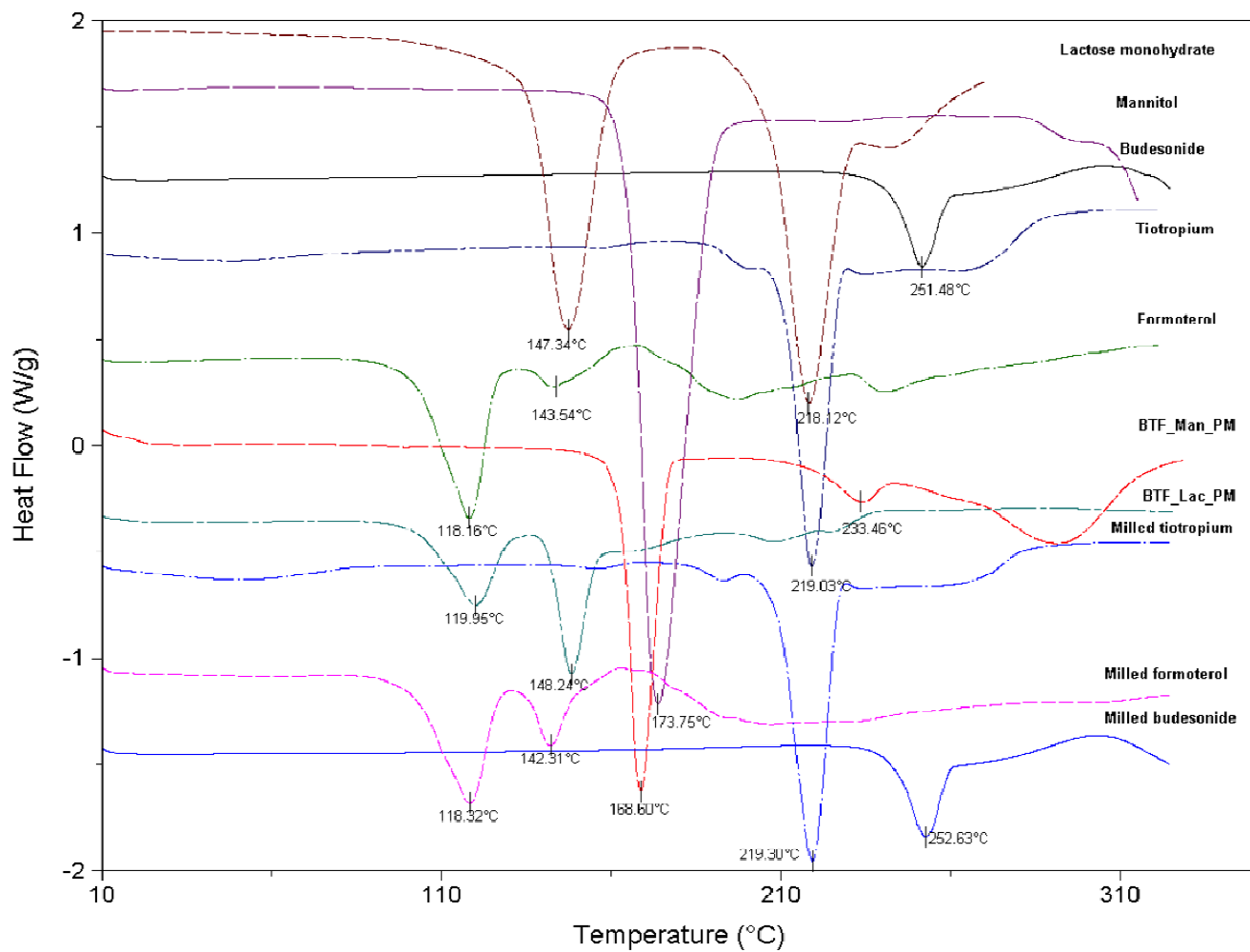


Figure 4.5 – Modulated DSC heat flow thermograms of unprocessed lactose monohydrate, mannitol, budesonide, tiotropium and formoterol, physical mixture formulation of jet milled budesonide, tiotropium and formoterol with mannitol (BTF_Man) and with lactose (BTF_Lac), and jet milled tiotropium, formoterol and budesonide.

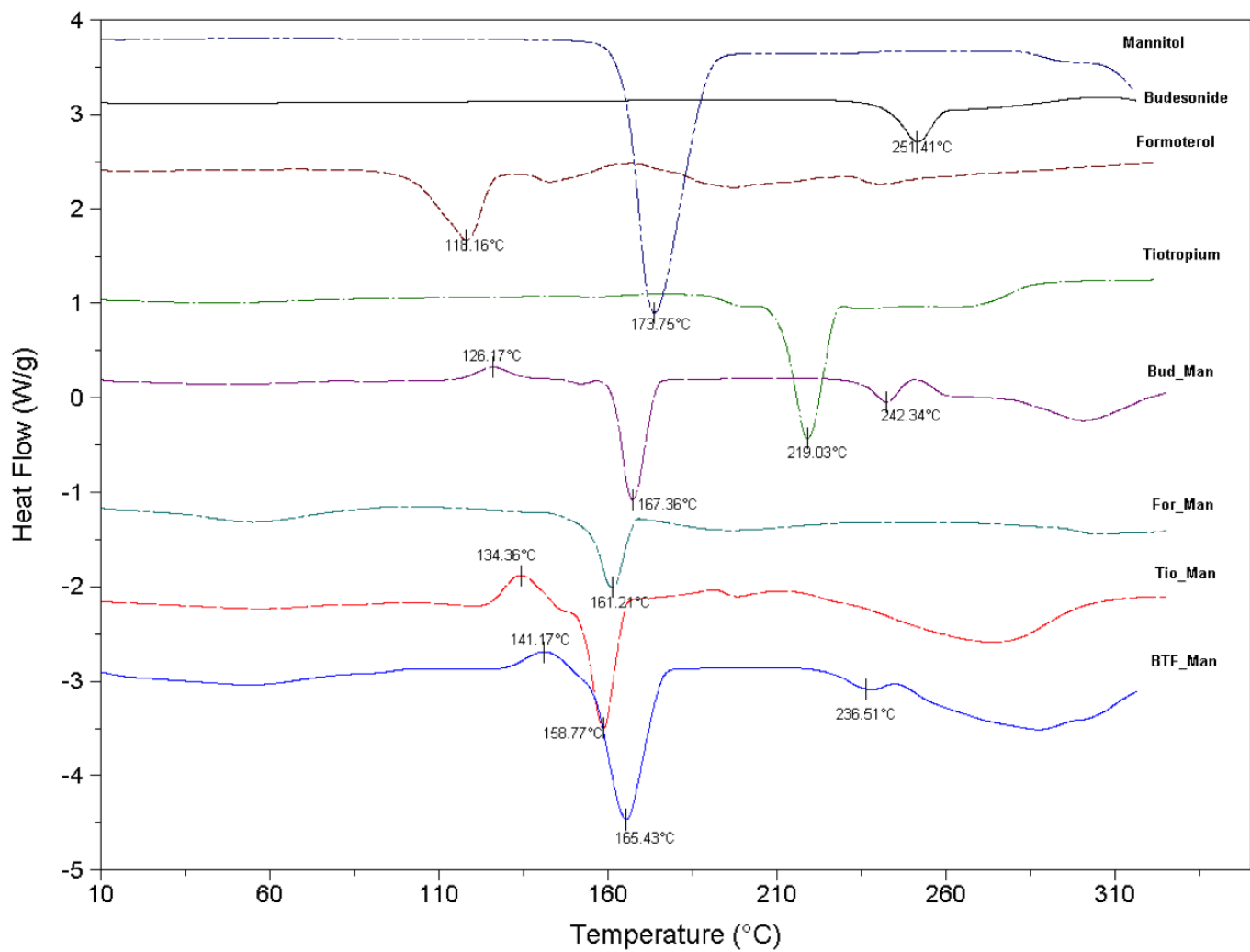


Figure 4.6 – Modulated DSC heat flow thermograms of unprocessed lactose monohydrate, mannitol, budesonide, formoterol and tiotropium, TFF formulations of Bud_Man, For_Man, Tio_Man and BTF_Man.

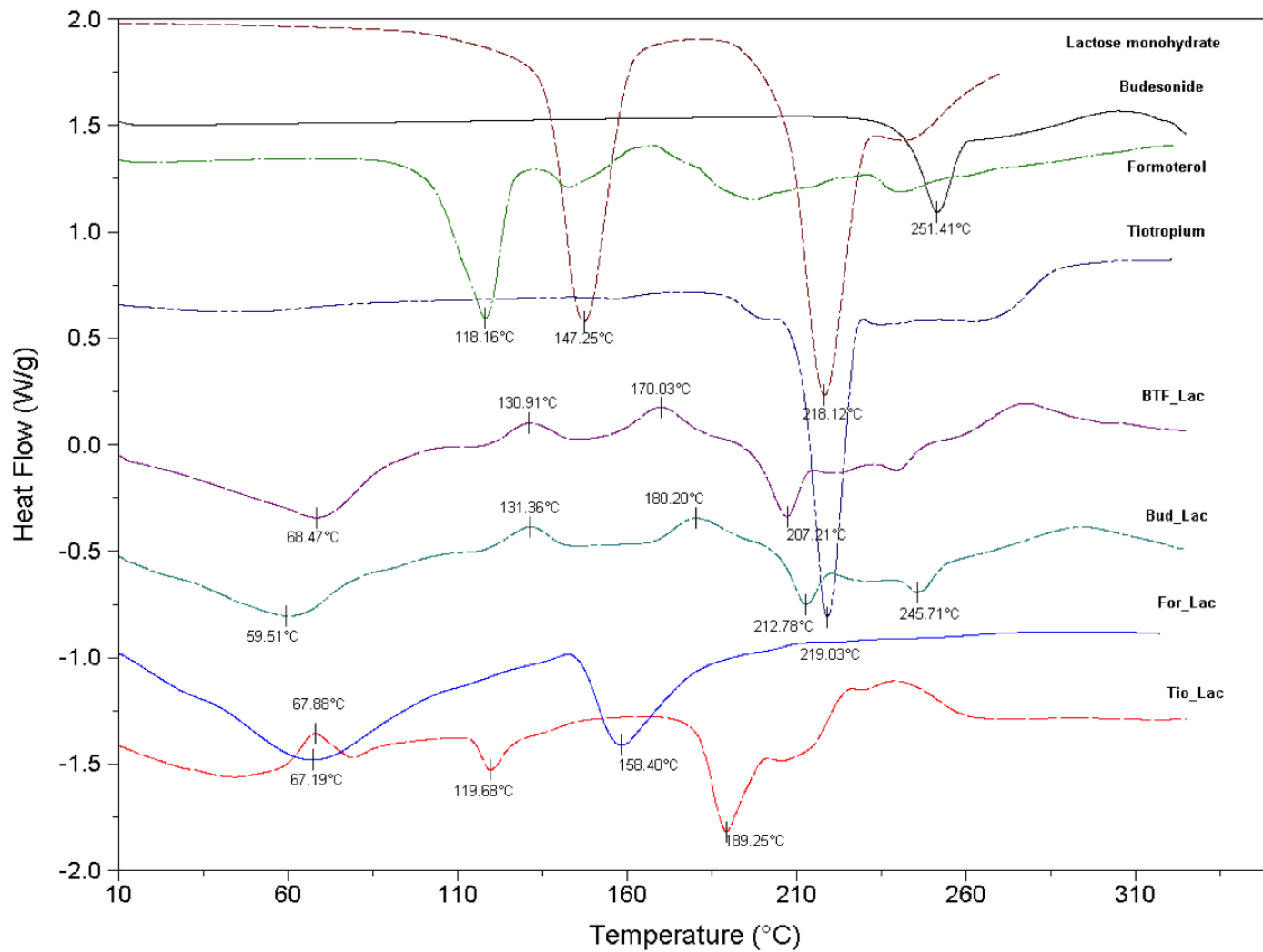


Figure 4.7 – Modulated DSC heat flow thermograms of unprocessed lactose monohydrate, mannitol, budesonide, formoterol and tiotropium, TFF formulations of BTF_Lac, Bud_Lac, For_Lac, and Tio_Lac.

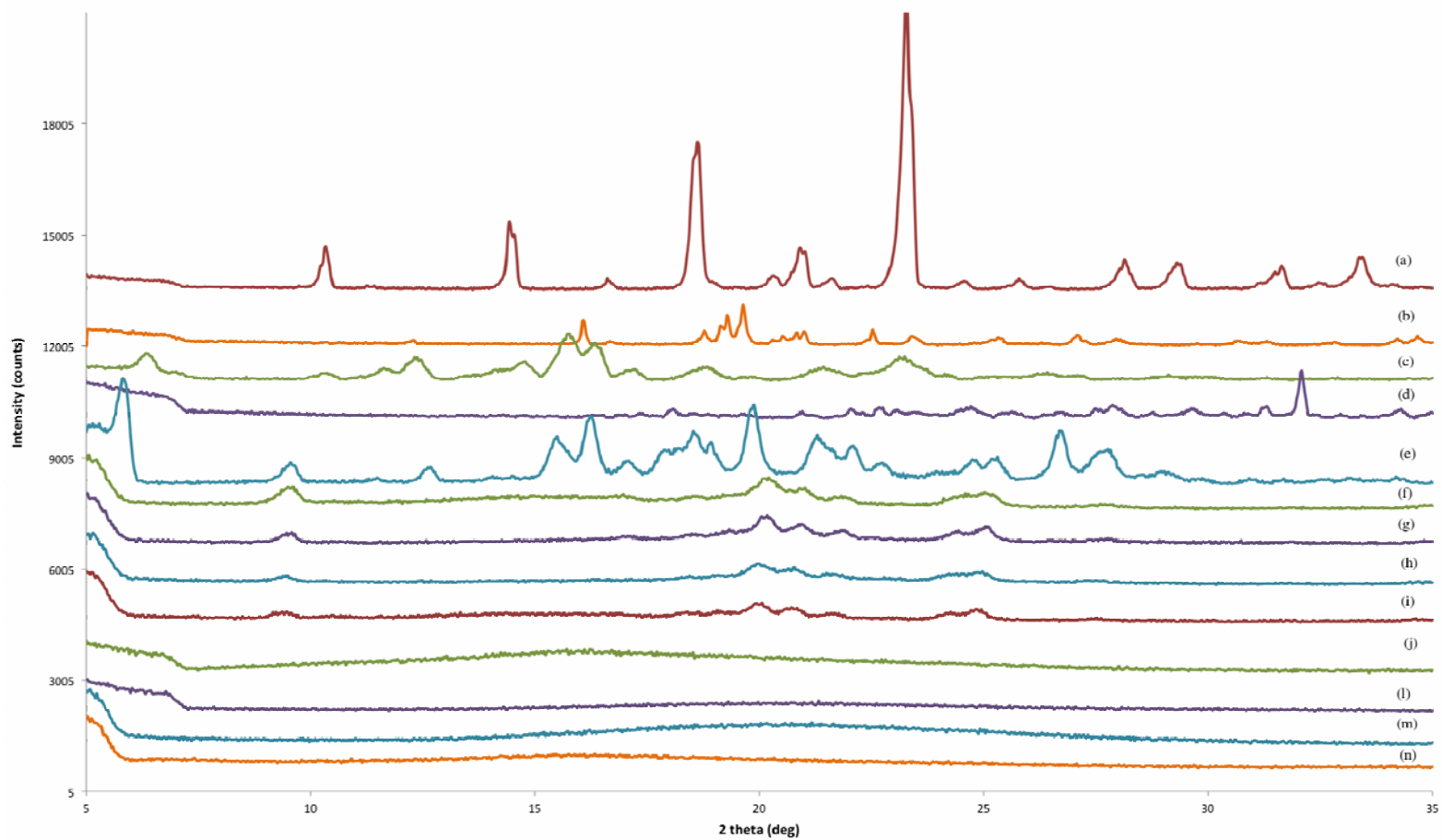


Figure 4.8 –Powder x-ray pattern of (a) mannitol, (b) lactose monohydrate, (c) budesonide, (d) tiotropium, (e) formoterol, (f) Bud_Man, (g) Tio_Man, (h) For_Man, (i) BTF_Man, (j) Bud_Lac, (l) Tio_Lac, (m) For_Lac and (n) BTF_Lac.

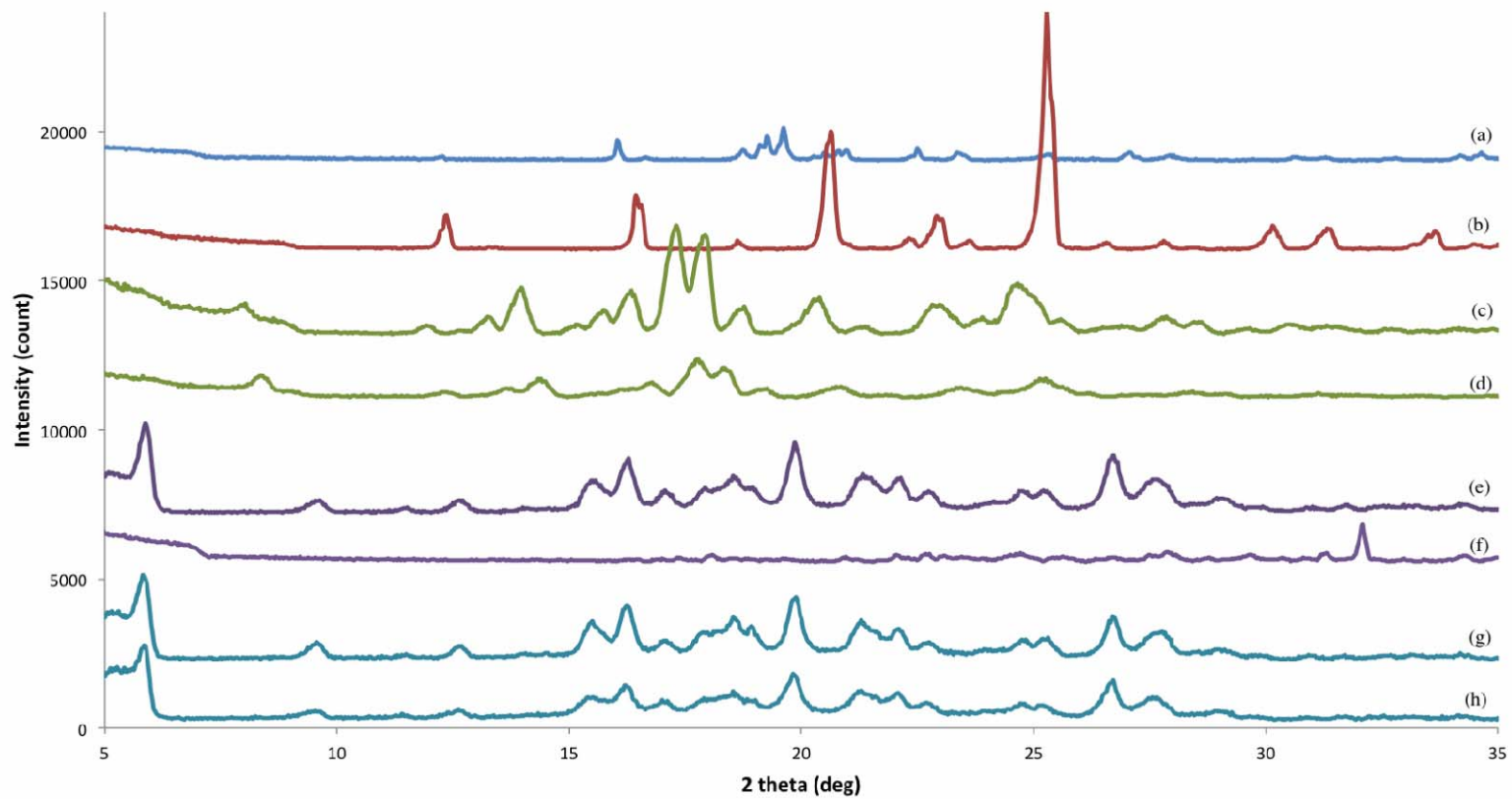


Figure 4.9 – Powder x-ray pattern of (a) lactose monohydrate, (b) mannitol, (c) budesonide, (d) jet milled budesonide, (e) tiotropium, (f) jet milled tiotropium, (g) formoterol, and (h) jet milled formoterol.

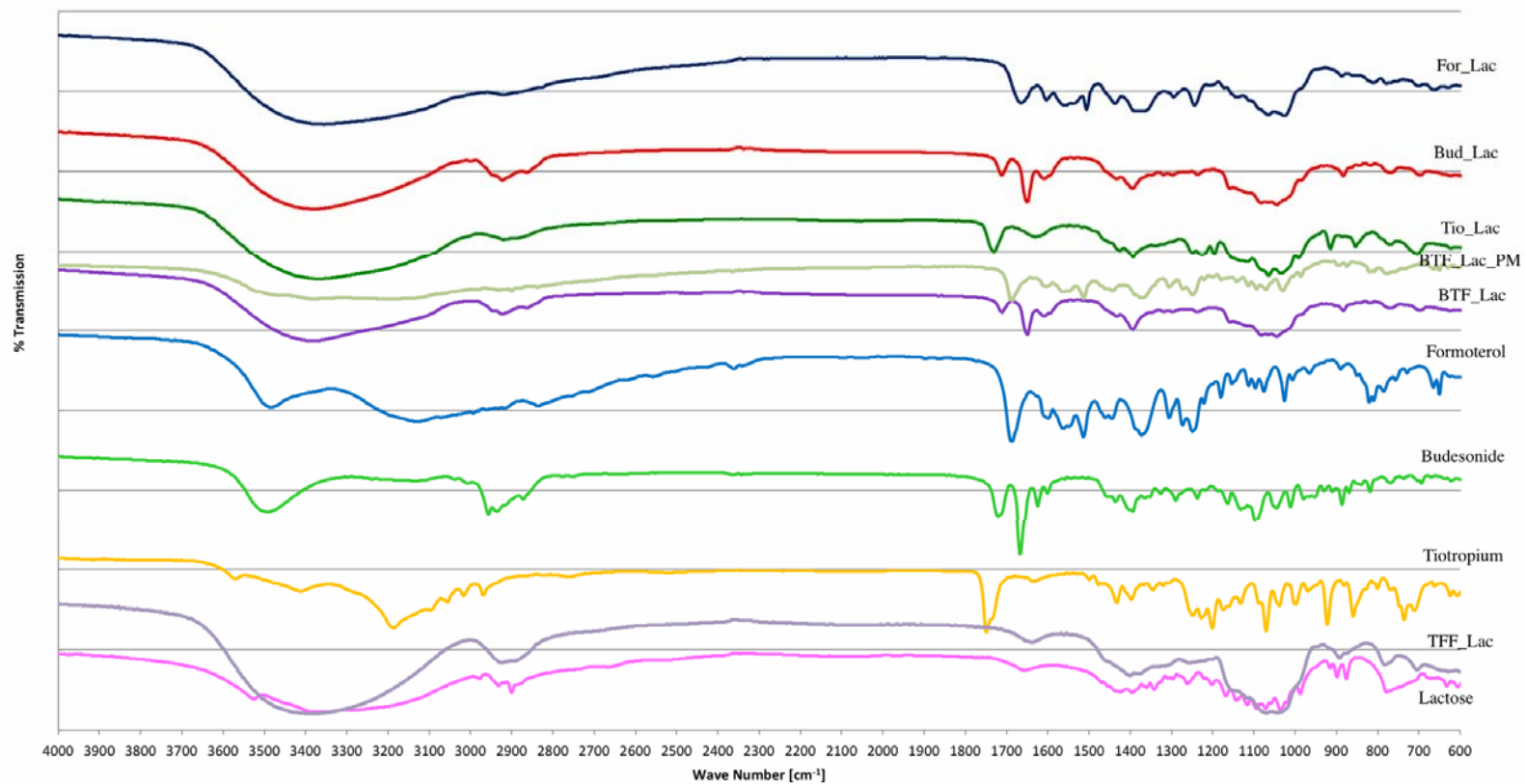


Figure 4.10 – FTIR scans of TFF formoterol_lactose, TFF budesonide_lactose, TFF tiotropium_lactose, physical mixture of triple drug combination, TFF triple drug combination, formoterol, budesonide, tiotropium, TFF lactose and lactose.

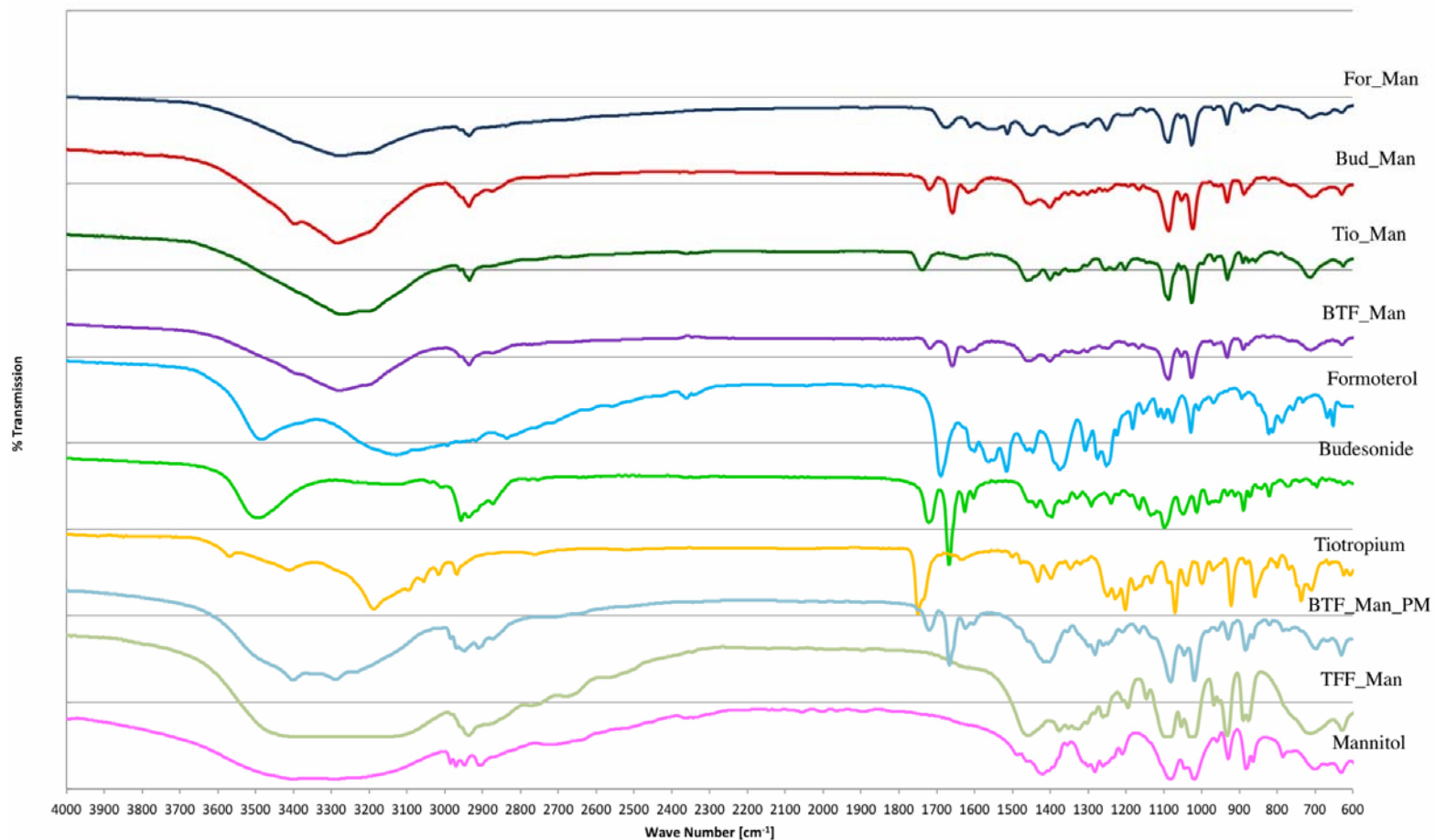


Figure 4.11 – FTIR scans of TFF formoterol_mannitol, TFF budesonide_mannitol, TFF tiotropium_mannitol, TFF triple drug combination, formoterol, budesonide, tiotropium, physical mixture of triple drug combination, TFF mannitol and mannitol.

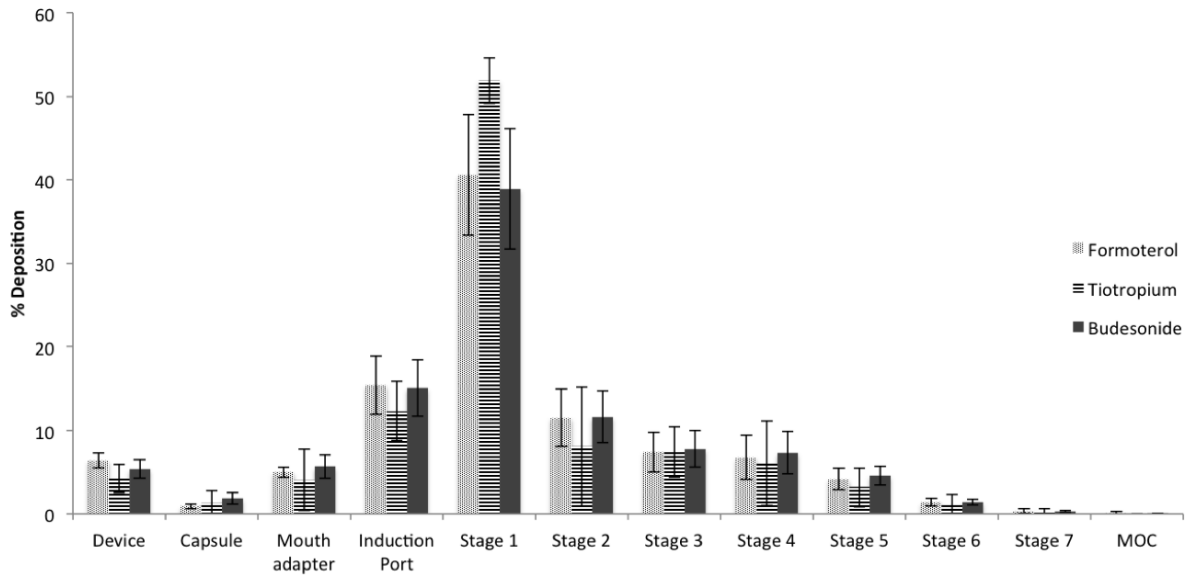


Figure 4.12a – Aerodynamic particle size distribution of TFF triple combo BTF_Lac formulations deposited on a next generation cascade impactor.

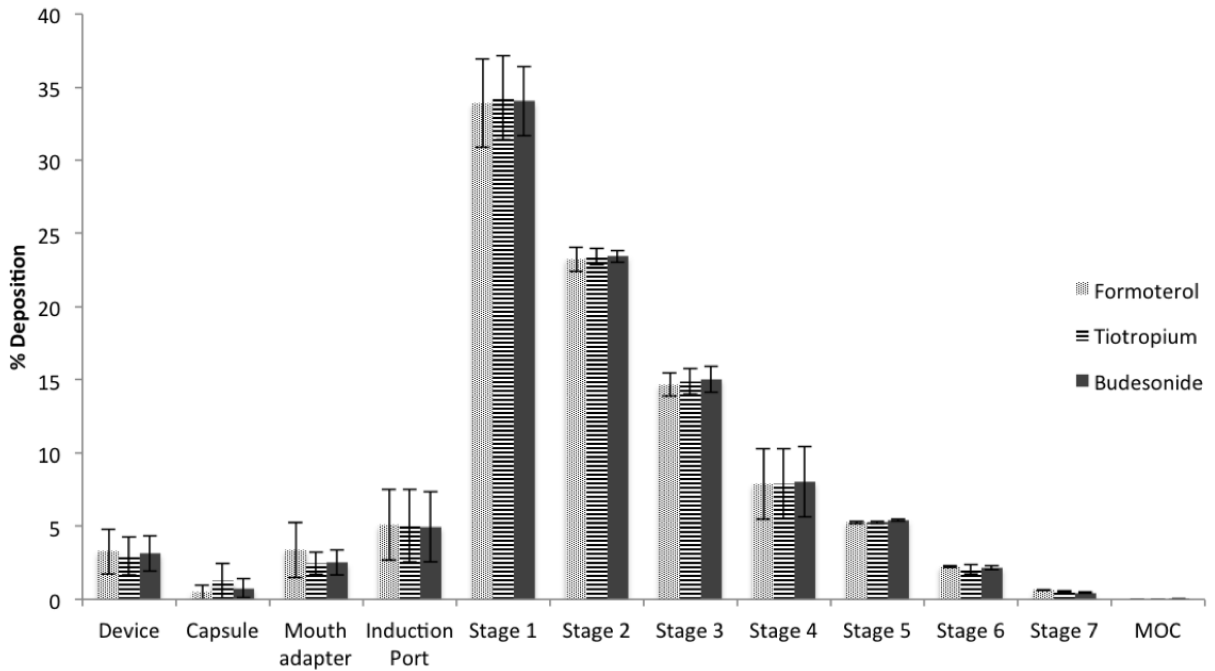


Figure 4.12b – Aerodynamic particle size distribution of TFF triple combo BTF_Man formulations deposited on a next generation cascade impactor.

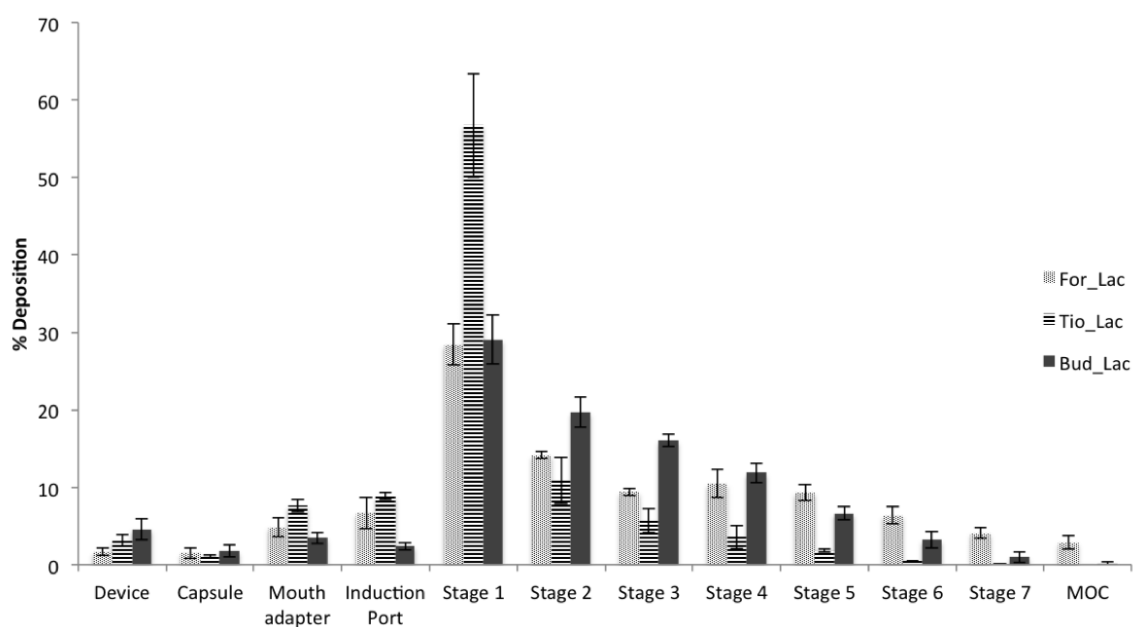


Figure 4.13a – Aerodynamic particle size distribution of TFF single drug formulations For_Lac, Tio_Lac and Bud_Lac, deposited on a next generation cascade impactor.

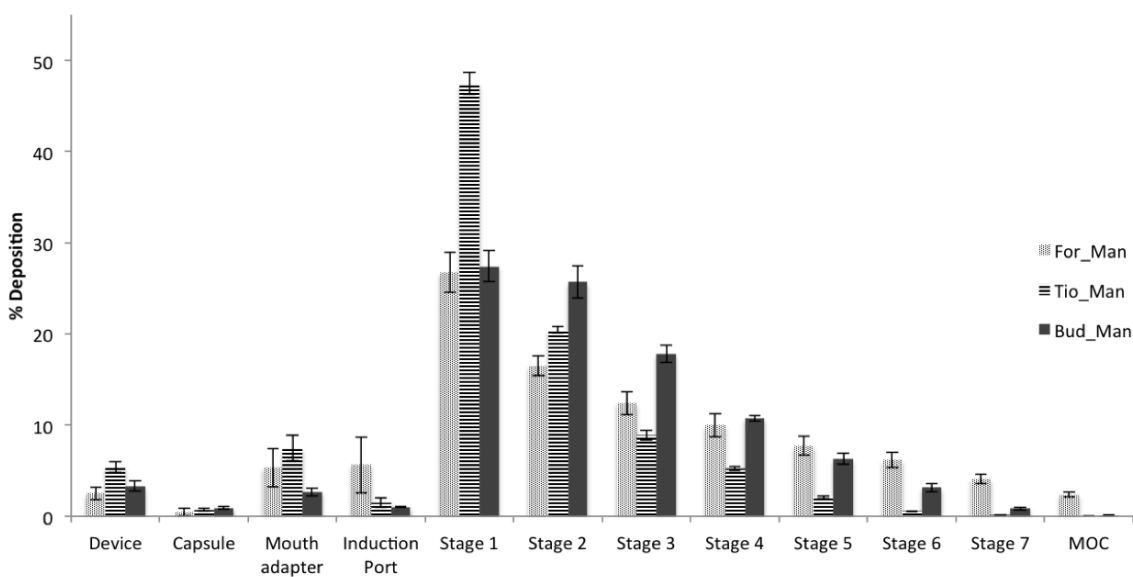


Figure 4.13b – Aerodynamic particle size distribution of TFF single drug formulations For_Man, Tio_Man and Bud_Man, deposited on a next generation cascade impactor.

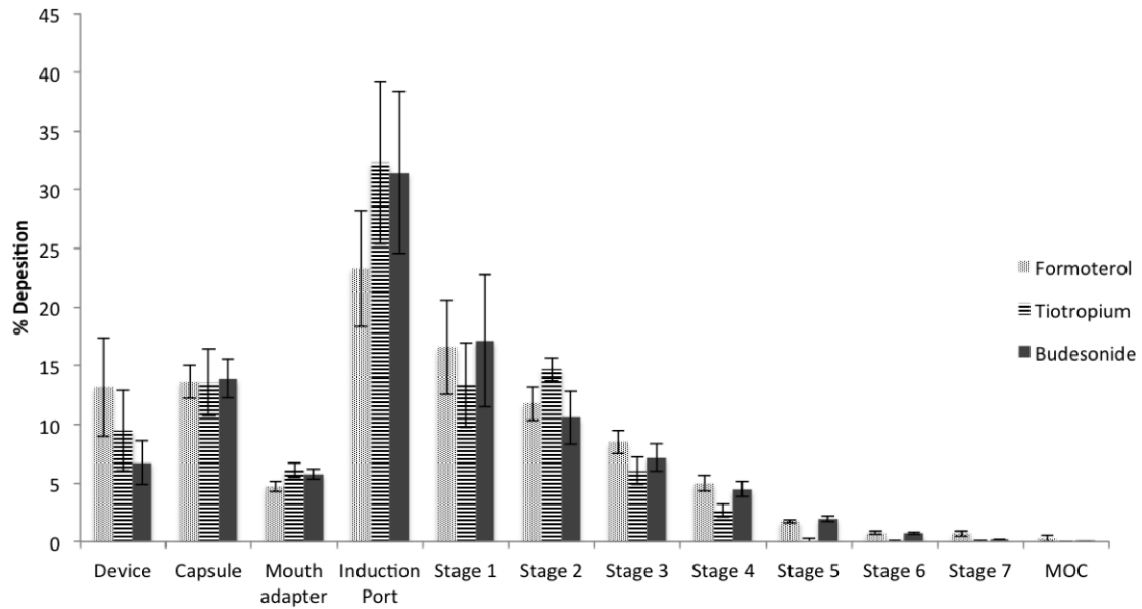


Figure 4.14a – Aerodynamic particle size distribution of triple combo physical mixture BTF_Lac_PM formulations deposited on a next generation cascade impactor.

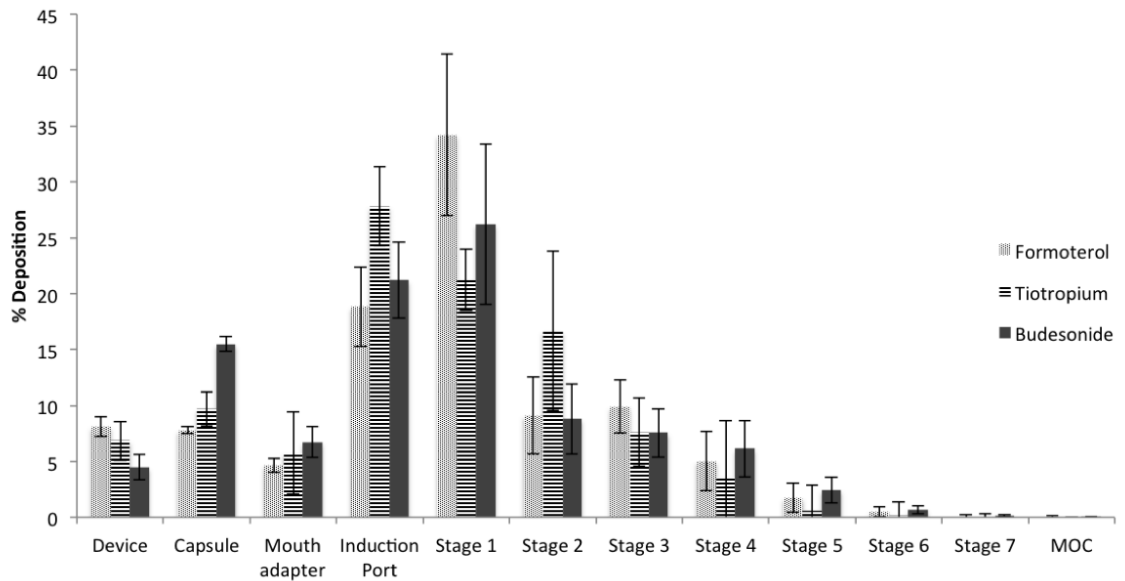


Figure 4.14b – Aerodynamic particle size distribution of triple combo physical mixture BTF_Man_PM formulations deposited on a next generation cascade impactor.

4.7 REFERENCES

1. Barnes PJ, Shapiro SD, Pauwels RA. Chronic obstructive pulmonary disease: molecular and cellular mechanisms. *Eur Respir J*. 2003 Oct;22(4):672–88.
2. Bjerg A, Lundbäck B, Lötvall J. The future of combining inhaled drugs for COPD. *Curr Opin Pharmacol*. 2012 Jun;12(3):252–5.
3. Barnes PJ, Stockley RA. COPD: current therapeutic interventions and future approaches. *Eur Respir J*. 2005 Jun;25(6):1084–106.
4. Price D, Yawn B, Brusselle G, Rossi A. Risk-to-benefit ratio of inhaled corticosteroids in patients with COPD. *Prim Care Respir J*. 2013 Mar;22(1):92–100.
5. Weers JG, Bell J, Chan H-K, Cipolla D, Dunbar C, Hickey AJ, et al. Pulmonary Formulations: What Remains to be Done? *J Aerosol Med Pulm Drug Deliv*. 2010 Dec;23:S5–S23.
6. Salama RO, Young PM, Rogueda P, Lallement A, Iliev I, Traini D. Advances in drug delivery: is triple therapy the future for the treatment of chronic obstructive pulmonary disease? *Expert Opin Pharmacother*. 2011 Aug;12(12):1913–32.
7. Barnes PJ. Triple inhalers for obstructive airways disease: will they be useful? *Expert Rev Respir Med*. 2011 Jun;5(3):297–300.
8. Williamson PA, Short PM, Clearie KL, Vaidyanathan S, Fardon TC, Howaniec LJ, et al. Paradoxical trough effects of triple therapy with budesonide/formoterol and tiotropium bromide on pulmonary function outcomes in COPD. *CHEST J*. 2010;138(3):595–604.
9. McKeage K, Keam SJ. Salmeterol/Fluticasone Propionate A Review of its Use in Asthma. *Drugs*. 2009;69(13):1799–828.

10. Parikh D, Burns J, Hipkiss D, Usmani O, Price R. Improved localized lung delivery using smart combination respiratory medicines. *Eur Respir Dis*. 2012;8(1):40–5.
11. Adi H, Young PM, Traini D. Co-deposition of a triple therapy drug formulation for the treatment of chronic obstructive pulmonary disease using solution-based pressurised metered dose inhalers. *J Pharm Pharmacol*. 2012 Sep;64(9):1245–53.
12. Vehring R, Lechuga-Ballesteros D, Joshi V, Noga B, Dwivedi SK. Cosuspensions of Microcrystals and Engineered Microparticles for Uniform and Efficient Delivery of Respiratory Therapeutics from Pressurized Metered Dose Inhalers. *Langmuir*. 2012 Oct 23;28(42):15015–23.
13. Vishweshwar P, McMahon JA, Bis JA, Zaworotko MJ. Pharmaceutical co-crystals. *J Pharm Sci*. 2006 Mar;95(3):499–516.
14. Alhalaweh A, Kaialy W, Buckton G, Gill H, Nokhodchi A, Velaga SP. Theophylline Cocrystals Prepared by Spray Drying: Physicochemical Properties and Aerosolization Performance. *AAPS PharmSciTech*. 2013 Jan 8;14(1):265–76.
15. Watts AB, Wang Y-B, Johnston KP, Williams RO. Respirable Low-Density Microparticles Formed In Situ from Aerosolized Brittle Matrices. *Pharm Res*. 2013 Mar;30(3):813–25.
16. Overhoff KA, Engstrom JD, Chen B, Scherzer BD, Milner TE, Johnston KP, et al. Novel ultra-rapid freezing particle engineering process for enhancement of dissolution rates of poorly water-soluble drugs. *Eur J Pharm Biopharm*. 2007 Jan;65(1):57–67.
17. Trivedi RK, Chendake DS, Patel MC. A Rapid, Stability-Indicating RP-HPLC Method for the Simultaneous Determination of Formoterol Fumarate, Tiotropium Bromide, and Ciclesonide in a Pulmonary Drug Product. *Sci Pharm*. 2012 Sep;80(3):591–603.

18. Tajber L, Corrigan DO, Corrigan OI, Healy AM. Spray drying of budesonide, formoterol fumarate and their composites—I. Physicochemical characterisation. *Int J Pharm.* 2009 Feb 9;367(1–2):79–85.
19. Velaga SP, Berger R, Carlfors J. Supercritical fluids crystallization of budesonide and flunisolide. *Pharm Res.* 2002 Oct;19(10):1564–71.
20. Rasenack N, Muller BW. Micron-size drug particles: Common and novel micronization techniques. *Pharm Dev Technol.* 2004;9(1):1–13.
21. Sin DD, Man SFP. Do chronic inhaled steroids alone or in combination with a bronchodilator prolong life in chronic obstructive pulmonary disease patients? *Curr Opin Pulm Med.* 2007 Mar;13(2):90–7.
22. Nelson HS, Chapman KR, Pyke SD, Johnson M, Pritchard JN. Enhanced synergy between fluticasone propionate and salmeterol inhaled from a single inhaler versus separate inhalers. *J Allergy Clin Immunol.* 2003 Jul;112(1):29–36.
23. French DL, Edwards DA, Niven RW. The influence of formulation on emission, deaggregation and deposition of dry powders for inhalation. *J Aerosol Sci.* 1996 Jul;27(5):769–83.
24. Hickey AJ, Mansour HM, Telko MJ, Xu Z, Smyth HD., Mulder T, et al. Physical characterization of component particles included in dry powder inhalers. I. Strategy review and static characteristics. *J Pharm Sci.* 2007;96(5):1282–301.
25. Zeng XM, Martin GP, Tee SK, Marriott C. The role of fine particle lactose on the dispersion and deaggregation of salbutamol sulphate in an air stream in vitro. *Int J Pharm.* 1998 Dec 30;176(1):99–110.

Chapter 5: Development of a Performance Verification Test for Cascade Impactors

Abstract

Cascade impactors are used as the standard test method for assessing therapeutic aerosols. A Performance Verification Test (PVT) for cascade impactors was developed to investigate the use of a standardized pressurized Metered Dose Inhaler (pMDI) with the Next Generation Cascade Impactor. A suitable propellant (HFA-134a) was used in conjunction with an easily detectable marker compound, rhodamine B. By adjusting the composition of the pMDI formulation, various loadings across the impactor plates of the NGI could be achieved. Two standardized formulations were selected to be fired sequentially into the NGI, thereby optimizing the impactor plate coverage to maximize the potential for detecting deviations in MMAD, as well as Total Stage Deposition (TSD). Introduction of the variable conditions to the NGI was found to significantly adjust the deposition patterns of the standardized formulations (B and E4), suggesting that their use as a PVT could be useful and that further investigation is warranted.

5.1 INTRODUCTION

The pulmonary route has been extensively explored for the delivery of drugs therapies. It possess numerous advantages for drug delivery, such as large alveolar surface area, avoidance of first pass metabolism, the potential for local and systemic administration (1). In order to enhance lung deposition, aerosol particles should be in the aerodynamic diameter range between 1-5 μm . Particles smaller than 1 μm will probably be exhaled from the lungs and particles above 5 μm will mostly deposit in the upper airways (2)(3).

Cascade impactors (CIs) are used as the standard test method for assessing the performance of therapeutic aerosols. CIs fractionate the dose emitted from the inhaler device according to aerodynamic particle size distribution. The samples are collected and chemically quantified for determination of drug mass deposition onto the various impaction plates (4). The United States Pharmacopeia (USP) guidance is very clear on how a variety of different impactor/impinger systems should be used for a variety of delivery methods, such as pressurized metered dose inhaler (pMDI), nebulizer or dry powder inhaler (DPI) (5). Because of this the impaction test methods used have become the industry standard and are routinely used for batch validation as well as NDAs for new therapies. It is widely known that variation in the cascade impactor data can occur over time, due to improper cleaning resulting in erosion, corrosion and/or occlusion of the nozzles or even a poorly implemented standard operational procedure (SOP). These deteriorations may influence stage cut-off diameters and therefore, data integrity(6). As such the impactor manufacturers and the USP recommend that routine mensuration of the test apparatus should be implemented (depending of the frequency of use and formulations that are routinely being tested) (5).

Mensuration is a specialized process, which measures the critical properties of the jet dimensions, the jets spatial arrangements in relation to its collection surfaces and the airflow passing through them. In most cases, it requires the use of a Vibrating Orifice Aerosol Generator (VOAG) to generate a monodisperse droplet size in the size range from 0.6 to 20 μm that is impinged onto the various stages of the cascade impactor in question. The droplets are formed using oleic acid with a uranine fluorescent dye tracer for liquid particles of ammonium fluorescein for solid particles (7). However the VOAG is difficult to use for individual laboratories that do not routinely use it and the apparatus is generally quite expensive to purchase. So the only real option is to send the apparatus away for cleaning and mensuration (back to the original manufacturer). There are several reasons why this may be undesirable: (i) the apparatus will have a down time during this process; (ii) the cost of mensuration is high (especially to academic institutions and startup companies – particularly if full mensuration is not really needed); (iii) one or more secondary impactor system(s) may be needed for continued operation(8).

It would be desirable if a standard performance verification test (PVT) could be used in house to provide routine validation of impactor apparatus. This PVT could be considered to be equivalent to PVTs that the USP indicates for other test apparatus such as the General Chapters: <711> Dissolution. The dissolution apparatus employs the use of standard dissolution test tablets to ensure that the dissolution test apparatus is being used effectively.

The objective of this research is to develop a standardized performance verification test for in-house use to provide routine validation of cascade impactor apparatus. For that, a reference (non-commercial) standard system including device and formulation will be developed for the reproducible generation of aerosols.

5.2 MATERIALS AND METHODS

5.2.1 Materials

Acetic acid (glacial) and rhodamine B were purchased from Thermo Fisher Scientific (Waltham, MA). Ethanol (200 proof) was purchased from Decon Labs, Inc. (King of Prussia, PA). 1,1,1,2-tetrafluoroethane (HFA-134a) propellant was kindly donated by Mexichem Fluor Inc. (St Gabriel, LA). Plastic coated glass bottles (20 mL volume) were generously donated by SGD-Pharma Group (Mers-les-Brains, France) and the metered-dose valves (50 μ L) were donated from Aptar (Crystal Lake, IL).

5.2.2 Formulation preparation

5.2.2.1 Rhodamine B/ethanol/propellant formulations

In order to maximize the coverage of the proposed PVT across the cascade impactor, a high polydispersity (i.e. a broad particle size distribution) was required. In order to obtain this two options were available: a single shot formulation with broad but uniform particle size distribution (PSD); or a two shot system with both a low mass median aerodynamic diameter (MMAD) and a high MMAD ranging from 0.6 and 3.5 μ m. Therefore, adjustments to the solubility and density of the propellant solutions were carried out for optimal deposition profiles.

A series of solution pMDIs were prepared using Rhodamine B as a tracer dye, ethanol 200 proof as a co-solvent, and the propellant 1,1,1,2-tetrafluoroethane (HFA-134a). First, a stock solution was prepared by dissolving rhodamine b in ethanol. Subsequently, an aliquot of this solution was transferred to a 20 mL plastic coated glass bottle, which was immediately crimped with metered-dose valves. The system was filled with the chosen volume of HFA-134a using an HFA filling machine (Pamasol model P2008, Switzerland). Table 5.1 shows the different types of formulations with their

respective compositions. After preparation, pMDIs were placed on a plate shaker for 24 hours at 250 rpm. Same 0.7 mm actuator was used for all pMDIs. All formulations were prepared in the same day and repeated in different days to test for system robustness.

5.2.2.2 Rhodamine B/ethanol/propellant/adjuvant excipients formulations

pMDI systems were prepared using several adjuvant excipients, e.g., poloxamer 338, poloxamer 188 and polyethylene glycol 400. The excipients were employed at different concentrations giving different amount of nonvolatile content for each formulation. The series of solution pMDIs were prepared in the same way as described previously. However, additionally to the aliquot of rhodamine b and ethanol stock solution, an aliquot of the adjuvant excipients were also added to the plastic coated glass bottles and immediately crimped by the Pamasol machine. Table 5.2 shows the different types of formulations with their respective compositions. After preparation, pMDIs were placed on a plate shaker for 24 hours at 250 rpm. Same 0.7 mm actuator was used for all pMDIs. All formulations were prepared in the same day and repeated in different days to test for system robustness.

5.2.3 NGI operation procedure – normal use

The aerodynamic particle size distributions (APSD) of the formulations were determined using the Next Generation Cascade Impactor (Copley Scientific, Nottingham, UK) and a United States Pharmacopeia (USP) induction port (neck). Cascade impactor (CI) was assembled and operated in accordance to the USP General Chapter <601> Aerosol, Nasal Spray, Metered-dose Inhalers and Dry Powder Inhalers (5). Each pMDI formulation was primed and then actuated twice with 10 seconds interval between

actuators before fired into the CI. The airflow rate through the system was calibrated at 30 L/min using a TSI mass flowmeter (Model 4000, TSI Inc., St. Paul, MN) attached to the open end of the induction port. After aerosolization, samples were collected using known volumes of 0.1M acetic acid solution and ethanol (1:1) at pH 3.0 and assayed with UV-vis spectroscopy on the same day.

The same experimental procedure was used on 3 different NGI systems to test the formulations for repeatability and reproducibility. The experiments were conducted in 3 different laboratories.

The NGI collection plates were coated with 1% (v/v) silicone oil in hexane to prevent particle bounce, fracture and reentrainment. Total stage deposition was calculated as the amount of drug deposited on the NGI stages. Mass median aerodynamic diameter (MMAD) and geometric standard deviation (GSD) were calculated based on the dose deposited on stages 1 through MOC.

5.2.4 NGI operation procedure for stress testing

After selection of the optimized formulations, three cascade impactor stress testing was performed in the same NGI. The tests were performed to evaluate the impact on the APSD of the formulations when different parameters of the NGI system are altered. Also, the tests will determine the sensitivity of the formulations (standard reference material) to detect any abnormality present on the NGI apparatus. The selected formulations were tested and actuated once each with 10 seconds interval between actuators. Samples were recovered with 0.1M acetic acid solution and ethanol (1:1) at pH 3.0 and assayed with UV-vis spectroscopy at the same day.

5.2.4.1 Air leakage simulation of stage 3 of the NGI

In order to simulate an unknown air leakage on the NGI system, we placed a damaged O-ring at stage 3 of the equipment body. Because of the air leakage in the system the airflow rate was recalibrated from 20 to 30 L/min. using a TSI mass flowmeter (Model 4000, TSI Inc., St. Paul, MN) attached to the open end of the induction port.

5.2.4.2 Simulation of nozzle clogging at stage 4

To test the impact of clogged nozzles on APSD of the formulations approximately 1/3 of the stage 4 nozzles were blocked using a tape. The airflow rate was recalibrated to 30 L/min. after obstruction of the nozzles.

5.2.4.3 NGI analysis at low airflow rate

The impact on APSD of pMDI formulations was also evaluated when the analyst use the equipment at lower airflow rate than 30L/min. Therefore, we recalibrated the system using a flowmeter to set the airflow rate at 25L/min. It is anticipated that the APSD of the formulations will shift to the right due to the increase of aerodynamic particle size distribution with decrease of the airflow rate.

5.2.5 UV-vis spectroscopy

Samples of rhodamine were quantified using the HP/Agilent 8453 UV-vis spectrophotometer with Chemstation equipped with UV detector set at 558 nm wavelength.

5.2.6 Statistical analysis

The data is expressed as mean \pm standard deviation (SD). Statistical analyses were performed using NCSS/PASS software Dawson edition. Student's t tests and one-way ANOVA were conducted to analyze statistically significant differences in aerodynamic particle size distribution and cascade impactor deposition between formulations ($p < 0.05$).

5.3 RESULTS AND DISCUSSION

5.3.1 Formulation design

Rhodamine B was selected as the fluorescent marker due to its ease of detection (UV-vis detection), solubility in ethanol (15 mg/mL) and good stability in propellant system (9). Also, ethanol has been widely used as a co-solvent system in pMDI formulations (10). HFA-134a is an inert and well characterized propellant exhibiting many advantages e.g., non-toxicity, odor and taste free and chemical stability (11). There are several pros and cons to consider when choosing the correct pMDI formulation type such as solution or suspension as summarized in Table 5.3 (12)(11). While aerosolization performance of suspension pMDIs depends on proper re-suspension techniques and particle size distribution of suspended particles, the performance of a solution pMDI system is mainly determined by its non-volatile fraction and its influence on vapor pressure(13). For this study, a solution-based system was selected as there is the potential for less operator dependent error, since the re-suspension step of the formulation can lead to emitted dose variability.

5.3.2 Performance of formulations

5.3.2.1 Rhodamine B/ethanol/propellant formulations

Formulations A, F, B, B.1 and B.2 were prepared using different concentrations of rhodamine b, ethanol and propellant containing no adjuvant excipient. Rhodamine B precipitated inside the pMDI glass bottles of formulations A, F, B.1 and B.2 after 24 hours. Only formulation B was able to maintain its solubilized state in HFA=134a. These results indicated that the highest levels of rhodamine b were set at 0.1% w/v in the presence of 10% (v/v) ethanol before reaching the saturation point. An MMAD of 1.12 μm with a GSD of 2.2 was obtained, demonstrating a deposition toward the lower particle size plates of the NGI. The aerodynamic particle size distribution of this formulation is shown in Figure 5.1.

5.3.2.2 Rhodamine B/ethanol/propellant formulations/adjuvant excipients

All formulations prepared with adjuvant excipients are described in Table 5.2. The size of the aerosols is determined by the evaporation of the propellant and any other volatile component in the formulation followed by the shrinkage of the droplets. The inclusion of non-volatile components in HFA solution formulations for pMDIs greatly increases the particle size distribution of the aerosol by increasing the size of the droplets (9). Poloxamer 338 and poloxamer 188 were first dissolved in ethanol before filled into the pMDI bottles. The pMDI systems prepared with adjuvant excipients, ethanol 5% (v/v) and 0.1% (w/v) rhodamine b (formulations B.1, C.1, D.1, E.1) precipitated when filled with propellant. Precipitation was due to the low solubility of poloxamers 338 and poloxamers 188 in HFA 134a. To enhance the solubility of poloxamers, the concentration of ethanol was increased to 10% (v/v). After 24 hours, the final pMDI systems remained in the solution state (formulations C and D) and were analyzed for particle size

distribution. Due to the relatively high solubility of PEG 400 in HFA 134a of about 4% (w/w), all pMDI systems prepared with PEG at different concentrations (E, E.2, E.3 and E.4) remained in solution state and were analyzed for particle size distribution(10). The deposition profiles for these formulations are in shown in Figures 5.2a, 5.2b and 5.3a.

From data shown for the deposition profiles of formulations C, D and E (Figure 5.2) was found that the APSD mainly covers the center stages of the NGI (S3, S4 and S5). Moreover, the deposition for formulation E.2 is significantly low with most of the aerosol depositing on the external filter. The deposition of formulation E.3 and E.4 were skewed to the left of the NGI with significant deposition on stages S0, S1, S2 S3 and S4. Therefore, it was found that the development of a formulation with a broad particle size distribution and significant deposition on all stages of the NGI was not possible. So, two formulations were selected which would cover all stage depositions.

From the data shown for the deposition profiles Formulation E4 was found to cover the lower value impaction plates that were not obtained with Formulation B. For E4 the MMAD was found to be 3.30 μm with a GSD of 2.5. The combined deposition of Formulations B and E4 is shown in Figure 5.3b. After selection, the formulations were prepared in different days and tested on NGI. The particle size distribution on the stages was compared using student's t-test and was not statistically different indicating to be a robust system. The mass of aerosol deposited on the NGI stages when formulations are actuated in sequence on the NGI was not exactly the same as shown by the deposition of the formulations actuated individually. This could be due to particle bouncing on NGI and increased deposition on the induction port.

5.3.2.3 Inter impactor variability

To test for the reproducibility of the PVT inter-impactor variability was evaluated in addition to intra-impactor variability. Three NGIs were tested and the mass deposition among them is shown in Figure 5.4. The data shows a similar pattern of particle distribution among the 3 NGIs, however there was some statistical difference between few stage depositions. The intermediate reproducibility found for aerosol deposition among the NGIs may be related to a small difference in NGI calibration (from supplier) and/or to difference between laboratory environments, such as temperature and humidity. Difference in environment temperature and humidity will influence the rate of evaporation and shrinkage of the aerosol droplets and consequently the final aerodynamic particle size distribution.

5.3.3 NGI stress testing

Figure 5.5 shows the APSD of formulations B and E.4 when NGI was set up at different parameters. The data shows a significant difference in the deposition pattern of the stress-tested formulations of B and E4 when compared to the standard deposition pattern as indicated by the control group (MMAD = 1.96 μm ; GSD = 2.7; TSD = 15.4 μg).

The presence of the damaged o-ring on the NGI caused airflow leaking throughout the NGI stages. Therefore, during the initial calibration of the airflow rate it was necessary to increase significantly the vacuum pump pressure to regulate the flow back to 30 L/min. The data obtained for the damaged o-ring deposition suggests that a slightly higher mass of drug is deposited on the stages (TSD = 23.1 μg). This could be indicative of the increased airflow through the NGI entraining more drugs on the aerosol and its faster evaporation. The faster evaporation decreased the amount of droplets

depositing on the induction port. The subsequent MMAD is also higher at 2.16 with a GSD of 2.4, which could indicate a higher velocity of the increased airflow through the system leaning toward a higher MMAD.

For the blockage of the Stage 4 jets a lower airflow rate through the NGI is expected. Indeed a TSD of 18.2 μg is observed. The mass of rhodamine b deposited on the stages S3 through EF is lower than that obtained when a damaged o-ring was observed, but it is still higher than that obtained for the control group. This is possibly due to the change in pressure and airflow rate through the stages due to the increased pressure on S4. A lower MMAD of 1.76 μm is seen with a GSD of 2.6, which is consistent with and overall lower air velocity through the impactor compared to the control group, resulting in a lower aerodynamic particle size since the optimal inertia of particles would not be achieved.

A higher mass of drug is again deposited on the NGI stages when compared to the control group when the airflow through the NGI is reduced to 25 L/min (TSD value of 19.7 μg). The reduction of airflow rate increases the stages cutoff resulting in lower particle inertia, consequently, shifting particle deposition to the high number stages the NGI. As expected, the MMAD values reduced to 1.70 μm with a GSD of 2.8.

5.4 CONCLUSION

Two standard reference formulations with broad aerodynamic particle size distribution were developed. The formulations showed good reproducibility and robustness. The NGI deposition of the formulations exhibited a slight difference among the three NGIs. Also, the formulations presented good sensitivity to changes in NGI apparatus parameters. The formulations showed to be suitable to be used as a standard reference material for the performance verification tests of the NGI apparatus. The APSD

of the standard reference material should be determined individually for each apparatus immediately after NGI calibration and/or mensuration.

5.5 TABLES

Formulation	Rhodamine b % (w/w)	Ethanol % (v/v)	HFA-134a % (w/v)
A	1	9.26%	89.74
F	0.5	9.26%	90.24
B	0.1	9.26%	90.64
B.1	0.1	4.80%	95.1
B.2	0.05	4.80%	95.15

Table 5.1 – Composition of the pMDI formulations (Rhodamine B/ethanol/propellant).

Formulation	Rhodamine % (w/v)	Alcohol % (v/v)	P338 % (w/w)	P188 %(w/w)	PEG %(w/v)	Glycerol % (w/v)	HFA-134a %(w/v)
C	0.1	9.26	0.1	-	-		90.54
D	0.1	9.26	-	0.1	-		90.54
E	0.1	9.26	-	-	0.6		90.04
C.1	0.1	4.8	0.1				95
D.1	0.1	4.8	-	0.1	-		95
E.1	0.1	4.8	-	-	0.6		94.5
C.2	0.05	4.8	0.05				95.1
D.2	0.05	4.8	-	0.05	-		95.1
E.2	0.05	4.8	-	-	0.65		94.5
E.3	0.05	4.8			1.5		93.65
E.4	0.05	4.8			2.4		92.75
F	0.05	4.8				1	94.15

Table 5.2 – Composition of the pMDI formulations (Rhodamine B/ethanol/propellant/ adjuvant excipients).

Solution	Suspension
<u>Particle size:</u> <ul style="list-style-type: none"> • Non-volatile fraction • Vapor pressure • Actuator design 	<u>Particle size:</u> <ul style="list-style-type: none"> • Suspended micronized particles
<u>Stability issues:</u> <ul style="list-style-type: none"> • High solubility of solutes • Propellant choice 	<u>Stability issues:</u> <ul style="list-style-type: none"> • Aggregation • Flocculation
Uniformity dependent on high solubility	Uniformity dependent on re-dispersion

Table 5.3 – General comparison of solution based and suspension based pMDIs.

5.6 FIGURES

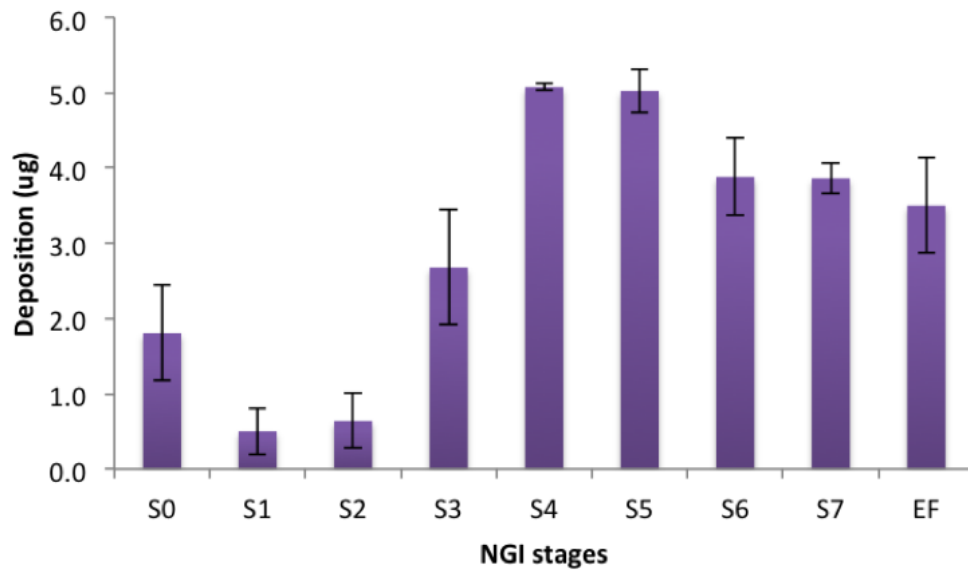


Figure 5.1 – Amount deposition of formulation B on a NGI. Data is presented as mean \pm SD, n = 3.

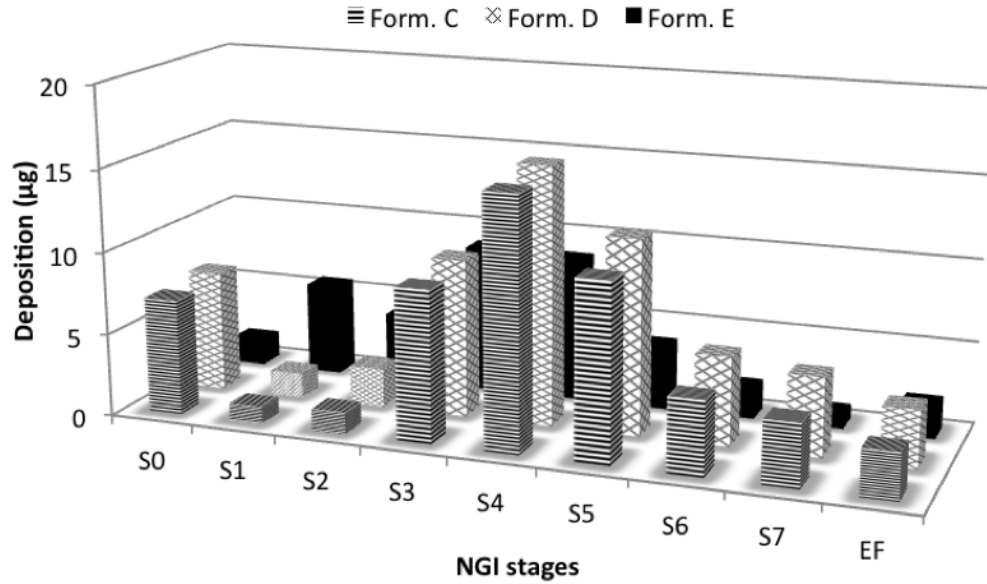


Figure 5.2a – Amount deposition of formulation C, D and E on a NGI. Data is presented as mean \pm SD, n = 3.

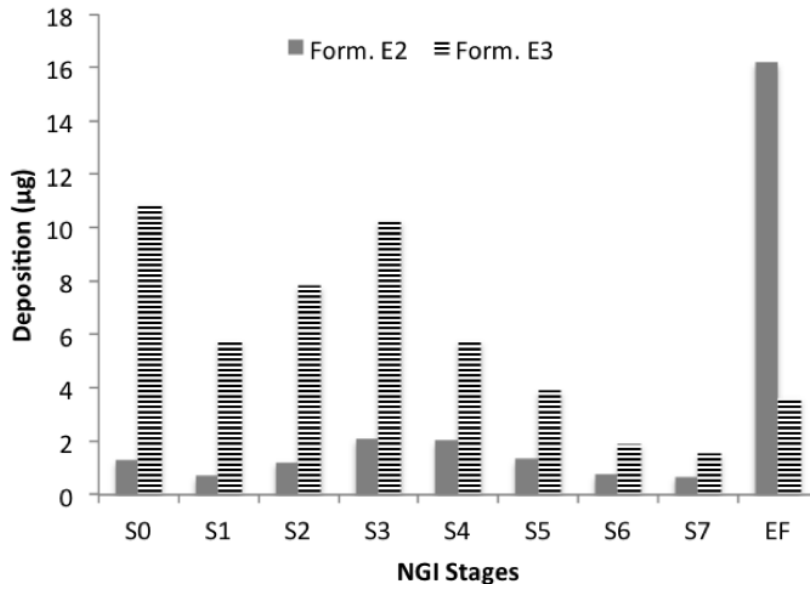


Figure 5.2b – Amount deposition of formulation E.2 and E.3 on a NGI. Data is presented as mean \pm SD, n = 3 .

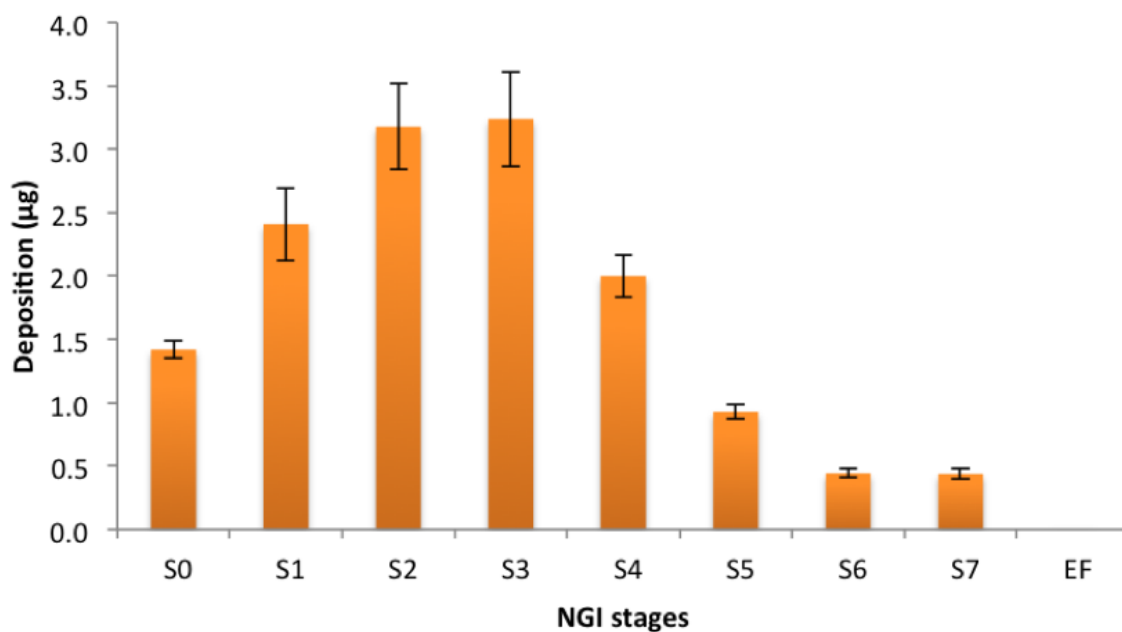


Figure 5.3a – Amount deposition of formulation E.4 on a NGI. Data is presented as mean \pm SD, n = 3.

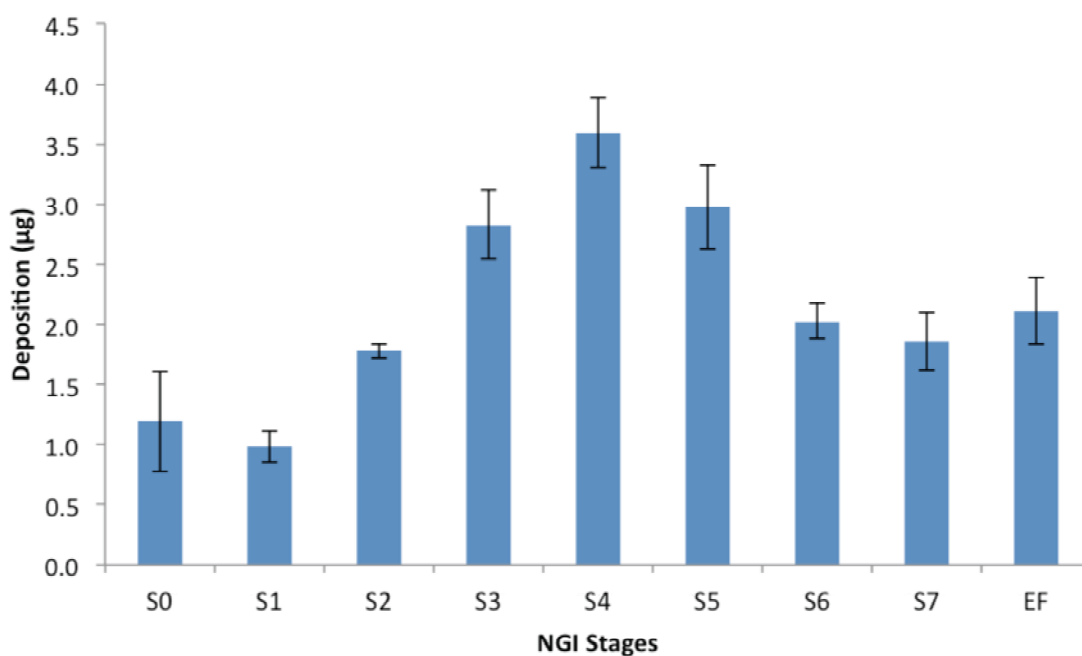


Figure 5.3b – Combined deposition of formulations B and E.4 on a NGI. Data is presented as mean \pm SD, n = 3.

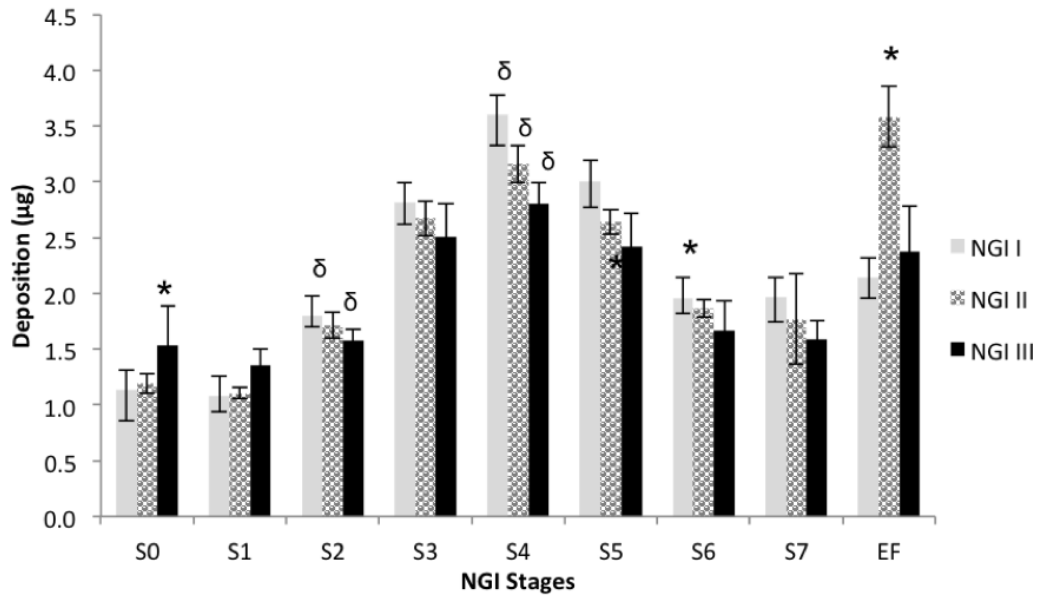


Figure 5.4. Amount deposition of formulations B and E.4 on NGI I, II and III. Data is presented as mean \pm SD, n = 3. The symbol * means $\alpha < 0.05$ when compared to other groups individually and δ means $\alpha < 0.05$ when compared to each other.

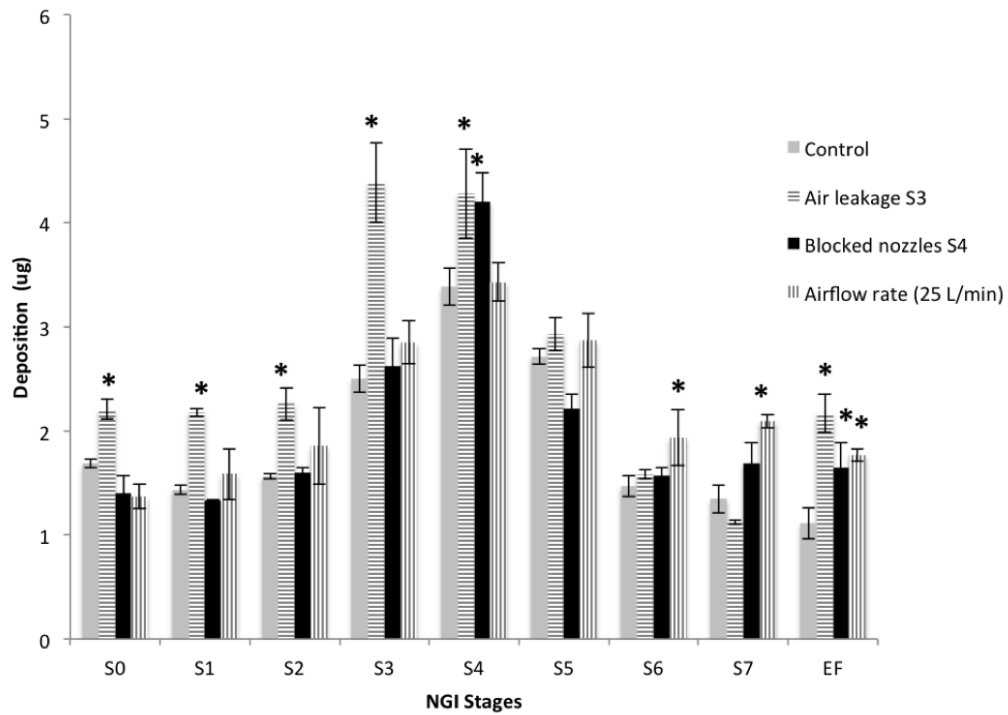


Figure 5.5 – Amount deposition of formulations B and E.4 on NGI I at different conditions: control, damaged o-ring, partial blockage of nozzles on stage 4, and reduction of airflow rate to 25 L/min. Data is presented as mean \pm SD, $n = 3$. The symbol * means $\alpha < 0.05$ when compared to other groups individually and δ means $\alpha < 0.05$ when compared to each other.

5.7 REFERENCES

1. Patton JS, Byron PR. Inhaling medicines: delivering drugs to the body through the lungs. *Nat Rev Drug Discov.* 2007 Jan 1;6(1):67–74.
2. Edwards DA, Hanes J, Caponetti G, Hrkach J, Ben-Jebria A, Eskew ML, et al. Large Porous Particles for Pulmonary Drug Delivery. *Science.* 1997 Jun 20;276(5320):1868–72.
3. Smyth HDC, Hickey AJ. Carriers in Drug Powder Delivery: Implications for Inhalation System Design. *Am J Drug Deliv.* 2005;3(2):117–32.
4. Marple VA, Roberts DL, Romay FJ, Miller NC, Truman KG, Holroyd MJ, et al. Next generation pharmaceutical impactor (A new impactor for pharmaceutical inhaler testing). Part I: Design. *J Aerosol Med-Depos Clear Eff Lung.* 2003 FAL;16(3):283–99.
5. General Chapters <601> Aerosols, Nasal Sprays, Metered-dose Inhalers, and Dry Powder Inhaler. *U S Pharmacop.* 35th-NF ed.
6. Svensson M, Pettersson G, Asking L. Mensuration and cleaning of the jets in Andersen cascade impactors. *Pharm Res.* 2005 Jan;22(1):161–5.
7. Marple VA, Olson BA. Good Laboratory Practice in Particle Measurement Calibration: Cascade Impactor. *Kona Powder Part J.* 2009;(27):206–16.
8. Roberts DL, Romay FJ. Relationship of stage mensuration data to the performance of new and used cascade impactors. *J Aerosol Med-Depos Clear Eff Lung.* 2005 WIN;18(4):396–413.
9. Brambilla G, Ganderton D, Garzia R, Lewis D, Meakin B, Ventura P. Modulation of aerosol clouds produced by pressurised inhalation aerosols. *Int J Pharm.* 1999;186(1):53–61.

10. Vervaet C, Byron PR. Drug-surfactant-propellant interactions in HFA-formulations. *Int J Pharm.* 1999 Sep 10;186(1):13–30.
11. Blondino FE, Byron PR. Surfactant dissolution and water solubilization in chlorine-free liquified gas propellants. *Drug Dev Ind Pharm.* 1998 Oct;24(10):935–45.
12. Dalby RN, Byron PR. Comparison of output particle size distributions from pressurized aerosols formulated as solutions or suspensions. *Pharm Res.* 1988 Jan;5(1):36–9.
13. Smyth HDC. The influence of formulation variables on the performance of alternative propellant-driven metered dose inhalers. *Adv Drug Deliv Rev.* 2003;55(7):807–28.

Bibliography

- Adi, Handoko, Daniela Traini, Hak-Kim Chan, and Paul M Young. 2008. "The Influence of Drug Morphology on the Aerosolisation Efficiency of Dry Powder Inhaler Formulations." *Journal of Pharmaceutical Sciences* 97 (7) (July): 2780–2788. doi:10.1002/jps.21195.
- Adi, Handoko, Paul M Young, Hak-Kim Chan, Peter Stewart, Helen Agus, and Daniela Traini. 2008. "Cospray Dried Antibiotics for Dry Powder Lung Delivery." *Journal of Pharmaceutical Sciences* 97 (8) (August): 3356–3366. doi:10.1002/jps.21239.
- Adi, Handoko, Paul M. Young, Hak-Kim Chan, Helen Agus, and Daniela Traini. 2010. "Co-Spray-Dried Mannitol–ciprofloxacin Dry Powder Inhaler Formulation for Cystic Fibrosis and Chronic Obstructive Pulmonary Disease." *European Journal of Pharmaceutical Sciences* 40 (3) (June 14): 239–247. doi:10.1016/j.ejps.2010.03.020.
- Adi, Handoko, Paul M. Young, and Daniela Traini. 2012. "Co-Deposition of a Triple Therapy Drug Formulation for the Treatment of Chronic Obstructive Pulmonary Disease Using Solution-Based Pressurised Metered Dose Inhalers." *Journal of Pharmacy and Pharmacology* 64 (9) (September): 1245–1253. doi:10.1111/j.2042-7158.2011.01370.x.
- Adi, S., H. Adi, P. Tang, D. Traini, H. Chan, and P. M Young. 2008. "Micro-Particle Corrugation, Adhesion and Inhalation Aerosol Efficiency." *European Journal of Pharmaceutical Sciences* 35 (1-2): 12–18.
- Al-Qadi, S., A. Grenha, D. Carrión-Recio, B. Seijo, and C. Remuñán-López. 2012. "Microencapsulated Chitosan Nanoparticles for Pulmonary Protein Delivery: In Vivo Evaluation of Insulin-Loaded Formulations." *Journal of Controlled Release* 157 (3) (February 10): 383–390. doi:10.1016/j.jconrel.2011.08.008.
- Al-Showair, Raid A.M., Walid Y. Tarsin, Khaled H. Assi, Stanley B. Pearson, and Henry Chrystyn. 2007. "Can All Patients with COPD Use the Correct Inhalation Flow with All Inhalers and Does Training Help?" *Respiratory Medicine* 101 (11) (November): 2395–2401. doi:10.1016/j.rmed.2007.06.008.
- Alemdar, A. Y., D. Sadi, V. C. McAalister, and I. Mendez. 2004. "Liposomal Formulations of Tacrolimus and Rapamycin Increase Graft Survival and Fiber

- Outgrowth of Dopaminergic Grafts.” *Cell Transplantation* 13 (3): 263–271.
doi:10.3727/000000004783983936.
- Alhalaweh, Amjad, Waseem Kaialy, Graham Buckton, Hardyal Gill, Ali Nokhodchi, and Sitaram P. Velaga. 2013. “Theophylline Cocrystals Prepared by Spray Drying: Physicochemical Properties and Aerosolization Performance.” *AAPS PharmSciTech* 14 (1) (January 8): 265–276. doi:10.1208/s12249-012-9883-3.
- Alhalaweh, Amjad, and Sitaram P. Velaga. 2010. “Formation of Cocrystals from Stoichiometric Solutions of Incongruently Saturating Systems by Spray Drying.” *Crystal Growth & Design* 10 (8) (August): 3302–3305. doi:10.1021/cg100451q.
- Alonzo, D. E, G. G.Z Zhang, D. Zhou, Y. Gao, and L. S Taylor. 2010. “Understanding the Behavior of Amorphous Pharmaceutical Systems during Dissolution.” *Pharmaceutical Research* 27 (4): 608–618.
- Amidi, Maryam, Enrico Mastrobattista, Wim Jiskoot, and Wim E. Hennink. 2010. “Chitosan-Based Delivery Systems for Protein Therapeutics and Antigens.” *Advanced Drug Delivery Reviews* 62 (1) (January 31): 59–82.
doi:10.1016/j.addr.2009.11.009.
- Asada, Mayumi, Hirokazu Takahashi, Hirokazu Okamoto, Hideo Tanino, and Kazumi Danjo. 2004. “Theophylline Particle Design Using Chitosan by the Spray Drying.” *International Journal of Pharmaceutics* 270 (1–2) (February 11): 167–174. doi:10.1016/j.ijpharm.2003.11.001.
- Baheti, Ankit, Lokesh Kumar, and Arvind Kumar Bansal. 2010. “Excipients Used in Lyophilization of Small Molecules.” *Journal of Excipients and Food Chemicals* 1 (1): 41–54.
- Bailey, Mark M., and Cory J. Berkland. 2009. “Nanoparticle Formulations in Pulmonary Drug Delivery.” *Medicinal Research Reviews* 29 (1) (January 1): 196–212.
doi:10.1002/med.20140.
- Barnes, P. J. 2002. “Scientific Rationale for Inhaled Combination Therapy with Long-Acting β 2-Agonists and Corticosteroids.” *European Respiratory Journal* 19 (1) (January 1): 182–191. doi:10.1183/09031936.02.00283202.

- Barnes, P. J., S. D. Shapiro, and R. A. Pauwels. 2003. "Chronic Obstructive Pulmonary Disease: Molecular and Cellular Mechanisms." *European Respiratory Journal* 22 (4) (October): 672–688. doi:10.1183/09031936.03.00040703.
- Barnes, P. J., and R. A. Stockley. 2005. "COPD: Current Therapeutic Interventions and Future Approaches." *European Respiratory Journal* 25 (6) (June): 1084–1106. doi:10.1183/09031936.05.00139104.
- Barnes, Peter J. 2011. "Triple Inhalers for Obstructive Airways Disease: Will They Be Useful?" *Expert Review of Respiratory Medicine* 5 (3) (June): 297–300. doi:10.1586/ers.11.26.
- Beck-Broichsitter, Moritz, Christoph Schweiger, Thomas Schmehl, Tobias Gessler, Werner Seeger, and Thomas Kissel. 2012. "Characterization of Novel Spray-Dried Polymeric Particles for Controlled Pulmonary Drug Delivery." *Journal of Controlled Release* 158 (2) (March 10): 329–335. doi:10.1016/j.jconrel.2011.10.030.
- Beinborn, Nicole A, Helene L Lirola, and Robert O. Williams. 2012. "Effect of Process Variables on Morphology and Aerodynamic Properties of Voriconazole Formulations Produced by Thin Film Freezing." *International Journal of Pharmaceutics* 429 (1-2) (June 15): 46–57. doi:10.1016/j.ijpharm.2012.03.010.
- Beinborn, Nicole A., Ju Du, Nathan P. Wiederhold, Hugh D.C. Smyth, and Robert O. Williams III. 2012. "Dry Powder Insufflation of Crystalline and Amorphous Voriconazole Formulations Produced by Thin Film Freezing to Mice." *European Journal of Pharmaceutics and Biopharmaceutics* (0). doi:10.1016/j.ejpb.2012.04.019. <http://www.sciencedirect.com/science/article/pii/S0939641112001348>.
- Bentham, A.C, C.C Kwan, R Boerefijn, and M Ghadiri. 2004. "Fluidised-Bed Jet Milling of Pharmaceutical Powders." *Powder Technology* 141 (3) (March 30): 233–238. doi:10.1016/j.powtec.2004.01.024.
- Bérard, V, E Lesniewska, C Andrès, D Pertuy, C Laroche, and Y Pourcelot. 2002. "Dry Powder Inhaler: Influence of Humidity on Topology and Adhesion Studied by AFM." *International Journal of Pharmaceutics* 232 (1–2) (January 31): 213–224. doi:10.1016/S0378-5173(01)00913-9.

- Berard, V., E. Lesniewska, C. Andres, D. Pertuy, C. Laroche, and Y. Pourcelot. 2002. "Affinity Scale between a Carrier and a Drug in DPI Studied by Atomic Force Microscopy." *International Journal of Pharmaceutics* 247 (1-2) (October 24): 127–137. doi:10.1016/S0378-5173(02)00400-3.
- Bhambere, Deepak, Birendra Shirivastava, Pankaj Sharma, Nisha Bukane, and Paraag Gide. 2013. "Preparation and Optimization of Dry PLGA Nanoparticles by Spray Drying Technique." *Particulate Science and Technology* 31 (5) (September 3): 533–540. doi:10.1080/02726351.2013.782932.
- Bhavna, Farhan Jalees Ahmad, Gaurav Mittal, Gaurav K Jain, Geena Malhotra, Roop K Khar, and Aseem Bhatnagar. 2009. "Nano-Salbutamol Dry Powder Inhalation: A New Approach for Treating Broncho-Constrictive Conditions." *European Journal of Pharmaceutics and Biopharmaceutics* 71 (2) (February): 282–291. doi:10.1016/j.ejpb.2008.09.018.
- Bittner, B., and T. Kissel. 1999. "Ultrasonic Atomization for Spray Drying: A Versatile Technique for the Preparation of Protein Loaded Biodegradable Microspheres." *Journal of Microencapsulation* 16 (3) (June): 325–341.
- Bjerg, Anders, Bo Lundbäck, and Jan Lötvall. 2012. "The Future of Combining Inhaled Drugs for COPD." *Current Opinion in Pharmacology* 12 (3) (June): 252–255. doi:10.1016/j.coph.2012.03.004.
- Blondino, F E, and P R Byron. 1998. "Surfactant Dissolution and Water Solubilization in Chlorine-Free Liquified Gas Propellants." *Drug Development and Industrial Pharmacy* 24 (10) (October): 935–945. doi:10.3109/03639049809097273.
- Bonam, M., D. Christopher, D. Cipolla, B. Donovan, D. Goodwin, S. Holmes, S. Lyapustina, et al. 2008. "Minimizing Variability of Cascade Impaction Measurements in Inhalers and Nebulizers." *AAPS PharmSciTech* 9 (2): 404–413.
- Bose, Sagarika, and Robin H Bogner. 2007. "Solventless Pharmaceutical Coating Processes: A Review." *Pharmaceutical Development and Technology* 12 (2): 115–131. doi:10.1080/10837450701212479.

- Brain, Joseph D. 2007. "Inhalation, Deposition, and Fate of Insulin and Other Therapeutic Proteins." *Diabetes Technology & Therapeutics* 9 (s1) (June): S-4-S-15. doi:10.1089/dia.2007.0228.
- Brambilla, G, D Cocconi, A Armani, S Smith, Emma Lesley Lye, and S Burge. 2006. "Designing a Novel Powder Inhaler: The NEXT DPI." In , 2:553-555. *Respiratory Drug Delivery*.
- Brambilla, G., D. Ganderton, R. Garzia, D. Lewis, B. Meakin, and P. Ventura. 1999. "Modulation of Aerosol Clouds Produced by Pressurised Inhalation Aerosols." *International Journal of Pharmaceutics* 186 (1): 53-61.
- Brown, Beth A.-S., Jack A. Rasmussen, Daniel P. Becker, and David R. Friend. 2004. "A Piezo-Electronic Inhaler for Local & Systemic Applications." *Drug Delivery Technology* 4 (8): 90-93.
- Carvalho, Thiago C., Jay I. Peters, and Robert O. Williams III. 2011. "Influence of Particle Size on Regional Lung Deposition – What Evidence Is There?" *International Journal of Pharmaceutics* 406 (1-2) (March 15): 1-10. doi:10.1016/j.ijpharm.2010.12.040.
- Cattaneo, Dario, Norberto Perico, and Flavio Gaspari. 2002. "Assessment of Sirolimus Concentrations in Whole Blood by High-Performance Liquid Chromatography with Ultraviolet Detection." *Journal of Chromatography B* 774 (2) (July 15): 187-194. doi:10.1016/S1570-0232(02)00204-0.
- Cegla, Ulrich H. 2004. "Pressure and Inspiratory Flow Characteristics of Dry Powder Inhalers." *Respiratory Medicine* 98, Supplement 1 (April): S22-S28. doi:10.1016/j.rmed.2004.02.003.
- Chan, Hak-Kim, Paul M. Young, Daniela Traini, and Matthew. Coates. 2007. "Dry Powder Inhalers: Challenges and Goals for next Generation Therapies." *Pharmaceutical Technology Europe* 19 (4): 19-24.
- Chang, Yoon Soo, Myung Jae Park, Chunxue Bai, Baiqiang Cai, Cissy Kartasmita, Benjamin P. Margono, Shirley Panganiban, et al. 2012. "Comparative Study of Patients in Correct Usage of and Preference for the Swinghaler and Turbuhaler Multidose Inhalers." *The Journal of Asthma* □: Official Journal of the Association for the Care of Asthma 49 (7): 750-6.

- Chapman, Kenneth R., Charles M Fogarty, Clare Peckitt, Cheryl Lassen, Dalal Jadayel, Juergen Dederichs, Mukul Dalvi, and Benjamin Kramer. 2011. "Delivery Characteristics and Patients' Handling of Two Single-Dose Dry-Powder Inhalers Used in COPD." *International Journal of Chronic Obstructive Pulmonary Disease* 6: 353–363. doi:10.2147/COPD.S18529.
- Chapman, Kenneth R., Stephen I. Rennard, Angeli Dogra, Roger Owen, Cheryl Lassen, and Benjamin Kramer. 2011. "Long-Term Safety and Efficacy of Indacaterol, a Long-Acting β 2-Agonist, in Subjects With COPD A Randomized, Placebo-Controlled Study." *Chest* 140 (1) (July 1): 68–75. doi:10.1378/chest.10-1830.
- Cheow, Wean Sin, Mabel Li Ling Ng, Katherine Kho, and Kunn Hadinoto. 2011. "Spray-Freeze-Drying Production of Thermally Sensitive Polymeric Nanoparticle Aggregates for Inhaled Drug Delivery: Effect of Freeze-Drying Adjuvants." *International Journal of Pharmaceutics* 404 (1–2) (February 14): 289–300. doi:10.1016/j.ijpharm.2010.11.021.
- Chhajed, Prashant N., Michael Dickenmann, Lukas Bubendorf, Michael Mayr, Juerg Steiger, and Michael Tamm. 2006. "Patterns of Pulmonary Complications Associated with Sirolimus." *Respiration* 73 (3): 367–374.
- Chow, Albert H. L., Henry H. Y Tong, Pratibhash Chattopadhyay, and Boris Y Shekunov. 2007. "Particle Engineering for Pulmonary Drug Delivery." *Pharmaceutical Research* 24 (3) (March): 411–437. doi:10.1007/s11095-006-9174-3.
- Chrystyn, H., and C. Niederlaender. 2012. "The Genuair (R) Inhaler: A Novel, Multidose Dry Powder Inhaler." *International Journal of Clinical Practice* 66 (3) (March): 309–317. doi:10.1111/j.1742-1241.2011.02832.x.
- Coates, M. S., H. K. Chan, D. F. Fletcher, and H. Chiou. 2007. "Influence of Mouthpiece Geometry on the Aerosol Delivery Performance of a Dry Powder Inhaler." *Pharmaceutical Research* 24 (8): 1450–1456.
- Coates, Matthew S., Hak-Kim Chan, David F. Fletcher, and Judy A. Raper. 2005. "Influence of Air Flow on the Performance of a Dry Powder Inhaler Using Computational and Experimental Analyses." *Pharmaceutical Research* 22 (9) (August 24): 1445–1453. doi:10.1007/s11095-005-6155-x.

- Commissioner, Office of the. 2013. "Inspection Guides - Lyophilization of Parenterals (7/93)". WebContent. Accessed September 17.
<http://www.fda.gov/ICECI/Inspections/InspectionGuides/ucm074909.htm>.
- Crowder, T., and A. Hickey. 2006. "Powder Specific Active Dispersion for Generation of Pharmaceutical Aerosols." *International Journal of Pharmaceutics* 327 (1–2) (December 11): 65–72. doi:10.1016/j.ijpharm.2006.07.050.
- Cun, Dongmei, Ditte Krohn Jensen, Morten Jonas Maltesen, Matthew Bunker, Paul Whiteside, David Scurr, Camilla Foged, and Hanne Mørck Nielsen. 2011. "High Loading Efficiency and Sustained Release of siRNA Encapsulated in PLGA Nanoparticles: Quality by Design Optimization and Characterization." *European Journal of Pharmaceutics and Biopharmaceutics* 77 (1) (January): 26–35. doi:10.1016/j.ejpb.2010.11.008.
- Dailey, L.A., N. Jekel, L. Fink, T. Gessler, T. Schmehl, M. Wittmar, T. Kissel, and W. Seeger. 2006. "Investigation of the Proinflammatory Potential of Biodegradable Nanoparticle Drug Delivery Systems in the Lung." *Toxicology and Applied Pharmacology* 215 (1) (August 15): 100–108. doi:10.1016/j.taap.2006.01.016.
- Dalby, R N, and P R Byron. 1988. "Comparison of Output Particle Size Distributions from Pressurized Aerosols Formulated as Solutions or Suspensions." *Pharmaceutical Research* 5 (1) (January): 36–39.
- Daniher, Derek Ivan, and Jesse Zhu. 2008. "Dry Powder Platform for Pulmonary Drug Delivery." *Particuology* 6 (4) (August): 225–238. doi:10.1016/j.partic.2008.04.004.
- Das, Shyamal, Ian Larson, Paul Young, and Peter Stewart. 2010. "Understanding Lactose Behaviour during Storage by Monitoring Surface Energy Change Using Inverse Gas Chromatography." *Dairy Science & Technology* 90 (2-3) (June): 271–285. doi:10.1051/dst/2009051.
- De Boer, A. H., D. Gjaltema, P. Hagedoorn, and H. W. Frijlink. 2002. "Characterization of Inhalation Aerosols: A Critical Evaluation of Cascade Impactor Analysis and Laser Diffraction Technique." *International Journal of Pharmaceutics* 249 (1-2) (December 5): 219–231. doi:10.1016/S0378-5173(02)00526-4.
- De Boer, A. H., P. Hagedoorn, D. Gjaltema, J. Goede, and H. W. Frijlink. 2006. "Air Classifier Technology (ACT) in Dry Powder Inhalation - Part 3. Design and

- Development of an Air Classifier Family for the Novolizer (R) Multi-Dose Dry Powder Inhaler.” *International Journal of Pharmaceutics* 310 (1-2) (March 9): 72–80. doi:10.1016/j.ijpharm.2005.11.030.
- De Boer, A. H., P. Hagedoorn, D. Gjaltema, J. Goede, K. D. Kussendrager, and H. W. Frijlink. 2003. “Air Classifier Technology (ACT) in Dry Powder Inhalation Part 2. The Effect of Lactose Carrier Surface Properties on the Drug-to-Carrier Interaction in Adhesive Mixtures for Inhalation.” *International Journal of Pharmaceutics* 260 (2) (July 24): 201–216. doi:10.1016/S0378-5173(03)00264-3.
- De Boer, A.H., H.K. Chan, and R. Price. 2012. “A Critical View on Lactose-Based Drug Formulation and Device Studies for Dry Powder Inhalation: Which Are Relevant and What Interactions to Expect?” *Advanced Drug Delivery Reviews* 64 (3) (March 15): 257–274. doi:10.1016/j.addr.2011.04.004.
- De Boer, A.H., P. Hagedoorn, D. Gjaltema, J. Goede, and H.W. Frijlink. 2003. “Air Classifier Technology (ACT) in Dry Powder Inhalation: Part 1. Introduction of a Novel Force Distribution Concept (FDC) Explaining the Performance of a Basic Air Classifier on Adhesive Mixtures.” *International Journal of Pharmaceutics* 260 (2) (July 24): 187–200. doi:10.1016/S0378-5173(03)00250-3.
- De Koning, J.P, Th.W van der Mark, P.M.J Coenegracht, Th.F.J Tromp, and H.W Frijlink. 2002. “Effect of an External Resistance to Airflow on the Inspiratory Flow Curve.” *International Journal of Pharmaceutics* 234 (1–2) (March 2): 257–266. doi:10.1016/S0378-5173(01)00969-3.
- Dhumal, Ravindra S., Shailesh V. Biradar, Anant R. Paradkar, and Peter York. 2009. “Particle Engineering Using Sonocrystallization: Salbutamol Sulphate for Pulmonary Delivery.” *International Journal of Pharmaceutics* 368 (1–2) (February 23): 129–137. doi:10.1016/j.ijpharm.2008.10.006.
- Dijoseph, Jf, Rn Sharma, and Jy Chang. 1992. “The Effect of Rapamycin on Kidney-Function in the Sprague-Dawley Rat.” *Transplantation* 53 (3) (March): 507–513. doi:10.1097/00007890-199203000-00002.
- Donovan, Martin J, Sin Hyen Kim, Venkatramanan Raman, and Hugh D Smyth. 2012. “Dry Powder Inhaler Device Influence on Carrier Particle Performance.” *Journal of Pharmaceutical Sciences* 101 (3) (March): 1097–1107. doi:10.1002/jps.22824.

- Dunbar, Craig, Abdo Kataya, and Tiba Tiangbe. 2005. "Reducing Bounce Effects in the Andersen Cascade Impactor." *International Journal of Pharmaceutics* 301 (1–2) (September 14): 25–32. doi:10.1016/j.ijpharm.2005.04.039.
- Duret, Christophe, Nathalie Wauthoz, Thami Sebti, Francis Vanderbist, and Karim Amighi. 2012. "New Respirable and Fast Dissolving Itraconazole Dry Powder Composition for the Treatment of Invasive Pulmonary Aspergillosis." *Pharmaceutical Research* 29 (10) (October 1): 2845–2859. doi:10.1007/s11095-012-0779-4.
- Edwards, David A., Justin Hanes, Giovanni Caponetti, Jeffrey Hrkach, Abdelaziz Ben-Jebria, Mary Lou Eskew, Jeffrey Mintzes, Daniel Deaver, Noah Lotan, and Robert Langer. 1997. "Large Porous Particles for Pulmonary Drug Delivery." *Science* 276 (5320) (June 20): 1868–1872. doi:10.1126/science.276.5320.1868.
- El-Sherbiny, Ibrahim M, Shayna McGill, and Hugh D. C Smyth. 2010. "Swellable Microparticles as Carriers for Sustained Pulmonary Drug Delivery." *Journal of Pharmaceutical Sciences* 99 (5) (May): 2343–2356. doi:10.1002/jps.22003.
- El-Sherbiny, Ibrahim M., and Hugh D.C. Smyth. 2010. "Biodegradable Nano-Micro Carrier Systems for Sustained Pulmonary Drug Delivery: (I) Self-Assembled Nanoparticles Encapsulated in Respirable/swellable Semi-IPN Microspheres." *International Journal of Pharmaceutics* 395 (1–2) (August 16): 132–141. doi:10.1016/j.ijpharm.2010.05.032.
- Ferin, Juraj. 1994. "Pulmonary Retention and Clearance of Particles." *Toxicology Letters* 72 (1–3) (June): 121–125. doi:10.1016/0378-4274(94)90018-3
- Ferrari, F., D. Cocconi, R. Bettini, F. Giordano, P. Santi, M. Tobyn, R. Price, P. Young, C. Caramella, and P. Colombo. 2004. "The Surface Roughness of Lactose Particles Can Be Modulated by Wet-Smoothing Using a High-Shear Mixer." *Aaps Pharmscitech* 5 (4).
- "FisherScientific, Material Safety Data Sheet: Acetonitrile [HPLC]." 2009.
- Fonseca, Cristina, Sergio Simoes, and Rogerio Gaspar. 2002. "Paclitaxel-Loaded PLGA Nanoparticles: Preparation, Physicochemical Characterization and in Vitro Anti-Tumoral Activity." *Journal of Controlled Release* 83 (2): 273–286.

- French, D. L., D. A. Edwards, and R. W. Niven. 1996. "The Influence of Formulation on Emission, Deaggregation and Deposition of Dry Powders for Inhalation." *Journal of Aerosol Science* 27 (5) (July): 769–783. doi:10.1016/0021-8502(96)00021-3.
- Friebel, Christian, and Hartwig Steckel. 2010. "Single-Use Disposable Dry Powder Inhalers for Pulmonary Drug Delivery." *Expert Opinion on Drug Delivery* 7 (12) (December): 1359–1372. doi:10.1517/17425247.2010.538379.
- Garnier, S., S. Petit, and G. Coquerel. 2002. "Dehydration Mechanism and Crystallisation Behaviour of Lactose." *Journal of Thermal Analysis and Calorimetry* 68 (2): 489–502. doi:10.1023/A:1016087702409.
- Geller, David E., Jeffrey Weers, and Silvia Heuerding. 2011. "Development of an Inhaled Dry-Powder Formulation of Tobramycin Using PulmoSphere™ Technology." *Journal of Aerosol Medicine and Pulmonary Drug Delivery* 24 (4) (August): 175–182. doi:10.1089/jamp.2010.0855.
- Geller, De. 2009. "Aerosol Antibiotics in Cystic Fibrosis... Including Discussion with Volsko TA, Flume PA, Ratjen FA, Geller DE, Davies JC." *Respiratory Care* 54 (5) (May): 658–670.
- "General Chapters <601> Aerosols, Nasal Sprays, Metered-Dose Inhalers, and Dry Powder Inhaler." In *United States Pharmacopeia*, 35th-NF ed.
- Grohgan, Holger, Yan-Ying Lee, Jukka Rantanen, and Mingshi Yang. 2013. "The Influence of Lysozyme on Mannitol Polymorphism in Freeze-Dried and Spray-Dried Formulations Depends on the Selection of the Drying Process." *International Journal of Pharmaceutics* 447 (1–2) (April 15): 224–230. doi:10.1016/j.ijpharm.2013.03.003.
- Guchardi, R., M. Frei, E. John, and J.S. Kaerger. 2008. "Influence of Fine Lactose and Magnesium Stearate on Low Dose Dry Powder Inhaler Formulations." *International Journal of Pharmaceutics* 348 (1–2) (February 4): 10–17. doi:10.1016/j.ijpharm.2007.06.041.
- "Guidance for Industry - Metered Dose Inhaler (MDI) and Dry Powder Inhaler (DPI) Drug Products - Chemistry, Manufacturing, and Controls Documentation." 1998. In *Food and Drug Administration*, 1 – 61.

- Haque, Md. Kamrul, Kiyoshi Kawai, and Toru Suzuki. 2006. "Glass Transition and Enthalpy Relaxation of Amorphous Lactose Glass." *Carbohydrate Research* 341 (11) (August 14): 1884–1889. doi:10.1016/j.carres.2006.04.040
- Hara, Kaori, Hiroyuki Tsujimoto, Yusuke Tsukada, C.C. Huang, Yoshiaki Kawashima, and Masahiro Tsutsumi. 2008. "Histological Examination of PLGA Nanospheres for Intratracheal Drug Administration." *International Journal of Pharmaceutics* 356 (1–2) (May 22): 267–273. doi:10.1016/j.ijpharm.2007.12.041.
- Harder, Christophe, Eric Lesniewska, and Christophe Laroche. 2011. "Study of Ageing of Dry Powder Inhaler and Metered Dose Inhaler by Atomic Force Microscopy." *Powder Technology* 208 (2) (March 25): 252–259. doi:10.1016/j.powtec.2010.08.013.
- Harper, Nancy J, Steven Gray, Jennifer De Groot, Joann M Parker, Negar Sadrzadeh, Carlos Schuler, Jacqueline D Schumacher, et al. 2007. "The Design and Performance of the Exubera((R)) Pulmonary Insulin Delivery System." *Diabetes Technology & Therapeutics* 9 (June): S16–S27. doi:10.1089/dia.2007.0222.
- Harrison, David E., Randy Strong, Zelton Dave Sharp, James F. Nelson, Clinton M. Astle, Kevin Flurkey, Nancy L. Nadon, et al. 2009. "Rapamycin Fed Late in Life Extends Lifespan in Genetically Heterogeneous Mice." *Nature* 460 (7253) (July 16): 392–U108. doi:10.1038/nature08221.
- Hassan, Meer Saiful, and Raymond Lau. 2010a. "Inhalation Performance of Pollen-Shape Carrier in Dry Powder Formulation with Different Drug Mixing Ratios: Comparison with Lactose Carrier." *International Journal of Pharmaceutics* 386 (1-2) (February 15): 6–14. doi:10.1016/j.ijpharm.2009.10.047.
- 2010b. "Feasibility Study of Pollen-Shape Drug Carriers in Dry Powder Inhalation." *Journal of Pharmaceutical Sciences* 99 (3) (March): 1309–1321. doi:10.1002/jps.21913.
- Hausen, B, K Boeke, G J Berry, I T Segarra, U Christians, and R E Morris. 1999. "Suppression of Acute Rejection in Allogeneic Rat Lung Transplantation: A Study of the Efficacy and Pharmacokinetics of Rapamycin Derivative (SDZ RAD) Used Alone and in Combination with a Microemulsion Formulation of Cyclosporine." *The Journal of Heart and Lung Transplantation: The Official*

- Publication of the International Society for Heart Transplantation 18 (2)
(February): 150–159.
- Hauss, David J. 2007. *Oral Lipid-Based Formulations: Enhancing the Bioavailability of Poorly Water-Soluble Drugs*. CRC Press.
- Hickey, A. J, H. M Mansour, M. J Telko, Z. Xu, H. D.C Smyth, T. Mulder, R. McLean, J. Langridge, and D. Papadopoulos. 2007. “Physical Characterization of Component Particles Included in Dry Powder Inhalers. I. Strategy Review and Static Characteristics.” *Journal of Pharmaceutical Sciences* 96 (5): 1282–1301.
- Hindle, M., and Pr Byron. 1995. “Dose Emissions from Marketed Dry Powder Inhalers.” *International Journal of Pharmaceutics* 116 (2) (March 28): 169–177.
doi:10.1016/0378-5173(94)00287-F.
- Hu, Jiahui, Keith P. Johnston, and Robert O. Williams III. 2003. “Spray Freezing into Liquid (SFL) Particle Engineering Technology to Enhance Dissolution of Poorly Water Soluble Drugs: Organic Solvent versus Organic/aqueous Co-Solvent Systems.” *European Journal of Pharmaceutical Sciences* 20 (3) (November): 295–303. doi:10.1016/S0928-0987(03)00203-3.
- Hwang, Sung-Joo, Min-Soo Kim, Jeong-Soo Kim, Hee Jun Park, Won Kyung Cho, and Kwang-Ho Cha. 2011. “Enhanced Bioavailability of Sirolimus via Preparation of Solid Dispersion Nanoparticles Using a Supercritical Antisolvent Process.” *International Journal of Nanomedicine* (November): 2997.
doi:10.2147/IJN.S26546.
- Islam, Nazrul, and Matthew J. Cleary. 2012. “Developing an Efficient and Reliable Dry Powder Inhaler for Pulmonary Drug Delivery – A Review for Multidisciplinary Researchers.” *Medical Engineering & Physics* 34 (4) (May): 409–427.
doi:10.1016/j.medengphy.2011.12.025.
- Islam, Nazrul, and Ellen Gladki. 2008. “Dry Powder Inhalers (DPIs)—A Review of Device Reliability and Innovation.” *International Journal of Pharmaceutics* 360 (1–2) (August 6): 1–11. doi:10.1016/j.ijpharm.2008.04.044.
- Jaspart, Séverine, Pascal Bertholet, Géraldine Piel, Jean-Michel Dogné, Luc Delattre, and Brigitte Evrard. 2007. “Solid Lipid Microparticles as a Sustained Release System for Pulmonary Drug Delivery.” *European Journal of Pharmaceutics and Biopharmaceutics* 65 (1) (January): 47–56. doi:10.1016/j.ejpb.2006.07.006.

- Jensen, Ditte Krohn, Linda Boye Jensen, Saeid Koocheki, Lasse Bengtson, Dongmei Cun, Hanne Mørck Nielsen, and Camilla Foged. 2012. "Design of an Inhalable Dry Powder Formulation of DOTAP-Modified PLGA Nanoparticles Loaded with siRNA." *Journal of Controlled Release* 157 (1) (January 10): 141–148. doi:10.1016/j.jconrel.2011.08.011.
- Jensen, Ditte Marie Krohn, Dongmei Cun, Morten Jonas Maltesen, Sven Frokjaer, Hanne Mørck Nielsen, and Camilla Foged. 2010. "Spray Drying of siRNA-Containing PLGA Nanoparticles Intended for Inhalation." *Journal of Controlled Release* 142 (1) (February 25): 138–145. doi:10.1016/j.jconrel.2009.10.010.
- Jones, Matthew D, Paul Young, and Daniela Traini. 2012. "The Use of Inverse Gas Chromatography for the Study of Lactose and Pharmaceutical Materials Used in Dry Powder Inhalers." *Advanced Drug Delivery Reviews* 64 (3) (March 15): 285–293. doi:10.1016/j.addr.2011.12.015.
- Kahan, B D, J Y Chang, and S N Sehgal. 1991. "Preclinical Evaluation of a New Potent Immunosuppressive Agent, Rapamycin." *Transplantation* 52 (2) (August): 185–191.
- Kaialy, Waseem, Amjad Alhalaweh, Sitaram P. Velaga, and Ali Nokhodchi. 2011. "Effect of Carrier Particle Shape on Dry Powder Inhaler Performance." *International Journal of Pharmaceutics* 421 (1) (December 12): 12–23. doi:10.1016/j.ijpharm.2011.09.010.
- Kaialy, Waseem, Gary P Martin, Hassan Larhrib, Martyn D Ticehurst, Ewa Kolosionek, and Ali Nokhodchi. 2012. "The Influence of Physical Properties and Morphology of Crystallised Lactose on Delivery of Salbutamol Sulphate from Dry Powder Inhalers." *Colloids and Surfaces B-Biointerfaces* 89 (January 1): 29–39. doi:10.1016/j.colsurfb.2011.08.019.
- Kelley, Jean, Stephen Stein, Tom Robison, Zhaolin Wang, Allan Bohlke, John Simons, Tucker Silberhorn, and Randy Bay. 2011. "Comparative Performance of the High Efficiency 3MTM Taper Dry Powder Inhaler Device." In , 2:247–252.
- Kinsey, P Spencer, Benoit Adamo, Chad C Smutney, John M Polidoro, and others. 2009. "Dry Powder Inhaler."

- Kling, Jim. 2011. "Dreamboat Sinks Prospects for Fast Approval of Inhaled Insulin." *Nature Biotechnology* 29 (3) (March): 175–176. doi:10.1038/nbt0311-175.
- Kohler, Dieter. 2004. "The Novolizer®: Overcoming Inherent Problems of Dry Powder Inhalers." *Respiratory Medicine* 98, Supplement 1 (April): S17–S21. doi:10.1016/j.rmed.2004.02.005.
- Kong, Xiaoyuan, Weidong Zhang, Richard F Lockey, Alexander Auais, Giovanni Piedimonte, and Shyam S Mohapatra. 2007. "Respiratory Syncytial Virus Infection in Fischer 344 Rats Is Attenuated by Short Interfering RNA against the RSV-NS1 Gene." *Genetic Vaccines and Therapy* 5: 4. doi:10.1186/1479-0556-5-4.
- Kuehl, Philip J., Tamara L. Anderson, Gabriel Candelaria, Benjamin Gershman, Ky Harlin, Jacob Y. Hesterman, Thomas Holmes, et al. 2012. "Regional Particle Size Dependent Deposition of Inhaled Aerosols in Rats and Mice." *Inhalation Toxicology* 24 (1) (January): 27–35. doi:10.3109/08958378.2011.632787.
- Labiris, N R, and M B Dolovich. 2003. "Pulmonary Drug Delivery. Part I: Physiological Factors Affecting Therapeutic Effectiveness of Aerosolized Medications." *British Journal of Clinical Pharmacology* 56 (6) (December): 588–599. doi:10.1046/j.1365-2125.2003.01892.x.
- Lavorini, Federico, Antoine Magnan, Jean Christophe Dubus, Thomas Voshaar, Lorenzo Corbetta, Marielle Broeders, Richard Dekhuijzen, et al. 2008. "Effect of Incorrect Use of Dry Powder Inhalers on Management of Patients with Asthma and COPD." *Respiratory Medicine* 102 (4) (April): 593–604. doi:10.1016/j.rmed.2007.11.003.
- Le, V. N. P, T. H. Hoang Thi, E. Robins, and M. P Flament. 2012. "Dry Powder Inhalers: Study of the Parameters Influencing Adhesion and Dispersion of Fluticasone Propionate." *Aaps Pharmscitech* 13 (2) (June): 477–484. doi:10.1208/s12249-012-9765-8.
- Lee, Hb, and Md Blaufox. 1985. "Blood-Volume in the Rat." *Journal of Nuclear Medicine* 26 (1): 72–76.
- Lertchanaruengrith, P., P. Rattanasukol, N. Suratannon, N. Voraphani, P. Chatchatee, and J. Ngamphaiboon. 2012. "The Ability and Predictive Factors of Preschool Children to Use Swinghaler Device." *Journal of Allergy and Clinical*

- Immunology 129 (2, Supplement) (February): AB74.
doi:10.1016/j.jaci.2011.12.603.
- Li, H.-Y., P. C. Seville, I. J. Williamson, and J. C. Birchall. 2005. "The Use of Amino Acids to Enhance the Aerosolisation of Spray-Dried Powders for Pulmonary Gene Therapy." *The Journal of Gene Medicine* 7 (3): 343–353. doi:10.1002/jgm.654.
- Li, Xiang, Nicolas Anton, Cordin Arpagaus, Fabrice Belleteix, and Thierry F. Vandamme. 2010. "Nanoparticles by Spray Drying Using Innovative New Technology: The Büchi Nano Spray Dryer B-90." *Journal of Controlled Release* 147 (2) (October 15): 304–310. doi:10.1016/j.jconrel.2010.07.113.
- Lombry, C., D. A. Edwards, V. Preat, and R. Vanbever. 2004. "Alveolar Macrophages Are a Primary Barrier to Pulmonary Absorption of Macromolecules." *American Journal of Physiology-Lung Cellular and Molecular Physiology* 286 (5) (May 1): L1002–L1008. doi:10.1152/ajplung.00260.2003.
- Luque de Castro, M.D., and F. Priego-Capote. 2007. "Ultrasound-Assisted Crystallization (sonocrystallization)." *Ultrasonics Sonochemistry* 14 (6) (September): 717–724. doi:10.1016/j.ultsonch.2006.12.004.
- MacDonald, Allan, Joseph Scarola, James T. Burke, and James J. Zimmerman. 2000. "Clinical Pharmacokinetics and Therapeutic Drug Monitoring of Sirolimus." *Clinical Therapeutics* 22, Supplement 2 (0): B101–B121. doi:10.1016/S0149-2918(00)89027-X.
- Magnussen, H., H. Watz, I. Zimmermann, S. Macht, R. Greguletz, M. Falques, D. Jarreta, and E. Garcia Gil. 2009. "Peak Inspiratory Flow through the Genuair® Inhaler in Patients with Moderate or Severe COPD." *Respiratory Medicine* 103 (12) (December): 1832–1837. doi:10.1016/j.rmed.2009.07.006.
- Majumder, Smita, Antonella Caccamo, David X. Medina, Adriana D. Benavides, Martin A. Javors, Ellen Kraig, Randy Strong, Arlan Richardson, and Salvatore Oddo. 2012. "Lifelong Rapamycin Administration Ameliorates Age-Dependent Cognitive Deficits by Reducing IL-1 Ss and Enhancing NMDA Signaling." *Aging Cell* 11 (2) (April): 326–335. doi:10.1111/j.1474-9726.2011.00791.x.
- Makhlof, Abdallah, Martin Werle, Yuichi Tozuka, and Hirofumi Takeuchi. 2010. "Nanoparticles of Glycol Chitosan and Its Thiolated Derivative Significantly Improved the Pulmonary Delivery of Calcitonin." *International Journal of*

- Pharmaceutics 397 (1–2) (September 15): 92–95.
doi:10.1016/j.ijpharm.2010.07.001.
- Maraskovsky, Eugene, Max Schnurr, Nick S Wilson, Neil C Robson, Jeff Boyle, and Debbie Drane. 2009. “Development of Prophylactic and Therapeutic Vaccines Using the ISCOMATRIX Adjuvant.” *Immunology and Cell Biology* 87 (5) (July): 371–376. doi:10.1038/icb.2009.21.
- Marple, V. A., D. L. Roberts, F. J. Romay, N. C. Miller, K. G. Truman, M. J. Holroyd, J. P. Mitchell, and D. Hochrainer. 2003. “Next Generation Pharmaceutical Impactor (A New Impactor for Pharmaceutical Inhaler Testing). Part I: Design.” *Journal of Aerosol Medicine-Deposition Clearance and Effects in the Lung* 16 (3): 283–299. doi:10.1089/089426803769017659.
- Marple, Virgil A., and Bernard A. Olson. 2009. “Good Laboratory Practice in Particle Measurement Calibration: Cascade Impactor.” *Kona Powder and Particle Journal* (27): 206–216.
- Martin, Gary, Helen MacRitchie, Christopher Marriott, and Xian-Ming Zeng. 2006. “Characterisation of a Carrier-Free Dry Powder Aerosol Formulation Using Inertial Impaction and Laser Diffraction.” *Pharmaceutical Research* 23 (9): 2210–2219. doi:10.1007/s11095-006-9056-8.
- Matinkhoo, Sadaf, Karlene H Lynch, Jonathan J Dennis, Warren H Finlay, and Reinhard Vehring. 2011. “Spray-Dried Respirable Powders Containing Bacteriophages for the Treatment of Pulmonary Infections.” *Journal of Pharmaceutical Sciences* 100 (12) (December): 5197–5205. doi:10.1002/jps.22715.
- Mayo, Aaron S, Balamurali K Ambati, and Uday B Kompella. 2010. “Gene Delivery Nanoparticles Fabricated by Supercritical Fluid Extraction of Emulsions.” *International Journal of Pharmaceutics* 387 (1-2) (March 15): 278–285. doi:10.1016/j.ijpharm.2009.12.024.
- McCormack, Francis X., Yoshikazu Inoue, Joel Moss, Lianne G. Singer, Charlie Strange, Koh Nakata, Alan F. Barker, et al. 2011. “Efficacy and Safety of Sirolimus in Lymphangioleiomyomatosis.” *New England Journal of Medicine* 364 (17): 1595–1606. doi:10.1056/NEJMoa1100391.
- McKeage, Kate, and Susan J. Keam. 2009. “Salmeterol/Fluticasone Propionate A Review of Its Use in Asthma.” *Drugs* 69 (13): 1799–1828.

- Meiser, B. M., J. Wang, and R. E. Morris. 1989. "Rapamycin: A New and Highly Active Immunosuppressive Macrolide with an Efficacy Superior to Cyclosporine." In *Progress in Immunology*, edited by Fritz Melchers, E. D. Albert, H. Boehmer, M. P. Dierich, L. Pasquier, K. Eichmann, D. Gemsa, et al., 1195–1198. Berlin, Heidelberg: Springer Berlin Heidelberg.
http://link.springer.com/content/pdf/10.1007/978-3-642-83755-5_159.pdf#page-1.
- Merkel, Olivia M, Andrea Beyerle, Damiano Librizzi, Andreas Pfestroff, Thomas M Behr, Brian Sproat, Peter J Barth, and Thomas Kissel. 2009. "Nonviral siRNA Delivery to the Lung: Investigation of PEG-PEI Polyplexes and Their in Vivo Performance." *Molecular Pharmaceutics* 6 (4) (August): 1246–1260.
 doi:10.1021/mp900107v.
- Merkel, Olivia M., and Thomas Kissel. 2012. "Nonviral Pulmonary Delivery of siRNA." *Accounts of Chemical Research* 45 (7) (July 17): 961–970.
 doi:10.1021/ar200110p.
- Miller, Richard A., David E. Harrison, C. M. Astle, Joseph A. Baur, Angela Rodriguez Boyd, Rafael de Cabo, Elizabeth Fernandez, et al. 2011. "Rapamycin, But Not Resveratrol or Simvastatin, Extends Life Span of Genetically Heterogeneous Mice." *The Journals of Gerontology Series A: Biological Sciences and Medical Sciences* 66A (2) (February 1): 191–201. doi:10.1093/gerona/glq178.
- Mittal, G., D. K. Sahana, V. Bhardwaj, and M. N. V. Ravi Kumar. 2007. "Estradiol Loaded PLGA Nanoparticles for Oral Administration: Effect of Polymer Molecular Weight and Copolymer Composition on Release Behavior< I> in Vitro</i> And< I> in Vivo</i>." *Journal of Controlled Release* 119 (1): 77–85.
- Mohammed, Hlack, Daryl L. Roberts, Mark Copley, Mark Hammond, Steven C. Nichols, and Jolyon P. Mitchell. 2012. "Effect of Sampling Volume on Dry Powder Inhaler (DPI)-Emitted Aerosol Aerodynamic Particle Size Distributions (APSDs) Measured by the Next-Generation Pharmaceutical Impactor (NGI) and the Andersen Eight-Stage Cascade Impactor (ACI)." *AAPS PharmSciTech* 13 (3) (June 8): 875–882. doi:10.1208/s12249-012-9797-0.
- Mohri, Kohta, Tomoyuki Okuda, Asami Mori, Kazumi Danjo, and Hirokazu Okamoto. 2010. "Optimized Pulmonary Gene Transfection in Mice by Spray–freeze Dried Powder Inhalation." *Journal of Controlled Release* 144 (2) (June 1): 221–226.
 doi:10.1016/j.jconrel.2010.02.018.

- Monajjemzadeh, Farnaz, Davoud Hassanzadeh, Hadi Valizadeh, Mohammad R. Siahi-Shadbad, Javid Shahbazi Mojarrad, Thomas A. Robertson, and Michael S. Roberts. 2009. "Compatibility Studies of Acyclovir and Lactose in Physical Mixtures and Commercial Tablets." *European Journal of Pharmaceutics and Biopharmaceutics* 73 (3) (November): 404–413. doi:10.1016/j.ejpb.2009.06.012.
- Morton, David A V, and J. N. Staniforth. 2006. "Systemic Pulmonary Delivery: Success through Integrated Formulation and Device Development." <http://www.ondrugdelivery.com/publications/pulmonary.pdf>.
- Mueannoom, Wunlapa, Amon Srisongphan, Kevin M. G Taylor, Stephan Hauschild, and Simon Gaisford. 2012. "Thermal Ink-Jet Spray Freeze-Drying for Preparation of Excipient-Free Salbutamol Sulphate for Inhalation." *European Journal of Pharmaceutics and Biopharmaceutics* 80 (1) (January): 149–155. doi:10.1016/j.ejpb.2011.09.016.
- Müller, Rainer, and Junghanns. 2008. "Nanocrystal Technology, Drug Delivery and Clinical Applications." *International Journal of Nanomedicine* (October): 295. doi:10.2147/IJN.S595.
- Murthy, Vinit S, Jennifer N Cha, Galen D Stucky, and Michael S Wong. 2004. "Charge-Driven Flocculation of poly(L-Lysine)-Gold Nanoparticle Assemblies Leading to Hollow Microspheres." *Journal of the American Chemical Society* 126 (16) (April 28): 5292–5299. doi:10.1021/ja038953v.
- Nakach, Mostafa, Jean-René Authelin, Alain Chamayou, and John Dodds. 2004. "Comparison of Various Milling Technologies for Grinding Pharmaceutical Powders." *International Journal of Mineral Processing* 74, Supplement (December 10): S173–S181. doi:10.1016/j.minpro.2004.07.039.
- Napoli, Kimberly L., Mou-Er Wang, Stanislaw M. Stepkowski, and Barry D. Kahan. 1997. "Distribution of Sirolimus in Rat Tissue." *Clinical Biochemistry* 30 (2) (March): 135–142. doi:10.1016/S0009-9120(96)00157-9.
- Needham, M, G Fradley, and AP Cocks. 2010. "Investigating the Efficiency of the 3M Conix™ of Reverse Cyclone Technology for DPI Drug Delivery." In , 2:369–372.
- Nelson, Harold S, Kenneth R Chapman, Stephen D Pyke, Malcolm Johnson, and John N Pritchard. 2003. "Enhanced Synergy between Fluticasone Propionate and

- Salmeterol Inhaled from a Single Inhaler versus Separate Inhalers.” *The Journal of Allergy and Clinical Immunology* 112 (1) (July): 29–36.
- Neumiller, Joshua J, R Keith Campbell, and Lindy D Wood. 2010. “A Review of Inhaled Technosphere Insulin.” *The Annals of Pharmacotherapy* 44 (7/8) (July 1): 1231–1239. doi:10.1345/aph.1P055.
- Newman, S. P, D. J Sutton, R. Segarra, R. Lamarca, and G. de Miquel. 2009. “Lung Deposition of Acclidinium Bromide from Genuair (R), a Multidose Dry Powder Inhaler.” *Respiration* 78 (3): 322–328. doi:10.1159/000219676.
- NEWMAN, S. P., and W. W. BUSSE. 2002. “Evolution of Dry Powder Inhaler Design, Formulation, and Performance.” *Respiratory Medicine* 96 (5) (May): 293–304. doi:10.1053/rmed.2001.1276.
- Overhoff, Kirk A., Josh D. Engstrom, Bo Chen, Brian D. Scherzer, Thomas E. Milner, Keith P. Johnston, and Robert O. Williams III. 2007. “Novel Ultra-Rapid Freezing Particle Engineering Process for Enhancement of Dissolution Rates of Poorly Water-Soluble Drugs.” *European Journal of Pharmaceutics and Biopharmaceutics* 65 (1) (January): 57–67. doi:10.1016/j.ejpb.2006.07.012.
- Parikh, Dipesh, John Burns, David Hipkiss, Omar Usmani, and Rob Price. 2012. “Improved Localized Lung Delivery Using Smart Combination Respiratory Medicines.” *Eur. Respiratory Disease* 8 (1): 40–45.
- Parry-Billings, M., C. Birrell, L. Oldham, and C. O’Callaghan. 2003. “Inspiratory Flow Rate through a Dry Powder Inhaler (Clickhaler (R)) in Children with Asthma.” *Pediatric Pulmonology* 35 (3) (March): 220–226. doi:10.1002/ppul.10234.
- Patton, John S., and Peter R. Byron. 2007. “Inhaling Medicines: Delivering Drugs to the Body through the Lungs.” *Nature Reviews Drug Discovery* 6 (1) (January 1): 67–74. doi:10.1038/nrd2153.
- Patton, John S., Fishburn, C. Simone, and Weers, Jeffrey G. 2004. “The Lungs as a Portal of Entry for Systemic Drug Delivery (thoracic).” *American Thoracic Society* 1 (4): 338–344. doi:10.1513/pats.200409-049TA.
- Pavkov, Richard, Stefan Mueller, Katrin Fiebich, Dilraj Singh, Frank Stowasser, Giovanni Pignatelli, Benoît Walter, et al. 2010. “Characteristics of a Capsule Based Dry Powder Inhaler for the Delivery of Indacaterol.” *Current Medical*

- Research and Opinion 26 (11) (November): 2527–2533.
doi:10.1185/03007995.2010.518916.
- Pavkov, Richard, Dilraj Singh, and Ilse Reitveld. 2008. “Concept1 (a New Single Dose Dry Powder Inhaler) Peak Inspiratory Flow Rate Study with COPD Patients.” In , 3:683–686.
- Pilcer, G, and K Amighi. 2010. “Formulation Strategy and Use of Excipients in Pulmonary Drug Delivery.” *INTERNATIONAL JOURNAL OF PHARMACEUTICS* 392 (1-2) (June 15): 1–19.
doi:10.1016/j.ijpharm.2010.03.017.
- Pilcer, Gabrielle, Francis Vanderbist, and Karim Amighi. 2008. “Correlations between Cascade Impactor Analysis and Laser Diffraction Techniques for the Determination of the Particle Size of Aerosolised Powder Formulations.” *International Journal of Pharmaceutics* 358 (1–2) (June 24): 75–81.
doi:10.1016/j.ijpharm.2008.02.014.
- Pilcer, Gabrielle, Nathalie Wauthoz, and Karim Amighi. 2012. “Lactose Characteristics and the Generation of the Aerosol.” *Advanced Drug Delivery Reviews* 64 (3) (March 15): 233–256. doi:10.1016/j.addr.2011.05.003.
- Pison, U, Welte, T, Giersig, M, and Groneberg, DA. 2006. “Nanomedicine for Respiratory Diseases.” *European Journal of Pharmacology* 533 (1-3) (March 8): 341–350. doi:10.1016/j.ejphar.2005.12.068.
- Preetham, A. C., and C. S. Satish. 2011. “Formulation of a Poorly Water-Soluble Drug Sirolimus in Solid Dispersions to Improve Dissolution.” *Journal of Dispersion Science and Technology* 32 (6): 778–783. doi:10.1080/01932691.2010.488129.
- Price, David, Barbara Yawn, Guy Brusselle, and Andrea Rossi. 2013. “Risk-to-Benefit Ratio of Inhaled Corticosteroids in Patients with COPD.” *Primary Care Respiratory Journal* 22 (1) (March): 92–100. doi:10.4104/pcrj.2012.00092.
- Rasenack, N., and B. W. Muller. 2004. “Micron-Size Drug Particles: Common and Novel Micronization Techniques.” *Pharmaceutical Development and Technology* 9 (1): 1–13. doi:10.1081/PDT-120027417.
- Raula, Janne, Anna Lahde, and Esko I Kauppinen. 2009. “Aerosolization Behavior of Carrier-Free L-Leucine Coated Salbutamol Sulphate Powders.” *International*

- Journal of Pharmaceutics 365 (1-2) (January 5): 18–25.
doi:10.1016/j.ijpharm.2008.08.017.
- Raula, Janne, Frank Thielmann, Majid Naderi, Vesa-Pekka Lehto, and Esko I. Kauppinen. 2010. “Investigations on Particle Surface Characteristics vs. Dispersion Behaviour of L-Leucine Coated Carrier-Free Inhalable Powders.” *International Journal of Pharmaceutics* 385 (1–2) (January 29): 79–85.
doi:10.1016/j.ijpharm.2009.10.036.
- Rave, K., E. Potocka, A. H. Boss, M. Marino, D. Costello, and R. Chen. 2009. “Pharmacokinetics and Linear Exposure of AFRESATM Compared with the Subcutaneous Injection of Regular Human Insulin.” *Diabetes, Obesity and Metabolism* 11 (7): 715–720. doi:10.1111/j.1463-1326.2009.01039.x.
- Ricciutelli, Massimo, Piera Di Martino, Luciano Barboni, and Sante Martelli. 2006. “Evaluation of Rapamycin Chemical Stability in Volatile-Organic Solvents by HPLC.” *Journal of Pharmaceutical and Biomedical Analysis* 41 (3) (June 7): 1070–1074. doi:10.1016/j.jpba.2006.02.009.
- Richardson, Peter C, and Anders H Boss. 2007. “Technosphere((R)) Insulin Technology.” *Diabetes Technology & Therapeutics* 9 (June): S65–S72.
doi:10.1089/dia.2007.0212.
- Roberts, D. L., and F. J. Romay. 2005. “Relationship of Stage Mensuration Data to the Performance of New and Used Cascade Impactors.” *Journal of Aerosol Medicine-Deposition Clearance and Effects in the Lung* 18 (4): 396–413.
doi:10.1089/jam.2005.18.396.
- Rogers, True L, Andrew C Nelsen, Jiahui Hu, Judith N Brown, Marazban Sarkari, Timothy J Young, Keith P Johnston, and Robert O Williams III. 2002. “A Novel Particle Engineering Technology to Enhance Dissolution of Poorly Water Soluble Drugs: Spray-Freezing into Liquid.” *European Journal of Pharmaceutics and Biopharmaceutics* 54 (3) (November): 271–280. doi:10.1016/S0939-6411(02)00063-2.
- Ruecroft, G., and D. Parikh. 2010. “Sonocrystallisation Particle Engineering for Inhalable Medicines.” *Journal of Pharmacy and Pharmacology* 62 (10) (October): 1470–1471.

- Salama, Rania O., Paul M. Young, Philippe Rogueda, Arthur Lallement, Ilian Iliev, and Daniela Traini. 2011. "Advances in Drug Delivery: Is Triple Therapy the Future for the Treatment of Chronic Obstructive Pulmonary Disease?" *Expert Opinion on Pharmacotherapy* 12 (12) (August): 1913–1932. doi:10.1517/14656566.2011.589837.
- Saleki-Gerhardt, Azita, Claes Ahlneck, and George Zografi. 1994. "Assessment of Disorder in Crystalline Solids." *International Journal of Pharmaceutics* 101 (3) (January 25): 237–247. doi:10.1016/0378-5173(94)90219-4.
- Saluja, V., J-P. Amorij, J.C. Kapteyn, A.H. de Boer, H.W. Frijlink, and W.L.J. Hinrichs. 2010. "A Comparison between Spray Drying and Spray Freeze Drying to Produce an Influenza Subunit Vaccine Powder for Inhalation." *Journal of Controlled Release* 144 (2) (June 1): 127–133. doi:10.1016/j.jconrel.2010.02.025.
- Schüle, S., T. Schulz-Fademrecht, P. Garidel, K. Bechtold-Peters, and W. Frieß. 2008. "Stabilization of IgG1 in Spray-Dried Powders for Inhalation." *European Journal of Pharmaceutics and Biopharmaceutics* 69 (3) (August): 793–807. doi:10.1016/j.ejpb.2008.02.010.
- Sehgal, S.N. 2003. "Sirolimus: Its Discovery, Biological Properties, and Mechanism of Action." *Transplantation Proceedings* 35 (3, Supplement) (May): S7–S14. doi:10.1016/S0041-1345(03)00211-2.
- Shah, Saiyam, Chad Smutney, Vincent Saviano, Spencer Kinsey, and Donald Ridley. 2012. "A Dry Powder Delivery Technology Embodied in a Single Use Re-Useable and Single Use Disposable Format." In , 2:577–580.
- Sharma, Garima, Wunlapa Mueannoom, Asma B.M. Buanz, Kevin M.G. Taylor, and Simon Gaisford. 2013. "In Vitro Characterisation of Terbutaline Sulphate Particles Prepared by Thermal Ink-Jet Spray Freeze Drying." *International Journal of Pharmaceutics* 447 (1–2) (April 15): 165–170. doi:10.1016/j.ijpharm.2013.02.045.
- Shen, Li-Juan, and Fe-Lin Lin Wu. 2007. "Nanomedicines in Renal Transplant Rejection - Focus on Sirolimus." *International Journal of Nanomedicine* 2 (1): 25–32. doi:10.2147/nano.2007.2.1.25.
- Shen, Zhi-Gang, Wen-Hao Chen, Nital Jugade, Ling-Yan Gao, William Glover, Jin-Ye Shen, Jimmy Yun, and Jian-Feng Chen. 2012. "Fabrication of Inhalable Spore

- like Pharmaceutical Particles for Deep Lung Deposition.” *International Journal of Pharmaceutics* 430 (1-2) (July 1): 98–103. doi:10.1016/j.ijpharm.2012.03.044.
- Shoyele, Sunday A. 2008. “Controlling the Release of Proteins/peptides via the Pulmonary Route.” In *Methods in Molecular Biology*, edited by K. K. Jain, 437:141–148.
- Shur, Jagdeep, and Robert Price. 2012. “Advanced Microscopy Techniques to Assess Solid-State Properties of Inhalation Medicines.” *Advanced Drug Delivery Reviews* 64 (4) (March 30): 369–382. doi:10.1016/j.addr.2011.11.005.
- Simamora, Pahala, Joan M Alvarez, and Samuel H Yalkowsky. 2001. “Solubilization of Rapamycin.” *International Journal of Pharmaceutics* 213 (1–2) (February 1): 25–29. doi:10.1016/S0378-5173(00)00617-7.
- Sin, Don D., and S. F. Paul Man. 2007. “Do Chronic Inhaled Steroids Alone or in Combination with a Bronchodilator Prolong Life in Chronic Obstructive Pulmonary Disease Patients?” *Current Opinion in Pulmonary Medicine* 13 (2) (March): 90–97.
- Sinha, Biswadip, Biswajit Mukherjee, and Gurudutta Pattnaik. 2013. “Poly-Lactide-Co-Glycolide Nanoparticles Containing Voriconazole for Pulmonary Delivery: In Vitro and in Vivo Study.” *Nanomedicine* □: Nanotechnology, Biology, and Medicine 9 (1) (January 1): 94–104.
- Smyth, H. D. C. 2003. “The Influence of Formulation Variables on the Performance of Alternative Propellant-Driven Metered Dose Inhalers.” *Advanced Drug Delivery Reviews* 55 (7): 807–828.
- Smyth, Hugh D.C., and Anthony J. Hickey. 2005. “Carriers in Drug Powder Delivery: Implications for Inhalation System Design.” *American Journal of Drug Delivery* 3 (2): 117–132.
- Son, Yoen-Ju, and Jason T McConville. 2011. “A New Respirable Form of Rifampicin.” *European Journal of Pharmaceutics and Biopharmaceutics* 78 (3) (August): 366–376. doi:10.1016/j.ejpb.2011.02.004.
- Son, Yoen-Ju, and Jason T. McConville. 2008. “Advancements in Dry Powder Delivery to the Lung.” *Drug Development and Industrial Pharmacy* 34 (9) (January): 948–959. doi:10.1080/03639040802235902.

2009. "Development of a Standardized Dissolution Test Method for Inhaled Pharmaceutical Formulations." *International Journal of Pharmaceutics* 382 (1–2) (December 1): 15–22. doi:10.1016/j.ijpharm.2009.07.034.
- Sou, Tomás, Lisa M. Kaminskas, Tri-Hung Nguyen, Renée Carlberg, Michelle P. McIntosh, and David A.V. Morton. 2013. "The Effect of Amino Acid Excipients on Morphology and Solid-State Properties of Multi-Component Spray-Dried Formulations for Pulmonary Delivery of Biomacromolecules." *European Journal of Pharmaceutics and Biopharmaceutics* 83 (2) (February): 234–243. doi:10.1016/j.ejpb.2012.10.015.
- Sou, Tomás, Els N Meeusen, Michael de Veer, David A V Morton, Lisa M Kaminskas, and Michelle P McIntosh. 2011. "New Developments in Dry Powder Pulmonary Vaccine Delivery." *Trends in Biotechnology* 29 (4) (April): 191–198. doi:10.1016/j.tibtech.2010.12.009.
- Steckel, Hartwig, and Nina Bolzen. 2004. "Alternative Sugars as Potential Carriers for Dry Powder Inhalations." *International Journal of Pharmaceutics* 270 (1-2) (February 11): 297–306.
- Stein, Stephen, Tom Robison, Zhaolin Wang, Dave Hodson, and Todd Alband. 2010. "The 3M Taper Dry Powder Inhaler Device." In , 2:377–380. *Respiratory Drug Delivery*.
- Steiner, Solomon S., Trent A. Poole, Per B. Fog, Roderike Pohl, Michael Crick, and Robert Feldstein. 2008. "United States Patent: 7464706 - Unit Dose Cartridge and Dry Powder Inhaler." <http://patft.uspto.gov/netacgi/nph-Parser?Sect1=PTO1&Sect2=HITOFF&d=PALL&p=1&u=%2Fnetacgi%2FPTO%2Fsrchnum.htm&r=1&f=G&l=50&s1=7,464,706.PN.&OS=PN/7,464,706&RS=PN/7,464,706>.
- Stevens, Nia, John Shrimpton, Mark Palmer, Dave Prime, and Bal Johal. 2007. "Accuracy Assessments for Laser Diffraction Measurements of Pharmaceutical Lactose." *Measurement Science & Technology* 18 (12) (December): 3697–3706. doi:10.1088/0957-0233/18/12/004.
- Stuckey, L.J., C.E. Bartos, H.A. McCullough, R.D. Florn, V.N. Lama, J. Lin, and K.M. Chan. 2013. "Use of Sirolimus in Lung Transplantation: A Single Center

- Experience.” *The Journal of Heart and Lung Transplantation* 32 (4, Supplement) (April): S89. doi:10.1016/j.healun.2013.01.990.
- Sung, Jean, Danielle Padilla, Lucila Garcia-Contreras, Jarod VerBerkmoes, David Durbin, Charles Peloquin, Katharina Elbert, Anthony Hickey, and David Edwards. 2009. “Formulation and Pharmacokinetics of Self-Assembled Rifampicin Nanoparticle Systems for Pulmonary Delivery.” *Pharmaceutical Research* 26 (8): 1847–1855. doi:10.1007/s11095-009-9894-2.
- Svensson, Mårten, Gunilla Pettersson, and Lars Asking. 2005. “Mensuration and Cleaning of the Jets in Andersen Cascade Impactors.” *Pharmaceutical Research* 22 (1) (January): 161–165.
- Tajber, L., D.O. Corrigan, O.I. Corrigan, and A.M. Healy. 2009. “Spray Drying of Budesonide, Formoterol Fumarate and Their composites—I. Physicochemical Characterisation.” *International Journal of Pharmaceutics* 367 (1–2) (February 9): 79–85. doi:10.1016/j.ijpharm.2008.09.030.
- Taki, Mohammed, Christopher Marriott, Xian-Ming Zeng, and Gary P. Martin. 2010. “Aerodynamic Deposition of Combination Dry Powder Inhaler Formulations in Vitro: A Comparison of Three Impactors.” *International Journal of Pharmaceutics* 388 (1–2) (March 30): 40–51. doi:10.1016/j.ijpharm.2009.12.031.
- Tarsin, Walid Y., Stanley B. Pearson, Khaled H. Assi, and Henry Chrystyn. 2006. “Emitted Dose Estimates from Seretide® Diskus® and Symbicort® Turbuhaler® Following Inhalation by Severe Asthmatics.” *International Journal of Pharmaceutics* 316 (1–2) (June 19): 131–137. doi:10.1016/j.ijpharm.2006.02.040.
- Taveira-DaSilva, Angelo M, Olanda Hathaway, Mario Stylianou, and Joel Moss. 2011. “Changes in Lung Function and Chylous Effusions in Patients with Lymphangiomyomatosis Treated with Sirolimus.” *Annals of Internal Medicine* 154 (12) (June 21): 797–805, W-292–293. doi:10.1059/0003-4819-154-12-201106210-00007.
- Thalberg, Kyrre, Elna Berg, and Magnus Fransson. 2012. “Modeling Dispersion of Dry Powders for Inhalation. The Concepts of Total Fines, Cohesive Energy and Interaction Parameters.” *International Journal of Pharmaceutics* 427 (2) (May 10): 224–233. doi:10.1016/j.ijpharm.2012.02.009.

- Thibert, Roch, Mark Parry-Billings, and Martin Shott. 2002. "Clickhaler® Dry Powder Inhaler: Focussed in Vitro Proof of Principle Evaluation of a New Chemical Entity for Asthma." *International Journal of Pharmaceutics* 239 (1–2) (June 4): 149–156. doi:10.1016/S0378-5173(02)00106-0.
- Tolman, Justin A., and Robert O. Williams. 2010. "Advances in the Pulmonary Delivery of Poorly Water-Soluble Drugs: Influence of Solubilization on Pharmacokinetic Properties." *Drug Development and Industrial Pharmacy* 36 (1): 1–30. doi:10.3109/03639040903092319.
- Tompkins, Stephen Mark, Chia-Yun Lo, Terrence M. Tumpey, and Suzanne L. Epstein. 2004. "Protection against Lethal Influenza Virus Challenge by RNA Interference in Vivo." *Proceedings of the National Academy of Sciences of the United States of America* 101 (23) (June 8): 8682–8686. doi:10.1073/pnas.0402630101.
- Trivedi, Rakshit Kanubhai, Dhairyshil S. Chendake, and Mukesh C. Patel. 2012. "A Rapid, Stability-Indicating RP-HPLC Method for the Simultaneous Determination of Formoterol Fumarate, Tiotropium Bromide, and Ciclesonide in a Pulmonary Drug Product." *Scientia Pharmaceutica* 80 (3) (September): 591–603. doi:10.3797/scipharm.1204-06.
- Tuli, Rinku A., Tim R. Dargaville, Graeme A. George, and Nazrul Islam. 2012. "Polycaprolactone Microspheres as Carriers for Dry Powder Inhalers: Effect of Surface Coating on Aerosolization of Salbutamol Sulfate." *Journal of Pharmaceutical Sciences* 101 (2) (February): 733–745. doi:10.1002/jps.22777.
- Ungaro, Francesca, Roberta d'Emmanuele di Villa Bianca, Concetta Giovino, Agnese Miro, Raffaella Sorrentino, Fabiana Quaglia, and Maria Immacolata La Rotonda. 2009. "Insulin-Loaded PLGA/cyclodextrin Large Porous Particles with Improved Aerosolization Properties: In Vivo Deposition and Hypoglycaemic Activity after Delivery to Rat Lungs." *Journal of Controlled Release* 135 (1) (April 2): 25–34. doi:10.1016/j.jconrel.2008.12.011.
- Ungaro, Francesca, Ivana d' Angelo, Ciro Coletta, Roberta d' Emmanuele di Villa Bianca, Raffaella Sorrentino, Brunella Perfetto, Maria Antonietta Tufano, Agnese Miro, Maria Immacolata La Rotonda, and Fabiana Quaglia. 2012. "Dry Powders Based on PLGA Nanoparticles for Pulmonary Delivery of Antibiotics: Modulation of Encapsulation Efficiency, Release Rate and Lung Deposition

- Pattern by Hydrophilic Polymers.” *Journal of Controlled Release* 157 (1) (January 10): 149–159. doi:10.1016/j.jconrel.2011.08.010.
- Ungaro, Francesca, Giuseppe De Rosa, Agnese Miro, Fabiana Quaglia, and Maria Immacolata La Rotonda. 2006. “Cyclodextrins in the Production of Large Porous Particles: Development of Dry Powders for the Sustained Release of Insulin to the Lungs.” *European Journal of Pharmaceutical Sciences* 28 (5) (August): 423–432. doi:10.1016/j.ejps.2006.05.005.
- Vandenheuvel, Dieter, Abhishek Singh, Katrien Vandersteegen, Jochen Klumpp, Rob Lavigne, and Guy Van den Mooter. 2013. “Feasibility of Spray Drying Bacteriophages into Respirable Powders to Combat Pulmonary Bacterial Infections.” *European Journal of Pharmaceutics and Biopharmaceutics: Official Journal of Arbeitsgemeinschaft Für Pharmazeutische Verfahrenstechnik e.V* 84 (3) (August): 578–582. doi:10.1016/j.ejpb.2012.12.022.
- Vaughn, Jason M., Jason T. McConville, Matthew T. Crisp, Keith P. Johnston, and Robert O. Williams III. 2006. “Supersaturation Produces High Bioavailability of Amorphous Danazol Particles Formed by Evaporative Precipitation into Aqueous Solution and Spray Freezing into Liquid Technologies.” *Drug Development & Industrial Pharmacy* 32 (5) (June): 559–567. doi:10.1080/03639040500529176.
- Vehring, Reinhard. 2008. “Pharmaceutical Particle Engineering via Spray Drying.” *Pharmaceutical Research* 25 (5) (May): 999–1022. doi:10.1007/s11095-007-9475-1.
- Vehring, Reinhard, David Lechuga-Ballesteros, Vidya Joshi, Brian Noga, and Sarvajna K. Dwivedi. 2012. “Cosuspensions of Microcrystals and Engineered Microparticles for Uniform and Efficient Delivery of Respiratory Therapeutics from Pressurized Metered Dose Inhalers.” *Langmuir* 28 (42) (October 23): 15015–15023. doi:10.1021/la302281n.
- Velaga, S. P., R. Berger, and J. Carlfors. 2002. “Supercritical Fluids Crystallization of Budesonide and Flunisolide.” *Pharmaceutical Research* 19 (10) (October): 1564–1571. doi:10.1023/A:1020477204512.
- Vervaet, C, and P R Byron. 1999. “Drug-Surfactant-Propellant Interactions in HFA-Formulations.” *International Journal of Pharmaceutics* 186 (1) (September 10): 13–30.

- Vishweshwar, Peddy, Jennifer A McMahon, Joanna A Bis, and Michael J Zaworotko. 2006a. "Pharmaceutical Co-Crystals." *Journal of Pharmaceutical Sciences* 95 (3) (March): 499–516. doi:10.1002/jps.20578.
- 2006b. "Pharmaceutical Co-Crystals." *Journal of Pharmaceutical Sciences* 95 (3) (March): 499–516. doi:10.1002/jps.20578.
- Vujanic, Ana, Janet L.K. Wee, Kenneth J. Snibson, Stirling Edwards, Martin Pearse, Charles Quinn, Margaret Moloney, Shirley Taylor, Jean-Pierre Y. Scheerlinck, and Philip Sutton. 2010. "Combined Mucosal and Systemic Immunity Following Pulmonary Delivery of ISCOMATRIX™ Adjuvanted Recombinant Antigens." *Vaccine* 28 (14) (March 19): 2593–2597. doi:10.1016/j.vaccine.2010.01.018.
- Watts, Alan B., Yi-Bo Wang, Keith P. Johnston, and Robert O. Williams. 2013a. "Respirable Low-Density Microparticles Formed In Situ from Aerosolized Brittle Matrices." *Pharmaceutical Research* 30 (3) (March): 813–825. doi:10.1007/s11095-012-0922-2.
- 2013b. "Respirable Low-Density Microparticles Formed In Situ from Aerosolized Brittle Matrices." *Pharmaceutical Research* 30 (3) (March): 813–825. doi:10.1007/s11095-012-0922-2.
- Wee, J. L. K., J-P Y Scheerlinck, K. J Snibson, S. Edwards, M. Pearse, C. Quinn, and P. Sutton. 2008. "Pulmonary Delivery of ISCOMATRIX Influenza Vaccine Induces Both Systemic and Mucosal Immunity with Antigen Dose Sparing." *Mucosal Immunology* 1 (6) (November): 489–496. doi:10.1038/mi.2008.59.
- Weers, Jeffry G, John Bell, Hak-Kim Chan, David Cipolla, Craig Dunbar, Anthony J Hickey, and Ian J Smith. 2010. "Pulmonary Formulations: What Remains to Be Done?" *Journal of Aerosol Medicine and Pulmonary Drug Delivery* 23 (December): S5–S23. doi:10.1089/jamp.2010.0838.
- Wetterlin, K. 1988. "Turbuhaler - a New Powder Inhaler for Administration of Drugs to the Airways." *Pharmaceutical Research* 5 (8) (August): 506–508. doi:10.1023/A:1015969324799.
- Williamson, Peter A., Philip M. Short, Karine L. Clearie, Sriram Vaidyanathan, Thomas C. Fardon, Laura J. Howaniec, and Brian J. Lipworth. 2010. "Paradoxical Trough Effects of Triple Therapy with Budesonide/formoterol and Tiotropium Bromide on Pulmonary Function Outcomes in COPD." *CHEST Journal* 138 (3): 595–604.

- Yanez, Jaime A., M. Laird Forrest, Yusuke Ohgami, Glen S. Kwon, and Neal M. Davies. 2008. "Pharmacometrics and Delivery of Novel Nanoformulated PEG-B-Poly(epsilon-Caprolactone) Micelles of Rapamycin." *Cancer Chemotherapy and Pharmacology* 61 (1) (January): 133–144. doi:10.1007/s00280-007-0458-z.
- Yang, Wei, Keith P. Johnston, and Robert O. Williams III. 2010. "Comparison of Bioavailability of Amorphous versus Crystalline Itraconazole Nanoparticles via Pulmonary Administration in Rats." *European Journal of Pharmaceutics and Biopharmaceutics* 75 (1) (May): 33–41. doi:10.1016/j.ejpb.2010.01.011.
- Yang, Yan, Nimisha Bajaj, Peisheng Xu, Kimberly Ohn, Michael D. Tsifansky, and Yoon Yeo. 2009. "Development of Highly Porous Large PLGA Microparticles for Pulmonary Drug Delivery." *Biomaterials* 30 (10) (April): 1947–1953. doi:10.1016/j.biomaterials.2008.12.044.
- Yu, Lian, and Kingman Ng. 2002. "Glycine Crystallization during Spray Drying: The pH Effect on Salt and Polymorphic Forms." *Journal of Pharmaceutical Sciences* 91 (11) (November): 2367–2375. doi:10.1002/jps.10225.
- Yu, Zhongshui, Keith P. Johnston, and Robert O. Williams III. 2006. "Spray Freezing into Liquid versus Spray-Freeze Drying: Influence of Atomization on Protein Aggregation and Biological Activity." *European Journal of Pharmaceutical Sciences* 27 (1) (January): 9–18. doi:10.1016/j.ejps.2005.08.010.
- Zeng, X. M., G. P. Martin, S. K. Tee, and C. Marriott. 1998. "The Role of Fine Particle Lactose on the Dispersion and Deaggregation of Salbutamol Sulphate in an Air Stream in Vitro." *International Journal of Pharmaceutics* 176 (1) (December 30): 99–110. doi:10.1016/S0378-5173(98)00300-7.
- Zeng, Xian-Ming, Helen MacRitchie, Christopher Marriott, and Gary Martin. 2006. "Correlation between Inertial Impaction and Laser Diffraction Sizing Data for Aerosolized Carrier-Based Dry Powder Formulations." *Pharmaceutical Research* 23 (9): 2200–2209. doi:10.1007/s11095-006-9055-9.
- Zhang, Xi, Yingliang Ma, Liqiang Zhang, Jingxu Zhu, and Fang Jin. 2012. "The Development of a Novel Dry Powder Inhaler." *International Journal of Pharmaceutics* 431 (1-2) (July 15): 45–52. doi:10.1016/j.ijpharm.2012.04.019.
- Zhou, Qi (Tony), John A Denman, Thomas Gengenbach, Shyamal Das, Li Qu, Hailong Zhang, Ian Larson, Peter J Stewart, and David A. V Morton. 2011.

“Characterization of the Surface Properties of a Model Pharmaceutical Fine Powder Modified with a Pharmaceutical Lubricant to Improve Flow via a Mechanical Dry Coating Approach.” *Journal of Pharmaceutical Sciences* 100 (8) (August): 3421–3430. doi:10.1002/jps.22547.

Zhou, Qi Tony, Li Qu, Ian Larson, Peter J Stewart, and David A. V Morton. 2010. “Improving Aerosolization of Drug Powders by Reducing Powder Intrinsic Cohesion via a Mechanical Dry Coating Approach.” *International Journal of Pharmaceutics* 394 (1-2) (July 15): 50–59. doi:10.1016/j.ijpharm.2010.04.032.

Zhu, Jingxu, Jianzhang Wen, Yingliang Ma, and Hui Zhang. 2011. “Dry Powder Inhaler.” <http://www.google.com/patents?id=GSn5AQAAEBAJ>.

Vita

Simone Raffa Carvalho attended Colegio Promove during high school. In 2004, she received the degree of Bachelor in Pharmacy from the College of Pharmacy at Unicentro Newton Paiva in Belo Horizonte, Minas Gerais, Brazil. During the following years she was employed as Quality Assurance Analyst by Novo Nordisk Produção Farmacêutica do Brasil, in Montes Claros, Brazil. In August 2009, she entered the doctorate program in Pharmaceutics at The University of Texas at Austin, under the supervision of Dr. Robert O. Williams III.

E-mail address: simonerc@utexas.edu

This dissertation was typed by the author.